Characteristics of Baculovirus-Expressed rClC-1

by David St.John Astill

Thesis submitted to The Department of Physiology, Faculty of Science, The University of Adelaide as partial fulfilment of the requirements for award of the degree of Doctor of Philosophy.

Work performed in the laboratories of The Department of Physiology, The University of Adelaide and School of Pharmacy and Medical Sciences, University of South Australia.

January 1996

for Amanda

Contents

List of figures and tables

Figures and Tables (continued)

Summary

The baculovirus/ Sf cell system was established and used to express rat skeletal muscle chloride channel ClC-1. Modified *clc*-1 reading frames were produced and the mutant proteins encoded thereby successfully expressed. Recombinant PCR techniques were employed to produce a 5'-histidine tagged protein for use in future protein purification and reconstitution experiments. Site-directed mutagenesis was also applied to produce a protein in which the highly conserved arginine at position 304 was replaced by a glutamic acid residue (R304E). Factors influencing protein yield were investigated, the data obtained being used to optimise expression in Sf cells. Removal of the upstream untranslated sequence of the cDNA was found to increase the level of expression suggesting the presence of regulatory sequences in this region. Wild type and modified forms of ClC-1 were expressed at high levels in Sf cells, protein being easily visualised on coomassie-stained polyacrylamide gels.

Whole-cell patch-clamping was used directly on ClC-1-expressing Sf9 cells to assess the biophysical properties of the channel in this system. Current kinetics were investigated and found to be similar to those reported by others using heterologously expressed rat and human ClC-1 protein in other cell lines and were in keeping with those expected for the channel responsible for the large chloride flux in skeletal muscle. Distinctive features of whole-cell currents included deactivation at hyperpolarising potentials and rectification at positive potentials. Under the conditions used here, the deactivating current was found to be made up of three components, two exponentially decaying and one constant. The time constants of the two exponential components, designated fast and slow, were around 6 and 25ms (test potential -120mV) respectively. On a small number of occasions when longer lasting voltage pulses were employed, a third exponentially deacying component could be

extracted with a time constant of several hundred milliseconds (Astill et al., 1995a). No attempt has been made, at this stage, to characterise this component in any detail. In contrast, the two faster components were studied in detail and their time constants were found to be voltage dependent, the fast component becoming faster and the slow component slower as the test potential became less negative. Increases in total instantaneous and quasi-steady state currents along with a slowing of the deactivation process were also noted during the first 10 - 20 minutes of current recording.

The effects of various compounds known to interfere with chloride permeation in muscle and other tissues were also assessed. Anthracene-9-carboxylate was found to be the most potent blocker exhibiting an IC_{50} of around 20μM. Most other compounds tested displayed potencies in the millimolar range with the exception of niflumate for which preliminary results indicated a potency in the 50 - 100μM range. Different compounds were found to alter channel behaviour in varying ways suggesting several, discrete sites of interaction with the channel protein. A number of compounds, including 2-(4-chlorophenoxy)-propionate (clofibric acid) and its enantiomers, induced changes in current kinetics remarkably similar to those observed by other investigators working with *in vitro* expressed ClC-1 incorporating mutations found in the human myotonic muscle disease dominant myotonia congenita (Thomsen's disease).

Results obtained with the point mutant produced in our laboratories (R304E), in particular its differing response to Zn^{++} at various external pHs, shed some doubt on the current proposed topological model of this protein and indicate the possible involvement of histidine residues in normal channel operation.

Declaration

This thesis contains no material which has been submitted for the award of any other degree or diploma in any University. To the best of my knowledge and belief, this thesis contains no material previously published or written by another person except where due reference is given in the text. I consent to this thesis being made available for photocopying and loan, if applicable, if accepted for the award of the degree of Doctor of Philosophy.

Signed this 31ST day of Jan. 1996

Acknowledgments

During the course of this study I was the recipient of an Australian Postgraduate Research Award, provided by the Australian Federal Government, and the Ross Stuart Postgraduate Award, provided by The Muscular Dystrophy Association (MDA) of South Australia Inc. I gratefully acknowledge the generous financial support provided by the MDA throughout the course of this work.

I wish to acknowledge the assistance of numerous people who contributed to the preparation of this thesis. Firstly, my supervisors Assoc. Prof. Allan H. Bretag and Dr. Michael L. Roberts, both of whom have been extraordinarily supportive and positive over the past 3 and 1/2 years. Their exceptional knowledge and experience in all areas was invaluable and their consistently positive and enthusiastic approach always uplifting. I thank them for managing to provide adequate guidance whilst still allowing me a great deal of freedom during the course of my work. I am particularly thankful to Allan for convincing me to change disciplines to do this research, it was his infectious enthusiasm for his subject which finally convinced me to take it on. I would also like to thank Michael for having a sense of humour as bizarre as my own.

Secondly, I would like to thank past and present members of our research group. Thanks to past members namely Drs. Trevor M. Lewis and Gregory K. Pike for much help getting started with the patch-clamp experiments and for their friendship and encouragement. I would also like to acknowledge the work done by Honours student Jacqueline D. Clarke in preparing the site-directed mutant of ClC-1 used in this work. Also to two current members of the group namely Grygori Y. Rychkov and Bernard P. Hughes. I thank Grygori for many useful discussions in the area of biophysics and patch-clamp technique. Special thanks to Bernie for allowing me unrestricted use of his laboratory, for being a

useful sounding board when formulating ideas for molecular experiments and for putting up with my irreverent sense of humour.

I also acknowledge the assistance of our collaborators, in particular Prof. Thomas J. Jentsch and Dr. Klaus Steinmeyer of the Centre for Molecular Neurobiology, The University of Hamburg, Germany, for the generous gift of the *clc*-1 cDNA on which all this work is based. I also thank Prof. Shirley H. Bryant of The Department of Pharmacology and Cell Biophysics, University of Cincinnati, Ohio, for much useful discussion on pharmacological matters and for preparing the enantiomers of CPP used in this study.

Numerous members of both technical and academic staff at The School of Pharmacy and Medical Science, University of South Australia, also deserve acknowledgment but in particular I wish to thank Drs. Ray J. Harris and Jan Williamson for many useful discussions on matters molecular and for the use of numerous items of equipment.

I am also extremely grateful for the assistance of Dr. Peter L. Ey of The Department of Microbiology and Immunology, The University of Adelaide, for a good deal of assistance and useful discussion regarding production of antibodies.

Last but certainly not least, I would like to give special thanks to my wife Amanda. Her continual support and encouragement was vitally important throughout this entire exercise. It would not be an exaggeration to say that without her support this thesis would never have been written.

Abbreviations

2,4-D	2,4-dichlorophenoxyacetate
4-NC	4-chloro-1-naphthol
A9C	Anthracene-9-carboxylate
AcMNPV	*Autographa californica* Multiply embedded nuclear polyhedrosis virus
BGG	Bovine gamma globulin
BGG::C12	Bovine gamma globulin/ peptide C12 conjugate
BGG::N12	Bovine gamma globulin/ peptide N12 conjugate
bis	N,N'-methylene-bis-acrylamide
BSA	Bovine serum albumin
BSA::C12	Bovine serum albumin/ peptide C12 conjugate
BSA::N12	Bovine serum albumin/ peptide N12 conjugate
CPP	2-(4-chlorophenoxy)-propionate
DIDS	4,4'-diisothiocyanostilbene-2,2'-disulphonic acid
DNDS	4,4'-dinitrostilbene-2,2'-disulphonic acid
DPC	diphenylamine-2-carboxylate
ECV	Extracellular virus
ELB	Enriched Luria broth
ELISA	Enzyme-linked immunosorbent assay
FBS	Fetal bovine serum
GV	Granulosis virus
HGT	High gelling temperature
hpi	Hours post infection
HRP	Horseradish peroxidase
HRP::C12	Horseradish peroxidase/ peptide C12 conjugate
hrs	Hours
iv	Intravenous
I/V	Current vs voltage
IAA	Indanyloxyacetate
IC_{50}	Concentration inducing 50% maximal inhibitory effect
IE	Immediate early
I_{inst0}	Instantaneous current at time = 0
I_{inst30}	Instantaneous current at time = 30 minutes
I_{qss0}	Quasi-steady state current at time = 0
I_{qss30}	Quasi-steady state current at time = 30 minutes
iu	International units
kb	kilobases
kbp	kilobase pairs
KLH	Keyhole limpet haemocyanin
MCS	Multiple cloning site
min	Minutes
MNPV	Multiply embedded nuclear polyhedrosis virus
MQ	Milli-Q (water) (*Millipore*)
M_r	Molecular weight
NOB	Non-occluded baculovirus
NPEB	5-nitro-2-(3-phenylethylylamino)-benzoate
NPPB	5-nitro-2-(3-phenylpropylamino)-benzoate

Abbreviations (continued)

NPV	Nuclear polyhedrosis virus
nts	Nucleotides
OPD	o-phenylenediamine dihydrochloride
PAG	Polyacrylamide gel
PAGE	Polyacrylamide gel electrophoresis
PBS	Phosphate buffered saline
PBS-T	PBS + 0.1% Tween-20
PBS-TB	PBS + 0.05% (v/v) Tween-20 + 0.1% (w/v) BSA
PEG	Polyethyleneglycol
pfu	Plaque forming units
pi	post infection
P_{open}	Open probability
RIA	Radio-immuno assay
sc	subcutaneous
s	Seconds
Sf	*Spodoptera frugiperda*
SITS	4-acetamido-4'-isothiocyanostilbene-2,2'-disulphonic acid
SNPV	Singly embedded nuclear polyhedrosis virus
TBS	150mM NaCl, 50mM Tris-Cl (pH 8)
TE	Tris/ EDTA
TEMED	N,N,N',N'-tetramethylethylene diamine
TMN-FH	Grace's anthracea medium plus lactalbumin hydrolysate and yeastolate
utr	Untranslated region
$V_{1/2}$	Voltage at which open probability = 0.5

I
General Introduction

Chloride-selective channels appear to be a feature of the plasmalemma of virtually every animal cell type. Normal operation of these channels is required for cellular functions as diverse as synaptic transmission, volume regulation, maintenance of intracellular pH and modulation of membrane excitability (for reviews see Bretag, 1987; Greger, 1992; Jentsch, 1993; Pusch and Jentsch, 1994). In keeping with their diverse range of functions the activity of different types of chloride channels is controlled by various factors including membrane voltage, ligand binding, osmotic pressure and phosphorylation.

The importance of the regulated activity of these channels is probably best illustrated by the disease states which result from perturbation of their normal function. Examples include cystic fibrosis, hyperekplexia, nephrolithiasis and myotonia. It is now clear that the broad range of physiological abnormalities exhibited by patients suffering from cystic fibrosis can be attributed to inherited mutations of the chloride channel known as the cystic fibrosis transmembrane conductance regulator (CFTR) (for review see Cutting, 1993). Hyperekplexia has recently been shown to be due to mutations in the α_1 subunit of the glycine receptor (Shiang et al., 1993; Schorderet et al., 1994) whilst another chloride channel, ClC-K2, has been linked to an X-linked hereditary nephrolithiasis (Dent's disease) (Fisher et al., 1994). The inherited myotonias, autosomal dominant myotonia congenita (MC) and autosomal recessive generalised myotonia (RGM) have also been known for some time to be the result of reduced chloride conductance of skeletal muscle (Rüdel and Lehmann-Horn, 1985). The channel responsible, ClC-1, was identified relatively recently (Steinmeyer et al.,

1991b; George et al., 1993). Since the identification of the gene encoding ClC-1, ClCN1, numerous mutations have been described in RGM and MC pedigrees (for recent reviews see Jentsch et al., 1995b and Meyer-Kleine et al., 1995) and myotonia levior has also been shown to be the result of a mutation in the same gene (Lehmann-Horn et al., 1995).

Despite the diverse and essential nature of chloride channels in cell membranes, they were for many years relatively poorly characterised compared to the cation-selective channels. Over the past decade or so, the situation has begun to change. Our knowledge of the mechanistic basis of the activity of various chloride-selective channels has increased rapidly following the application of various biophysical methods including patch-clamping and reconstitution into artificial bilayers. Much of the increase in our knowledge of this area can also be attributed to the application of molecular biological techniques to chloride channel research.

Whilst there exists a large body of work dealing with ligand-gated channels, such as γ-amino butyric acid and glycine receptors, and an equally extensive list of publications concerning CFTR, a comprehensive coverage of what is now known about these channels is beyond the scope of this thesis. Its focus will be on chloride channels found in skeletal muscle with reference to channels found in other tissues made mainly for the purposes of comparison.

I.1 Skeletal muscle chloride conductance

Early investigations of the characteristics of the large chloride conductance measurable in mammalian skeletal muscle had included studies on numerous species and had revealed a number of inter-species similarities including a large conductance at resting membrane potentials, high selectivity for chloride over other ions and

sensitivity to changes in pH (for comprehensive review see Bretag, 1987). Reduction of normal muscle chloride conductance, be it due to hereditary defects or pharmacological blockade, was also found to lead to myotonia (Bryant and Morales-Aguilera, 1971; Morgan et al., 1975; Rüdel and Lehmann-Horn, 1985; Rüdel et al., 1988; Steinmeyer et al., 1994 and reviewed in Jentsch et al., 1995b). Stimulation, which in normal muscle would lead to a single action potential, induces a run of action potentials in myotonic muscle. This hyperexcitability is primarily due to a slightly slowed return to resting potential following membrane depolarisation. Normally, by the time sodium channels have recovered from depolarisation-induced inactivation, the membrane potential has returned to a value below their activation threshold. In myotonic muscle, however, as a result of the slowed membrane repolarisation, sufficient sodium channels have recovered from inactivation before the membrane potential has become sufficiently negative. The result is reactivation of sodium channels and initiation of another action potential. Clinically these trains of action potentials, known as myotonic runs, manifest as prolonged muscle contractions. Pioneering studies of the characteristics of skeletal muscle chloride conductance also revealed some notable differences between species. Amphibian muscle, for example, showed a similar permeability series to mammalian muscle (*vide infra*) at neutral pH but this series reversed at low pH (Hutter et al., 1969). Toad, compared to mammalian, muscle was found to be around 100 times less sensitive to the blocking effects of anthracene-9-carboxylate (Bretag et al., 1980). Avian muscle exhibits an exquisite sensitivity to I^-, inclusion of iodide (0.5% (w/v) KI or NaI) in the drinking water of newly hatched chickens or adult pigeons being sufficient to induce myotonic symptoms within days (Morgan et al., 1975). Whilst these inter-species differences are of interest, the focus of the work presented herein concerns the chloride channel

from rat skeletal muscle and so the remainder of this introduction will deal with findings in mammals with the necessary exception of work concerning the electric organ of elasmobranch fishes since it formed the basis of our understanding of the operation of mammalian skeletal muscle chloride channels and was the starting material for the molecular work associated with the ClC chloride channel family (Jentsch et al., 1990).

Following the isolation of the cDNA encoding the major chloride permeation pathway in mammalian skeletal muscle (Steinmeyer et al., 1991b), designated ClC-1, various molecular techniques have been applied to this area of research. As a result, over the past 4 years our understanding of the basis of skeletal muscle chloride conductance has expanded rapidly.

I.1.1 Whole-cell studies

It had been known for some time that skeletal muscle exhibited an unusually high permeability to chloride. At rest, ca. 70 - 80% of membrane conductance is attributable to this halide anion (Bryant and Morales-Aguilera, 1971; Palade and Barchi, 1977a). Although cation channels in muscle had been characterised, analogous studies of anion channels in this tissue had failed to identify the major permeation pathway for chloride (for review see Bretag, 1987).

During the late 1970s Palade and Barchi (1977a) published a comprehensive characterisation of the chloride current in rat skeletal muscle fibres. These workers found the permeation pathway for chloride to be highly selective for chloride over potassium and reported the selectivity sequence to be $Cl^- > Br^- \geq I^- > CH_3SO_4^-$. Bromide and iodide both showed signs of interaction with chloride that was indicative of channel block. The chloride conductance at the resting membrane potential was found

to be dependent on pH, acidification of the bathing solution reducing membrane conductance with an apparent pKa of 5.5.

The instantaneous and steady state current/voltage relationships (I/V) were also determined between 15mV depolarised and 90mV hyperpolarised from the resting potential. With depolarisation, the instantaneous and steady state I/V was linear under all conditions tested. At potentials of more than 20mV negative to the resting potential, whilst the instantaneous I/V remained linear, a time dependent increase in membrane resistance was detected with a time constant of between 100 and 300ms. The steady state I/V thus showed a marked reduction in current with increasing hyperpolarisation at normal pH and was similar at alkaline pH (pH 10). Under these conditions, the current passed through a maximum, at around 20mV hyperpolarised, and then decreased with further hyperpolarisation, the effect being more marked under alkaline conditions. At normal pH, reduction of the chloride concentration reduced the degree of rectification in a dose dependent manner with virtually no rectification detectable when chloride was reduced to 25% of its normal concentration. The steady state I/V at pH 4, however, displayed rectification in the opposite direction with the current increasing as hyperpolarisation increased.

Palade and Barchi (1977a) also reported the finding that detubulated fibres had a markedly decreased chloride permeability, and suggested that at least 60% of the chloride conductance was located in the T-tubular system. Other researchers have also reported results indicating that a large proportion of the chloride conductance measured in muscle can be localised to the T-tubular membranes (Dulhunty et al., 1984; Heiny et al., 1990b). Other experiments by Dulhunty (1979, 1982) suggested that this was the case in rat muscle but that much less of the conductance could be attributed to these membranes in amphibia. Overall, the localisation of muscle

chloride conductance to either T-tubules or sarcolemma had not been particularly convincing with conflicting reports being published by different laboratories (reviewed in Bretag, 1987).

Other aspects of chloride conductance in muscle preparations had also been investigated. Study of its metabolic regulation had shown that stimulation of protein kinase C-mediated phosphorylation reduced chloride permeation in rat muscle (Brinkmeier and Jockusch, 1987; Tricarico et al., 1991). If phosphorylation activity was sufficiently up regulated, chloride conductance was reduced to the point of induction of myotonia. Various pharmacological agents, notably aromatic carboxylic acids, had also been shown to reduce conductance and at sufficient dose to induce myotonia. An overview of the findings obtained with various channel blockers is presented in the introduction to Section V. Studies of mechanisms controlling development and maintenance of normal chloride permeability indicated that, in rats, innervation was required (Conte Camerino et al., 1989).

I.1.2 Single channel studies

Single channel recording techniques have been applied to skeletal muscle with limited success. Much of this work has been performed on cultured muscle tissue ie. myotubes and myoballs. *In vitro*, mature myocytes do not survive well but myoblasts, which form part of the starting material for culture, are able to survive for relatively long periods. Myotubes form in these cultures as a result of the spontaneous fusion of myoblasts to form long tubular syncytia. Myoballs are produced by treatment of myotubes with a cytoskeleton disrupting agent, eg colchicine, which results in what are essentially spherical myotubes.

A number of chloride-selective channels have also been described in studies using other muscle-derived preparations including sarcolemmal vesicles and enzymatically dissociated mature muscle fibres.

Using vesicles derived from mature myocytes, Burton et al. (1988) described a 15 - 50pS chloride-selective channel which is probably the same channel as that described later by Rivet-Bastide et al. (1993). A channel of similar size was also found, albeit rarely, in a patch-clamp study of enzymatically dissociated myocytes (Chua and Betz, 1991). Blatz and Magleby (1983, 1985) have described 3 chloride channels in myotubes of 430, 60 and 45pS. The 45pS channel was described as exhibiting "fast" kinetics and was later the subject of detailed kinetic analysis (Blatz and Magleby, 1986). A more recent study involving patch-clamping of cultured human myoballs (Fahlke et al., 1992) uncovered three chloride-selective channels which the authors designated small, intermediate and large. The unitary conductances of these channels were reported as 10, 31 and 250pS respectively. The intermediate channel was the most common with a calculated density of 0.23 channels /μm^2 of membrane. It exhibited an open channel substructure with two sub-conductance states of equal amplitude both exhibiting outward rectification.

The small channel was less common with a calculated density of 0.07 channels/ μm^2 of membrane. These channels were never detected singly leading to the suggestion that they exist in the membrane as clusters. The channel was only slightly voltage dependent exhibiting very slight outward rectification. The investigation of its substructure was hampered by the presence of multiple channels in each patch.

The large conductance channel was seen in only 4 patches indicative of a very low density. This channel was activated by depolarisation but quickly inactivated. It was

not possible to characterise this channel adequately and the unitary conductance was calculated on the assumption of a linear current/voltage relationship.

In a later report (Fahlke et al., 1993), myoballs cultured from human subjects suffering from RGM were investigated and compared with those from normal individuals. The same three channels were detected in myoballs from myotonic subjects and the behaviour of the small and large channels were not significantly different from controls. The intermediate channel, however, exhibited a conductance of ca. half that of controls, the conductance of both open sub-states being equally affected. This led the authors to suggest that the intermediate channel may be responsible for the majority of chloride conductance in skeletal muscle which is markedly reduced in some forms of myotonic disease.

Given that development and maintenance of the large chloride conductance in mature muscle requires continued neural input (Conte Camerino et al., 1989) and the consistent finding that the conductance of myoballs is substantially lower than in muscle fibres, it would seem unlikely that myoballs would contain the channel responsible for the majority of muscle chloride conductance, at least not in any substantial numbers. Added to this is the reported inconsistency of whole-cell currents measured in myoballs, some showing deactivating currents whilst others show currents with activating kinetics (Fahlke et al., 1993). Thus whilst various studies have revealed some interesting chloride channels which are characterisable at the single channel level, given the characteristics of the channels detected and the obvious limitations of using cultured muscle tissue, the contribution of these channels to the large chloride flux in mature muscle cannot be significant.

Single channel recordings have also been made from reconstituted mature skeletal muscle membrane preparations. Using indanyloxyacetic acid (IAA) affinity

chromatography on fractionated membrane preparations of rabbit skeletal muscle, Weber-Schürholz et al. (1993) isolated 2 chloride-selective channels which appeared to be localised to the sarcolemma. One of these channels was IAA insensitive and showed a unitary conductance of ca. 200pS with kinetics which were described as "slow", although little detail was given. The second channel exhibited bursting kinetics described as "fast", showed at least 2 open sub-states of 100 and 280pS and was IAA sensitive. Eluates taken after stringent washing of IAA affinity columns were enriched for this second channel. On the basis of polyacrylamide gel electrophoresis of wash and eluate fractions, the authors suggest that the fast channel probably corresponds to a protein of 110 - 120kDa molecular mass. The lack of detailed kinetic analysis and the conditions used make it difficult to assess the authors' claim that the fast channel exhibits characteristics consistent with whole-cell chloride conductance.

In summary, whilst single channel studies of skeletal muscle preparations had demonstrated chloride-selective channels, none of these channels convincingly accounted for the general characteristics of the chloride conductance measured in whole skeletal muscle fibres.

I.2 *Torpedo* electroplaque

Much of our current understanding of skeletal muscle chloride channels has arisen from studies of the ionic conduction pathways of the electroplaque, a muscle derived tissue, of electric fishes. These organs are composed of what are essentially modified and aligned muscle cells. Whilst there are some differences in the details of the mode of operation of these organs in different species (Bennett, 1961), the general principle is the same. The electrocytes making up the organ are polar, having an innervated and

non-innervated face. Differential control of the permeability of the opposite poles of each cell allows the establishment of large potentials across them and current flows along the cellular axis as a result (Bennett, 1961). Within the organ the cells are arranged in an ordered fashion enabling them to act like batteries in series and parallel which, when discharged in unison, produce the large currents used by these fish to stun prey and protect themselves from predators. Electroplaques were originally of interest with regard to the high density of nicotinic acetylcholine receptors found at the innervated face of the electrocyte. During investigation of these channels, electrocytes were also found to contain chloride channels at high density (White and Miller, 1979) which appeared to be localised to the non-innervated membrane (Goldberg and Miller, 1991).

Early studies of these channels, employing membrane vesicles isolated from *Torpedo californica* incorporated into artificial lipid bilayers, demonstrated their voltage dependent behaviour and sensitivity to block by 4,4'-diisothiocyanostilbene-2,2'-disulphonic acid (DIDS) and 4-acetamido-4'-isothiocyanostilbene-2,2'-disulphonic acid (SITS) (White and Miller, 1979). Block by these stilbenes was later shown to be effective from only one side of the bilayer (Miller,C and White, 1980). In the same report, the selectivity of the channel was determined to be $Cl^- > Br^- > SO_4^- > NO_3^- > F^- > CH_3COO^-$ and the relative open probability curve was shown to shift to more negative potentials with decreasing pH. The effect of pH has been investigated further showing that decreased pH increases the channel's open probability (Hanke and Miller, 1983). The pKa of the pH sensitive residue involved apparently changes depending on the state of the channel. In the open state the apparent pKa was approximately 6 whilst in the closed state it was closer to 9.

With the application of higher resolution recording techniques, the channel has been shown to have two equally spaced (≈ 9pS) conductance levels (Miller,C, 1982; Hanke and Miller, 1983). It exhibits unusual gating behaviour with long closed periods interspersed with bursts of activity in which it gates rapidly between the fully closed state and the two sub-conductance levels of 9 and 18pS (Miller,C, 1982). A model proposed to explain this behaviour suggests a double barrelled structure, each channel unit being made up of two independently gating protochannels each of around 9pS conductance. Transitions between the closed state and two sub-conductance levels during periods of activity are controlled by a fast gate operating on each protochannel on a millisecond time scale, whilst a slow gate operating on both protochannels, on a time scale of seconds, closes both protochannels during extended periods of inactivity (Miller,C, 1982; Hanke and Miller, 1983). The apparent gating charge involved in single protochannel openings was reported to be around 1. Further evidence for this model has been gained by the demonstration that the application of DIDS initially blocks only the 18pS sub-conductance level leaving the channel gating between the closed state and 9pS substate. After prolonged exposure to DIDS the remaining conductance also finally becomes blocked (Miller,C and White, 1984).

A complimentary DNA encoding the equivalent channel from *T. marmorata* was isolated using a hybrid-depletion approach and expression screening in *Xenopus* oocytes (Jentsch et al., 1990). The open reading frame included in this cDNA encoded an 805 amino acid protein with a predicted molecular mass of ca. 89kDa. Hydropathy analysis revealed 13 hydrophobic domains, the authors suggesting 12 of these were likely to span the membrane (Figure 1). Whole-cell currents measured from oocytes expressing this protein, designated ClC-0, were in keeping with the previously published characteristics of the channel isolated from *T. californica*. More

detailed single channel analysis left virtually no doubt that ClC-0 was the same channel as described from *T. californica* as it exhibited the same selectivity series, unitary conductance and gating behaviour (Bauer et al., 1991).

I.3 ClC-1

The *clc*-0 cDNA was used as a probe to isolate an homologous sequence from a rat skeletal muscle library (Steinmeyer et al., 1991b). The isolated rat cDNA, designated *clc*-1, encoded a 994 amino acid protein (M_r ca. 110kDa) which was 55% identical to ClC-0 and showed a similar predicted topology. Expression in *Xenopus* oocytes showed that the protein acted as a chloride-selective channel with biophysical characteristics consistent with the macroscopic chloride conductance measured in whole muscle preparations. Further, Northern analysis showed it to be expressed almost exclusively in skeletal muscle and its level of expression to be developmentally regulated in neonatal rats. The time course of increasing mRNA levels during development coinciding with increasing chloride permeability in skeletal muscle (Steinmeyer et al., 1991b). These findings led Steinmeyer et al. to suggest that ClC-1 was the major chloride permeation pathway in skeletal muscle.

Further evidence supporting this contention was provided by the finding that in ADR ("Arrested Development of Righting Response") myotonic mice the equivalent gene was interrupted by a large retroposon resulting in destruction of its coding potential (Steinmeyer et al., 1991a). Electrophysiological investigation of muscle fibres in these mice had previously revealed typical myotonic behaviour (Mehrke et al., 1988). Later, the human *clc*-1 cDNA was cloned, localised to chromosome 7 and linked to the T cell receptor β (*TCR*β) locus (Koch et al., 1992). Tight linkage of the *clc*-1 and the *TCR*β locus in German families suffering from RGM and MC implied the

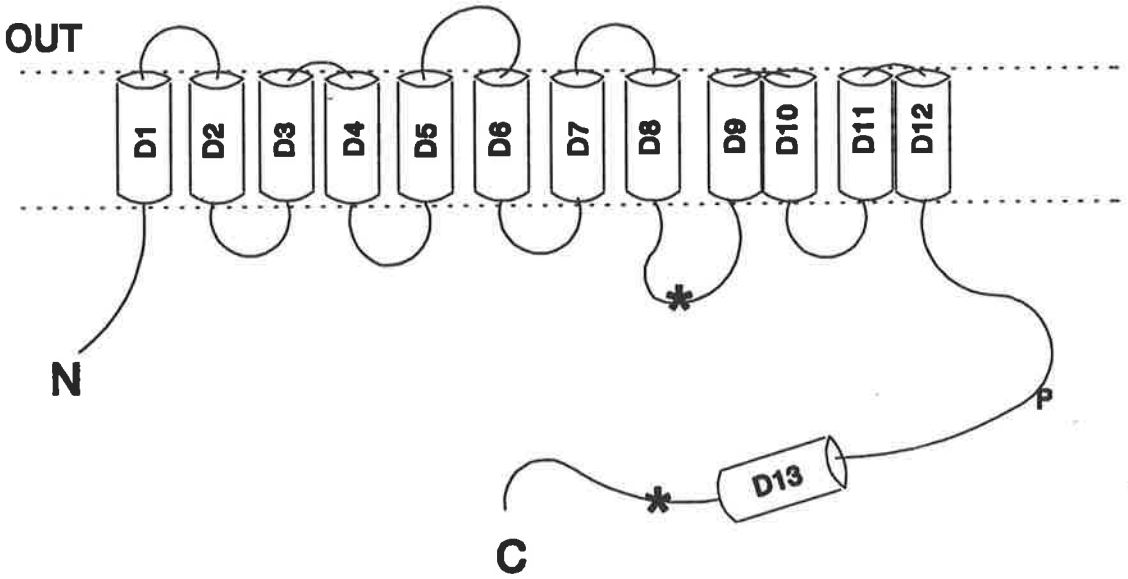

Figure 1: Proposed structure of ClC-0 according to Jentsch et al. (1990). * = putative N-linked glycosylation sites. **P** = consensus sequence for cAMP dependent phosphorylation.

involvement of ClC-1 in these forms of myotonia, both of which are characterised by reduced muscle chloride permeability. In the same report, a point mutation was demonstrated in two families suffering from RGM, adding weight to the case that ClC-1 was the major chloride channel of skeletal muscle.

This introduction summarises the state of knowledge at the commencement of this study. Reviews of more recent developments in the areas of the biophysical and molecular characteristics of ClC-1 are presented in the introductions to Sections IV and VI repectively.

I.4 Project Aims

Late in 1992 Prof. T J Jentsch and Dr. K Steinmeyer of the Centre for Molecular Neurobiology in Hamburg generously provided us with the rat ClC-1 cDNA which was used in this work. Against the background given above, the work presented in this thesis was commenced with the following aims:

1. To express ClC-1 at high levels in a heterologous system with the eventual aim of protein purification and reconstitution into artificial bilayers.
2. To produce a specific anti-ClC-1 antibody for use in immuno-localisation and protein purification.
3. To examine the biophysical characteristics of ClC-1 in the chosen expression system.
4. To investigate the pharmacological characteristics of ClC-1, in particular its response to various aromatic carboxylates.
5. To apply site-directed mutagenesis for the purpose of structure vs function studies, particularly searching for mutations affecting pharmacological responses.

II
Protein Expression

II.1 Introduction

II.1.1 Baculovirus expression vectors

Baculoviruses are a very diverse group which are pathogenic only for invertebrates, most members of the family being pathogens of insects. These organisms have been the subject of a great deal of research over the last two decades (for an overview of their general and molecular biology see Appendix a). Their use as expression vectors, however, has only become widespread over the last 5 or so years with the most commonly used virus being *Autographa californica* Multiply embedded Nuclear Polyhedrosis Virus (*Ac*MNPV). Their application to the area of heterologous protein expression stems from research into the nature of two of their so called very late, or δ, genes. Investigation of these genes, *p10* and *polh* (polyhedrin), clearly demonstrated the non-essential nature of their protein products for *in vitro* propagated virus. Experiments where foreign sequences were inserted in place of the natural coding sequence illustrated the suitability of the δ gene promoters for expression of foreign proteins in cultured insect cells (Smith,GE et al., 1983; Pennock et al., 1984; Possee and Howard, 1987; Rankin et al., 1988; Ooi et al., 1989; Weyer and Possee, 1989; Williams et al., 1989). Whilst yields vary with different proteins expressed using this system, they are generally much higher than those achieved with other heterologous expression systems and can approach the levels of those found with the natural viral proteins ie. 50% (w/w) of total cell protein (equivalent to $1g/10^9$ cells).

The relatively large size (ca. 130kbp) of the covalently closed circular viral genome is not conducive to direct manipulation, necessitating the use of an indirect method for

introduction of foreign sequences. The method most commonly used employs a bacterial plasmid, known as a transfer vector, which contains viral sequences normally found flanking the polyhedrin or p10 coding region and including the relevant promoter elements. Foreign DNA is inserted between these sequences in the position and orientation normally occupied by the viral δ gene. Cultured insect cells are then co-transformed with the recombinant transfer vector and viral DNA. Within the cell the foreign DNA is transferred to the viral genome via homologous recombination facilitated by the viral sequences flanking the inserted open reading frame (Smith,GE et al., 1983). Numerous different transfer vectors have been developed over the last 5 - 10 years (for reviews see Luckow and Summers, 1988; Jarvis, 1991; King and Possee, 1992) including vectors with up to 4 promoters (Belyaev and Roy, 1993) and others with specialised features, eg. the inclusion of a signal sequence for secretion of normally cytoplasmic proteins (Mroczkowski et al., 1994) or the inclusion of an M13 bacteriophage replicon allowing production of single stranded DNA (Livingstone and Jones, 1989).

Variations of the original system have also been reported. Patel et al. (1992) constructed an *Ac*MNPV genome containing yeast sequences which enable it to replicate in *S. cerevisae*. Insertion of foreign coding sequences is still achieved by the use of a transfer vector but the recombination occurs in yeast. Recombinant DNA is then purified and used to transfect insect cells wherein it replicates and produces recombinant baculovirus progeny. Another approach was reported by Luckow et al., (1993). In this work a mini-F replicon was introduced into an *Ac*MNPV genome allowing it to be maintained in *E. coli.* The target sequence for the bacterial transposon *att*Tn*7* was also inserted. This allows the transfer of foreign genes carried by an expression cassette, which includes the left and right ends of Tn*7*, via a

transposition event when the Tn*7* transposition functions are provided in *trans* by a helper plasmid. As with the yeast approach, recombinant DNA is isolated from the intermediate host and transformed into cultured insect cells wherein it behaves as a baculovirus.

Originally, wild type virus was employed and recombinants were selected on the basis of a polyhedrin negative phenotype. More recently, virus vector combinations which provide a higher relative yield of recombinants and easier detection thereof have become available. The system used in this work, known as the BacPAK system (*Clonetech*), utilises a virus, Bac6, which contains the bacterial *lac*Z gene in place of *polh* (Kitts and Possee, 1993). For production of recombinants the viral DNA used is first restricted with *Bsu*36I. This results in linearised viral DNA which is missing a section of sequence either side of the gene insertion site. The use of linear viral DNA has been shown to increase the efficiency of recombination compared to the closed circular form (Kitts et al., 1990). Further, the deleted sequence downstream of the gene insertion site includes part of a gene essential for viral replication (Kitts and Possee, 1993). The upstream deleted sequence interrupts an apparently non-essential gene of unknown function known as ORF603 (Gearing and Possee, 1990). The missing viral sequences are included in the transfer vector either side of the foreign DNA insertion site. Thus when both restricted Bac6 and transfer vector DNA are introduced into the same cell, recombination results in the rescue of replication deficient virus. Using this approach more than 80% of recovered viruses are likely to be recombinants (*Clontech* sales literature).

II.1.2 Sf insect cell lines

The original cell line, IPLB-Sf-21, was derived from pupal ovarian tissue of the "fall army worm" (*Spodoptera frugiperda*) at the USDA Insect Pathology Laboratory at

Bethesda (IPLB), Maryland (Vaughn et al., 1977). This line was adapted in England during the early 1970s to TC-100 medium by H. Stockdale to produce Sf-21AE (**A**dapted in **E**ngland). Later (1983) a clonal line was derived from Sf-21AE by G Smith and C Cherry and named Sf9 (American Type Culture Collection: Accession Number CRL-1711). These two derivatives of the original IPLB line are the most commonly used with the *Ac*MNPV expression vectors.

All three lines show very similar growth characteristics (for reviews see Summers and Smith, 1987; Cameron et al., 1989; King and Possee, 1992; O'Reilly et al., 1994) which are quite different from cell lines of mammalian origin. The cells have an optimal growth temperature of 28°C, do not require a CO_2 enriched atmosphere and have no apparent minimal plating density. They are also neither anchorage dependent nor contact inhibited allowing cells to be cultured as monolayers or in suspension, the latter allowing growth to high cell densities. When grown as monolayers the cells do not adhere strongly to surfaces and can be resuspended, without the use of proteases such as trypsin, by simply squirting medium over the monolayer. Under optimal conditions Sf cells have a doubling time of around 20 hours and appear able to be passaged continuously. The cells are generally spherical in shape ranging in size from 22 - 28 μm in diameter with occasional larger cells of approximately 50μm. Sf9 populations in our laboratory tend to have a smaller average size than IPLB-Sf-21 populations but the two are otherwise morphologically identical. The two lines do show some slight differences in other characteristics. For example, IPLB-Sf-21 cells have been reported to give larger, better defined plaques than Sf9s whilst Sf9s are reported to be electrophysiologically quieter (King and Possee, 1992). In our laboratory, the former appears to be the case whilst the latter has not been definitively

tested. There have also been unpublished reports of differences in levels of expression of particular proteins between the two lines (King and Possee, 1992).

Insect cells are capable of performing many of the post-translational processing events demonstrated in mammalian cells (reviewed in Miller,LK, 1988; King and Possee, 1992; O'Reilly et al., 1994). Processing events demonstrated in these cells include glycosylation, phosphorylation, acylation, amidation, proteolysis including signal sequence cleavage, and oligomer and complex formation. Glycosylation of proteins expressed in these cells appears to occur at the same sites as in mammalian cells but the side chains are less complex and consist mainly of mannose residues. To date, hundreds of biologically active proteins, including glycoproteins, from various species have been successfully expressed in Sf cells (see Luckow, 1991; O'Reilly et al., 1994; Grisshammer and Tate, 1995 for recent reviews).

II.1.3 Baculovirus expressed channels

A search of the available literature undertaken at the commencement of this work uncovered very few reports of ion channels expressed using the baculovirus/Sf cell system. Exceptions were the cystic fibrosis trans-membrane conductance regulator (Kartner et al., 1991) and the *shaker* potassium channel (Klaiber et al., 1990). Expression of the human multidrug resistance protein had been reported as early as 1990 (Germann et al., 1990) although its ability to function as a chloride channel was not suggested until 1992 (Gill et al., 1992; Valverde et al., 1992). A more recent report by De Greef et al. (1995) has cast doubt on the ability of this protein to act as a chloride-selective channel. During the course of this study reports of the functional expression of other channels and membrane transporters in Sf cells have been published. These include a cardiac Na^+/Ca^{2+} exchanger (Li et al., 1992), a Na^+/glucose co-transporter (Smith,CD et al., 1992), a Na^+-K^+-ATPase (DeTomaso et

al., 1993), two potassium channels (Human K^+ channel, (Kamb et al., 1992) and G-protein-gated inward rectifier, (Krapivinsky et al., 1995)) and the $GABA_A$ activated chloride channel (Birnir et al., 1992). ClC-1 expressed in this work is, to the best of my knowledge, the only mammalian skeletal muscle channel to be functionally expressed in this system.

II.2 Materials and methods

II.2.1 *Clc*-1 cDNA

The complimentary DNA encoding the ClC-1 protein was kindly provided by Prof. Thomas J Jentsch and Dr. Klaus Steinmeyer of the Centre for Molecular Neurobiology, University of Hamburg, Germany (Steinmeyer et al., 1991b).

II.2.2 Bacterial cultivation

All bacterial cultivation was performed using ELB medium (pH 7.5), composed of Bacto tryptone (*Difco*) (10 g/l), Bacto yeast extract (*Difco*) (10 g/l) and NaCl (10 g/l). For solid media, Bacto agar (*Difco*) was added at 1.5% (w/v).

Where appropriate, ampicillin was added to broth and solid media at a final concentration of 50 µg/ml. All cultures were incubated at 37°C in air. Aeration of liquid cultures was achieved by incubation in a rotary shaker/incubator with the shaker set at 250 rpm.

II.2.3 Chemicals and reagents

All chemicals were Analar or Molecular Biology grade and were purchased from established suppliers (*Ajax Chemicals*, *BDH Chemicals*, *Biorad*, *Boehringer Mannheim*, *Merck*, *Sigma*). High gelling temperature molecular biology grade agarose for DNA electrophoresis was purchased from *Biorad*. Low gelling temperature agarose used in plaque assays was from *Sigma*. Polyacrylamide gel electrophoresis

reagents (acrylamide, N,N'-methylene-bis-acrylamide, N,N,N',N'-tetramethylethylene diamine (TEMED), ammonium persulphate) were from *Biorad*. All solutions were prepared using milli-Q (MQ) water (*Millipore*) with an electrical resistance of >18MΩ/cm.

II.2.4 Enzymes

Deoxyribonuclease I (DNAase I) and ribonuclease A (RNAase A) were obtained from *Sigma*. Proteinase K was from *Promega* as were restriction endonucleases, T4 DNA ligase and *E. coli* DNA polymerase I large (Klenow) fragment. *Taq* DNA polymerase was purchased from *Boehringer Mannheim* or *Bresatec*.

II.2.5 Oligodeoxynucleotides

Oligodeoxynucleotides (oligos) were purchased from the Department of Haematology, Institute of Medical and Veterinary Science, Frome Rd. Adelaide, 5000. Synthesis was performed on an *Applied Biosystems* 391 DNA synthesiser. All oligos were supplied on their synthesis columns and were eluted by the author by use of concentrated ammonium hydroxide. After elution, de-protection was achieved by incubating the eluted DNA at 55°C overnight. Oligos of greater than 40nts in length were synthesised with trityls on and were subsequently purified, by the author, on an *Applied Biosystems* oligonucleotide purification column following the method recommended by the manufacturer. Oligo stocks were stored at -20°C in ammonium hydroxide and aliquots were extracted using butanol (Sawadogo and Van Dyke, 1991) as required.

Oligonucleotide primers, their sequences and applications were as follows:

CLCHIS
5'-ATTCTAGATGCATCATCATCATCATCATATC
GAAGGACGGATGGAGCGGTCCCAGTCCCAG-3'
PCR primer for replacement of *clc*-1 5' untranslated sequence with His purification tag.

CLCXBA
5'-ATTCTAGATGGAGCGGTCCCAGTCCCAG-3'
PCR primer for removal of *clc*-1 5' untranslated sequence.

CLCTTH
5'-TCCTTCTCAGCACACGTCCCAGGCGAT-3'
PCR primer homologous to *clc*-1 complimentary strand adjacent to *Tth*111I restriction site used with primers CLCHIS and CLCXBA.

TTHSEQ
5'-GCTAACATAGTCCATGCACCA-3'
Sequencing primer homologous to *clc*-1 complimentary strand down stream of CLCTTH primer binding site used to check integrity of subclones made with CLCXBA/HIS/TTH.

PBPRIM1 (Bac1)
5'-ACCATCTCGCAAATAAATAAG-3'
pBacPAK forward sequencing primer.

PBPRIM2 (Bac2)
5'-ACAACGCACAGAATCTAGCG-3'
pBacPAK reverse sequencing primer.

-21 M13
5'-TGTAAAACGACGGCCAGT-3'
Standard sequencing primer used in Dye labelled primer sequencing reactions.

II.2.6 Bacterial strains and cloning vectors

E. coli strain DH5α was obtained from Dr. RJ Harris, Centre for Advanced Biomedical Studies, University of South Australia, North Terrace Adelaide, 5000.

Plasmids pBacPAK1 and pBacPAK8 were purchased from *Clonetech*.

II.2.7 Bacterial transformation

Bacteria in early log phase growth were made competent and transformed with plasmid DNA using a modified version of the method described by Brown,MGM et al. (1979) as follows. Cells from an overnight culture were diluted 1:20 with fresh, pre-warmed medium and incubated with shaking until early log phase (ca. 90 min). After cooling on ice and pelleting (6000X g/10 min/4°C), the bacteria were resuspended in 10 ml of ice cold 100mM $MgCl_2$. Centrifugation was repeated as above followed by resuspension of the pellet in 2 ml of ice cold 100mM $CaCl_2$. After standing on ice for a minimum of 60 minutes, 200µl aliquots were transferred to pre-cooled microcentrifuge tubes, DNA was added and incubation on ice continued for a further 20 minutes. The bacteria were then heat shocked at 42°C for 2 minutes and returned to ice for 20 minutes. Following this, 1 ml of growth medium was added and the cells were allowed to recover at 37°C for 30 minutes. Transformed bacteria were then plated on selective media and incubated overnight. When transforming cells with freshly ligated DNA (new constructs) a negative and positive control were run in parallel. The negative control consisted of competent cells to which no DNA was added whilst the positive control was an aliquot of competent cells transformed with 100ng of clean plasmid DNA carrying the same selection marker as the new construct.

II.2.8 Plasmid isolation

Large scale plasmid purification was performed by ion exchange chromatography using the Qiagen plasmid purification kit (*Qiagen*) following the method recommended by the manufacturer. Small scale ('mini-prep') plasmid purification was performed using a three step alkali lysis method (Birnboim and Doly, 1979) as described in Sambrook et al. (1989) (*vide* Appendix b).

II.2.9 Analysis and manipulation of DNA

II.2.9.1 DNA quantitation

The concentration of DNA in solutions was determined by measurement of absorption at 260 nm and assuming an ABS_{260} of 1.0 is equal to 50 µg of double stranded DNA/ml (Sambrook et al., 1989) or for oligonucleotides 33 µg of single stranded DNA (Brown,TA, 1991).

II.2.9.2 Restriction endonuclease digestion

Cleavage reactions with restriction enzymes were performed as recommended by the manufacturer. Where possible (single enzyme digests), the optimal buffer supplied with the enzyme was used. In cases where digestion with multiple enzymes with different salt requirements was performed, either a multi-purpose buffer eg multicore (*Promega*) was used or else DNA was incubated with the enzyme with the lowest salt requirement first followed by adjustment of the salt concentration and addition of the next enzyme. Typically 0.5-1.0 µg of DNA was incubated with 2 units of each enzyme at optimal temperature in a final volume of 20 µl for 1-2 hr.

II.2.9.3 Restriction of PCR products

Prior to digestion with endonucleases, PCR products were extracted from their reaction mixture using the magic PCR preps DNA purification system (*Promega*) according to the manufacturer's protocol. In cases where the restriction site was located more than 40 bp from the primer sites, cleavage reactions were carried out as described above. For restriction reactions where the cutting site was close to product ends, enzymes were used at high concentration (10 -20 iu/µg of target) and incubation was carried out overnight.

II.2.9.4 Analytical and preparative separation of restriction fragments

Electrophoresis of digested DNA was carried out at room temperature on horizontal, 0.8% or 2% (w/v) agarose gels (high strength analytical grade (HGT)) containing ethidium bromide (ca. 0.5µg/ml). Typically, gels were run at 100V for 1.5 - 2 hours

in 1X TAE buffer (see appendix b). DNA bands were visualised by trans-illumination with UV light.

For isolation and purification of restriction fragments, the band of interest was excised using a scalpel, sliced into thin pieces and placed in a microcentrifuge tube. The DNA was then recovered using Qiaex resin (*Qiagen*) following the protocols supplied by the manufacturer.

II.2.9.5 Calculation of restriction fragment size

The sizes of restriction enzyme fragments were calculated by comparing their relative mobility with that of *Eco*RI digested *Bacillus subtilis* bacteriophage SPP1 DNA. The calculated sizes of the SPP1 *Eco*RI standard fragments differ from those published (Ratcliff et al., 1979). The sizes used were as described by the supplier (*Bresatec*) having been calculated by comparison of SPP1 fragment mobilities with those of lambda phage DNA fragments of known molecular weight (M_r) using the TRACKTEL system (Forensic Science Technology International, Adelaide S.A.). The revised sizes are (kilobases): 8.5; 7.35; 6.11; 4.84; 3.59; 2.81; 1.95; 1.86; 1.51; 1.39; 1.16; 0.98; 0.72; 0.48; 0.36.

II.2.9.6 DNA sequencing

DNA sequencing was performed by the Microbial Pathogenesis Unit, Department of Microbiology and Immunology, University of Adelaide, South Australia 5005 using the *Applied Biosystems* Model 370A/373A DNA Cycle Sequencing system. Double stranded DNA templates were prepared according to the manufacturers protocols and were amplified by cycling in a *Perkin Elmer Cetus* TC1 DNA Thermal Cycler using the recommended cycling parameters. The *Applied Biosystems* DyeDeoxy Terminator sequencing protocol was used with primers PBPRIM1, PBPRIM2 and TTHSEQ. When sequencing the 5' end of modified *clc*-1 constructs in pBluescript KS+ (*vide*

infra), the standard sequencing primer -21 M13 was used with the Dye Labelled Primer protocol.

Gel and sequence data from the analyser was down loaded to diskette. Verification and correction of raw data was performed by the author on an Apple Macintosh CXII using *Applied Biosystems* 373A software kindly made available by Dr. RJ Harris. Edited sequence data was also analysed using the computer programs DNASIS (*Hitachi LKB*) and MailfastA (EMBL (Pearson,WR and Lipman, 1988)). For comparison of DNA and protein sequences with other published data, GENECOMPAR (*Applied Maths*, Kortrijk Belgium) and PROSIS (*Hitachi LKB*) were used in addition to the aforementioned programs.

II.2.9.7 End filling

End-filling of 5' overhangs created by endonuclease digestion was performed using *E. coli* DNA Polymerase I Large (Klenow) Fragment at a concentration of 1 unit/µg of target DNA. Reactions were carried out in Klenow buffer (see appendix b) at 37°C for 30 minutes in a final volume of 30µl. After incubation., the reaction was stopped by addition of EDTA to a final concentration of 20mM.

II.2.9.8 DNA ligation

Ligation of DNA with compatible overhangs was performed using insert and vector DNA in a molar ratio of 3:1. Reactions were incubated overnight at 4°C in the buffer supplied by the manufacturer and containing 2 weiss units of T4 DNA ligase. For ligation of blunt-ended DNA, the insert to vector ratio was 2:1, 5 weiss units of ligase were used, incubation was performed overnight at room temperature and the reaction was carried out in blunt end ligation buffer (see appendix b).

In all cases two controls were included. The positive control contained SPP1 marker DNA (500ng) in place of insert/vector and was used to check enzyme activity. The

negative control consisted of an aliquot of the ligation mixture which was removed immediately after addition of ligase and heated at 65°C for 10 minutes to stop the reaction. Following incubation of the ligation reaction, a second aliquot was removed and electrophoresed in parallel with the two controls to assess the success of the reaction.

II.2.10 Construction of Transfer Vectors

II.2.10.1 Complete cDNA (pDA1bvr and pDA2bvr)

The original *clc*-1 cDNA was received in pBluescript KS+ having been cloned into this vector via the *Eco*R1 site by the use of linker oligonucleotides (Steinmeyer et al., 1991b). In our laboratory this construct was designated TJJ Clone (Figure 2.1). On receipt, the plasmid was transformed into DH5α and ampicillin resistant colonies isolated. Plasmids isolated from these clones were screened by digestion with *Eco*RV, one being selected at random for amplification and large scale plasmid extraction. At the time of these experiments, our laboratory did not have a transfer vector which contained a multiple cloning site (MCS), pBacPAK1 containing only a single *Bam*H1 cloning site. For this reason it was decided to carry over part of the pBluescript MCS when subcloning the *clc*-1 cDNA to allow later production of a more flexible transfer vector for use in future experiments.

For construction of transfer vectors, TJJ Clone was sequentially digested using *Xba*I, *Cla*I and *Pvu*I resulting in excision of the cDNA and fragmentation of the vector. Enzymes were then removed from the mixture by extraction with an equal volume of 1:1 (v/v) TE (pH 8) (see appendix b) equilibrated phenol: $CHCl_3$ and the DNA precipitated using 1/10X volume of 3M ammonium acetate (pH 5.2), 2X volume of 100% ethanol and overnight incubation at -20°C. After pelleting (15000X g/10 min) and washing with 500µl of 70% ethanol, the precipitated DNA was resuspended in TE

(pH 8). Total digested DNA was then end-filled and the cDNA fragment was separated from unincorporated nucleotides and vector DNA fragments by gel electrophoresis and recovered using Qiaex resin (*Qiagen*). Transfer vector pBacPAK1 was cleaved with *Bam*H1 then cleaned, end-filled and gel purified as for insert DNA. Insert and vector DNAs were ligated using the blunt-end protocol and the resulting DNA mixture was then used to transform competent *E. coli* DH5α. Plasmids isolated from the resultant bacterial clones were first screened for the presence of insert DNA by digestion with *Eco*RV. Two clones apparently containing insert DNA were further analysed by digestion using *Cla*I, *Eco*R1, *Eco*RV, *Hin*dIII, and *Pvu*I. Final confirmation of integrity and orientation of insert DNA in both clones, designated pDA1bvr and pDA2bvr, was achieved by sequence analysis using primers PBPRIM1 and PBPRIM2.

II.2.10.2 modified cDNA (pDA5bvr and pDA6bvr)

Two 5'-modified versions of original construct (TJJ Clone) were produced by recombinant PCR using primers designed to amplify the region of the open reading frame from the start codon to 30bp downstream of the unique *Tth*111I site. In one reaction the 5' primer, CLCXBA, was designed to incorporate an *Xba*I site immediately adjacent to the ATG whilst removing the upstream untranslated region. In a second reaction the upstream primer, CLCHIS, was designed to replace the 5' untranslated DNA with sequence encoding an *Xba*I cleavage site followed by an in frame ATG, 6 consecutive histidine residues and a factor Xa endopeptidase site (Ile-Glu-Gly-Arg). CLCHIS also introduces a unique *Nsi*I restriction site. Both constructs were produced using the same procedure and down stream primer (CLCTTH) as follows.

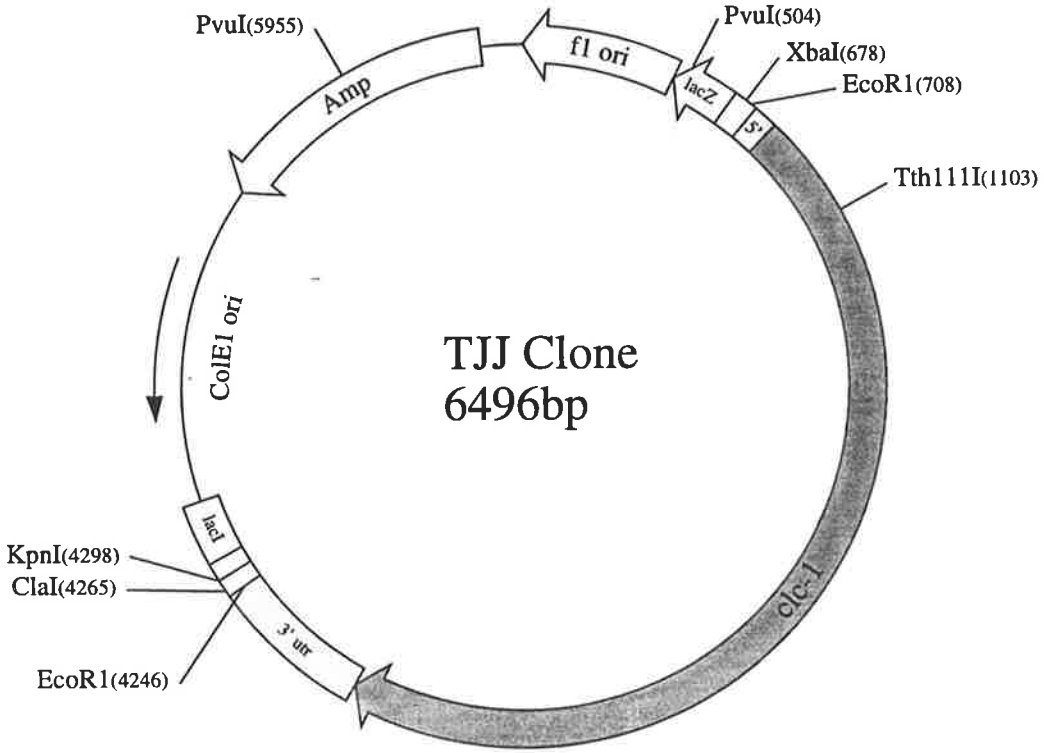

Figure 2.1. Plasmid TJJ Clone.
Clc-1 cDNA cloned into pBluescript KS+ (*Stratagene*) via the *Eco*R1 site, obtained from Prof. TJ Jentsch and Dr. K Steinmeyer (Steinmeyer et al. 1991b).
5' = upstream untranslated sequence. 3' utr = downstream untranslated sequence (actual length as determined by DNA sequencing (see results)). clc-1 = coding region. Relevant restriction sites are marked and numbered according to actual cutting site.

PCR reactions contained 50ng of target DNA (plasmid pDA1bvr), 200ng of each oligonucleotide primer, 3.5mM $MgCl_2$, 2 units of *Taq* DNA polymerase, 10mM (each) dNTPs and *Taq* reaction buffer supplied with the enzyme (see appendix b). Reactions were performed in a final volume of 100 µl overlayed with sterile mineral oil. Cycling was performed in a *Perkin Elmer Cetus* TC1 thermal cycler using the following parameters, "hot start" (94°C/7 min), denaturation (94°C/1 min), annealing (55°C/1 min), extension (72°C/1 min), 30 cycles followed by final extension (72°C/10 min) and cooling to 4°C. A negative control, containing no target DNA, was run in parallel with each set of reactions. Reaction products were separated from unincorporated primers, nucleotides and target DNA using the magic PCR preps DNA purification system (*Promega*).

The purified DNA was then sequentially digested with *Tth*111I and *Xba*I. The success of endonuclease digestion was checked by comparing the relative mobilities of aliquots of DNA after each enzyme treatment with that of undigested DNA on a standard polyacrylamide sequencing gel, kindly run by Ms. J. Williamson (School of Pharmacy and Medical Sciences, University of South Australia, Adelaide 5000). Visualisation of DNA on this gel was achieved by soaking the gel in aqueous ethidium bromide (0.5µg/ml) followed by soaking in MQ water to remove excess stain and examination by UV transillumination. Following digestion, the products were separated from cleaved ends by TAE agarose (2% gel) electrophoresis. The cleaved product band was excised from the gel and extracted using Qiaex resin (*Qiagen*), then ligated into similarly cleaved, purified TJJ Clone. The ligated constructs were transformed into DH5α and plasmids isolated from resultant bacterial clones. Plasmid DNA was then screened using single digestion with *Eco*R1, *Eco*RV and *Nsi*I.

Further analysis was by double enzyme digestion using *XbaI/Eco*RV, *XbaI/Kpn*I and *XbaI/Tth*111I. The integrity of 2 clones of each construct was confirmed by DNA sequencing using primers -21 M13 and TTHSEQ. One of each was chosen for use in production of recombinant transfer vectors. The construct produced using CLCHIS as the upstream primer (His tagged) was designated pDA7cl whilst the other construct (5'-untranslated sequence deleted) was designated pDA8cl.

The entire modified *clc*-1 insert was excised from pDA7cl and pDA8cl using *Xba*I and *Kpn*I, gel purified and ligated into similarly cleaved and purified pBacPAK8. After transformation of DH5α and screening of resultant clones by restriction analysis, using *Eco*RV, *Nsi*I single and *XbaI/Kpn*I, *XbaI/Tth*111I, *ScaI/Bam*H1 double digestion, one of each recombinant transfer vector was chosen for use in production of recombinant virus. The transfer vectors were designated pDA5bvr (His tagged construct) and pDA6bvr (5' untranslated region deleted).

II.2.11 Cell Culture

Methods used for routine passage, virus infection and recombinant virus production were essentially as described by King and Possee (1992).

II.2.11.1 Cell lines

Cell line IPLB-Sf-21 was purchased from *Clontech*. For the sake of simplicity, IPLB-Sf-21 cells will be referred to simply as Sf21 throughout the remainder of this document. Sf9 cells were a generous gift from Dr B Birnir, John Curtin School of Medical Research, Australian National University.

II.2.11.2 Maintenance of Cell Lines.

Both cell lines were maintained in TMN-FH medium consisting of Grace's Anthracea medium (*Gibco*) plus lactalbumin hydrolysate (3.3g/L) (*Difco*), yeastolate (3.3g/L)

(*Difco*) and $NaHCO_3$ (0.35g/L). Fetal bovine serum (FBS, *CSL*) and gentamicin were routinely added at 10% (v/v) and 50μg/ml respectively (TMN-FH/FBS).

Monolayer cultures were routinely passaged twice per week after reaching about 80% confluence. Fresh flasks were seeded at the following densities, $25cm^2$, 0.5 -1.0 X 10^6; $75cm^2$, 1.0 -2.0 X 10^6.

Cells maintained in suspension culture, in μ-carrier flasks (*Belco*), were passaged after reaching a density of 2 -3 X 10^6 cells/ml (ca. once per week). Fresh suspension cultures were seeded at 1 - 2 X 10^5 cells/ml or existing cultures were diluted with an appropriate volume of fresh medium to achieve a density of 2 X 10^5 cells/ml.

All cell cultures were incubated at 28 - 30°C in a bench top heater/refrigerator incubator without added CO_2. Suspension cultures were mixed at 50 - 75 rpm using a *Belco* μ-carrier 4 station magnetic stirrer. Routine passage of uninfected cell lines was performed using aseptic technique in a class II laminar flow cabinet (*Gelman Scientific*).

II.2.12 Recombinant virus production and amplification

II.2.12.1 Cell seeding densities

Cultures to be infected were used at the following densities, 35mm dish, 1.5 X 10^6; $25cm^2$ flask, 2.0 X 10^6; $75cm^2$ flask, 6 X 10^6; spinner flasks, 5.0 X 10^5(cells/ml).

In the case of monolayer cultures, flasks/dishes were seeded at the above densities and allowed to settle for 1 hour at ambient temperature before infection. Spinner cultures were seeded at lower density (1 - 2 X 10^5 cells/ml), and incubated until the required cell density was reached.

The Sf21 cell line was routinely used for amplification of virus stocks and plaque assays. Protein production and biophysical studies (*vide* Section IV) were performed using Sf9 cells.

II.2.12.2 Infection of Cells

After settling, the medium was removed from monolayers and replaced with virus inoculum in a total volume of 100µl for 35mm dishes, 250µl for 25cm^2 flasks and 500 µl for 75cm^2 flasks. The cells were incubated for 1 hour at room temperature to allow virus adsorption, the inoculum being distributed over the monolayer every 15 - 20 minutes by gently rocking the dish/flask. The inoculum was then removed and the appropriate volume of fresh medium added (1.5 ml for 35mm dishes, 4 ml for 25cm^2 flasks and 10 ml for 75cm^2 flasks). Infected cells were then incubated for the desired period, typically 6 - 7 days for amplification of virus stocks, 4 days for plaque assays and 1 - 3 days for protein production.

When amplifying virus stocks, cells were infected at a low multiplicity of infection (moi), typically 0.1 (ie. 0.1 plaque forming units (pfu)/cell, *vide infra*). For protein production and biophysical studies a higher moi was used, typically 50 - 100.

II.2.12.3 Co-transformation

For production of recombinant baculoviruses, Sf21 cells were co-transformed with linearised, replication deficient Bac6 virus (*Clonetech*) and recombinant transfer plasmid DNA using lipofectin (*Gibco BRL*) as follows. Two hundred ng of virus DNA and 1µg of transfer vector were mixed with an equal volume of lipofectin (diluted 2:1 in sterile MQ water) in a sterile polystyrene tube. The DNA/ lipofectin mixture was left at ambient temperature for 15 minutes and then added to a 35mm dish containing 1 X 10^6 cells which had been washed twice with TMN-FH (no FBS) and then covered with 1 ml of same.

After 5 hours incubation at 28°C in a humidified atmosphere, 1 ml of TMN-FH/FBS was added and the cells were incubated until 48 hours post infection (hpi). At this

point, the culture medium containing a mixture of putative recombinant viruses was collected and used in plaque assays for isolation of virus clones.

II.2.12.4 Plaque assays

Plaque assays were used for determination of titres of virus stocks and isolation of recombinant virus clones as follows.

Thirty five mm dishes were seeded with Sf21 cells at the abovementioned density and allowed to settle. The medium was removed and the cells were infected with 100µl of virus dilution (10^0 - 10^{-4} (single set) for co-transformation supernatants or 10^{-5} - 10^{-7} (in triplicate) for virus stocks) in medium. After adsorption at ambient temperature for 1 hour, the inoculum was removed and the cells overlayed with 2 ml of 2% low gelling temperature agarose/TMN-FH/FBS (50/50 v/v) which had been cooled to 35°C. The agarose/medium overlay was allowed to set at room temperature and was then overlayed with 1 ml of liquid medium.

Following 4 days incubation (28°C, humidified atmosphere), monolayers were stained by the addition to the medium of 1 ml of 0.025% (w/v) neutral red in PBS. After staining for 2 hours at 28°C in the dark, the neutral red/liquid medium was removed and the plaques allowed to clear by standing the plates overnight in an inverted position at room temperature in the dark.

For determination of viral titres, plaques were counted on dilutions which gave approximately 30 plaques per plate. Plaques were also examined under an inverted microscope (400X total magnification) to ensure they contained unstained cells and were not simply holes in the monolayer. Viral titres were calculated by using the plaque counts averaged from three plates inoculated with the same dilution of stock and multiplying by the appropriate figure to yield a titre expressed as plaque forming units per ml (pfu/ml).

II.2.12.5 Isolation of recombinant virus clones

Individual, isolated plaques were picked from plaque assays using sterile pasteur pipettes. The agarose plugs collected in this manner were placed in microcentrifuge tubes containing 0.5 ml of medium, vortexed briefly and then eluted overnight at 4°C. Virus clones obtained from co-transformation using transfer vectors pDA1bvr and pDA2bvr were designated BVDA1.x and BVDA2.x respectively. The clones produced using vectors pDA5bvr and pDA6bvr were designated BVDA5.x and BVDA6.x respectively.

II.2.12.6 Virus amplification

For amplification of plaque derived virus, 250 µl of plaque eluate was used to infect $25cm^2$ flasks of Sf21 cells and the infection allowed to proceed until the cells appeared well infected (typically 6 - 7 days). Following incubation, the culture medium and cells were collected and centrifuged (2500X g/10 min). Pelleted cells were retained for use in confirmation of recombinant clones by PCR (*vide infra*). One ml of the resultant 4 ml virus-containing supernatant was stored at 4°C as seed stock whilst the remaining 3 ml was stored at -80°C in 500µl aliquots. Seed stocks were further amplified to produce intermediate stocks by using 250µl, in a total volume of 500µl, to infect Sf21 monolayers in $75cm^2$ flasks in the same manner. As for seed stocks, 1 ml of intermediate stock was stored at 4°C whilst the remainder (9 ml) was stored in aliquots at -80°C.

Large scale, high titre working stocks were produced by infection of 50 ml suspension cultures with intermediate stock at a moi of 0.2. Cultures were harvested after 6 - 7 days incubation and the cells removed by centrifugation (2500X g/10 min) in a bench-top centrifuge. Working virus stocks were stored at 4°C. Titres of intermediate and working stocks were determined using standard plaque assay (*vide supra*).

II.2.12.7 Confirmation of Recombinant Virus Clones by PCR

Cells collected from amplified plaque cultures (*vide supra*) were resuspended in 1 ml of PBS and transferred to microcentrifuge tubes. The cells were then repelleted (3500X g/2 min), resuspended in 500µl PBS, pelleted again (3500X g/2 min) and finally suspended in 250µl of 1X TE (pH 8). Whole-cell DNA (cellular and virus) was then extracted as described by King and Possee (1992) (see appendix b).

The presence of insert DNA was confirmed by PCR using primers PBPRIM1 and PBPRIM2 and by restriction analysis of the resulting products. PCR reactions were performed in a final volume of 100µl overlayed with sterile mineral oil and contained, 10µl (ca. 1µg) of infected whole-cell DNA, 200ng of each primer, 3.5mM $MgCl_2$, 10mM (each) dNTPs, 2 units of *Taq* DNA polymerase and 1X *Taq* reaction buffer. Thermal cycling was performed in a *Perkin Elmer Cetus* TC1 DNA thermal cycler using the following parameters, "hot start" 94°C/10 min, denaturation 94°C/1 min, annealing 45°C/1 min, extension 72°C/2 min and increasing by 15s each cycle, 30 cycles followed by final extension (72°C/10 min) and cooling to 4°C. Each set of reactions was performed in parallel with negative and positive controls. The positive control contained 2ng of pDA1bvr plasmid DNA in place of virus infected cell DNA. The negative controls consisted of two reactions. One contained no target DNA (reagent control) whilst the other contained whole-cell DNA from mock infected Sf21 cells incubated in parallel with virus infected cultures.

The identity of inserted DNA was assessed by endonuclease restriction of PCR products using *Eco*RV and *Tth*111I. Due to the high yield of products (see results), only small volumes (2µl) of the reaction mix were required for enzyme digests.

Amplified DNA was therefore added directly to digestion reactions without any prior purification.

II.2.13 Protein Expression

II.2.13.1 Polyacrylamide gel electrophoresis

Polyacrylamide gel electrophoresis (PAGE) was performed on 7cm X 8cm X 0.75cm discontinuous polyacrylamide gels using the method of Laemmli (1970) (4% stacking gel, 9% resolving gel) in Tris/Glycine/SDS running buffer (see appendix b for buffer and gel formulations). Gels were typically electrophoresed at a constant 250V for 30 minutes at room temperature using a mini-PROTEAN II electrophoresis apparatus (*Biorad*). Fixation and staining was achieved by soaking gels for 30 minutes, with gentle rocking, in an aqueous solution containing 0.25% (w/v) coomassie brilliant blue R250, 25% (v/v) ethanol and 10% (v/v) glacial acetic acid. Excess stain was removed with the same solution, minus coomassie blue, using four changes of solution over 24 - 48 hours. For sizing of proteins, *Biorad* broad range protein M_r markers were run in parallel with samples.

II.2.13.2 Expression screening

Sf9 cells in 35mm dishes were infected with intermediate virus stock at a moi of 60 - 100 and incubated for 48 hrs. The cells were suspended in their culture medium, 1.5 ml was transferred to microcentrifuge tubes and a small volume was placed in a haemocytometer (Improved Neubauer) for determination of cell concentration. After centrifugation (3500X g/2 min), the cells were resuspended in 500µl PBS, repelleted and finally resuspended in PBS to a concentration of 10^4 cells/µl. Cells were then disrupted by sonication (10 min) in a bath type sonicator and an equal volume of PAGE sample buffer (see appendix b) was added. Samples (15µl, ca. 8µg total

protein) were heated at 100°C for 10 minutes and briefly centrifuged (15000X g/30s) before loading on PAGs for electrophoresis.

Following screening for protein expression one clone of each recombinant virus was selected for use in further experiments.

II.2.13.3 Determination of expression time course

The time course of ClC-1 expression was assessed by PAGE as described above. Sf9 cells were infected in 35mm dishes and collected at 24, 30, 36, 42, 48, 54, 60, 66 and 72 hpi.

II.3 Results

II.3.1 Construction of Transfer Vectors

II.3.1.1 Complete cDNA (pDA1bvr and pDA2bvr)

II.3.1.1.1 Subcloning

Transformation of TJJ Clone into DH5α resulted in numerous colonies on selective plates. All of the colonies screened (12 in total) proved to be carrying the plasmid. A 40 ml overnight culture of one colony, selected at random, yielded 90µg of clean plasmid DNA. Single enzyme digestion with *Eco*R1, *Kpn*I and *Pvu*I produced fragments similar in size to those predicted from the published sequence (Steinmeyer et al., 1991b). The size of the insert fragment however did appear to be larger than predicted by around 300bp.

Five µg of pBacPAK1 was completely digested by 10iu of *Bam*H1 to produce the expected sized (ca 5.5kbp) DNA fragment. One µg of cut plasmid was used in the endfilling reaction and after gel purification 300ng of clean blunt ended DNA remained. Similarly, 5µg of TJJ Clone DNA was completely digested by 10iu each of *Xba*I, *Cla*I and *Pvu*I. Again the *Xba*I-*Cla*I fragment appeared to be approximately 300bp larger than expected whilst the other 3 fragments were of the expected size.

After endfilling 2µg of total digested DNA and gel purification 300ng of the insert fragment was recovered.

After incubation of the ligation reaction containing the two DNA species, electrophoresis of an aliquot (in parallel with controls) confirmed that ligation had occurred. Transformation of DH5α with 10µl of the remaining ligation mix resulted in more than 100 isolated colonies on ampicillin-containing plates. Restriction analysis, using *Eco*RV, of plasmids isolated from randomly selected clones gave fragments of sizes indicative of religated vector DNA in 22/24 cases. The remaining two clones produced fragments of the sizes expected for pBacPAK containing the desired insert, one in the forward and one in the reverse orientation. Extraction of plasmid DNA from 40 ml cultures of these two clones yielded about 80µg of each. Screening of this DNA by single digestion with enzymes *Eco*RV, *Cla*I, *Pvu*I, *Hin*dIII and *Eco*R1 gave the expected sized fragments with the exception that the fragments which contained the 3' end of the *clc*-1 cDNA had an apparent size approximately 300bp larger than predicted. The construct containing *clc*-1 in the forward orientation was designated pDA1bvr whilst the other construct was designated pDA2bvr.

II.3.1.1.2 DNA sequencing

For pDA1bvr, around 400bp of readable sequence was obtained with each primer. Data from PBPRIM1 included the ligation junction, 5' untranslated sequence and around 300 bp of the *clc*-1 protein coding region (Figure 2.2). PBPRIM2 data was readable from 35 bp beyond the ligation site and extended into the 3' untranslated region of *clc*-1 (Figure 2.2). For pDA2bvr, PBPRIM1 gave 429 bp of readable sequence whilst PBPRIM2 yielded 519 bp. In both cases the ligation junctions were readable along with significant amounts of *clc*-1 cDNA (Figure 2.3). The results

Primer PBPRIM1

*Bam*H1 *Spe*I *Bam*H1 *Sma*I *Pst*I *Eco*R1

1 GGATCCTAGA ACTAGTGGAT CCCCCGGGCT GCAGGAATTC CGGCAAAAGC AGAGGCTTAA
61 GGAGGTACTA GGGGGAGACT AGGAGCAAGC AGGCCAAGGC CTGGCTGGGG CTTGGGGGGA
121 GGACAC**ATGG AGCGGTCCCA GTCCCAGCAA CATGGAGGTG AACAAAGCTG GTGGGGCACT**
181 **GCCCCCCAGT ACCAGTACAT GCCCTTCGAA CATTGTACCA GCTATGGACT GCCCTCAGAG**
241 **AATGGGGGCC TTCAGCACCG GCCCCGAAAG GACCTGGGTC CCAGGCACAA TGCCCACCCA**
301 **ACACAGATAT ATGGCCATCA CAAAGAACAA TATTCATATC AGGCACAGGA CAGGGGAATA**
361 **CCCAAGAAGA CGGACTCCAG TTCTACTGTG GACAGCTTGG ATGAGGACCA CTATTCTAAA**
421 **TGTCAAGACT GTGTCCATCG CCTGGG**

Primer PBPRIM2

1 GTAGTCAATC CACATGGCAA TATTGTGGTC CCACATGCCC TTCCAATGTG ACACTTGCGG
61 ATTCTTTCAA TCTGGGCCTC CACTCACCTA CTCCATATGG AAACTGAAAT ATAGACAGGC
121 ATGCCGGGCC AGGATGGTGA CAGAATGACA CTGGGAACTG TGGGGCATTA GAGTGACAGG
181 GACTGAACCT GCACAGCAGG AACACAGAAG TCCTTTGAGC ATGGGGGCTT GAACCCTCCC
241 TGGAAATGGG GAGGGGGGTC TTGATGGACC CAAATTCTTC CCTGCCAAGA TCAAGTTCTC
301 CTTAAGATCC ATCAACCATC ACCTTTCATA GTGGGGTAGG AACAACGATG AAATGGAGGT
361 CTCCCCAACT TCAGGGCACC CATTTT

Figure 2.2

Sequence data from pDA1bvr

Primers used are indicated above sequence. Restriction sites are labelled and boxed. Nucleotides derived from pBacPAK1 are indicated by dotted underlining. 5' (PBPRIM1 sequence) and 3' (PBPRIM2 sequence) untranslated regions are underlined, unpublished 3' sequence double underlined. *Clc*-1 coding region marked in bold.

Primer PBPRIM1

*Bam*H1 *Hin*dIII *Eco*RV *Eco*R1

1 AAATACGGAT CCGATAAGCT TGATATCGAA TTCCGGTTTA GGGTAGTCAA TCCACATGGC
61 AATATTGTGG TCCCACATGC CCTTCCAATG TGACACTTGC GGATTCTTTC AATCTGGGCC
121 TCCACTCACC TACTCCATAT GGAAACTGAA ATATAGACAG GCATGCCGGG CCAGGATGGT
181 GACAGAATGA CACTGGGAAC TGTGGGGCAT TAGAGTGACA GGGACTGAAC CTGCACAGCA
241 GGAACACAGA AGTCCTTTGA GCATGGGGGC TTGAACCCTC CCTGGAAATG GGGAGGGGGG
301 TCTTGATGGA CCCAAATTCT TCCCTGCCCA AGATCAAGTT CTCCTTAAGA TCCATCAACC
361 ATCACCTTTC ATAGTGGGGT AGGAACAACG ATGAAATGGA GGTCTCCCCA ACTTCAGGGC
421 ACCCATTTT

Primer PBPRIM2

*Bam*H1 *Spe*I *Bam*H1 *Sma*I *Pst*I *Eco*R1

1 GGATCCTAGA ACTAGTGGAT CCCCCGGGCT GCAGGAATTC CGGCAAAAGC AGAGGCTTAA
61 GGAGGTACTA GGGGGAGACT AGGAGCAAGC AGGCCAAGGC CTGGCTGGGG CTTGGGGGGA
121 GGACACATGG AGCGGTCCCA GTCCCAGCAA CATGGAGGTG AACAAAGCTG GTGGGGCACT
181 GCCCCCCAGT ACCAGTACAT GCCCTTCGAA CATTGTACCA GCTATGGACT GCCCTCAGAG
241 AATGGGGGCC TTCAGCACCG GCCCCGAAAG GACCTGGGTC CCAGGCACAA TGCCCACCCA
301 ACACAGATAT ATGGCCATCA CAAAGAACAA TATTCATATC AGGCACAGGA CAGGGGAATA
361 CCCAAGAAGA CGGACTCCAG TTCTACTGTG GACAGCTTGG ATGAGGACCA CTATTCTAAA
421 TGTCAAGACT GTGTCCATCG CCTGGGACGT GTGCTGAGAA GGAAGCTGGG GGAAGACTGG
481 ATCTTTCTTG TGCTCCTGGG CCTACTGATG GCTCTTGTCA

Figure 2.3

Sequence data from pDA2bvr

Primers used are indicated above sequence. Restriction sites are labelled and boxed. Nucleotides derived from pBacPAK1 are indicated by dotted underlining. 5' (PBPRIM2 sequence) and 3' (PBPRIM1 sequence) untranslated regions are underlined, unpublished 3' sequence double underlined. *Clc*-1 coding region marked in bold.

confirmed the orientation of the insert in both constructs and the identity of the inserted sequence. The DNA sequence of the 5' end of the *clc*-1 insert was exactly as expected whilst the 3' end included 326 bp of unpublished sequence accounting for the larger than expected size of some restriction fragments. This sequence was not published in the original paper (Steinmeyer et al., 1991b) due to its poor quality and since it was outside the protein coding region (TJ Jentsch, personal communication). A comparison of the data for the unpublished 3' sequence obtained by K Steinmeyer and the author is presented in Figure 2.4. Plasmid maps showing relevant restriction sites are presented in Figures 2.1 (TJJ Clone), 2.5 (pDA1bvr) and 2.6 (pDA2bvr).

II.3.1.2 modified cDNA (pDA5bvr and pDA6bvr)

II.3.1.2.1 Recombinant PCR

For the production of both 5'-modified constructs, 10 PCR reactions were performed using each pair of primers and the reaction products of each set were pooled. Extraction using the magic PCR preps DNA purification system (*Promega*) yielded in the vicinity of 2µg of each. One µg of each product was sequentially digested with *Xba*I and *Tth*111I. Aliqouts of digestion reactions collected before and after treatment with each enzyme and separated on a 12% polyacrylamide DNA sequencing gel clearly demonstrated successful digestion of the products as evidenced by their relative mobilities. After agarose gel purification of the digested fragments approximately 800ng of each was recovered.

Two µg of TJJ Clone was completely digested with *Xba*I and *Tth*111I and after gel purification around 1.5µg of clean 6071bp fragment was recovered. Ligation reactions containing 0.25pmol of this DNA and 0.75pmol of each digested PCR product appeared to be successful as evidenced by the relative mobility of an aliquot electrophoresed in parallel with controls. Transformation of competent DH5α with

1/3 of each of these ligation mixes yielded 42 and 54 ampicillin resistant colonies for the histidine tagged and 5'-deleted constructs respectively. Three of each of these clones were selected at random and their plasmid content examined. Single digestion with *Eco*R1 and *Nsi*I as well as double digestion using *Xba*I in combination with *Eco*RV, *Tth*111I and *Kpn*I produced fragments of the predicted sizes in all 6 clones. Two clones of each construct were selected at random for confirmation by DNA sequencing.

II.3.1.2.2 DNA sequencing

Sequencing reactions of both the 5'-deleted clones and one of the histidine tagged clones gave clean readable sequence of approximately 400bp in length. The second histidine tagged clone gave poor quality sequence which was deemed to be unreliable. The DNA sequence of both 5'-deleted clones confirmed the integrity of the inserts exactly matching that predicted. One clone was selected for production of a recombinant transfer vector and was designated pDA8cl (for plasmid map see Figure 2.7). The readable histidine tagged clone was also exactly as predicted with the exception of a single bp substitution at nt 138. This point mutation affects the third nucleotide of a codon encoding a phenylalanine residue. Since this C to T transition does not alter the amino acid sequence it was deemed insignificant. The construct was designated pDA7cl (for plasmid map see Figure 2.8). Edited and corrected sequence data obtained with pDA7cl and pDA8cl and showing relevant features are presented in Figure 2.9.

II.3.1.2.3 Recombinant transfer vectors

Two µg of pBacPAK8 DNA was successfully cut with *Xba*I and *Kpn*I. Gel purification yielded about 1.5µg of digested vector. Similarly, 2µg each of pDA7cl

3116 GTGAT GGTTGATGGA TCTTAAGGAG AACTTGATCT TGGGCAGGGA AGAATTTGGG TCCATCAAGA
GG_ TGATG_ A TCCATC_AGA
3181 CCCCCCTCCC CATTTCCAGG GAGGGTTCAA GCCCCCATGC TCAAAGGACT TCTGTGTTCC
GGCCCCATGC
3241 TGCTGTGCAG GTTCAGTCCC TGTCACTCTA ATGCCCCACA GTTCCCAGTG TCATTCTGTC

3301 ACCATCCTGG CCCGGCATGC CTGTCTATAT TTCAGTTTCC ATATGGAGTA GGTGAGTGGA

3361 GGCCCAGATT GAAAGAATCC GCAAGTGTCA CATTGGAAGG GCATGTGGGA CCACAATATT

3421 GCCATGTGGA TTGACTACCC TAAA

Figure 2.4
Unpublished *clc*-1 cDNA 3' sequence.
Sequence shown is from TJ Jentsch (personal communication) and numbered according to published data (Steinmeyer et al., 1991b). Areas of sequence differences obtained by the author are presented under the original sequence. Nucleotide differences are indicated by bold type.

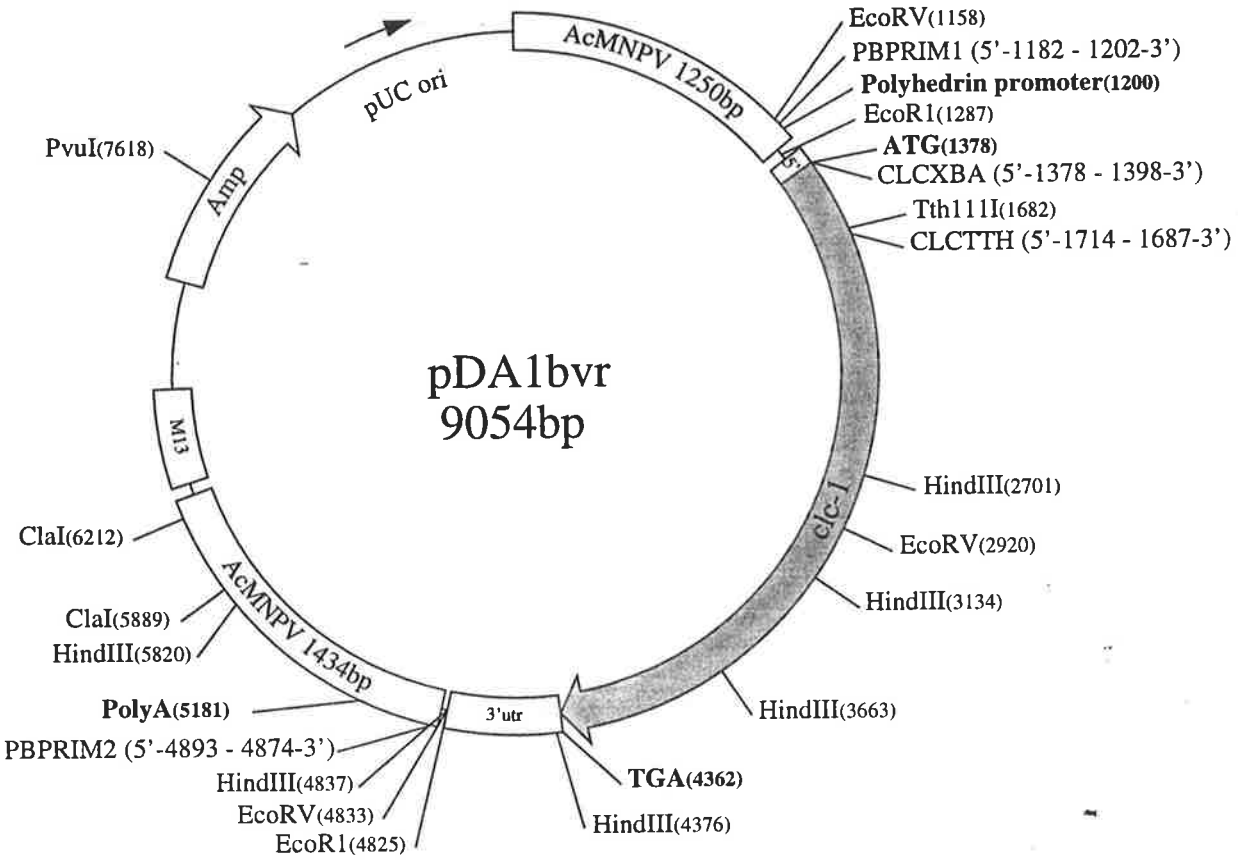

Figure 2.5. Plasmid pDA1bvr.
Clc-1 cDNA cloned into pBacPAK1.
5' = *clc*-1 upstream untranslated sequence. 3' utr = *clc*-1 downstream untranslated sequence. clc-1 = *clc*-1 coding region. AcMNPV = baculovirus derived DNA. PolyA = polyadenylation signal. Polyhedrin promoter numbered according to transcription initiation site. Relevant restriction sites are marked and numbered according to actual cutting site. Primer binding sites (PBPRIM1, PBPRIM2, CLCXBA, CLCTTH) are marked. Primer orientation is indicated by 5'/ 3' and nucleotide numbering. For primer CLCXBA, bps numbered correspond to only those to which the primer binds.

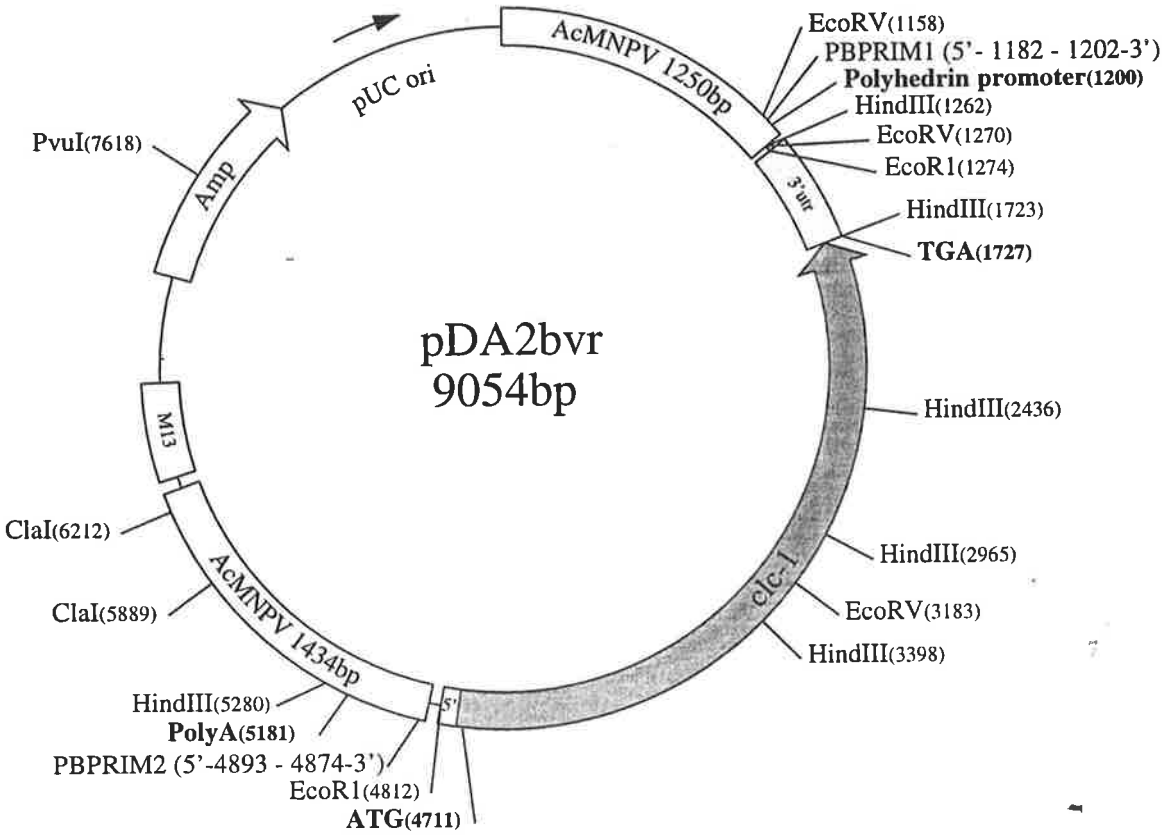

Figure 2.6. Plasmid pDA2bvr.
Clc-1 cDNA cloned into pBacPAK1.
5' = *clc*-1 upstream untranslated sequence. 3' utr = *clc*-1 downstream untranslated sequence. clc-1 = *clc*-1 coding region. AcMNPV = baculovirus derived DNA. PolyA = polyadenylation signal. Polyhedrin promoter numbered according to transcription initiation site. Relevant restriction sites are marked and numbered according to actual cutting site. Primer binding sites (PBPRIM1, PBPRIM2) are marked. Primer orientation is indicated by 5'/ 3' and nucleotide numbering.

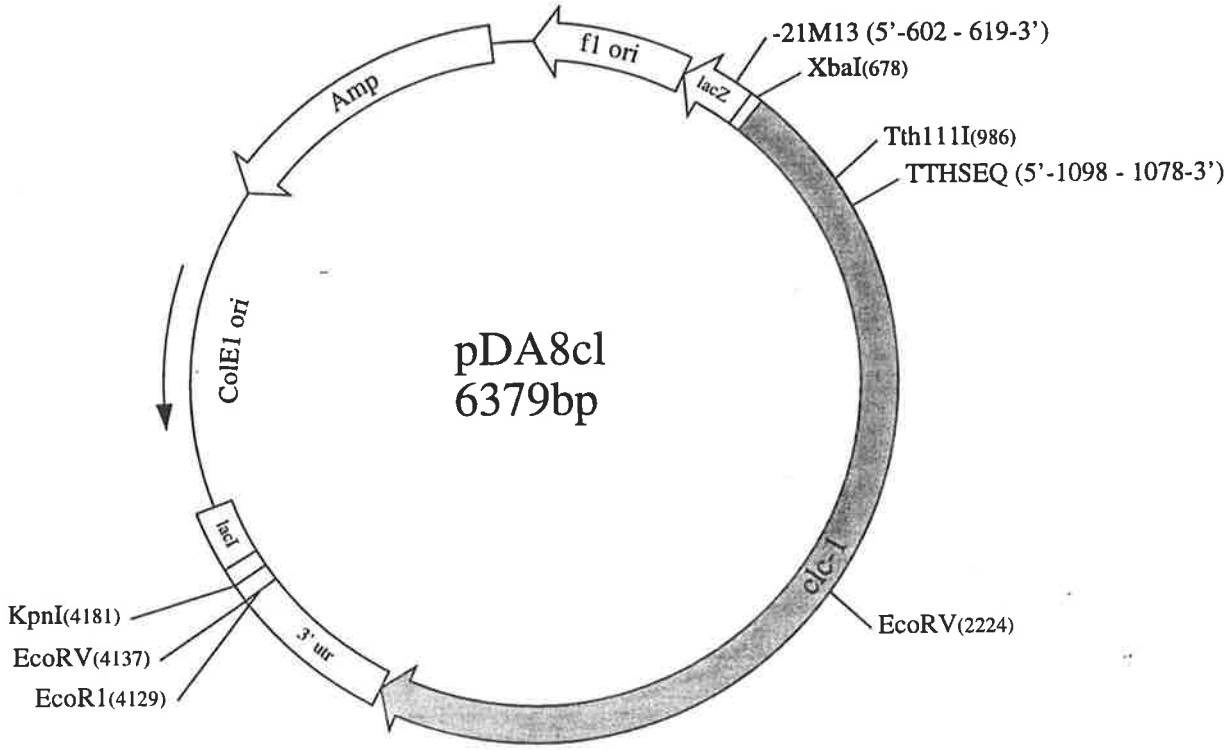

Figure 2.7. Plasmid pDA8cl.
5' modified *clc*-1 cDNA in pBluescript.
3' utr = *clc*-1 downstream untranslated sequence. clc-1 = *clc*-1 coding region. Relevant restriction sites are marked and numbered according to actual cutting site. Sequencing primer binding sites (-21M13 and TTHSEQ) are marked. Primer orientation is indicated by 5'/ 3' and nucleotide numbering.

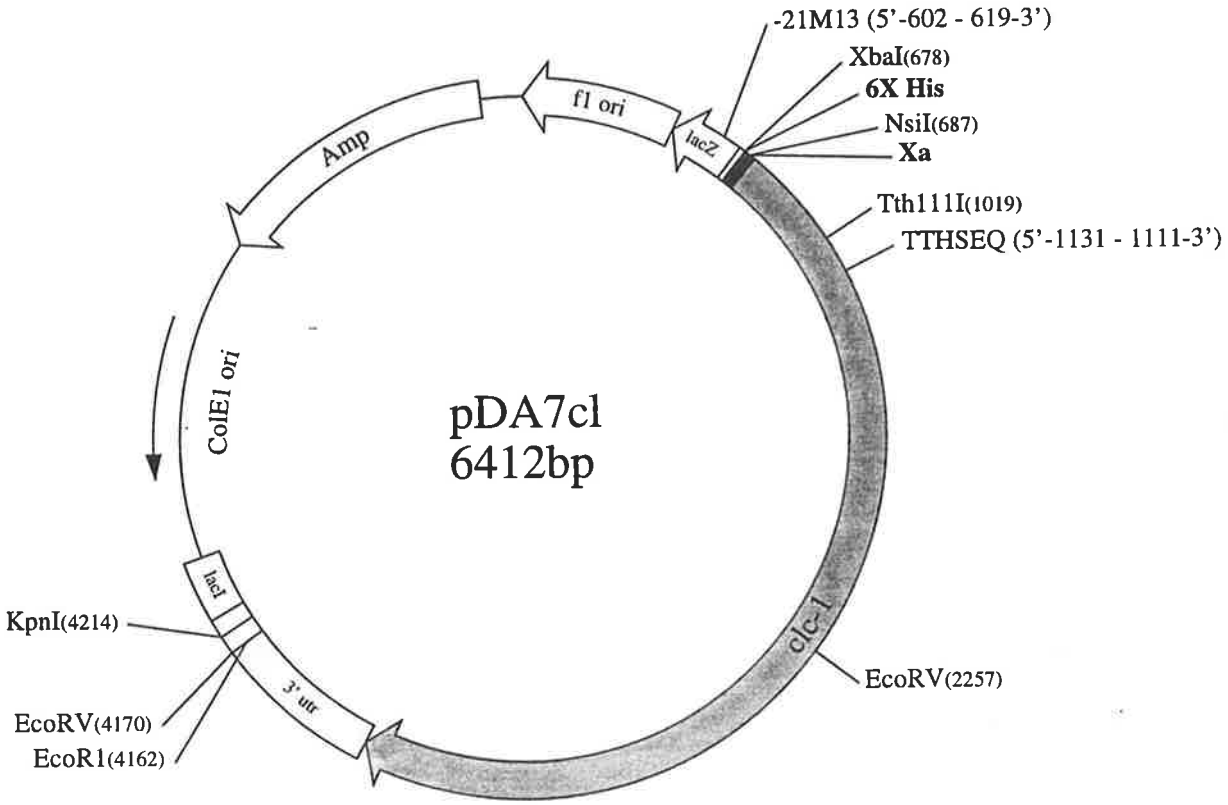

Figure 2.8. Plasmid pDA7cl.
5' modified *clc*-1 cDNA in pBluescript.
6X His = sequence encoding 6 consecutive histidine residues. Xa = sequence encoding a factor Xa endopeptidase site. 3' utr = *clc*-1 downstream untranslated sequence. clc-1 = *clc*-1 coding region. Relevant restriction sites are marked and numbered according to actual cutting site. Sequencing primer binding sites (-21M13 and TTHSEQ) are marked. Primer orientation is indicated by 5'/ 3' and nucleotide numbering.

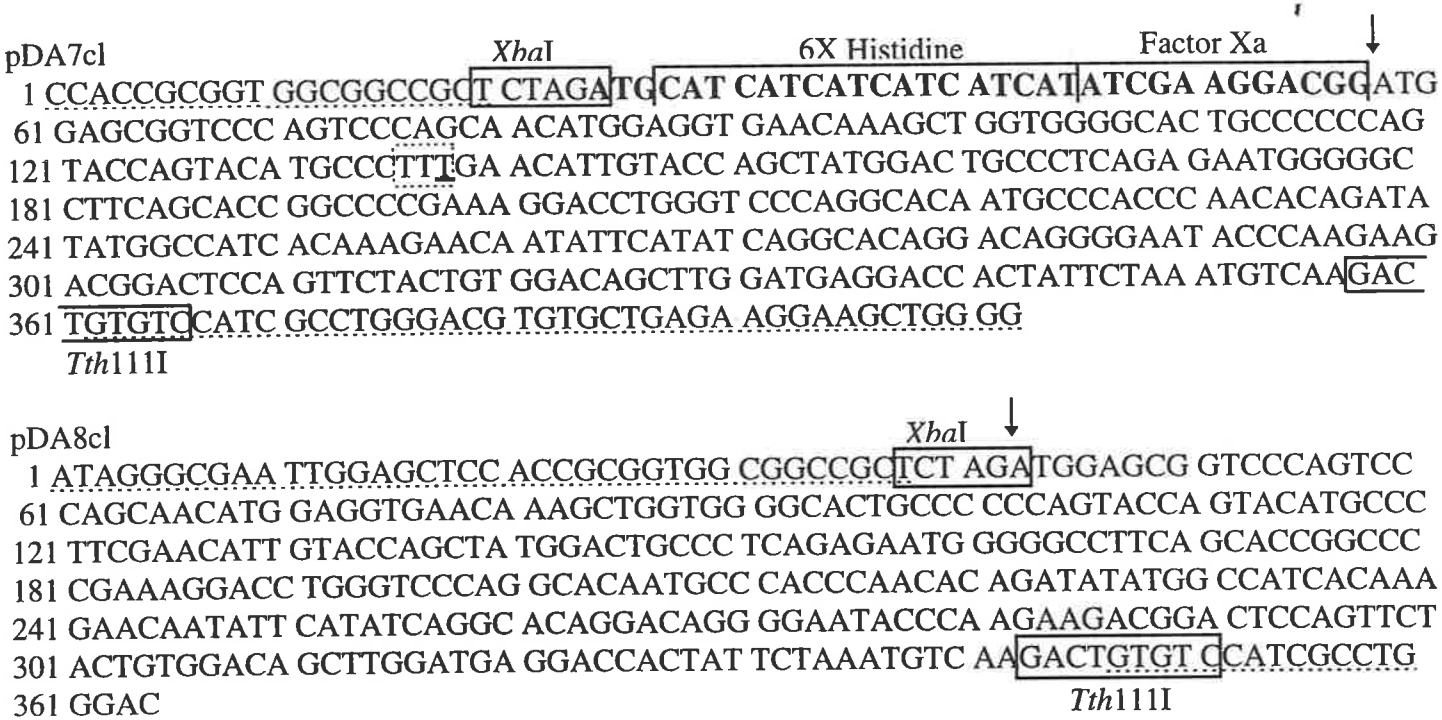

Figure 2.9
Sequence data showing PCR 5' modified *clc*-1 inserts. Sequences were constructed by combining data obtianed using primers -21M13 and TTHSEQ (complimentary strand). Restriction sites are labelled and boxed. DNA derived from TJJ Clone is marked by dotted underline. Native *clc*-1 translation start site arrowed. For pDA7cl, extra codons introduced upstream of native ATG are in bold-face type, codon affected by PCR induced C to T exchange is marked by dotted box with nucleotide involved double underlined.

and pDA8cl were completely digested with the same enzyme combination and approximately 800ng of each modified *clc*-1 insert was recovered after gel purification. Following ligation of each insert into the cut vector and transformation of competent DH5α, numerous (>200) ampicillin resistant colonies were recovered in each case. Six colonies from each transformation were selected at random and plasmid DNA extracted therefrom. Digestion of these plasmids with *Eco*RV and *Nsi*I singly yielded fragments of the expected sizes in all 12 cases as did double digestion with *Xba*I/*Kpn*I, *Xba*I/*Tth*111I and *Sca*I/*Bam*H1. One of each type was selected at random for use in further experiments and designated pDA5bvr and pDA6bvr for the histidine tagged and 5'-deleted constructs respectively. Plasmid extraction of 40 ml overnight cultures of these constructs using Qiagen columns yielded 60μg of clean pDA5bvr and 70μg of clean pDA6bvr plasmid DNA. Plasmid maps of these two constructs are presented in Figs. 2.10 and 2.11.

II.3.2 Recombinant virus production

II.3.2.1 Co-transformations

All 4 recombinant transfer vectors gave similar results in co-transformation experiments. Co-transformation supernatants collected after 2 days incubation and used in standard plaque assays gave titres ranging between 2 X 10^3 and 5 X 10^4 pfu/ml. The plaques produced were well defined and easily distinguished from background uninfected cells and any holes introduced into the monolayer during the course of the procedure.

II.3.2.2 Selection and confirmation of recombinant clones

Ten isolated plaques were picked from each co-transformation plaque assay and eluted overnight in 500μl of growth medium. Of these, 4 of each type were amplified by infection of monolayers in 25cm^2 flasks. In every case cells began to show signs of

virus infection after 24 hours incubation. By 6 - 7 days post inoculation all cultures were well infected. Total cellular DNA collected from these cultures at 6 - 7 days post infection (pi) yielded between 5 and 10µg of DNA per culture.

PCR amplification of whole-cell DNA extracts using primers PBPRIM1 and PBPRIM2 produced a distinct product band of the expected size in all 16 cases with a yield in the vicinity of 10µg of product per reaction. This product was not present in DNA extracts from mock infected cells incubated in parallel with virus infected cells nor in PCR reactions to which no DNA had been added (reagent control). A product of appropriate size was also present in the positive control reaction containing 2ng of pDA1bvr plasmid DNA. Restriction of products with *Eco*RV and *Tth*111I also gave fragments of the sizes predicted for the inserts in each case.

II.3.3 Virus amplification and protein expression

II.3.3.1 Virus amplification

Two hundred and fifty µl of virus seed stock (BVDA2.1, 5.2 and 6.3) in a total volume of 500µl was used to inoculate 75cm^2 flasks of Sf21 cells to produce intermediate virus stocks. All flasks showed signs of infection within 24 hours of inoculation and were well infected by 6 days incubation. Culture supernatants collected at this point showed titres of 1 - 2 X 10^8 pfu/ml by plaque assay. Using this intermediate stock to infect 50 ml suspension cultures at a moi of 0.2 resulted in working virus stocks with titres of between 8 X 10^8 and 1 X 10^9 pfu/ml.

II.3.3.2 Expression time course

The first recombinant viruses produced contained the entire *clc*-1 cDNA in forward and reverse orientation ie. BVDA1 and 2 respectively. Cells analysed 48 hours after infection with 4 clones of each of these viruses showed a protein profile distinctly different from that of mock infected cells (Figure 2.12). Many host cell protein bands

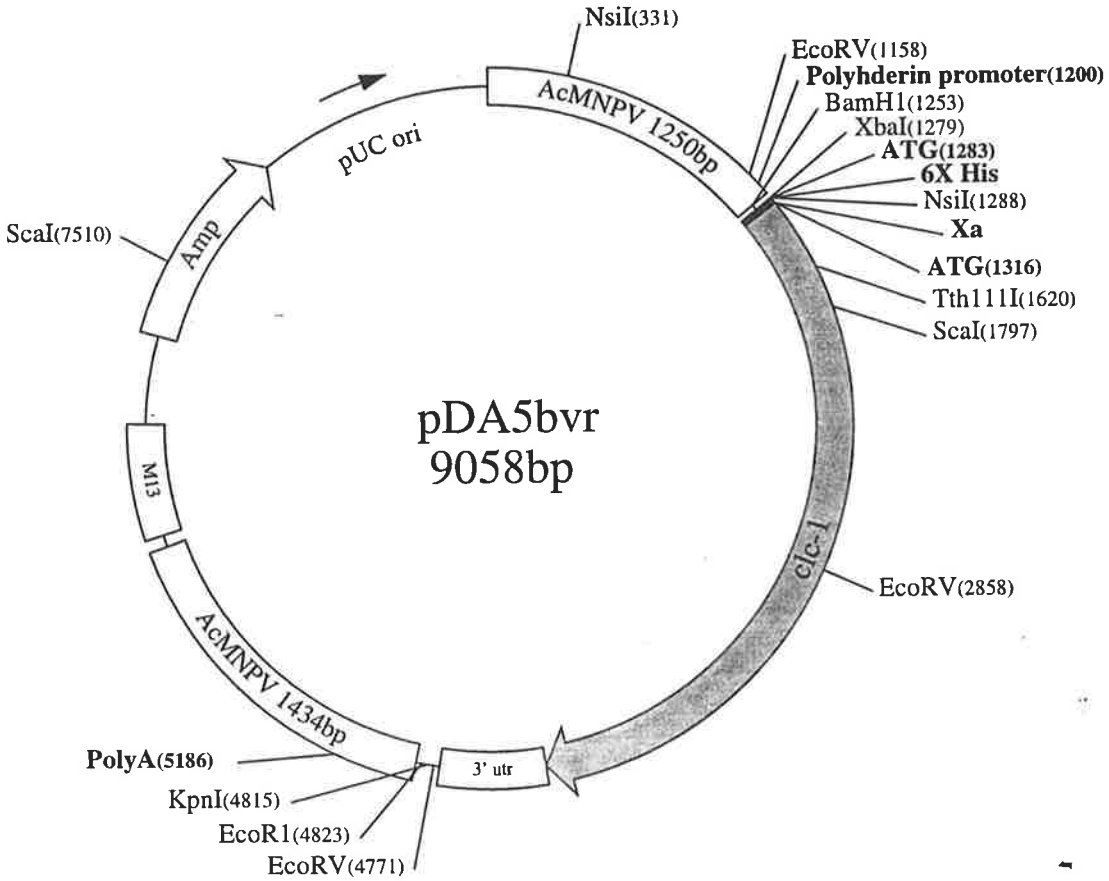

Figure 2.10. Plasmid pDA5bvr.
5' modified clc-1 cDNA cloned into pBacPAK8.
AcMNPV = baculovirus derived DNA. PolyA = polyadenylation signal. Polyhedrin promoter numbered according to transcription initiation site. 6X His = sequence encoding 6 consecutive histidine residues. Xa = sequence encoding a factor Xa endopeptidase site. 3' utr = *clc*-1 downstream untranslated sequence. clc-1 = *clc*-1 coding region. Relevant restriction sites are marked and numbered according to actual cutting site.

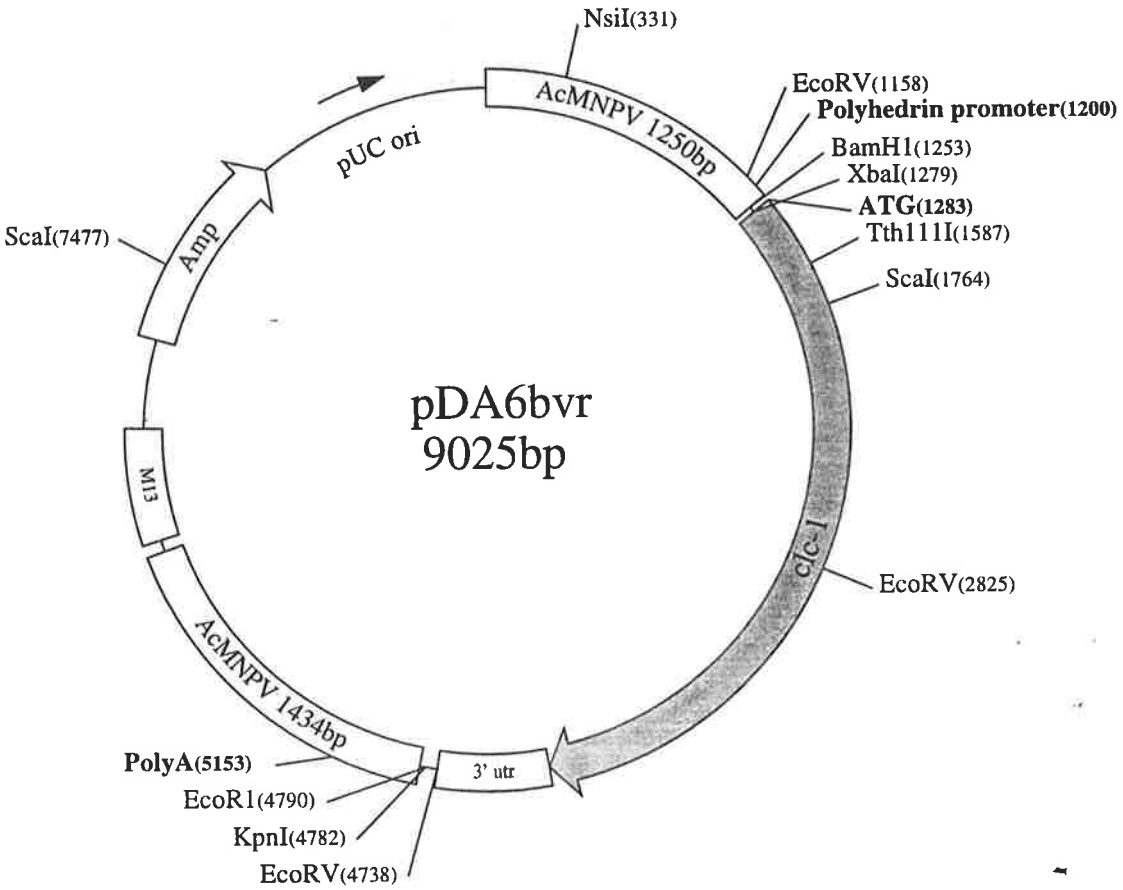

Figure 2.11. Plasmid pDA6bvr.
5' modified clc-1 cDNA cloned into pBacPAK8.
AcMNPV = baculovirus derived DNA. PolyA = polyadenylation signal. Polyhedrin promoter numbered according to transcription initiation site. 3' utr = *clc*-1 downstream untranslated sequence. clc-1 = *clc*-1 coding region. Relevant restriction sites are marked and numbered according to actual cutting site.

Figure 2.12. Whole cell protein extracts of Sf9 cells infected with baculovirus expression vectors separated on 9% discontinuous polyacrylamide gel and stained with coomassie blue. Cells collected at 48 hours post infection (**a**, **b**) or times indicated (**c**) and processed as described in II 2.13.2. Molecular weight markers indicated.

a: Extracts from cells infected with vectors containing different constructs and uninfected control cells.
Lane 1: Mock infected.
Lane 2: BVDA2 infected (negative control).
Lane 3: BVDA1 infected (complete cDNA).
Lane 4: BVDA6 infected (5' utr deleted).
Lane 5: BVDA5 infected (5' utr replaced with His purification tag).

b: Cells infected with 4 different BVDA6 virus clones.
Lane 1: mock infected.
Lane 2: BVDA6.1 infected.
Lane 3: BVDA6.2 infected.
Lane 4: BVDA6.3 infected.
Lane 5: BVDA6.4 infected.

c: Time course of CLC-1 expression. Cells infected with virus BVDA6.3.

Lane 1: 24 hours.
Lane 2: 30 hours.
Lane 3: 36 hours.
Lane 4: 42 hours.
Lane 5: 48 hours.
Lane 6: 54 hours.
Lane 7: 60 hours.
Lane 8: 66 hours.
Lane 9: 72 hours.

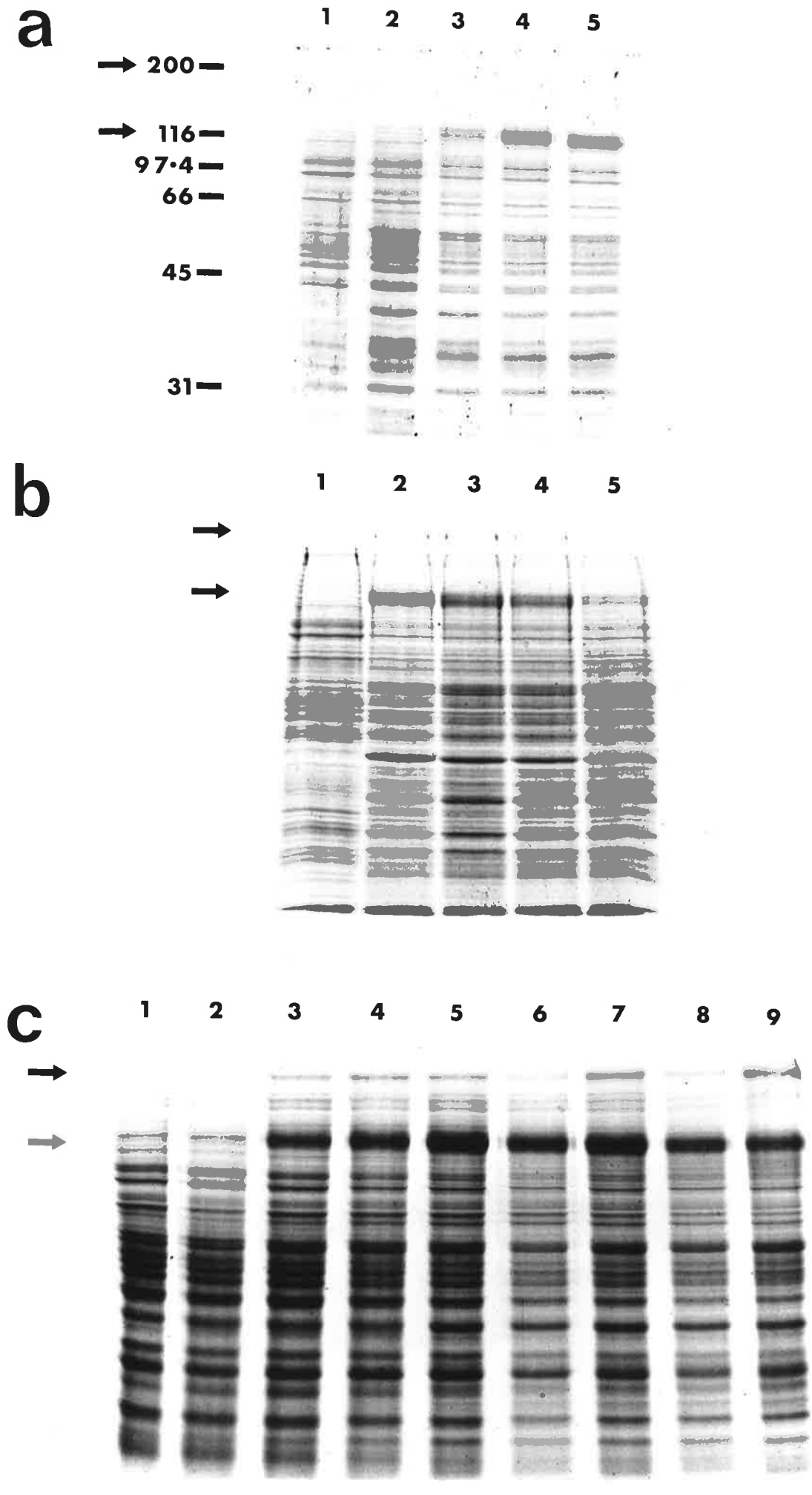
a
1
2
3
4
5
200
116
97·4
66
45
31
b
1
2
3
4
5
c
1
2
3
4
5
6
7
8
9

reduced in intensity or were no longer visible by the staining method used whilst numerous apparently virus encoded proteins appeared. None of the BVDA2 infected cultures produced a protein with a mobility expected for ClC-1 whereas the BVDA1 infected cells exhibited a vague, diffuse protein band with an apparent M_r of approximately 116kDa which we presume to be ClC-1. The intensity of this band varied from clone to clone. A second unique but very faint band was also visible and had an apparent M_r of around 200kDa.

Due to the disappointing results with BVDA1, vectors BVDA5 and 6 (5' untranslated region deleted) were produced and screened as above. Cells infected with clones of these two viruses produced protein profiles almost identical to those of BVDA1 with the exception that the extra bands at 116kDa and 200kDa were of much greater intensity (Figure 2.12a). Clonal variation was again evident (Figure 2.12b) but the level of expression was consistently higher having increased by about 5 - 10 fold. The intensity of the higher M_r band was consistently much less than that of the lower (Figure 2.12a).

BVDA1 virus clones were not pursued further. One clone of each of the other vectors was selected and amplified for use in further experiments, these being BVDA2.1, 5.2 and 6.3.

II.3.3.3 Expression time course

During the first 24 hpi with BVDA6.3 ClC-1 protein was not detectable by coomassie staining. At 30 hours the bands at both 200 and 116kDa were visible and by 42 hours maximum intensity appeared to have been reached. The intensity of the bands did not appear to diminish over the next 6 hours but thereafter declined along with many other cell and virus encoded proteins (Figure 2.12c).

Identical results were achieved with BVDA5.2 whereas ClC-1 protein was not detected in cells infected with BVDA2.1 at any of the time points tested (results not shown).

II.4 Discussion

II.4.1 Clc-1 cDNA

Sequencing of the original *clc*-1 cDNA, performed in this work for confirmatory purposes, revealed the presence of an additional 326 bp of 3' untranslated DNA which was not published with the rest of the sequence Steinmeyer et al. (1991b). A comparison of the sequence data covering this region obtained by this author with that obtained by Steinmeyer et al. reveals disagreement at only 4 nucleotides (Figure 2.4). Three of these nucleotides, at positions 3123, 3129 and 3177, were not present in data obtained here. The fourth point of disagreement occurred at nucleotide 3212 where a C appears to be a G according to the data gained in this work.

All but 6 bp of this region was covered by data, of good quality, from two clones (pDA1bvr and pDA2bvr (Figs. 2.2 and 2.3)) albeit on the same strand in both cases. Further, the sequence not covered in both clones was identical to that obtained by Steinmeyer et al. Due to the high level of agreement between our collaborators' data and my own and since both clones in this work gave identical sequence which included the areas of discrepancy I am confident that the sequence presented here accurately represents this region of the cDNA. However, since both strands of this region have not yet been verified, this additional sequence has not been submitted to GENBANK.

Taking the unpublished sequence into account, the *clc*-1 cDNA obtained from rat skeletal muscle used in this work is 3526 bp in length and is composed of 83 bp of 5' untranslated sequence, a 2985 bp open reading frame (including the stop codon) and

458 bp of 3' untranslated DNA. The complete cDNA sequence is presented in appendix c.

II.4.2 Construction of expression vectors

II.4.2.1 Transfer vectors

The production of transfer vectors containing the entire cDNA in both orientations (pDA1bvr and pDA2bvr) was achieved using blunt end cloning techniques. Using this method the number of recombinants was low compared to religated vector DNA. This result is typical of the approach used since ligation of blunt ended DNA species occurs at much lower efficiency than for DNA bearing compatible overhangs. Further, since the ends of the cut and end-filled vector were not dephosphorylated a relatively high level of vector religation is to be expected.

Modification of the 5' end of the cDNA, including the introduction of additional protein coding sequence, was successfully achieved using recombinant PCR. The efficiency of recombination of cleaved PCR products with similarly cut parental plasmid appeared to be quite high. Again, this is to be expected when using directional cloning methods with DNAs which have compatible overhangs. Cleavage of the PCR products did however require relatively high concentrations of restriction enzymes. Difficulty in cutting PCR products at sites close to their ends is a commonly reported problem. Sequence verification of the cloned, PCR modified fragments revealed a single base pair substitution in one of the clones. *Taq* DNA polymerase is known not to have a 3'-5' proof reading activity and is therefore prone to this sort of error. This problem can largely be avoided by the use of other thermo-stable DNA polymerases which possess proof reading activity eg. *Pfu*. The error in this case, fortuitously, did not alter the protein sequence and was therefore of no significance.

The error does however serve to highlight the need for sequence verification of cloned PCR products when using *Taq* polymerase.

II.4.2.2 Expression vectors

Four recombinant baculovirus expression vectors were produced during the course of this work. In all cases co-transformation procedures yielded culture supernatants with virus titres typical of those reported for the techniques used (King and Possee, 1992). Amplification of selected clones also resulted in virus stocks with titres in the range expected (King and Possee, 1992).

Screening of viral clones by PCR using primers designed to amplify the entire cDNA insert demonstrated the presence of insert in every clone investigated. Using linearised, replication deficient virus the suppliers (*Clonetech*) claim that more than 80% of recovered viruses are likely to be recombinant. Although in this work only small numbers of clones were screened, given the results it would appear that this claim is not unreasonable and may even be a little conservative.

II.4.2.3 Protein expression

II.4.2.3.1 Level of expression

ClC-1 protein was successfully expressed using the polyhedrin promoter in the baculovirus /Sf cell system. In all vectors which were expected to express ClC-1 the level of expression was high enough for protein to be detectable on coomassie-stained polyacrylamide gels. Although the protein yield was much lower than has been described for polyhedrin, it is in the range of other membrane bound proteins expressed using this system (reviewed in O'Reilly et al., 1994).

PAGE analysis clearly demonstrated a marked increase in protein yield when using vectors from which the 5' untranslated region (5'utr) of the cDNA had been removed. Removal of foreign 5' leader sequences is a suggested procedure when attempting to optimise yields of poorly expressed proteins in this system (Cameron et al., 1989).

Maximal transcription from the polyhedrin promoter has also been shown to be influenced by the presence and integrity of the entire viral leader sequence, 50 bp, between the initiation start site and the polyhedrin ATG (Matsuura et al., 1987; Possee and Howard, 1987). This sequence is present and intact in all expression vectors used here. The translation start site in vector BVDA1 is 127 bp downstream of the position where the natural start site would occur. In the 5'-modified constructs this distance is reduced to 32 bp. It is possible that the spacing of these elements may influence the efficiency of transcription and/or, more likely, translation leading to a reduction in the level of expression achieved using BVDA1. It is also possible that the 5'utr of *clc*-1 contains *cis* acting elements which act to reduce the level of protein expressed. The expression of this cDNA in *Xenopus* oocytes was only achieved after the 5'utr was replaced with that from *clc*-0 (Steinmeyer et al., 1991b). Further, a search of the GENBANK database reveals an identical sequence upstream of the human *clc*-1 gene. Although the evidence is circumstantial, the author favours the view that the *clc*-1 leader sequence encodes *cis* acting regulatory elements.

It would be an interesting exercise to investigate the role of this sequence in regulation of ClC-1 expression. This could probably best be achieved by linking this sequence to a reporter gene, eg. chloramphenicol acetyl transferase, and examining the effects of various mutations introduced into the sequence in an approach similar to that used in the investigation of the polyhedrin leader sequence (Matsuura et al., 1987). Investigation of this sequence may give some insight into the regulation of ClC-1 expression *in vivo*.

II.4.2.3.2 Protein size

Baculovirus expressed ClC-1 investigated using SDS-PAGE migrates with an apparent M_r of approximately 116kDa. Translation of the *clc*-1 reading frame predicts

an unprocessed mass of 110,068 Da. This discrepancy could simply be due to the hydrophobic nature of ClC-1 causing anomalous migration. It is also possible that the protein is subject to post-translational processing in Sf cells. The ClC-1 sequence does include 3 potential N-linked glycosylation sites one of which, between D8 and D9, is conserved in other members of the ClC family. Human ClC-1, ClC-2 and the ClC-K group, have been shown to be glycosylated at this site when expressed in a cell free expression system (Kieferle et al., 1994). It is therefore possible that the rat ClC-1 expressed here is also glycosylated. Preliminary experiments using the glycosylation inhibitor tunicamycin did not, however, reduce the apparent size of the protein (results not shown). Recently published work (Gurnett et al., 1995) using Western blotting of rat ClC-1 extracted directly from muscle reported a size of 130kDa. Experiments using glycanase F failed to clearly demonstrate whether or not the protein was glycosylated *in vivo*, giving a 2 - 3kDa mobility shift which was difficult to detect and reproduce. The 130kDa size reported by Gurnett et al. is not consistent with the figures published in their paper. Size calculations using measurements taken directly from the figures and assuming correct marking of M_r standards suggest a size for ClC-1 which is closer to 115kDa and is consistent with the size of the protein expressed in this work. The issue of glycosylation of rat ClC-1 is yet to be resolved. The presence or otherwise of glycoslylation in the Sf cell could best be investigated using radio-labelled sugars and autoradiography. If glycosylation were detected, the definitive identification of which residues are involved would require site-directed mutagenesis.

PAGE analysis also revealed a second protein band with an apparent M_r of about 200kDa which appears to be peculiar to ClC-1-expressing cells. Other workers using the baculovirus/Sf system have reported the presence of protein bands of higher M_r

unique to their protein expressing vectors (Grabenhorst et al., 1993; Voss et al., 1993). Investigation revealed that these bands were due to glycosylation variants of the expressed protein (Voss et al., 1993). The use of tunicamycin, mentioned above, did not reduce the size or intensity of this higher M_r band. There is some evidence to suggest that ClC-1 forms multimers in the membrane (Steinmeyer et al., 1994). To investigate the possibility that this 200kDa band was due to undissociated ClC-1 multimers, preliminary experiments were performed using samples prepared under harsh denaturing conditions (8M urea). PAGE analysis of these samples showed no reduction in size or intensity of this band (results not shown) suggesting that it is unlikely to be due to multimer formation. The best way to establish the identity of this band would be by Western blot using ClC-1 specific antibodies. Attempts in our laboratory to produce such an antibody (*vide* Section III) have thus far been unsuccessful. Another possible approach would be extraction of this band for N-terminal protein sequencing.

Although Sf cell expressed ClC-1 exhibits some, thus far, unexplained characteristics on polyacrylamide gels, given its functionality in these cells (*vide* Section IV) it would appear that they are of no obvious functional significance.

II.4.2.3.3 Expression time course

The time course of expression of ClC-1 in Sf cells is generally in keeping with the reported timing of *polh* promoter activity (reviewed in O'Reilly et al., 1994 and *vide* appendix a). Peak expression occurs approximately 24 hours earlier than reported for β-galactosidase expressed in Sf cells in suspension cultures (Licari and Bailey, 1991; Hara et al., 1993; Power et al., 1994) although the decline in intracellular yield following peak production follows a similar time course (Hara et al., 1993). The timing of peak expression appears to depend on the culture and infection conditions

used (moi, cell growth phase, temperature) as well as the protein being expressed (cf. Licari and Bailey, 1991; Hara et al., 1993; Reuveny et al., 1993; Wang, M-Y et al., 1993; Power et al., 1994). Glucocerebrosidase expressed in Sf9 cells (Reuveny et al., 1993) showed peak expression at 4 days post infection when medium was replaced during the infective process but a lower yield and earlier peak, at 48 hours, when it was not. In the work described by Wang et al. (1993) the membrane bound enzyme epoxide hydrolase showed peak expression at around 50 hpi. ClC-1 is detectable by coomassie staining from around 30 hpi, although it may be detectable earlier using more sensitive methods, and peaks at around 42 hpi. Although direct comparison of published expression time course data is difficult due to the different conditions used by various workers, it appears that ClC-1 is expressed with a time course expected for an integral membrane protein under the conditions applied.

II.4.3 Conclusions

The baculovirus/Sf cell system is appropriate for expression of ClC-1 and produces a product of very similar size to that predicted for and observed with the native protein. Expression using this approach yields high levels of product which are readily detectable using standard protein staining techniques. The high yield and successful expression of a histidine tagged version of ClC-1 demonstrate the system's applicability to protein purification experiments, which are planned in the future. Differences in the level of expression of full length and 5'-modified *clc*-1 cDNAs suggest the 83bp 5'utr contains some *cis* acting element(s) involved in regulation of expression of this protein.

III
Antibody Production

III.1 Introduction

For many years the exact location of the protein responsible for the large chloride conductance observed in skeletal muscle was unknown. Various researchers had suggested that the channel responsible was located predominantly in the T-tubular system (Palade and Barchi, 1977a; Dulhunty, 1979, 1982; Dulhunty et al., 1984; Heiny et al., 1990b) though results from different laboratories and species were contradictory (reviewed in Bretag, 1987). Later, single channel studies performed directly on the surface of whole muscle cells also failed to detect a chloride-selective channel with characteristics which could account for the chloride conductance measured in the whole cell (reviewed in Pusch and Jentsch, 1994). These results provided further support for the view that this channel may have been predominantly T-tubular in location although other explanations were possible eg. low single channel conductance. Although chloride channels had been purified from sarcolemma (eg. Weber-Schürholz et al., 1993), none of these showed appropriate biophysical characteristics. Clearly, a direct method of localising the protein *in situ* was required to resolve the issue. Immuno-localisation with a specific anti-channel antibody would provide such a method, however, since the protein had not been isolated and no information about its amino acid sequence was available, production of such an antibody was all but impossible.

Following the cloning of the *clc*-1 cDNA (Steinmeyer et al., 1991b) and the demonstration that the protein encoded by this sequence was probably the major chloride permeation pathway in skeletal muscle (Steinmeyer et al., 1991a), the way

was open for the application of various approaches to production of anti-ClC-1 antibodies. One possible approach was to express ClC-1, or a fusion protein, in an heterologous system and use it in animal inoculation. Another was to use the deduced amino acid sequence as a guide for the production of synthetic oligopeptides which could be linked to protein carriers and used as antigens.

Dr. K. Steinmeyer and Prof. TJ Jentsch provided us with the *clc*-1 cDNA, but as part of our collaborative agreement we were requested not to use the cDNA for production of anti-ClC-1 antibodies. For this reason we pursued the use of synthetic oligopeptides.

The use of peptides linked to protein carriers as antigens in antibody production has become a commonly applied approach (reviewed in Butler and Beiser, 1973). Choosing which peptide from an entire protein sequence will elicit a response is still a largely empirical process. Hydrophilic domains and protein termini, however, appear more likely to be antigenic epitopes (Hopp and Woods, 1981; Walter, 1986). By employing the right carrier, inoculation protocol and animal, virtually any peptide, including completely conserved sequences, may produce a response (reviewed in Walter, 1986). Numerous methods for peptide/ carrier conjugation are available (reviewed in Van Regenmortal et al., 1988); the choice of method depends on the sequence of the peptide and the characteristics of the carrier.

Given the above, the N and C termini of ClC-1 were selected on the basis of their position, hydrophilicity (Steinmeyer et al., 1991b) and the absence of these sequences in ClC-0 and ClC-2, the only other known members of the ClC family at the time.

Specific anti ClC-1 antibodies produced using the above approach were to be applied in a number of ways to the investigation of this channel. Used in Western blots, they would allow detection of small amounts of protein which would be of great use during

protein expression, solubilisation and purification experiments. Since the source of antigen was independent of the heterologous expression system, they could also be used to confirm the identity of protein(s) expressed therein. Possibly of greater importance though, was their application to the problem of localising this channel in native membranes.

III.1.1 Approach to anti-ClC-1 antibody production

Set out in detail below are three approaches applied sequentially in this work to the problem of producing a ClC-1 specific antibody. The second and third approaches were formulated following review of the results achieved with the previous protocol(s). Conjugation to horseradish peroxidase (HRP) was chosen in initial experiments on the basis that this method had, on more than one occasion, been successful in eliciting specific anti-peptide antibodies in experiments performed in a colleague's laboratory (P.L. Ey, personal communication). The inoculation protocol was formulated after discussion with the Chief Veterinary Officer (Dr. T. Kuchel) at the Veterinary Services Division, Institute of Medical and Veterinary Science (Frome Rd. Adelaide, 5000). The original protocol included only subcutaneous inoculations but an additional intravenous booster was included after assessment of the results achieved following the subcutaneous inoculations.

III.2 Materials and methods

III.2.1 Synthetic oligopeptides

Peptides representing the termini of ClC-1 were purchased from *Auspep* and had the following sequences:

Peptide N12 (ClC-1 N-terminus): NH_2- M E R S Q S Q Q H G G E -COO.
Peptide C12 (ClC-1 C-terminus): NH_2- S T D E E D E D E L I L -COO.

III.2.2 Chemicals, reagents and media

All chemicals and reagents were of RIA grade or better and were purchased from established suppliers (*Ajax, BDH, Boehringer Mannheim, Sigma*). Goat anti-rabbit IgG HRP conjugate and Tween-20 were from *Biorad*. Donkey anti-rabbit IgG HRP conjugate was from *Amersham*. Bovine serum albumin (BSA), HRP used in peptide conjugation and substrate 4-chloro-1-naphthol (4-NC) were from *Sigma*. Bovine gamma globulin (BGG) was from *Calbiochem* as was enzyme substrate o-phenylenediamine dihydrochloride (OPD). Phosphate buffered saline (PBS), Dulbecco A, was from *Oxoid*. All solutions were prepared using MQ quality water with a resistance of at least 18MΩ/ cm.

Microtitre trays were purchased from *COSTAR* (EIA/ RIA, High binding U-bottomed Strip plate cat.# 2585) or *Dynatech* (Immulon3, Removawell strips). Application of each plate type is specified in the description of the methods.

Biorad Trans-Blot transfer medium (nitrocellulose, 0.45µm pore size) was used for all dot blots.

III.2.3 Peptide conjugation procedures

III.2.3.1 Conjugation efficiency

Since neither peptide contained any residues which are easily detectable, eg. by spectrophotometry at a wavelength of 280nm, more complex methods would need to be employed, eg. peptide labelling, to accurately quantitate them. Consequently, in all experiments reported here the efficiency of conjugation was not systematically assessed. Given that in all cases peptides were added at a vast molar excess, the number of peptides bound per carrier molecule was assumed to parallel the number of available interaction sites. In the case of HRP the expected peptide to carrier ratio would be 1:1 whereas for BGG and BSA it would be in the region of 50:1.

III.2.3.2 Conjugation to horseradish peroxidase

Four mg of HRP was dissolved in 2ml of 0.1M $NaHCO_3$ and 120µl of freshly prepared 0.15M $NaIO_4$ was added followed by immediate mixing. The solution was further mixed gently for 2 hours at room temperature in the dark after which 100µl of 100mM Na_2CO_3 was added. Two mg of peptide dissolved in 2 ml of 0.2M bicarbonate buffer (pH 9.5) was added to the periodate treated HRP and the mixture incubated overnight at 4°C in the dark with gentle agitation. Following this, excess aldehyde groups were blocked by addition of 200µl of freshly prepared $NaHB_4$ (5mg/ml in 100mM NaOH, this reagent is used due to its small size which allows it access to the aldehyde groups formed on HRP where larger reagents, eg. diethanolamine, may be sterically hindered). Following this treatment the entire solution was dialysed overnight at 4°C against 3 changes of 2L of PBS. The peptide conjugate was stored in 200µl aliquots at -20°C until required.

III.2.3.3 Conjugation to bovine serum albumin and bovine γ globulin

III.2.3.3.1 In solution

Carrier proteins (BSA and BGG) were dissolved in 100mM bicarbonate buffer (pH 9) at a final concentration of 10mg/ml. Aldehyde groups were formed by addition of a vast molar excess of gluteraldehyde (2% final concentration) followed by gentle mixing at room temperature in the dark for 2 hours. Excess gluteraldehyde was then removed by dialysis against 3X 2L 100mM bicarbonate buffer (pH 9). Each solution was further de-salted using a Sephadex G50 column. The yellowish colour of the solutions, due to the aldehyde groups, allowed them to be tracked through the columns visually and be collected virtually undiluted. Peptides were added to the de-salted carriers in a 50X molar excess and coupling allowed to proceed overnight in the dark at room temperature with gentle mixing. Excess aldehyde groups were then blocked

by addition of diethanolamine to a final concentration of 100mM. The conjugates were dialysed overnight against 3X 2L changes of PBS and stored at -20°C in 200µl aliquots. After dialysis, approximate concentrations of conjugates were determined by measuring their absorbance at a wavelength of 280nm and comparing the values to those obtained with 1mg/ml solutions of the appropriate carrier protein (BSA or BGG). Due to their amino acid composition, the peptides were assumed not to add significantly to the absorbance of the conjugates at this wavelength.

III.2.3.3.2 Solid phase

COSTAR trays were coated by addition of 100µl of BSA (200ng/ml in PBS) to each well and incubation at 4°C overnight. After removing the BSA solution and washing once with PBS, aldehyde groups were formed by addition of 0.5% gluteraldehyde in PBS (100µl/well) and incubation at room temperature for 20 minutes. Wells were then washed thoroughly (10 times) with MQ H_2O, and peptide added at a 10X molar excess compared to BSA (50ng/ml in PBS, 100µl/well). Coupling was allowed to proceed overnight at 4°C. The peptide solution was then removed and excess aldehyde groups were blocked by addition of 100µl 0.1M glycine and incubation at room temperature for 2 hours (glycine was used as the blocking agent, in preference to diethanolamine, since it has the added advantage of also acting as a blocking agent of non-specific protein binding sites). Wells were then washed 5 times with PBS containing 0.1% Tween-20 (PBS-T) and used in ELISA assays as for other antigen coated plates (*vide infra*).

III.2.4 Enzyme-linked immunosorbent assay (ELISA)

Costar plates were employed with sera obtained using approach 1 (*vide infra*). Optimal blocking conditions were established by testing various concentrations of

BSA, Tween-20 and casein in PBS at room temperature and 4°C and incubation from 30 minutes to overnight. The blocking conditions quoted below were found to give the lowest background in negative control wells with these plates. Due to continuing problems with background, plates from various manufacturers were tested using the blocking conditions quoted below. *Dynatek* Immulon3 plates were found to give no detectable background and were used for all ELISA screening of sera obtained using approaches 2 and 3 (*vide infra*).

Microtitre plates were coated by addition of 50µl of antigen (2µg/ml in PBS) per well and incubation at ambient temperature for 2 hours. Wells were washed twice with PBS-T then blocked by filling completely with blocking solution (3% Casein, 0.1% BSA, 0.5% Tween-20 in PBS) and incubating at room temperature for 2 hours. The blocking solution was then decanted and the plates were tapped, inverted, on a bench covered with absorbent paper towel to remove any remaining traces of solution. Dilutions of test serum were made in blocking solution and added to wells according to the format shown in the following diagram.

96 (12 X 8) well mictotitre tray.

	1	2	3	4	5	6	7...12
A		1/2	1/4	1/8	1/16	etc.	
B		1/2	1/4	1/8	1/16	etc.	
C		1/10	1/20	1/40	etc.		
D		1/50	1/100	etc.			
E		1/250	etc.				
F...H		etc.					

Controls: Row A; test serum, no antigen. Column 1; antigen, no test serum.
Test serum dilutions:

Across rows: 1/2 serial dilution
Down columns (B-H): 1/5 serial dilution

One hundred µl of the appropriate dilution of serum was added to each of the wells in column 2 and 50µl of blocking solution was added to all other wells. Serial 1/2

dilutions were then made by using a multi-channel pipettor to carry 50µl from column to column and mixing by repeated aspiration and replacement of the solution with the pipettor. The 50µl removed from the final column was discarded. Typically, dilutions were produced using 4 rows (B - E) and 9 columns (2 - 10) giving a range from 1/2 to 1/64000. After incubation at room temperature for 2 hours, wells were washed 4 times with PBS and 50µl of goat anti-rabbit IgG HRP conjugate (1/3000 dilution of stock in blocking solution) was added. Following at least 30 minutes incubation at room temperature, unbound secondary antibody was removed by washing 4 times with PBS-T. Just prior to use, enzyme substrate was prepared by dissolving OPD in phosphate-citrate buffer (pH 5.0) (see appendix b) to a final concentration of 8mg/ml and adding H_2O_2 (100vol. 3µl/ ml of OPD solution). Fifty µl of this reagent was added to all wells and colour allowed to develop at ambient temperature in the dark for 15 minutes. The reaction was then stopped by addition of 50 µl of 0.1M H_2SO_4 and the absorbance of each well measured at a wavelength of 492nm using a *Titertek* Multiskan MC ELISA plate reader.

III.2.5 Dot blots

One µl of antigen solutions (approx. 1mg/ml) was blotted onto nitrocellulose membranes and allowed to dry at room temperature. Membranes were then blocked by soaking in a small volume of blocking solution (1% (w/v) casein, 0.1% (v/v) Tween-20, 0.5% (w/v) BSA in PBS) for 10 minutes with gentle rocking. This was followed by washing twice for 2 - 3 minutes with gentle rocking in PBS containing 0.05% (v/v) Tween-20 and 0.1% (w/v) BSA (PBS-TB). Immediately after the final wash, membranes were incubated at room temperature with test antisera, diluted in PBS-TB (0.15ml/cm^2 of membrane), in heat sealed plastic bags. After 30 minutes at

room temperature with gentle rocking, excess primary antibody was removed by washing 4 times with PBS-T for 2 minutes followed by one 5 minute wash in PBS. Secondary antibody solution was prepared by adding 12.5µl of donkey anti-rabbit IgG HRP conjugate to 10ml of PBS containing 1mg/ml BSA. Membranes were incubated in this solution for 30 minutes at room temperature with gentle rocking, then excess secondary antibody was removed by washing as for primary antibody. Enzyme substrate was prepared by dissolving 15mg of chilled (-20°C) 4-NC in 5ml chilled (-20°C) methanol. This was then mixed with 25ml PBS containing 24µl of 100vol. H_2O_2 and immediately poured over membranes. Colour was allowed to develop at room temperature with gentle rocking for 30 minutes and the reaction then stopped by thoroughly washing the membranes with MQ H_2O.

III.2.6 Inoculation protocols and serum screening

New Zealand white rabbits weighing approximately 3kg were used for all protocols. All inoculations, phlebotomy and exsanguinations, under anaesthesia, were performed by staff of the Veterinary Services Division, Institute of Medical and Veterinary Science (Frome Road, Adelaide Sth. Australia, 5000) following methods approved by the in house animal ethics committee.

Subcutaneous (sc) inocula were in a total volume of 1ml given at 4 separate sites ie. 250µl per site. Primary subcutaneous inocula were prepared by mixing 300µl of immunogen with 700µl of complete Freund's adjuvant whilst boosters were prepared using incomplete Freund's adjuvant. Intravenous (iv) inocula contained no adjuvant and were given as a bolus dose of not more than 300µl. Test bleeds were collected from the animal's marginal ear vein and were generally of not more than 5ml in volume. Pre-immune serum was collected from each animal prior to primary

inoculation. Whole blood was collected into 10ml blood collection tubes (no anticoagulant) and allowed to clot at ambient temperature. Clot and serum were separated by centrifugation (3500X g/10 min) and the serum collected by aspiration. Sera were stored in 500µl aliquots at -20°C.

III.2.6.1 Approach 1

III.2.6.1.1 Inoculation protocol

Two animals, designated 1A and 1B, were inoculated with peptide C12 conjugated to HRP (HRP::C12). Subcutaneous inoculations of 100µg of immunogen were given at days 1 and 21. One iv dose of 300µg of immunogen was given at day 36. Test bleeds were collected at days 14, 35 and 50.

III.2.6.1.2 Serum screening

All sera were screened by ELISA using *Costar* plates coated with BSA-coupled peptide C12 (BSA::C12). Serum from the final test bleed was additionally screened using *Costar* plates prepared using the solid phase conjugation procedure.

III.2.6.2 Approach 2

III.2.6.2.1 Inoculation protocol

A total of 4 rabbits, designated 2A - 2D, were inoculated with BGG-coupled peptide. Rabbits 2A and 2B were inoculated using peptide C12 and animals 2C and 2D using peptide N12. One of each pair, 2A and 2C, received doses containing a total of 300µg of immunogen whilst the other received 600µg doses. Inoculation and bleeding protocols were as follows.

Primary sc inoculation was one week after collection of pre-immune serum. Five sc booster doses were given at 21 day intervals thereafter with test bleeds being taken 14 days after the second, third and fourth boosters. Animals were exsanguinated under anaesthesia 14 days after the fifth booster.

III.2.6.2.2 Serum screening

Sera from the first test bleed were screened by ELISA using the homologous peptide linked to BSA as antigen. As a control, sera were also screened against untreated BGG.

Second test bleed sera were screened against the homologous peptide coupled to BSA as well as the heterologous peptide also coupled to BSA and against BSA alone. All sera were tested both unabsorbed and following absorption using BGG (100µg/ml serum). Additionally, sera from rabbits 2B and 2C were tested after absorption with homologous and heterologous peptide linked to BSA (300µg/ml serum).

All sera from test bleed three were screened by ELISA against homologous peptide linked to BSA. The sera were tested unabsorbed and after absorption with homologous and heterologous peptide/BSA conjugate (300µg/ml serum). Testing was also performed after absorption with un-conjugated homologous and heterologous peptide (25µg/ml serum). Additionally, sera absorbed with homologous peptide/BSA conjugate were screened against the heterologous peptide/BSA conjugate. Serum from rabbit 2C was further tested in dot blot assays at dilutions of 1/20, 1/100, 1/500 and 1/1000. Each of the antigens (BSA-conjugated peptide N12 (BSA::N12), BSA-conjugated peptide C12 (BSA::C12), un-conjugated peptide N12 and C12) were spotted on filters at totals of 1ng, 10ng, 100ng and 1µg per spot. Spots containing 2µg of rabbit IgG and 1µg BGG were included on each filter as controls.

No further sera were obtained from rabbits 2A and 2D due to the death of these animals. Sera from animals 2B and 2C collected at exsanguination were screened by dot blot at dilutions of 1/10, 1/20, 1/40 and 1/50. Antigens spotted on filters were BSA::N12 and BSA::C12, BGG and Sf cell (uninfected) whole-cell lysate.

III.2.6.3 Approach 3

III.2.6.3.1 Inoculation protocol

Three animals, designated 3A -3C, were inoculated with BGG-coupled peptide C12 (BGG::C12). Subcutaneous inocula contained a total of 300µg of immunogen whilst iv inocula contained a total of 100µg. The inoculation and bleeding protocol was essentially as described by Van Bueren et al. (1993), as follows.

Primary sc inoculation was performed 7 days after collection of pre-immune serum. Four sc boosters were administered at 4 weekly intervals. This was followed by 3 iv inoculations at 4 day intervals. Test bleeds were collected 1 week after the third sc booster and 11 and 18 days after the final iv dose. One animal, 3A, was given a second round of 3 iv inoculations using 200µg of immunogen/ dose beginning 4 weeks after the final iv dose of the first round. The animal was exsanguinated under anaesthesia 7 days after the final dose.

III.2.6.3.2 Serum screening

Sera from all three animals collected after sc and iv inoculations were screened by ELISA against BSA::C12. Post- iv sera from rabbit 3A were further tested by ELISA using BSA::N12 as antigen and by dot blot against BSA-coupled peptides, BSA, BGG and whole-cell lysates of Sf cells both expressing and not expressing ClC-1.

III.3 Results

III.3.1 Approach 1

(*Rabbits*: 1A, 1B; *Antigen*: HRP::C12; *Inoculation*: 2X sc, 1X iv)

After subtraction of background, pre-immune sera gave no detectable titre to BSA::C12 as did test bleeds collected after each sc inoculation. Testing of sera collected after iv inoculation also gave no reaction using ELISA plates coated with peptide C12 coupled to BSA in solution or in the plates (solid phase conjugation).

After reviewing these results, a change of carrier species was deemed appropriate. It was decided that a desirable carrier must have, 1) a high molecular weight, 2) known immunogenicity, 3) multiple peptide linkage sites, in contrast to HRP, 4) easy availability and 5) be suitable for conjugation to peptides via the same groups as a second carrier and AH-Sepharose. This final characteristic was considered desirable for two reasons. Firstly, sera were to be screened using ELISA techniques and since the 12 amino acid peptides were too small to bind efficiently to microtitre trays, conjugated peptides were to be used. Clearly the carrier used in screening must differ from that used in immunisation but linkage of peptide via the same groups in both conjugates would maximise the chances of the same peptide epitope(s) being exposed on the immunisation and screening antigens. Secondly, it was envisaged that an affinity column might be employed in peptide specific antibody purification. The proposed method of production of such a column was to link peptides to AH-Sepharose via aldehyde groups produced by treatment with periodate (Ey, 1993) and, as with the screening conjugate, linkage via the same groups on the peptide and affinity column would seem desirable.

After further discussions with Dr. T. Kuchel the immunisation protocol was revised to include additional inoculations and different doses of antigen.

III.3.2 Approach 2

(*Rabbits*: 2A - 2D; *Antigen*: BGG::C12 (2A, 2B), BGG::N12 (2C, 2D); *Inoculation*: 5X sc (2A, 2C dose = 300µg; 2B, 2D dose = 600µg,).

Pre-immune sera from all four animals gave no detectable titre to BSA-coupled homologous peptide nor to untreated BGG or BSA.

Sera from test bleed 1 again showed no detectable titre to homologous BSA-coupled peptides or untreated BSA in any animal but all showed an anti-BGG titre of approximately 1/400.

Second test bleed sera gave no titre to untreated BSA but the following titres to BSA-coupled homologous peptides: 2A, 1/1000; 2B, 1/8000; 2C, 1/12800; 2D, 1/2560. Screening against BSA-coupled heterologous peptides gave titres as follows: 2A, 1/1000; 2B, 1/3200, 2C, 1/6400; 2D, 1/1000. Absorption of all sera using untreated BGG did not reduce any of these titres. Serum from rabbit 2B gave no detectable titre against BSA::C12 or BSA::N12 when absorbed with BSA::C12. After absorption with BSA::N12, however, titres of 1/200 and 1/400 were obtained against BSA::N12 and BSA::C12 respectively. Rabbit 2C gave no titre against BSA::N12 and C12 after absorption with BSA::N12 and no titre against BSA::C12 after absorption with BSA::C12. BSA::C12 absorbed serum gave a titre of around 1/800 against BSA::N12.

Unabsorbed sera from test bleed 3 gave titres of 1/1280 in all four animals when tested against BSA-coupled homologous peptides. Absorption with BSA::N12, BSA::C12, un-conjugated peptide N12 and un-conjugated peptide C12 did not significantly reduce the measurable titre in any case. Sera absorbed with BSA-coupled homologous peptide gave the following titres against BSA-coupled heterologous peptides. 2A, 1/320; 2B, 1/640; 2C, 1/320; 2D, 1/320. Dot blots using serum from rabbit 2C gave a weak positive result on 0.1 and 1µg spots of BSA::N12 and BSA::C12 at serum dilutions of 1/100 and 1/20. Spots containing un-conjugated peptides gave negative results. Strong positives were obtained on the control rabbit and bovine IgG at all serum dilutions.

Serum collected at exsanguination of rabbits 2B and 2C gave the following titres on dot blots using 1µg spots of antigen. 2B, 1/50 against BSA::N12 and C12; 2C, 1/20 against BSA::N12, 1/50 against BSA::C12. In all blots a strong positive was observed on the control IgG spots. Both sera gave a weak reaction to uninfected Sf9 whole-cell extracts up to 1/50.

In view of the results obtained with approaches 1 and 2, it was decided to persist with the same carrier but to concentrate on peptide C12 since this appeared to produce the most promising results. The inoculation protocol of Van Bueren et al. (1993) was adopted given the success they reported with two different peptides and the marked increase in specific titre they achieved after multiple iv inoculations administered 3 to 4 days apart.

III.3.3 Approach 3

(*Rabbits*: 3A - 3C; *Antigen*: BGG::C12; *Inoculation*: 4X sc, 3X or 6X iv (3A)).

Pre-immune sera from all three animals gave no detectable titre against BSA::C12.

Following the third sc inoculation with BGG::C12, the following anti-BGG::C12 titres were detected: rabbit 3A, 1/640; rabbit 3B, 1/160; rabbit 3C, 1/160.

Test sera collected 7 days after 1 round of iv inoculation gave titres of 1/2560, 1/320 and 1/160 for animals 3A, 3B and 3C respectively. Sera collected 18 days post iv boosters produced no significant change in titre in 3B and 3C. Serum from 3A gave titres of 1/4000 against BSA::C12 and 1/1000 against BSA::N12.

Dot blots using serum from rabbit 3A (18 days post iv boosters) gave no detectable titre against unmodified BSA or whole insect cell lysates both expressing and not expressing ClC-1. The same serum gave an anti-BGG response which titred to beyond 1/5000 and a 1/1000 titre against both BSA::N12 and BSA::C12.

ELISA screening of serum from 3A collected at exsanguination, 7 days after a second round of iv inoculations, gave a titre of 1/2000 against BSA::C12.

III.4 Discussion

III.4.1 Approach 1

(*Rabbits*: 1A, 1B; *Antigen*: HRP::C12; *Inoculation*: 2X sc, 1X iv)

The lack of success with approach 1 could conceivably be due to an inability of the two animals used to recognise the antigen as foreign. The same approach used on a number of other animals may induce an immune response. It is also possible that the number of inoculations and relatively small doses were not sufficient to stimulate a response of a detectable magnitude.

III.4.2 Approach 2

(*Rabbits*: 2A - 2D; *Antigen*: BGG::C12 (2A, 2B), BGG::N12 (2C, 2D); *Inoculation*: 5X sc (2A, 2C dose = 300µg; 2B, 2D dose = 600µg).

The lack of any significant specific response, as evidenced by the low titres and the level of cross reactivity with heterologous antigens, by animals 2A and 2D could again be due to the inability of these animals to respond adequately. The titres obtained with these two animals are indicative of the presence of non-specific antibodies. The results obtained with rabbits 2B and 2C with sera collected at the second test bleed suggest some specific response directed against the peptides. This response appears to be mixed with a reaction against a common epitope on both BGG-coupled peptide conjugates which is also found on the BSA-coupled peptides used in screening eg. the aldehyde carrier linkage.

Following the third inoculation, the apparent drop in titre against homologous peptide conjugates, which was no longer absorbable, detected with rabbits 2B and 2C suggests the induction of tolerance and the presence of a mixture of non-specific antibodies.

Tolerance and loss of specificity has been described by other workers (Vaitukaitis, 1981; Van Regenmortal et al., 1988), however, in those reports these phenomena occurred only after more extensive inoculation than used in this case.

III.4.3 Approach 3

(*Rabbits*: 3A - 3C; *Antigen*: BGG::C12; *Inoculation*: 4X sc, 3X or 6X iv (3A)).

Animals 3B and 3C appeared to be unable to respond specifically to the antigens. The increasing titre and lower level of cross reactivity demonstrated in animal 3A was suggestive of a specific response. Following the second round of iv inoculation, apparent reduction in titre against homologous peptide conjugate and the increased level of cross reactivity with heterologous antigen is again suggestive of the beginnings of tolerance and a response against some common epitope in BSA- and BGG-coupled peptides.

III.4.4 General comments

Overall, attempts to produce a specific anti-ClC-1 polyclonal antiserum have not been successful. Of the animals used here (8 in total), animal 3A gave the most promising results. A number of explanations for the lack of success are possible. It may simply be that none of the animals used here were able to respond adequately to the antigens and that more animals need to be inoculated before a strong responder is found. The number of animals that would need to be inoculated to give a reasonable chance of success is not easy to determine since few authors reporting successful production of anti-peptide antibodies report how many animals were inoculated and of these how many gave a reasonable response. A handbook on the subject (Harlow and Lane, 1988) suggests, when using outbred species such as rabbits, that 3 to 6 animals should be sufficient. However, a total of 5 rabbits were inoculated with BGG::C12 in this study, albeit not all using the same protocol, without success.

It is also possible that the use of BGG as a carrier is inappropriate with these peptides. Gamma-globulins from one species are able to induce a specific immune response in a different species, as evidenced by the availability of commercially prepared cross-species anti-immunoglobulins. However, without an extensive, systematic assessment of the immunogenicity of the BGG::peptide conjugates it is impossible to be sure that the bound peptides are presented in a manner which is optimal from the point of view of immunogenicity. What is apparent from the results obtained is that low titre, non-specific antibodies were induced with BGG-coupled peptides.

Cross-reactivity may be due to an immune response directed against the peptide carrier linkage although other workers have successfully employed immunisation and screening antigens produced by linkage of peptides to different protein carriers using the same method (eg. Fuller et al., 1992), ie. gluteraldehyde treatment, without any apparent problem. Reported successes may simply reflect the induction of higher specific anti-peptide titres allowing use of antisera at dilutions which make the presence of low titres of cross reactive antibodies inconsequential.

Given the results obtained here, the application of a different carrier and conjugation procedure are worth considering. A possible alternative could be keyhole limpet haemocyanin (KLH), given past successes with its use in production of anti-peptide antibodies directed against membrane proteins (cf. Fuller et al., 1992; Brewster et al., 1993; Gurnett et al., 1995). An effective coupling method employed with this carrier, and others, is activation of carboxyl groups using carbodiimide. Whilst this approach could be used with peptide N12, it is probably not the best choice for peptide C12 in view of the large number of aspartic and glutamic acid residues included in its sequence. In retrospect, a good approach to the problem of carrier/ peptide conjugation would have been to incorporate an extra, unique residue, at the desired

position, specifically for the purpose eg. a terminal cysteine which could be treated with *m*-maleimidobenzoyl-N- hydroxysuccinimide ester (cf. Harlow and Lane, 1988; Gurnett et al., 1995). This would allow coupling via a single, defined residue leaving the entire peptide free to act as an epitope.

Recently, the production of anti-ClC-1 antibodies has been reported (Gurnett et al., 1995). These workers used a synthetic peptide representing the 15 C-terminal amino acids of ClC-1 linked to KLH. Specific antibody purification techniques were employed in isolation of the antibodies. Whilst no indication is given of the number of animals inoculated nor of the titres obtained, the results clearly indicate that the approach used here was valid. It is possible that the extra 3 amino acids included in the oligopeptide used by Gurnett et al. make up the antigenic epitope, or part thereof, against which the antibodies are directed. It is also possible that KLH as a carrier is more effective than BGG in this instance and/ or that the presentation of the antigen differs due to the coupling method used. Since the C-terminus of ClC-1 is completely conserved in human and rat, it is likely that in rabbits this sequence will also be very similar if not identical. The results reported by Gurnett et al. serve to illustrate that despite the highly conserved nature of this sequence, under the right circumstances it can elicit an immune response.

III.4.4.1 Future directions

Despite the *in vivo* sarcolemmal location of ClC-1 having been reported (Gurnett et al., 1995), an anti-ClC-1 antibody would still be of use in future work. We believe that the use of whole ClC-1 as an antigen is the preferred approach to the production of polyclonal sera. For this reason negotiations with our collaborators (TJ Jentsch et al.) are being initiated in the hope of being able to use heterologously expressed ClC-1 in antibody production experiments.

Whilst polyclonal antibodies, raised using the entire protein as antigen, would be of use for various procedures including tracking of protein during solubilisation and purification experiments, antibodies directed against specific regions of the protein would also be extremely useful. For this reason, and in view of the titres observed in serum collected from rabbit 3A, methods for purification of specific anti-C12 antibodies are currently being appraised. The most appropriate method is likely to involve the use of an antigen affinity column. A proposed approach to the production of such a device is linkage of peptide C12 to AH-Sepharose (Ey, 1993). Methods for the production of monoclonal antibodies directed against various regions of ClC-1 are also being investigated with a view to their application to the problem of mapping the structure of the protein in the membrane (cf. Casadei et al., 1984; Adamo et al., 1992).

IV
Biophysics

IV.1 Introduction

IV.1.1 ClC-1

As discussed in Section I, the characteristics of the chloride conductance in mammalian skeletal muscle had been known for some time but the channel responsible had proved to be elusive using various biophysical and biochemical methods. It was the application of molecular biological methods which finally proved successful (Steinmeyer et al., 1991b). Since 1992, a number of reports concerning ClC-1 have appeared in the literature. Most have been regarding mutations in the *Clc-1* gene (ClCN1) particularly with respect to myotonic muscle diseases (*vide* Section VI).

Some new biophysical information has also been published. Expression of the human protein (hClC-1) in HEK293 cells has allowed the calculation of its unitary conductance by non-stationary noise analysis (Pusch et al., 1994). Using this approach, Pusch et al. calculate a value of approximately 1pS. The relative open probability (P_{open}) of the channel was also discussed, these workers finding the apparent P_{open} to be voltage dependent with 0.5 probability occurring at a membrane potential ($V_{1/2}$) of -100mV. It was also suggested that even when maximally activated by voltage, the channel still gates between open and closed states.

Co-expression of mutant and wild type hClC-1 (Steinmeyer et al., 1994) has provided evidence of a multimeric structure for this channel. The results of Steinmeyer et al. suggest that subunits containing particular mutations reduce or destroy the function of normal subunits when both occur in the same multimer. This would explain why

some mutations in the *Clc*-1 gene exhibit a dominant inheritance pattern, as occurs in autosomal dominant myotonia congenita, whilst others are recessive (autosomal recessive generalised myotonia). In the same report, both human and rat ClC-1 were expressed and displayed almost identical biophysical properties with the exception that hClC-1 showed slightly slower kinetics at positive potentials.

Effects of pH on the opening and closing process(es) have also been reported (Fahlke et al., 1995a). Working with hClC-1 expressed in HEK293 cells, Fahlke et al report reduction of internal pH leads to less complete deactivation with hyperpolarisation along with a slowing of the deactivation rate. Reducing external pH was reported to increase the proportion of steady state current without affecting the rate of deactivation. These workers suggest several titratable residues are involved in the opening and closing of the channel. The same group also report that protein kinase C-mediated phosphorylation reduces whole-cell current amplitudes in both muscle fibres (rat) and HEK293 cells expressing hClC-1 (Rosenbohm et al., 1995). This effect was highly dependent on pH with ca. 80% block reported at pH 6 and ca. 40% block at pH 8.5. The fast deactivation time constant also slowed. The use of different phorbol esters produced effects with different time courses leading the authors to suggest the possible involvement of several phosphorylation sites.

Recently, a study, using the double Vaseline gap method, of the characteristics of G_{Cl} in rat psoas muscle fibre segments has been published by Fahlke and Rüdel (1995). This technique allows internal perfusion of fibre segments affording researchers the ability to control the ionic environment on both sides of the membrane. The characteristics of the chloride conductance measured in this preparation were in keeping with the biophysical behaviour of heterologously expressed ClC-1. In their publication, Fahlke and Rüdel report a conductivity sequence of $Cl^- > Br^- > I^-$ and

complete block of membrane G_{Cl} following application of 0.1mM A9C. Using a holding potential of -85mV, voltage steps to hyperpolarising potentials evoked deactivating currents whilst steps to depolarising potentials resulted in activating current kinetics. Three components could be extracted from both activating and deactivating currents, 2 of these being exponential and one constant. The time constants of the exponential components differed for activating and deactivating currents. The time constant of the faster component of activating and deactivating currents was found to be voltage dependent giving values of 37.5 and 67ms at +55 and -5mV respectively (activating current) and 99.3 and 30.6ms at -35 and -105mV respectively (deactivating current). The slower component was reported to be essentially voltage independent for activating currents (τ = 450ms at potentials > -5mV) but displayed voltage dependence for deactivating currents (τ = 738.5 or 139.4ms at -35 or -105mV respectively). Steady-state activation data were well fitted by a Boltzmann distribution with $V_{1/2}$ occurring at -39mV and the apparent gating charge calculated to be 1.5. Other characteristics reported included incomplete deactivation in response to hyperpolarising potentials, a lack of sensitivity to changes in internal chloride concentration (5 vs 61mM), inward rectification of instantaneous and steady state I/V curves and activation which was followed by current decline following prolonged depolarisations (>5s). The authors also suggested that they were measuring a real inactivation process on the basis of the response to increasing duration of prepulses positive to the holding potential followed by test pulses negative to it. This manoeuvre resulted in currents in response to test and prepulses which decreased with similar time constants.

From all of the above it is apparent that whilst our knowledge of the basic biophysical properties of ClC-1 is rapidly increasing, there is clearly still much to be investigated.

IV.1.2 Other ClC family members

At the commencement of this work the ClC family numbered only three, the members being ClC-0 (Jentsch et al., 1990), ClC-1 (Steinmeyer et al., 1991b) and ClC-2 (Thiemann et al., 1992). At the time of writing the family had grown to include an additional eight members, yClC-1 (Huang et al., 1994), ClC-3 (Kawasaki et al., 1994), ClC-4 (van Slegtenhorst et al., 1994), ClC-Ka, ClC-Kb, ClC-K1, ClC-K2 (Uchida et al., 1993; Kieferle et al., 1994) and ClC-2g (Malinowska et al., 1995). Whilst all members of the family show similarities in their predicted primary structure, their individual biophysical characteristics vary.

ClC-0 had been extensively studied at the single channel level in lipid vesicles and artificial bilayers (*vide* Section I). More recently, expression in *Xenopus* oocytes of the cDNA encoding this channel (Jentsch et al., 1990) has suggested the action of the permeating anion as the gating charge, at least in the case of the fast gate (Middleton et al., 1994; Pusch et al., 1995a). The channel shows deactivation at hyperpolarising voltages similar to that seen with ClC-1 but, in contrast to ClC-1, there is no evidence of outward current saturation (inward rectification) at depolarising potentials.

ClC-2 is ubiquitously expressed and is thought to be involved in cell volume regulation (Thiemann et al., 1992). Its cDNA encodes a 907 amino acid protein of ca. 99kDa molecular mass with 55% homology to ClC-1. Expression in oocytes shows it to be activated slowly by hypotonicity (Gründer et al., 1992) and strong non-physiological hyperpolarisation. Once activated it shows a linear instantaneous current/voltage relationship and exhibits halide selectivity $Cl^- \geq Br^- > I^-$. Noise

analysis estimates its unitary conductance to be in the range 3 - 5pS (Jentsch et al., 1995a).

The cDNA encoding ClC-2g was isolated from a rabbit gastric library (Malinowska et al., 1995) and shows 93% sequence homology to ClC-2. The encoded protein is 898 amino acids in length with a predicted molecular mass of ca. 98kDa and is thought to be involved in HCl secretion. Biophysical investigation of *Xenopus* oocyte expressed protein in lipid bilayers demonstrated a linear current/voltage relationship with a unitary conductance of ca. 7pS and selectivity $I^- > Cl^- > NO_3^-$. The channel was also shown to be active at pH 3 and activated by PKA-mediated phosphorylation.

Clc-3 cDNA isolated from rat kidney (Kawasaki et al., 1994) encodes a 760 amino acid protein with 24% identity to other members of the ClC-family. Despite being isolated from kidney, ClC-3 is abundantly expressed in brain. Kawasaki et al. reported that this channel conducted inward rectifying currents which were blocked by 4,4'-diisothiocyanatostilbene-2,2'-disulphonic acid (DIDS) but not by A9C-or diphenylamine-2-carboxylate (DPC). The channel was also shown to be blocked following activation of PKC-and displayed selectivity $I^- > Cl^- = Br^-$ > acetate > gluconate. Some doubt was later cast as to whether the currents recorded in oocytes were due to expressed ClC-3 or native *Xenopus* channels (Jentsch et al., 1995a). In a more recent report, Kawasaki et al. (1995) have presented convincing whole-cell and single channel data from ClC-3 expressed in CHO cells. In these cells the channel shows the same properties as were found in oocytes. Additional experiments performed by Kawasaki et al (1995) clearly demonstrated its sensitivity to Ca^{++} and its multistate single channel behaviour.

The same research group isolated a cDNA, designated *Clc*-K1, from rat kidney (Uchida et al., 1993) which encodes a 686 amino acid protein with ca. 40% identity to

other ClC-channels. The protein was found to be predominantly expressed in the thin ascending limb of the loop of Henle . Expression in oocytes produced currents with similar properties to ClC-3 which were blocked by DIDS and A9C. The selectivity series reported was $Br^- > Cl^- > I^-$.

Kieferle et al (1994) independently isolated *Clc*-K1 (r*Clc*-K1) cDNA. These workers also isolated a second highly homologous cDNA from rat kidney, designated r*Clc*-K2, and two human homologues h*Clc*-Ka and Kb. The rat sequences show 83% identity whilst the human proteins are 91% identical. Between species the sequences show ca. 80% identity. Defects in hClC-K2 have recently been linked to Dent's disease, an X-linked hereditary nephrolithiasis (Fisher et al., 1994). In contrast to Kawasaki and co-workers, Kieferle et al. were unable to obtain functional expression of any of these cDNAs in *Xenopus* oocytes despite demonstrating adequate protein expression. They report finding similar currents to those reported for ClC-K1 (Uchida et al., 1993) in control oocytes and therefore suggest that the ClC-K group should be classified as putative chloride channels at this stage.

No report of attempts to express yClC-1 has appeared in the literature to date. This sequence was discovered on the X chromosome of *Saccharomyces cerevisae* (Huang et al., 1994) and apparently encodes a 779 amino acid protein with homology to other ClC-channels, particularly in the putative trans-membrane domains.

As with yClC-1, ClC-4 was identified purely on DNA sequence data (van Slegtenhorst et al., 1994). The gene, ClCN4, is found on the human X chromosome and encodes a 760 amino acid protein. Northern blot analysis showed ClC-4 mRNA to be abundant in skeletal muscle with lower levels detectable in heart and brain. The transcript was also shown to be conserved in other mammals including mouse and hamster. No attempt was made to express ClC-4.

It is clear from the above that our knowledge of the molecular biology of this group of channels is expanding at a faster rate than our understanding of their functions and biophysics. It seems likely that more members will be added to this family on the basis of DNA/ protein sequence as research continues.

IV.2 Materials and Methods

IV.2.1 Chemicals and Reagents

All chemicals and reagents were purchased from established suppliers (*Ajax, BDH, Sigma*) and, except where stated otherwise, were Analar grade. Solutions were prepared in MQ quality water with a resistance of >18MΩ/cm.

IV.2.2 Patch-clamping

IV.2.2.1 Cells

General cell culture and infection methods are described in Section II. Sf9 cells were seeded at low density in 35mm tissue culture dishes and incubated until reaching ca. 50% confluence (typically 2-3 days). Cells were then infected with virus (BVDA6.3 or BVDA2.1) at a moi of 50. After adsorption, the virus inoculum was left on the cells and 1ml of fresh medium was added. After 24-26 hours incubation, cells were resuspended in their medium and 10µl aliquots were seeded onto glass coverslip fragments (ca. 1 x 0.5cm). After settling for at least 20 minutes at room temperature - the cells were covered with fresh culture medium and kept at ambient temperature, for up to 10 hours, until needed. Cells were typically patched between 30 and 36 hpi.

IV.2.2.2 Solutions

Bath solution contained NaCl 170mM, $MgCl_2$ 2mM, $CaCl_2$ 2mM and HEPES-Na 10mM at pH 7.4. Except where indicated otherwise, pentobarbitone-Na (BP grade, *Faulding*) was added to bath solution at a final concentration of 0.5mM. In experiments where different anion permeabilities were determined, NaCl

concentration was reduced to 30mM and either NaI, NaBr or $NaNO_3$ was added to a final concentration of 140mM.

Pipette solution contained KCl 40mM, K-glutamate 120mM, EGTA 10mM and HEPES-Na 10mM at pH 7.2.

IV.2.2.3 Pipettes

Pipettes were of borosilicate glass and were pulled on a *Kopf* model 720 two step vertical pipette puller. Tips were coated with Sylgard (*Dow Corning*) and fire polished using a glass coated element. Employing the above solutions, pipette resistances were typically of the order of 2-4 MΩ.

IV.2.2.4 Apparatus and establishment of whole-cell configuration

Coverslip fragments carrying cells for patch-clamping were mounted in a glass bottomed bath with a main chamber of ca. 1 x 4 cm on an inverted phase contrast microscope. The main chamber was connected to 1cm diameter wells at each end via 5mm long, 1mm radius semicircular channels. Rapid solution exchange was effected by addition of new solution to one well whilst the other was attached to vacuum. The bath volume (main chamber) was set by the depth of the suction tube and was kept to a minimum, typically 500-900µl.

Silver/ silver chloride wires were used at both pipette and reference electrodes with the reference electrode being connected to the bath solution via a salt bridge composed of pipette solution containing 1% agar.

Whilst entering the bath and approaching cells, positive pressure (ca. 10cm H_2O) was maintained at the pipette tip via a water column. Once in contact with the cell membrane, the positive pressure was removed and cell-attached mode was established by application of slight negative pressure per mouth. After establishment of a high resistance seal, whole-cell mode was obtained by application of a pulse of negative

pressure, again by mouth. During the course of current recording in whole-cell mode the pipette was exposed to atmospheric pressure. Establishment and maintenance of whole-cell mode was determined by monitoring capacitance in response to a 50mV voltage step.

IV.2.2.5 Data collection and analysis

Currents were recorded using a *List* EPC-7 patch-clamp amplifier connected via a TL1-125 interface (*Axon Instruments*) to an IBM compatible PC-running pCLAMP v5.5 software (*Axon Instruments*). Data were filtered at 3kHz using a 3 pole Bessel filter and sampled at a rate of 10kHz. During recording, capacitance transients were corrected using the circuitry on the EPC-7 amplifier and series resistance compensation adjustment was set as high as was possible without inducing "ringing", typically 70 - 90%.

IV.2.2.6 Voltage protocols

Three voltage step protocols were used routinely, all employing a holding potential of -30mV and a 2 second delay between individual voltage pulses. One protocol (activation protocol, Figure 4.1a) consisted of eleven 100ms test pulses from -120 to +80mV (20mV increments) each preceded by a 100ms prepulse to +40mV. The second protocol (-120mV deactivation protocol, Figure 4.1b) consisted of eleven 100ms prepulses from -120 to +80mV (20mV increments) each followed by a 100ms test pulse at -120mV. The third protocol (-80mV deactivation protocol, Figure 4.1c) was similar to the -120mV deactivation protocol except that 10 100ms prepulses ranging from -100 to +80mV were used followed by a test pulse at -80mV.

IV.2.2.7 Analysis

All data analysis was performed using pCLAMP v5.5 software (*Axon Instruments*), predominantly with the "clampfit" program.

Data are quoted as mean ± SEM with the exception of $V_{1/2}$ values, obtained from fitting of Boltzmann functions, which are quoted as mean ± 95% confidence interval (C.I.). Statistical analyses (analysis of variance and paired t-test) were performed using the data analysis tools supplied with EXCEL (*Microsoft*). When testing for statistical significance, probabilities of >0.05 were regarded as not significant. When comparing two $V_{1/2}$ values, differences were considered significant if the mean of each of the two values being compared lay outside the 95% C.I. of the other.

IV.3 Results

IV.3.1 Cell-attached

High resistance (>10GΩ) seals were generally easily obtained with both infected and uninfected cells. No single channel activity was detected in any cell-attached patch nor was there any detectable current non-linearity in response to voltage steps (activation protocol) which might be attributed to the presence of channels with a conductance too small to be resolved at the single channel level. The amenability of uninfected Sf9 cells to patch-clamping was unaffected by the age of the cells with high resistance seals obtained in around 90% of attempts even after 4 days incubation. Infected cells, however, became progressively more difficult to patch and increasingly fragile after ca. 48 hours infection.

IV.3.2 Whole-cell

IV.3.2.1 BVDA2.1 (negative control virus) and uninfected cells

The activation protocol evoked currents which were almost linear with respect to voltage (Figure 4.2a, b). All cells tested showed similar sized currents with maxima typically of 50 - 80pA inward and outward (Figure 4.2a, b). Slightly larger currents could be induced under hypoosmotic conditions which could be attributed to native, volume regulatory channels (G. Rychkov, unpublished observations). These currents

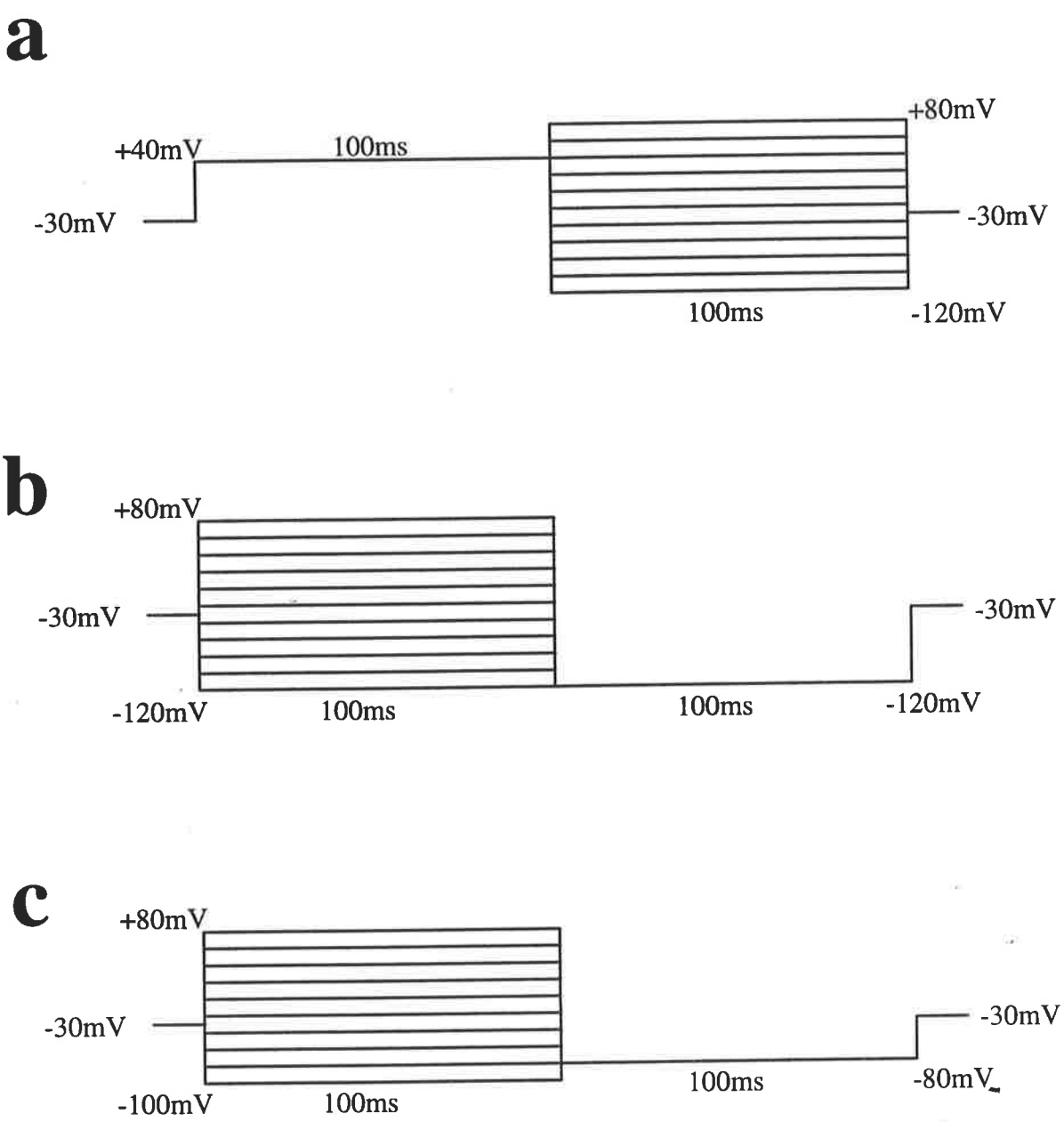

Figure 4.1. Patch clamping voltage protocols.
Voltage protocols used in whole cell patch clamp experiments. Holding potential for all protocols was -30mV. Delay between pulses was 2 seconds.
a: Activation protocol. 100ms test pulses ranging from -120mV to +80mV in 20mV increments each preceded by a 100ms prepulse to +40mV.
b: -120mV deactivation protocol. 100ms prepulses ranging from -120mV to +80mV in 20mV increments each followed by a 100ms test pulse to -120mV.
c: -80mV deactivation protocol. As for b except prepulse range -100 to +80mV followed by test pulses at -80mV.

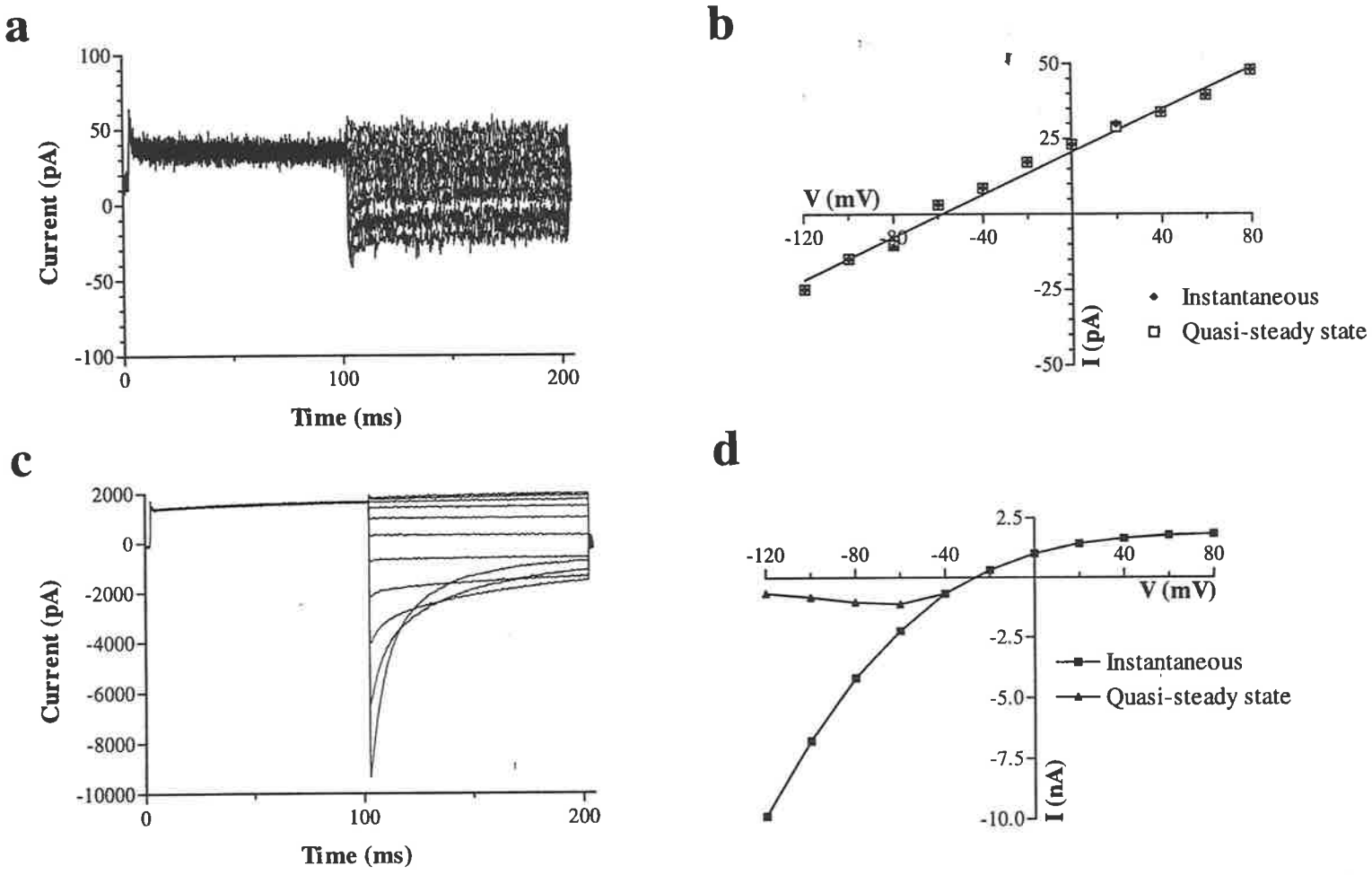

Figure 4.2 Comparison of ClC-1 positive and negative cells.
a: Current traces elicited by the activation voltage protocol in a typical BVDA2 infected cell. **b:** Peak and steady state current/voltage relationships for Sf9 cell infected with expression vector BVDA2 (negative control) derived from current traces in **a**. **c:** Current traces elicited by the activation voltage protocol in a typical BVDA6 infected cell. **d:** Peak and steady state current/voltage relationships for Sf9 cell expressing ClC-1 (expression vector BVDA6) derived from current traces depicted in **c**.

were readily blocked by the addition of pentobarbitone 0.5mM (G. Rychkov, unpublished observations) to leave the abovementioned small, whole-cell currents. No difference in current shape or amplitude was detected in BVDA2.1 infected or uninfected cells regardless of the time pi (up to 48 hours).

IV.3.2.2 BVDA6.3 infected

Before ca. 28 hpi most cells exhibited similar currents to those seen in negative control cells. A small proportion of cells do show voltage and time dependent currents at this stage, however the currents are quite small with maximum inward currents of no more than 400pA in response to a -120mV pulse. After ca. 30 hours pi and in contrast to BVDA2.1 infected and uninfected cells, a high proportion of cells exhibit large inwardly rectifying currents. These currents varied in magnitude from cell to cell but were typically of the order of 3nA inward and 0.5nA outward with many cells exhibiting currents as large as 10 - 15nA inward and 2 - 2.5nA outward (Figure 4.2c, d). The currents were unaffected by pentobarbitone at concentrations up to 10mM (G. Rychkov, unpublished observations). The measured reversal potential was -23.9 ± 1.4mV (mean ± SD, n = 25) which, after correction for a junction potential of -14.6mV, is close to that calculated from the Nernst equation (-36.6mV) for the imposed chloride gradient.

Deactivation of peak inward current was evident at voltage steps negative to -60mV, rectification occurred at positive voltage steps and saturation of outward current occurred at steps positive to +40mV (Figure 4.2c, d). Using the -120mV deactivation voltage protocol, maximal inward current was found to be induced by 100ms prepulses to +40mV (Figure 4.3). No further significant increase in current was induced by prepulses positive to this value (Figure 4.3 inset).

Throughout this thesis total peak currents measured in response to, and at the beginning of, voltage steps will be referred to as instantaneous currents whilst total currents measured at the end of each 100ms test pulse will be referred to as quasi-steady state currents, this being distinct from the constant current component discussed below.

IV.3.2.3 Kinetics

IV.3.2.3.1 Effect of voltage

The deactivating currents evoked by hyperpolarising voltage steps were made up of 3 resolvable components, two exponentially decaying and one constant (Figure 4.4a). The time constants of the two exponentially decaying components varied with voltage. At steps to -140mV the fast (component 1) and slow (component 2) components had time constants of 7.1 ± 0.3 (τ_1) and 22.1 ± 1.2 (τ_2) ms (n = 7) respectively. As voltage steps became less negative, τ_1 became smaller and τ_2 larger until finally merging, at around -60mV, with the capacitive transient and quasi-steady state current respectively. Time constants for both components at the various voltage steps are presented in Table IVa. Analysis of variance showed the effect of voltage on both time constants to be significant ($P<0.0001$).

The relative contributions of the three components to the total current also varied with voltage. At -140mV the fast component contributes 70.5 ± 2.3%, the slow 23.8 ± 2.1% and the constant 6.5 ± 0.5% (n=8). As the potential became less negative, the proportion of constant current component increased whilst the relative amplitude of component 1 decreased. Component 2 first increased in proportion, reaching a maximum of ca. 50% at -100mV, before decreasing between -100 and -60mV (Table IVa). As with the time constants, analysis of variance showed the voltage effect on relative component amplitudes to be significant ($P<0.0001$).

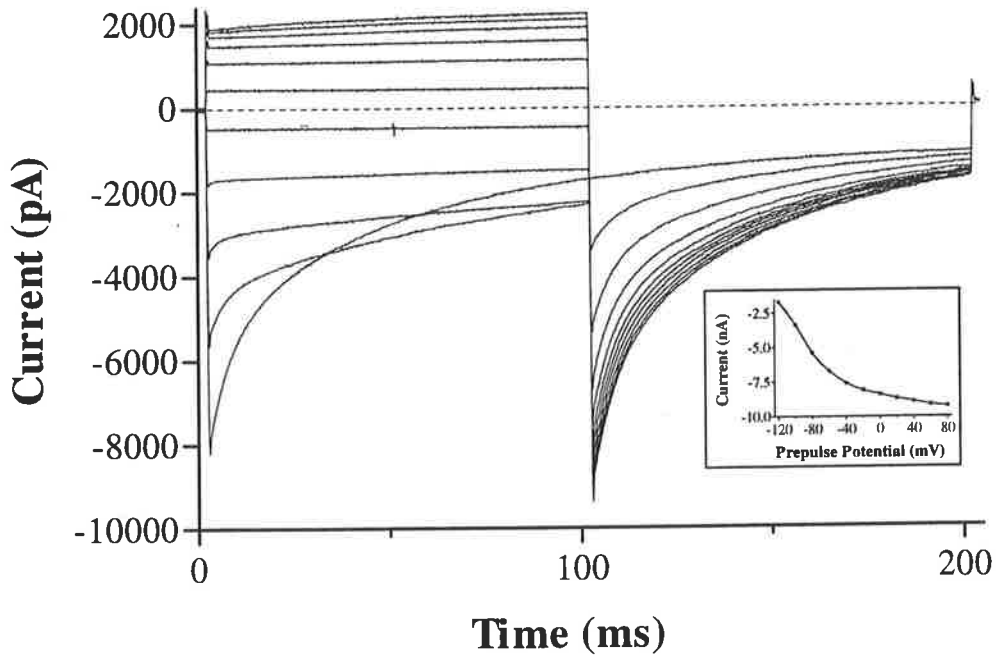

Figure 4.3
Currents elicited using the inactivation voltage protocol in an Sf9 cell expressing ClC-1. **inset:** Instantaneous currents measured at the beginning of the -120mV test pulse as a function of the prepulse potential.

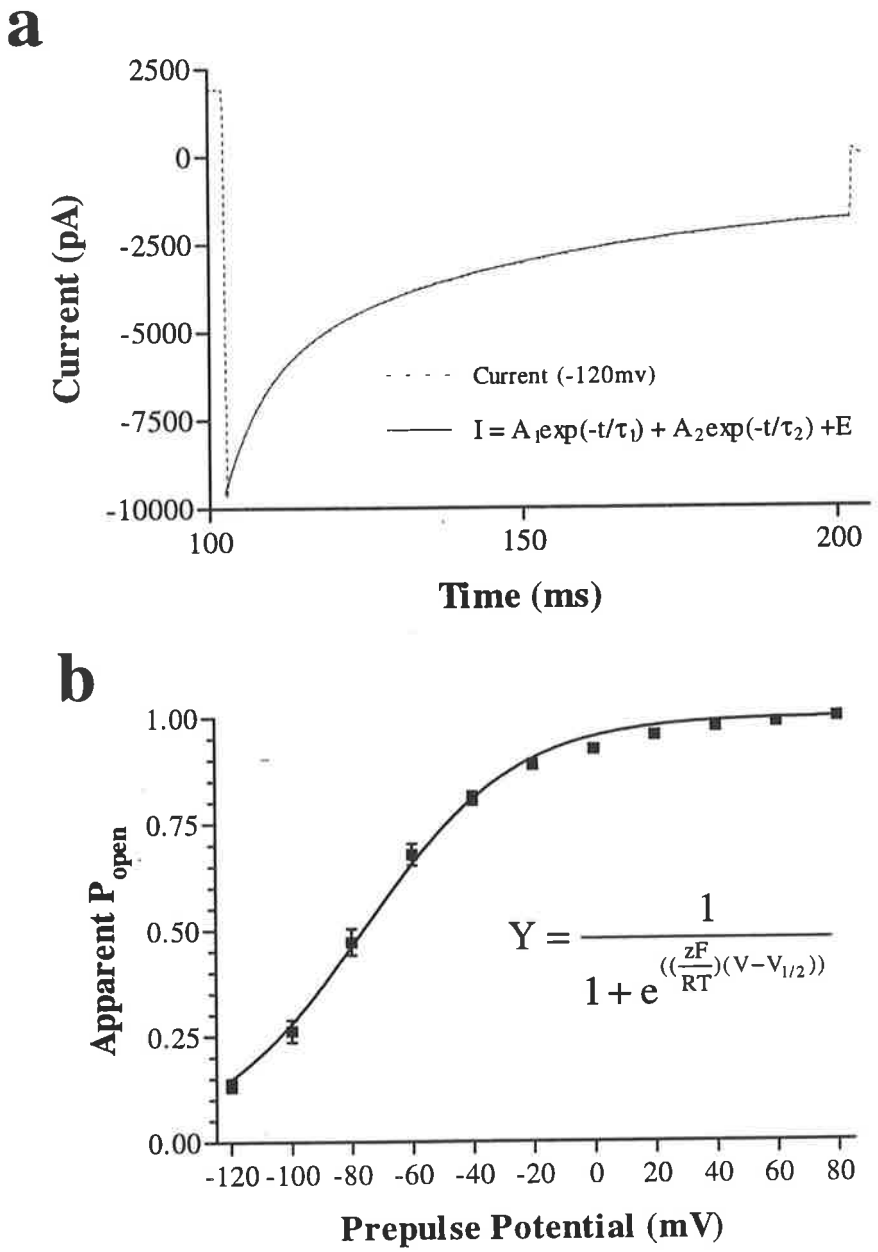

Figure 4.4

a: Current trace (broken line) recorded during a -120mV test pulse, following a 100ms prepulse to +40mV, in an Sf9 cell expressing ClC-1 fitted with equation (solid line) of the form $I = A_1 e^{(-t/\tau_1)} + A_2 e^{(-t/\tau_2)} + E$ where A_1 = -3477pA, τ_1 = 6.58ms, A_2 = -4979pA, τ_2 =48.48ms and E = -1146pA (R^2 = 0.9999). **b:** Apparent open probability immediately following establishment of whole-cell configuration, calculated by division of instantaneous currents measured after stepping from each prepulse to -120mV by the value obtained following a +80mV prepulse. Data are fitted with a Boltzmann funtion of the form shown on the graph where z = -1.01 and $V_{1/2}$ = -76.1mV (R^2 = 0.9996)

Component	Parameter	Membrane potential (mV) -140	-120	-100	-80	-60
Fast	Amplitude	70.5 ± 2.3 (8)	47.2 ± 1.7 (16)	33.1 ± 1.7 (16)	21.4 ± 1.0 (16)	12.6 ± 0.8 (16)
	τ_1	7.1 ± 0.3 (7)	5.9 ± 0.2 (23)	5.1 ± 0.1 (23)	4.0 ± 0.1 (23)	3.0 ± 0.2 (23)
Slow	Amplitude	22.8 ± 2.1 (8)	43.6 ± 1.9 (16)	49.6 ± 1.7 (16)	42.4 ± 2.4 (16)	25.4 ± 2.6 (16)
	τ_2	22.1 ± 1.2 (7)	26.1 ± 1.4 (23)	39.9 ± 2.0 (23)	59.2 ± 2.2 (23)	80.4 ± 4.2 (23)
Constant	Amplitude	6.5 ± 0.5 (8)	9.1 ± 0.6 (16)	17.7 ± 1.7 (16)	36.1 ± 2.7 (16)	62.1 ± 2.8 (16)

Table IVa:
Time constants in milliseconds and relative component amplitudes, expressed as percentage of total current, (mean ± SEM) measured immediately following establishment of whole cell configuration (t=0). Number of observations is given in brackets below each value.

Component	Parameter	Membrane potential (mV) -120	-100	-80	-60
Fast	Amplitude	39.8 ± 1.7 (19)	27.9 ± 1.1 (19)	17.5 ± 0.8 (19)	11.0 ± 0.6 (10)
	τ_1	7.1 ± 0.2 (20)	5.9 ± 0.2 (20)	4.7 ± 0.2 (20)	2.9 ± 0.2 (15)
Slow	Amplitude	43.3 ± 1.4 (19)	40.1 ± 1.3 (19)	26.8 ± 1.1 (19)	13.6 ± 0.6 (10)
	τ_2	40.2 ± 2.2 (20)	62.8 ± 3.1 (20)	76.9 ± 2.6 (17)	99.5 ± 4.1 (5)
Constant	Amplitude	16.9 ± 0.9 (19)	32.1 ± 1.7 (19)	55.7 ± 1.6 (19)	75.5 ± 0.7 (10)

Table IVb:
Time constants, in milliseconds, and relative component amplitudes, expressed as percentage of total current, (mean ± SEM) measured 30 minutes after establishment of whole cell configuration (t=30). Number of observations is given in brackets below each value.

Potential (mV)	I_{inst30}/ I_{inst0}	I_{qss30}/ I_{qss0}
-120	1.22 ± 0.16	2.39 ± 0.39
-100	1.23 ± 0.14	2.55 ± 0.37
-80	1.29 ± 0.15	2.16 ± 0.22
-60	1.20 ± 0.09	1.67 ± 0.15
-40	1.19 ± 0.17	1.35 ± 0.19
-20	1.70 ± 0.23	1.71 ± 0.22
0	1.32 ± 0.07	1.31 ± 0.06
20	1.27 ± 0.06	1.25 ± 0.06
40	1.25 ± 0.07	1.21 ± 0.07
60	1.23 ± 0.07	1.19 ± 0.07
80	1.18 ± 0.07	1.16 ± 0.07

Table IVc:
Instantaneous and quasi-steady state ratios (mean ± SEM, t=30/ t=0) at different membrane potentials. n = 6 throughout.

The apparent open probability (P_{open}) was calculated using currents elicited by the -120mV deactivation voltage protocol. Instantaneous currents, measured at the beginning of the -120mV test pulse, following each prepulse were divided by the value obtained following the +80mV prepulse. At positive potentials the apparent P_{open} was close to 1. The minimal value obtained following the -120mV prepulse was close to 0.1 (Figure 4.4b). The data were well fitted by a Boltzmann function with a $V_{1/2}$ of -76.1 $\pm$ 2.5mV and an apparent gating charge of approximately -1.

IV.3.2.3.2 Effect of time

During the first 20 minutes post establishment of whole-cell configuration, current amplitude gradually increased. The amount of increase was highly variable from cell to cell and did not appear to be related to the size of the initial currents or cell dimensions. All cells, however, exhibited the same pattern and time course of current increase and had stabilised by 20 - 25 minutes post perforation after which no further change in any current parameter was detected.

At 30 minutes post establishment of whole-cell, and over the voltage range tested (activation voltage protocol), instantaneous current (I_{inst30}) divided by the initial current (I_{inst0}) gave an average of 1.28 $\pm$ 0.04 (n = 6). The current increase was fairly consistent across the voltage range, no significant difference being found when comparing the degree of increase at the different voltages. Analysis of variance did however demonstrate a significant difference between currents measured at each voltage at the 30 minute time point compared to those measured at time 0 (P = 0.0028).

At voltage steps between -40 and +80mV, the quasi-steady state current (I_{qss}), measured at the end of the 100ms test pulse, showed increases comparable with those

seen with instantaneous current (I_{qss30}/ I_{qss0} = 1.22 ± 0.03, n = 6). At more negative potentials a consistently greater increase in I_{qss} compared to I_{inst} was observed. Analysis of variance returned a significant value when comparing I_{qss30} with I_{qss0} at each voltage (P<0.0001) and finds a significant difference between the amount of increase at the different potentials (P = 0.0006). Post-hoc testing (Tukey's test) finds the mean values obtained at -120 and -100mV to be significantly different from those obtained at voltages positive to -20mV. No significant difference was found between the mean values of the other voltages.

Two way analysis of variance comparing I_{inst30}/ I_{inst0} with I_{qss30}/ I_{qss0} at the different voltages reveals a significant difference (P <0.0001) between the two ratios. A post-hoc Tukey's test finds significant differences only between means of values obtained at -120 and -100mV. A comparison of I_{inst30}/ I_{inst0} and I_{qsst30}/ I_{qss0} at the different voltages is presented in Table IVc.

Time constants for the exponential components also differed at 30 minutes. Time constants measured during a -120mV step were 7.1 ± 0.2 and 40.2 ± 2.2 ms (n = 20) for τ_1 and τ_2 respectively. Both time constants show the same trend with regard to size in response to voltage as is seen immediately after perforation of the cell-attached patch (Table IVb). The relative contribution of each component to the total current at different voltages also follows the same trend as seen initially (Table IVb). As with currents measured immediately after membrane perforation, variance analysis returns significant values when comparing time constants and relative component amplitudes at the different voltages (P<0.0001). Statistical analysis comparing values of both time constants and the relative component amplitudes at each voltage obtained at the two time points returned significant values for all parameters (P<0.0001).

At the 30 minute time point the apparent P_{open} at negative potentials also varies significantly ($P<0.0001$) from that calculated for initial currents. The data fit a Boltzmann function with a valence of approximately -1 but the $V_{1/2}$ occurs at a more negative potential (ca. -90.4 ± 1.6mV, Figure 4.5a), the difference between $V_{1/2}$ values being significant. The overall shape of current/voltage curves remains very similar at 30 minutes compared to that recorded immediately after patch perforation (Figure 4.5b).

IV.3.2.4 Foreign anions

Currents measured in the presence of other anions clearly show the selectivity of ClC-1 for chloride over bromide, iodide and nitrate (Figure 4.6). The selectivity series for those anions tested was $Cl^- > Br^- > NO_3^- > I^-$. All three foreign anions reduce both outward and inward current to varying degrees and shift the reversal potential to less negative values (Figure 4.7). These phenomena are consistent with channel block induced by these ions.

IV.4 Discussion

IV.4.1 Negative control cells

The currents measured in both uninfected and BVDA2 infected cells are typical of those reported by other workers using this system (Klaiber et al., 1990; Kartner et al., 1991; Birnir et al., 1992; Joyce et al., 1993). The current amplitudes reported here are very similar to those reported by Kartner et al. (1991) and slightly smaller than reported by Birnir et al. (1992). The use of pentobarbitone to reduce currents through native channels reported by the latter researchers was also found to be effective in our laboratory. The ease with which high resistance seals were formed on Sf9 cells, infected or uninfected, is also typical of previous reports, the rate of successful seal formation being similar to that reported by Joyce et al. (1993). As was also reported

by these researchers when using lytic virus, we find the cells increasingly difficult to patch after around 48 hours infection.

IV.4.2 ClC-1-expressing cells

The variability of current amplitude from cell to cell and the increase in the size of instantaneous currents over the course of infection, as reported here, is a feature of the baculovirus/ Sf cell system which has previously been noted (Klaiber et al., 1990). Due to the transient nature of recombinant protein expression and the lytic nature of the virus, it has been suggested that electrophysiological studies of baculovirus infected Sf9 cells are best performed between about 24 and 72 hpi (Joyce et al., 1993). Our experience suggests that the experimental window for patch-clamping is even narrower, spanning ca. 14 hours from 30 to 44 hpi. PAGE analysis has clearly shown that ClC-1 is being expressed in infected Sf9 cells before 30 hpi (*vide* Section II). The apparent lack of measurable channel activity between 24 and 30 hpi suggests that even though the protein is being expressed it is predominantly located intracellularly, probably throughout the post-translational machinery of the cell, and is not yet inserted in the plasma membrane in measurable quantities. After this time there would appear to be a rapid increase in the number of recombinant channels inserted into the plasmalemma of many cells as evidenced by the relative abundance of ClC-1 positive cells and the size of whole-cell currents measured therefrom.

IV.4.2.1 Kinetics

The general characteristics of ClC-1 currents as measured in Sf9 cells are very similar to those reported for this protein when expressed in other heterologous systems (Steinmeyer et al., 1991b, 1994; Pusch et al., 1994; Fahlke et al., 1995b) and as measured in skeletal muscle fibres (Fahlke and Rüdel, 1995). Inward rectification above -20mV and saturation at potentials positive to +40mV are consistent features of

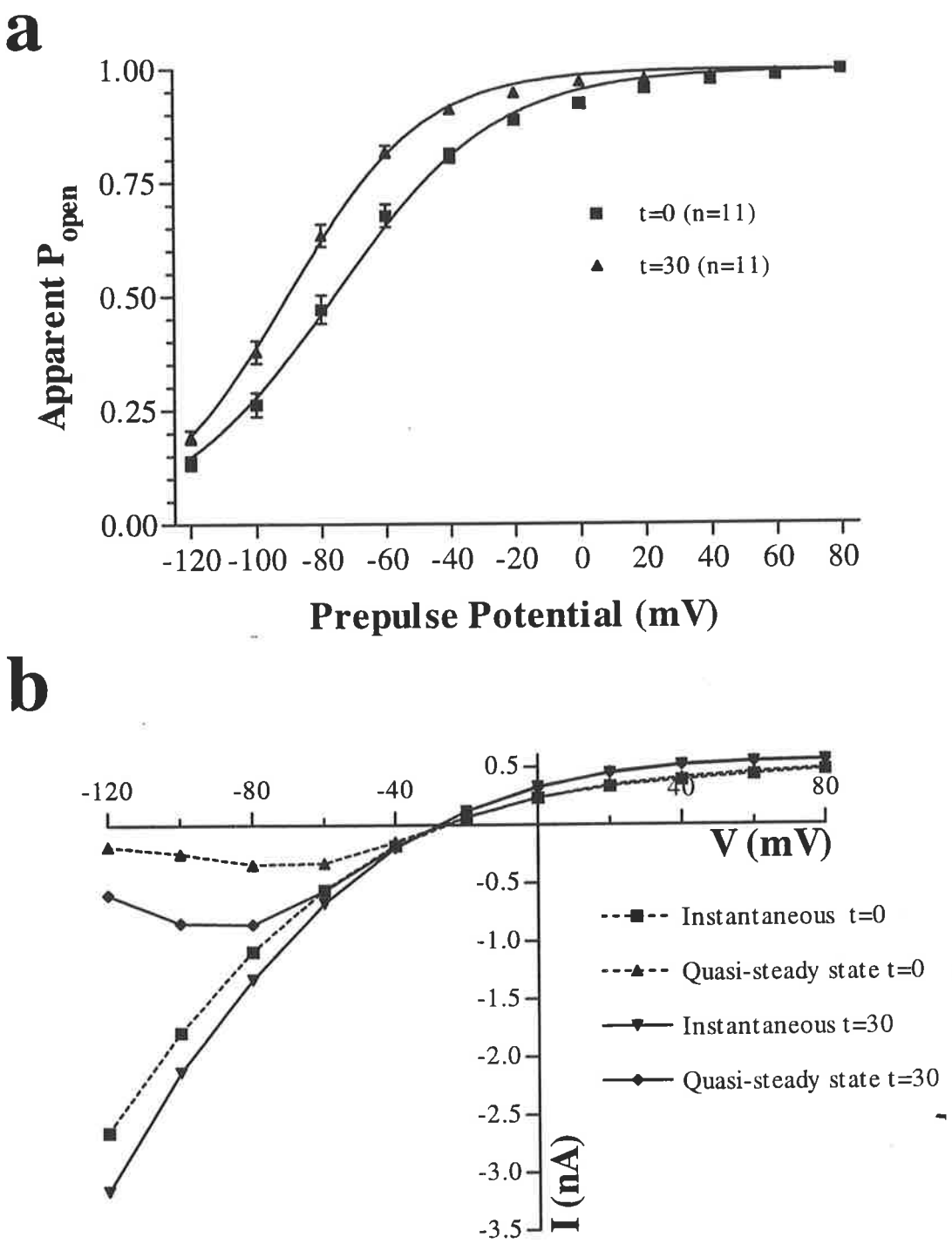

Figure 4.5. Effect of time.
a: Relative open probabilities at time = 30 minutes, calculated as described in Figure 4.4b. Data for time = 0 are included for comparison. Data are fitted with Boltzmann functions as described in Figure 4.4b. For t = 30, z = -1.22 and $V_{1/2}$ = -90.4mV (R^2 = 0.9998) **b:** Current/voltage relationships for peak and quasi-steady state currents in the same cell measured immediately after establishment of whole cell configuration (t=0) and 30 minutes later (t=30).

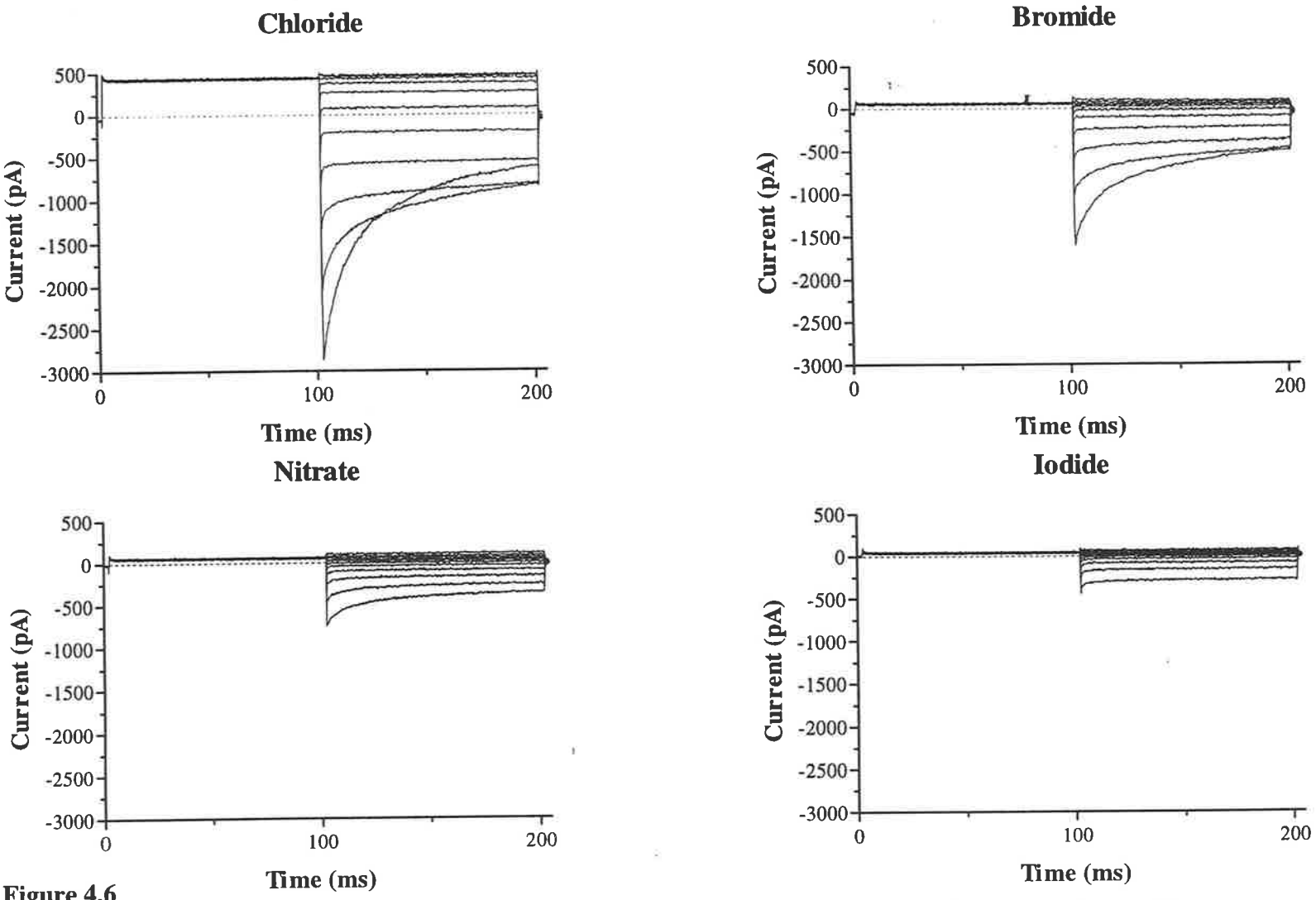

Figure 4.6
Current traces elicited using the activation voltage protocol in the same cell in bath solutions contianing 30mM Cl- plus the indicated anion at 140mM final concentration.

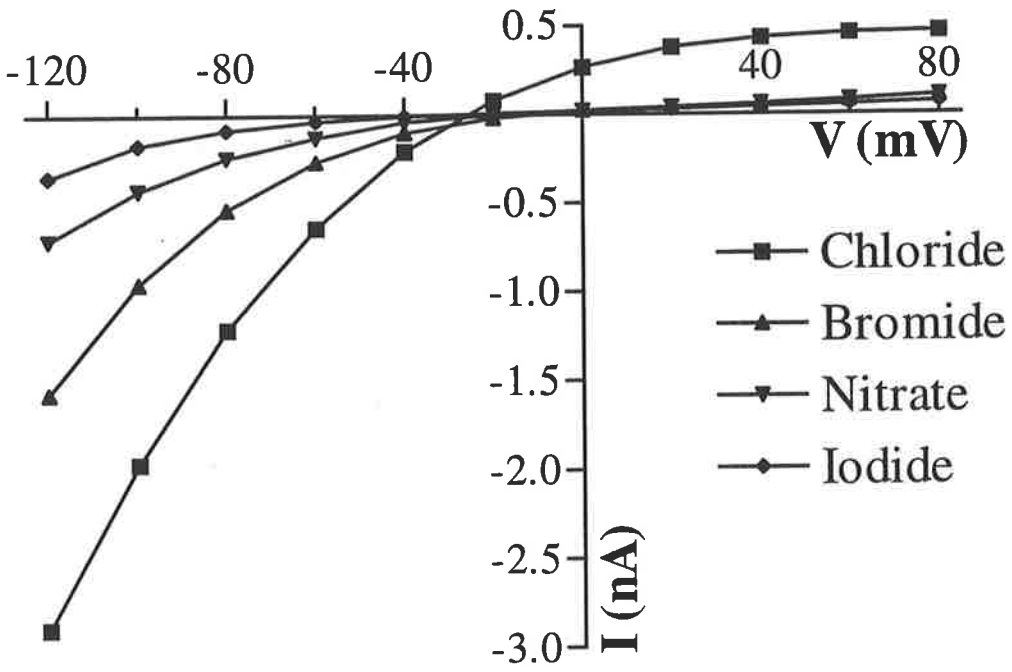

Figure 4.7. Instantaneous current/voltage relationships in the presence of different anions. Plots derived from current traces depicted in Figure 4.6.

all reports as is the deactivation of currents at hyperpolarising potentials, the degree of deactivation increasing with greater hyperpolarisation. There is also consensus on the block of ClC-1 by foreign anions such as iodide and bromide (Steinmeyer et al., 1991b, 1994; Fahlke and Rüdel, 1995; Fahlke et al., 1995b), nitrate also being shown to block ClC-1 in this work.

The details of the kinetics of this channel do, however, vary in the different reports. Deactivation at hyperpolarising potentials in Sf cells is incomplete, as it is in other cell types (Pusch et al., 1994; Fahlke and Rüdel, 1995; Fahlke et al., 1995b). Fitting of a Boltzmann functions to steady state activation data has returned $V_{1/2}$ values ranging from ca. -39mV (Fahlke and Rüdel, 1995) to ca. -100mV (Pusch et al., 1995a). The $V_{1/2}$ values reported here from measurements taken immediately after membrane perforation (t=0) and 30 minutes later (t=30) are within this range and are closest to that reported by Pusch et al. (1994) for hClC-1 measured in HEK cells.

$V_{1/2}$ has been shown to be dependent on external chloride concentration in both ClC-1 (Fahlke et al., 1995b, Rychkov et al., 1995) and ClC-0 (Pusch et al., 1995a). Interestingly, Fahlke et al. (1995b) report $V_{1/2}$ shifts, in response to decreasing chloride concentration, in the opposite direction to that described by others. This effect is most likely due to the use of methane sulphonate as a chloride replacement in their low chloride solutions since this compound has been found to interact in a similar manner to many other foreign anions, such as Br^- and I^- (Rychkov et al., 1995). Whilst all reports from other laboratories describe the deactivating current being made up of two exponentially decaying and one constant component, the reported time constants of the exponents vary widely. The human protein expressed in oocytes exhibits time constants of 40 - 80ms and 300 - 700ms for the fast (τ_1) and slow (τ_2) components respectively (Steinmeyer et al., 1994), similar to those measured for the

rat channel in skeletal muscle fibres (Fahlke and Rüdel, 1995). In contrast, the values for hClC-1 measured in HEK cells are reported to be in the region of 10ms for component 1 and 55ms for component 2 (Fahlke et al., 1995b) which are close to those reported here. Furthermore, whilst the time constants of both components are found to be voltage dependent here and in rat fibres (Fahlke and Rüdel, 1995), the effect of voltage varies. The first time constant, τ_1, becomes smaller and the second, τ_2, larger in Sf cells as the degree of hyperpolarisation is increased whilst both are reported to become larger when measured in muscle fibres. Fahlke et al. (1995b) working with HEK cells expressing hClC-1 find the time constants of both time dependent components to be voltage independent whilst the relative contributions of all three components vary with voltage in a manner virtually identical to that found in this work.

In the cases where slower time constants are reported, relatively long time scales and voltage pulses (seconds) are employed. In these cases the values for τ_1 are very similar to those measured in Sf and HEK cells for τ_2. Where fast kinetics are reported, the time scales and voltage pulses are much shorter (several hundred milliseconds). On a small number of occasions longer lasting pulses have been used with Sf cells expressing ClC-1 and in these cases a third exponentially decaying component is sometimes resolvable with a time constant in the range of those reported for the slower τ_2 (hundreds of milliseconds) (Rychkov and Bretag, unpublished observations). The behaviour of this component in response to voltage etc. has not been thoroughly detailed in our laboratory but its existence raises the possibility that there are in fact three exponentially decaying components involved in the deactivation process and that the discrepancies in reported time constants are due to different

laboratories selectively extracting different pairs of exponents due to the time scales used. If this were the case, then τ_1 reported here and by Fahlke et al. (1995b) correspond to the same very fast component whereas τ_2 in Sf and HEK cells corresponds to the slower τ_1 reported elsewhere (Steinmeyer et al., 1994; Fahlke and Rüdel, 1995). The time constants of the component designated here as τ_2 and the component designated as fast in muscle fibres (Fahlke and Rüdel, 1995) show a similar response to voltage.

Alternatively, ClC-1 may behave differently in different cell types due to an inherent sensitivity to the cytoplasmic and/ or membrane lipid environment. Inward rectification is more pronounced in HEK293, and Sf cells, than in *Xenopus* oocytes (Fahlke et al., 1995b), although this may have more to do with the relative size of leakage currents in the different cell types than differences in cellular environments. Deactivation of hClC-1 at hyperpolarising potentials has been found to be faster in HEK cells than in oocytes (Pusch et al., 1994) but it is not clear whether the same time scales were used with both cell types in that report. Differences in the behaviour of the rat protein compared to the human homologue have also been reported, for example the activation process of the human protein has been reported to be slightly slower than the rat channel when both were measured in *Xenopus* oocytes (Steinmeyer et al., 1994).

One factor which clearly does affect the behaviour of ClC-1 is pH (Rychkov et al., 1995). Reduction in extracellular pH markedly reduces the level of deactivation seen at hyperpolarising voltages. The effect is due to an increase in the relative amplitude of the constant component with a concomitant decrease in the contribution from both exponential components. There is, however, no apparent change in the size of the

time constants, or voltage dependence thereof, for either exponent. Reduction of internal pH, on the other hand, slows deactivation kinetics and shifts the deactivation curve to more hyperpolarised values. Raising the intracellular pH has the opposite effect. Whilst the effect of pH cannot explain the differences in time constants reported by different laboratories, all use solutions of similar pH, it could, at least partly, explain the slowing of time constants, reduced deactivation and the shift of the steady state activation curve which occurs over the first 20 minutes of whole-cell recording in Sf cells. The internal pH of Sf9 cells has not, to my knowledge, been determined. These cells grow optimally at an external pH of 6.2 and thus one might expect their intracellular pH to be low. However, unlike most cell lines, these cells actually raise the pH of their medium as they grow suggesting the possibility of an alkaline cytoplasmic environment. If the internal pH of these cells is higher than that of the pipette solution (pH 7.2) and it takes some time to affect dialysis of the cell interior, then a gradual shift to a more acidic internal pH would occur. This would be seen as a slowing of deactivation kinetics, an increase in constant current and a gradual shift of the steady state activation curve to more hyperpolarised potentials.

Both the rat and human proteins have been reported to be sensitive to protein kinase C (PKC) -mediated phosphorylation (Rosenbohm et al., 1995). In this case the peak current amplitude was reduced and the time constant of the "fast component" became larger, although no specific values were reported, in response to stimulation of PKC activity. The increase in current amplitude over the first 20 or so minutes of whole-cell recording seen here could conceivably be due to a reduction in the protein's phosphorylation state as the cytoplasmic contents of the cell are dialysed with the pipette solution. The concomitant slowing of the deactivation process during this

time, however, is not in keeping with the findings of Rosenbohm et al. being opposite to what would be predicted.

The possibility that the drift in current parameters during the first 20 minutes of whole-cell recording is purely due to a Donnan effect has been considered. The ca. 15mV difference for $V_{1/2}$ between t=0 and t=30 is within the range of voltage shift expected due to a dissipating Donnan equilibrium (Barry and Lynch, 1991) and shows an appropriate time course. If this shift were purely due to a Donnan effect, the t=30 values for relative current amplitudes and time constants would be expected to be the same at -100mV as the t=0 values at ca. -85mV. Correction of t=0 values by -15mV results in good alignment of relative amplitude values for component 1 and the constant component as well as for τ_2. The relative amplitude values for component 2, however, are not well aligned and τ_1 values are actually less comparable than before "correction". Furthermore, instantaneous current amplitudes would be predicted to be smaller at any given hyperpolarising voltage after equilibration of the cell with the pipette solution, the membrane potential now being accurate rather than ca. 15mV negative to that set. The finding that instantaneous currents actually increase with time along with the lack of correlation of other current parameters after "correction", leads this author to suggest that the effect is not caused entirely, if at all, by a dissipating Donnan equilibrium but rather a change in some other parameter eg. changing internal pH and/ or removal of some cytoplasmic factor which modulates the deactivation process as mentioned above.

IV.4.3 Conclusions

The baculovirus/ Sf9 cell system is appropriate for the investigation of this channel, the cells being highly amenable to patch-clamping and exhibiting relatively small

leakage currents through native channels. The general characteristics of Sf cell expressed ClC-1 are in keeping with those reported in other heterologous systems and as measured in skeletal muscle fibres.

ClC-1 is clearly deactivated, albeit incompletely, by hyperpolarising potentials, the deactivation process involving at least 3 if not four components comprising 2 or 3 exponentially decaying and one constant component. The relative contribution of the three components measured here to the time dependent current is voltage dependent as is the time course of deactivation.

There is some evidence of ClC-1 being regulated by a soluble cytoplasmic factor which when removed by intracellular dialysis shifts the steady state open probability curve to more hyperpolarised voltages and slows the rate of deactivation.

V
Pharmacology

V.1 Introduction

V.1.1 Chloride channel blockers

Various compounds have been tested for their effectiveness as blockers of chloride-selective channels. Agents which have been found to be effective in this regard are many and varied and include various aromatic carboxylates, benzoates, phenoxyacetates, sulphonic acids, divalent cations, foreign anions and even some commonly used pH and Ca^{++} buffers (for reviews see Bretag, 1987; Franciolini and Petris, 1990; Greger, 1990). The potency of a given blocker is highly variable from channel to channel eg. anthracene-9-carboxylate (A9C) is highly effective on mammalian skeletal muscle (Palade and Barchi, 1977b) but only poorly in the thick ascending limb of the loop of Henle (Wangemann et al., 1986). Even within a particular tissue there is found to be inter-species variation eg. iodide is more effective in avian muscle than mammalian (reviewed in Bretag, 1987). Further, structurally quite dissimilar compounds can demonstrate similar potencies with a given channel whilst even subtle structural changes to a compound can alter its effectiveness dramatically (Wangemann et al., 1986).

There have been many detailed studies of the pharmacology of the ligand-gated chloride channels eg. γ-aminobutyric acid and glycine receptors (for reviews see Eldefrawi and Eldefrawi, 1987; Franciolini and Petris, 1990; Greger, 1990; Stephenson, 1995). Investigation of these channels has revealed a range of distinct binding sites on both the receptor and chloride channel components of these multimeric membrane proteins which interact with different compounds. Whilst some

compounds act to either increase or decrease the affinity of the receptor for its ligand, other compounds act as blockers of the chloride channel component eg. picrotoxin and various insecticides. While this large body of work is interesting in a general sense, these ligand-gated channels and the compounds which act to block their chloride channel activity clearly form a discrete group which differ from voltage-gated channels and their blockers. Consequently, ligand-gated channels and their pharmacology will not be dealt with further.

Despite the apparent complexities uncovered by research into this area, much useful information has been, and is to be, gained from the use of blockers in the investigation of the structure and function of chloride channels in various tissues including skeletal muscle.

V.1.2 Mammalian chloride channels

V.1.2.1 Epithelia

Compounds which block chloride conductance in various epithelial tissues have been the subject of a number of detailed studies mostly aimed at investigation of the structural elements required for efficient block. One such study examined the potency of numerous compounds including diphenylamine-2-carboxylate (DPC), 112 derivatives thereof and 108 other agents not directly related to DPC (Wangemann et al., 1986). This investigation allowed general conclusions to be drawn regarding the which structural elements influence efficacy. Most of the active compounds were aromatic carboxylates and were highly lipophilic. Substitutions which reduced lipophilicity drastically reduced efficacy. Most of the effective compounds were secondary amines, the amine being found to be required since its replacement with any other group abolished activity. Further, the spacing between the carboxylate and the amine also had an influence, the optimum being 2 - 3 carbons, and a partial positive

charge on this group was found to be required. Two phenyl rings were found not to be essential as long as an appropriately spaced secondary amine and carboxylate were present. With regard to the DPC derivatives, substitution on the benzoate moiety with Cl or NO_2, at the *para* and *meta* positions respectively, had either no effect or increased potency.

From all of the above, and various other findings, the authors suggested that effective compounds interact with the channel protein via at least 4 sites namely the carboxylate, a partial negative charge *meta* to COO^-, the bridging amino group and a hydrophobic site provided by a phenyl, cycloalkyl, pyrrole or pyrrolidino ring.

An investigation of the action of indanyloxyacetic acid (IAA) enantiomers, anthranilic acid, ethacrynic acid and derivatives thereof on chloride transport in membrane vesicles derived from bovine kidney cortex and trachea has also been published (Landry et al., 1987). The conclusions regarding structure vs potency for the anthranilic acid derivatives were very similar to those of Wangemann et al (1986). The presence of an appropriately placed nitro group and its position relative to the carboxylate were found to be important as was the degree of hydrophobicity. Further, the efficacy with which a given compound blocked chloride transport was mirrored by its ability to displace tritiated IAA-94 enantiomer in competitive binding assays. A surprising finding was that ^{3}H-IAA-94 could be displaced by compounds which were structurally quite dissimilar to it. Also of interest were the deviations from ideal behaviour reported between some enantiomers eg. IAA-94 vs IAA-95 but not others eg. IAA-74 vs 75 ie. with some enantiomers the ability to displace tritiated IAA-94 did not correlate with their effectiveness as a blocking agent. This finding led the authors to suggest the presence of two inhibitory binding sites on the channel each of which binds a different enantiomer.

The effects of a number of compounds on the intermediate conductance outwardly rectifying (ICOR) chloride channel in the HT_{29} colon carcinoma cell line and respiratory epithelium have been studied at the single channel level (Tilmann et al., 1991). In this study, 4,4'-diisothiocyanostilbene-2,2'-disulphonic acid (DIDS), 4-acetamido-4'-isothiocyanostilbene-2,2'-disulphonic acid (SITS), 4,4'-dinitrostilbene-2,2'-disulphonic acid (DNDS), IAA, amidine, 5-nitro-2-(3-phenylpropylamino)-benzoate (NPPB) and 5-nitro-2-(3-phenylethylylamino)-benzoate (NPEB) were applied to channels in excised membrane patches. All these compounds produced a reversible, flicker type block when applied at low concentration to the cytosolic face of inside out patches with higher concentrations inducing complete block. In this configuration the effect of most compounds was seen almost instantaneously following application. The effect of NPPB, which was the most potent agent exhibiting an IC_{50} of 0.9μM, however, was detected after a short delay and was only slowly reversible. Application of 1μM NPPB to the external face of outside out patches resulted in immediate and complete block implying that the binding site was located on the external face of the channel and that when using the inside out patch configuration NPPB must diffuse across the membrane to exert its effect. This interpretation was supported by experiments using NPPB and NPEB linked to polyethylene glycol (PEG) inhibiting their ability to cross the membrane. The PEG-linked NPPB was ineffective when applied to the cytoplasmic face of patches but was almost instantly effective when applied to outside out patches, exhibiting an IC_{50} of 30nM.

V.1.2.2 Skeletal muscle

Possibly the most comprehensive study of the effects of aromatic carboxylates on chloride conductance (G_{Cl}) in mammalian skeletal muscle published to date is that of

Palade and Barchi (1977b). Testing of 25 benzoic acid derivatives revealed 19 which were effective in reducing chloride conductance in rat diaphragm, A9C being the most potent with a measured K_i of 11μM. The potency of the various blockers was highly variable ranging over 3 orders of magnitude and all were reversible as long as exposure time was limited. Reduction of G_{Cl} by all blockers was voltage independent and followed a dose dependence consistent with interaction at a single site or multiple sites with similar affinities.

Comparison of the potencies of these structurally related compounds led to similar conclusions regarding the structural requirements for efficient block as were reached with studies in epithelia (Wangemann et al., 1986; Landry et al., 1987). Some 59% of the difference in potency of the effective analogues could be attributed to variation in their calculated octanol-water partition coefficient. An additional 29% could be accounted for by differences in each compound's Hammett σ value, ie. the dissociability of a functional group, in this case the carboxyl, relative to the parent compound (benzoic acid), and steric hindrance effects of ring substituents. On the basis of their results Palade and Barchi suggested that these blockers bind to an intramembrane site and that interaction involves 2 regions one of which is polar and the other relatively non-polar. The additional finding that increasing concentrations of A9C progressively alter the conductivity sequence until, at relatively high concentrations, it reverses, added weight to the premise that, in contrast to earlier proposals (Bryant and Morales-Aguilera, 1971), these compounds do not produce channel blockade by occluding the pore. It was also noted in this work that a number of the compounds tested also altered potassium conductance in this preparation, some causing a detectable increase whilst others a caused a reduction.

Another group of compounds which has been the subject of detailed investigation is clofibric acid (2-(*p*-chlorophenoxy)-isobutyric acid) and its derivatives (Bettoni et al., 1987). Most of this work has dealt with the differing effects of the enantiomers of these chiral compounds (Bettoni et al., 1987; Conte-Camerino et al., 1988a, b; De Luca et al., 1992). In summary, the body of work dealing with these compounds has shown that 2-(4-chlorophenoxy)-propionate (CPP) is among the most potent of the derivatives (Conte-Camerino et al., 1988b) and that the R(+) and S(-) forms of all optically active analogues produce markedly different effects. The S(-) form was shown to be more potent than the racemate by a factor exceeding 2 whilst the R(+) enantiomer at concentrations below 10μM actually increased muscle G_{Cl}. Higher concentrations of R(+) reduced G_{Cl} but the level of reduction plateaued to leave approximately 75% of the original value (Conte-Camerino et al., 1988a).

A model to explain this behaviour has been proposed (De Luca et al., 1992) in which the chloride channel contains two binding sites (cf. Landry et al., 1987). Ligand binding to one site blocks the channel whilst opening results from interaction with the other. According to the proposed model the S(-) enantiomer binds only to the inhibitory site whilst the R(+) binds to both, albeit with lower affinity than S(-) at the inhibitory site. Dose responses for the S(-) form of CPP were also performed in the presence of R(+) at either 3 or 10μM. The results gained using this approach indicated antagonism between the two optical isomers which was overcome by high concentrations of S(-) (De Luca et al., 1992). This data suggested competition for a common binding site between the enantiomers and was in support of the proposed model.

Other unrelated work has revealed that the R(+) form of CPP is also able to potentiate the mechanical response of amphibian muscle possibly via some interaction with the voltage sensor in the T-system (Heiny et al., 1990a).

IAA-94 has also been shown to be effective on rat skeletal muscle (Weber-Schürholz et al., 1993). Intracellular application via microinjection induced myotonic responses in 16 of 36 fibres whereas addition to the bath up to a concentration of 100μM had no detectable effect. Weber-Schürholz et al. went on to use IAA affinity chromatography to isolate functional chloride channel proteins from muscle membrane preparations. The contribution of these channels to the large chloride flux in rat muscle remains unclear (*vide* Section I).

V.1.3 Concluding remarks

From the above it is apparent that the best characterised blockers of mammalian skeletal muscle chloride conductance are the aromatic carboxylates. In these investigations muscle preparations have been used and the effect of blockers assessed, somewhat indirectly, from changes in whole-cell G_{Cl} and membrane resistance. Given the ability of some of these compounds to influence the behaviour of proteins other than the major chloride permeation pathway, it would seem advantageous to test these substances in a system devoid of other muscle membrane proteins. Further, more detailed information about the mode of action of these compounds could be gained by directly examining their effects on the currents flowing through the channel.

With all this in mind, the work set out below was undertaken in an effort to gain more detailed knowledge of the effects of various channel blockers on ClC-1 as expressed in Sf9 cells and to highlight compounds worthy of further investigation.

V.2 Materials and Methods

V.2.1 Chemicals and reagents

V.2.1.1 Blockers

Substances tested for their ability to block heterologously expressed ClC-1, their structures and sources are listed in Table Va. Carboxylic acids were prepared as the sodium salt by addition of an equimolar concentration of NaOH and then diluted to 200mM by addition of MQ quality water (resistance >18MΩ). Stock solutions were prepared fresh on the day of use and added to standard bath solution at the concentrations indicated in Results. The pH of bath solutions containing blockers was checked and adjusted as necessary using HCl.

V.2.2 Patch-clamping

All solutions and methods were as described in Section IV. Cells were infected with baculovirus and prepared for patch-clamping as described in Sections II and IV.

V.2.2.1 Dose response

Except where stated otherwise, cells were held in whole-cell configuration and monitored until current parameters had stabilised (*vide* Section IV) prior to the addition of any blocking agent. Dose response values were obtained by addition of increasing concentrations of the blocker being tested ie. they are cumulative dose responses. Each solution addition was of at least 3 times the volume in which the cell was bathed.

Dose response data were fitted, using GraphPad Prism (*GraphPad Software Inc.*), with sigmoidal dose response curves of the form $Y = b + \frac{(t-b)}{1+10^{\left((\log_{10} IC_{50} - X)\,Z\right)}}$

where b = Y value at bottom of plateau, t = Y value at top of plateau, Z = slope of curve (Hill slope), $\log_{10} IC_{50}$ = value of X when Y is half way between t and b, and X is expressed as $\log_{10}$ concentration. Except where stated otherwise, values for 50%

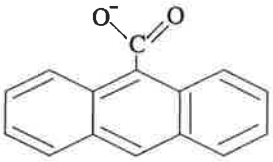

Anthracene-9-carboxylate (**A-9-C**)
Aldrich

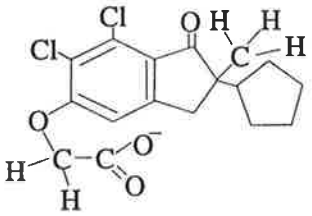

Indanyloxyacetate, 94/95 (**IAA**)
D.W. Landry
(see Landry et al., 1987)

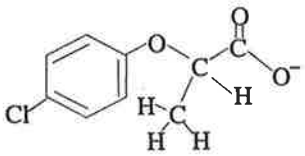

2-(4-chlorophenoxy) propionate (**CPP**)
Sigma

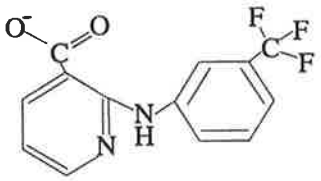

2-(3-trifluoromethylanilino)-nicotinic acid
(**niflumate**)
Squibb

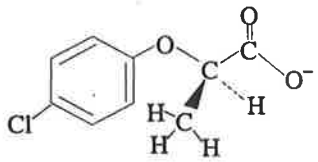

CPP R(+) enantiomer
Prof. SH Bryant
(see Bettoni et al., 1987)

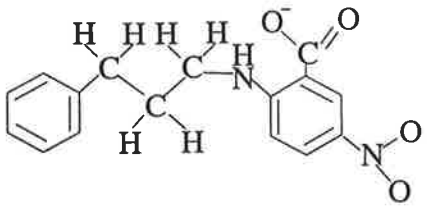

5-nitro-2-(3-phenylpropylamino) benzoate
(**NPPB**)
D.W. Landry
(see Landry et al., 1987)

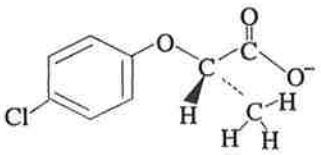

CPP S(-) enantiomer
Prof. SH Bryant
(see Bettoni et al., 1987)

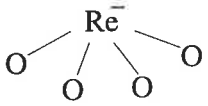

Perrhenate
Koch-Ligh

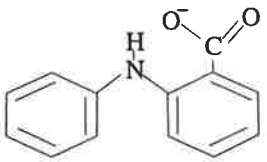

diphenylamine-2-carboxylate (**DPC**)
D.W. Landry
(see Landry et al., 1987)

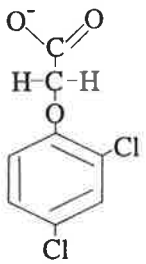

2,4-dichlorophenoxyacetate (**2,4-D**)
Sigma

Table Va: Structures and sources of blockers used in this study.

inhibitory concentration (IC_{50}) were calculated from data averaged from a minimum of three cells. Error bars on graphically presented, averaged data represent ± SEM. Confidence intervals, also calculated using GraphPad Prism, were used when comparing $V_{1/2}$ values calculated from fitting of Boltzmann functions. Differences between two $V_{1/2}$ values were considered significant if the means of each of the values being compared lay outside the 95% confidence interval of the other. Throughout the text, $V_{1/2}$ values are quoted as mean ± 95% confidence interval.

Statistical analysis of other data was as described in Section IV.

V.3 Results

V.3.1 Anthracene-9-carboxylate

Application of A9C at final concentrations ≥1μM resulted within seconds in a measurable reduction in both instantaneous and quasi-steady state currents. At concentrations above 1μM, there was a concentration dependent reduction in current which was consistent across the entire voltage range (Figure 5.1) There was no apparent change in current kinetics (Fig 5.1 and 5.2a) with regard to deactivation in the hyperpolarising voltage range or rectification at positive potentials, although both exponential components were impossible to extract from currents measured in the presence of concentrations above 100μM. The overall shape of current/voltage relationships remained unaltered at all tested concentrations (Figure 5.2b). Cumulative dose response data yielded IC_{50} values, at a test voltage of -100mV, of 21 and 29μM for the instantaneous and quasi-steady state currents respectively (Figure 5.2b). Calculated IC_{50} values for all other test voltages were of a similar magnitude ie. around 20 - 25μM.

A9C-induced block was easily reversible (Figure 5.3) regardless of the applied concentration as long as exposure time was limited (< 10 minutes). With prolonged exposure, block became increasingly difficult to reverse with cells needing to be rinsed with larger volumes (>20ml) of bath solution before control conditions could be re-established. Following prolonged (>15 minutes) exposure to concentrations above 10μM cells appeared to be irreparably damaged as evidenced by the loss of resting membrane potential, increasing leakage current and finally breakdown of the patch (not shown).

V.3.2 Perrhenate

A detectable reduction in instantaneous current became apparent at concentrations ≥ 100μM. As with A9C the response was virtually immediate, proportional to concentration and consistent across the voltage range (Figure 5.4). By contrast, quasi-steady state currents elicited by hyperpolarising voltage pulses were not noticeably affected at concentrations below 500μM. Following exposure to concentrations of 500μM and 1mM the quasi-steady state current amplitude actually increased before decreasing in a concentration dependent manner at higher concentrations (Figure 5.5a).

The shape of the instantaneous current/voltage curve remained similar across the concentration range whilst for the quasi-steady state current the curve shape differs at the different test concentrations (Figure 5.5b, c). IC_{50} values for instantaneous and quasi-steady state currents, calculated from currents elicited by a -100mV test pulse, were 1.1 and 3.5mM respectively (Figure 5.5d) with similar values being obtained for both at all other voltages tested.

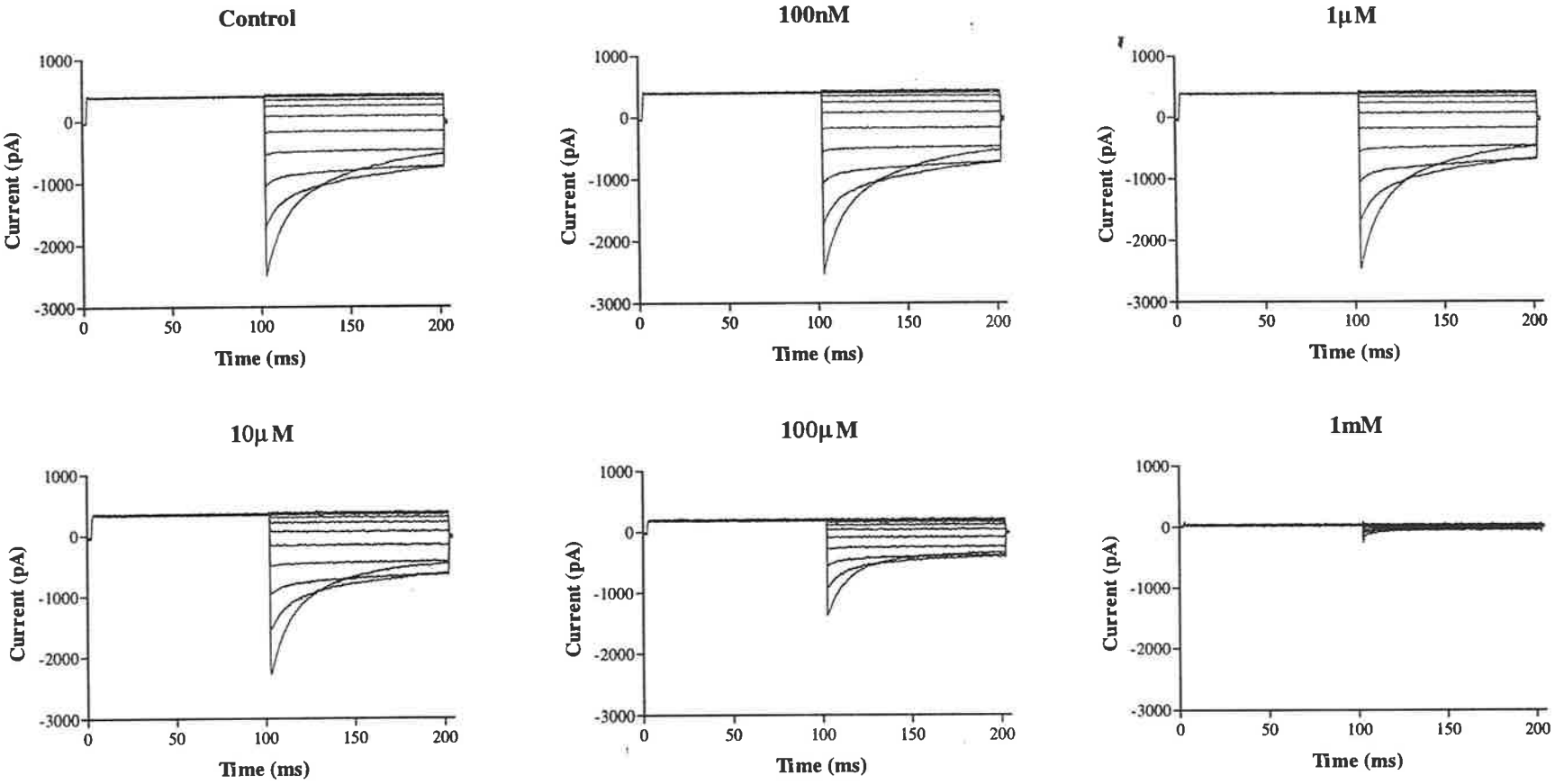

Figure 5.1: Typical families of current traces elicited using the activation voltage protocol in the presence of the concentration of anthracene-9-carboxylate indicated above each graph. All sets of current traces were recorded from the same cell.

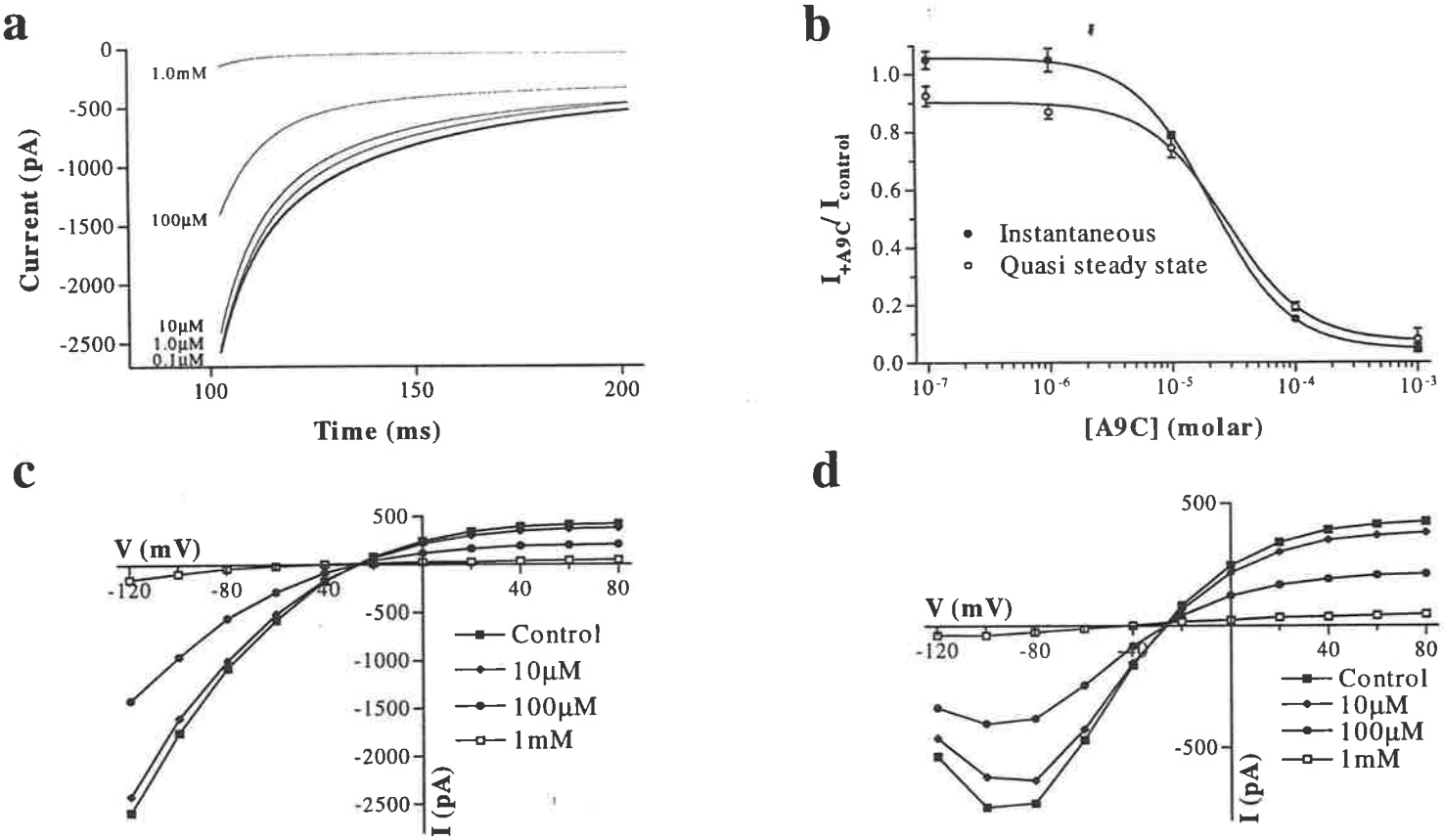

Figure 5.2: **a:** Currents averaged from 4 cells and fitted with the sum of 2 exponential and one constant component. Currents were measured during a -120mV test pulse, preceded by a 40ms pulse to +40mV, and in the presence of anthracene-9-carboxylate at the concentrations indicated. **b:** Instantaneous and quasi-steady state dose response data for A9C. Data are fitted with sigmoidal functions as described in materials and methods. **c and d:** Typical instantaneous (**c**) and quasi-steady state (**d**) current/voltage relationships measured from the same cell in the presence of the indicated concentrations of A9C.

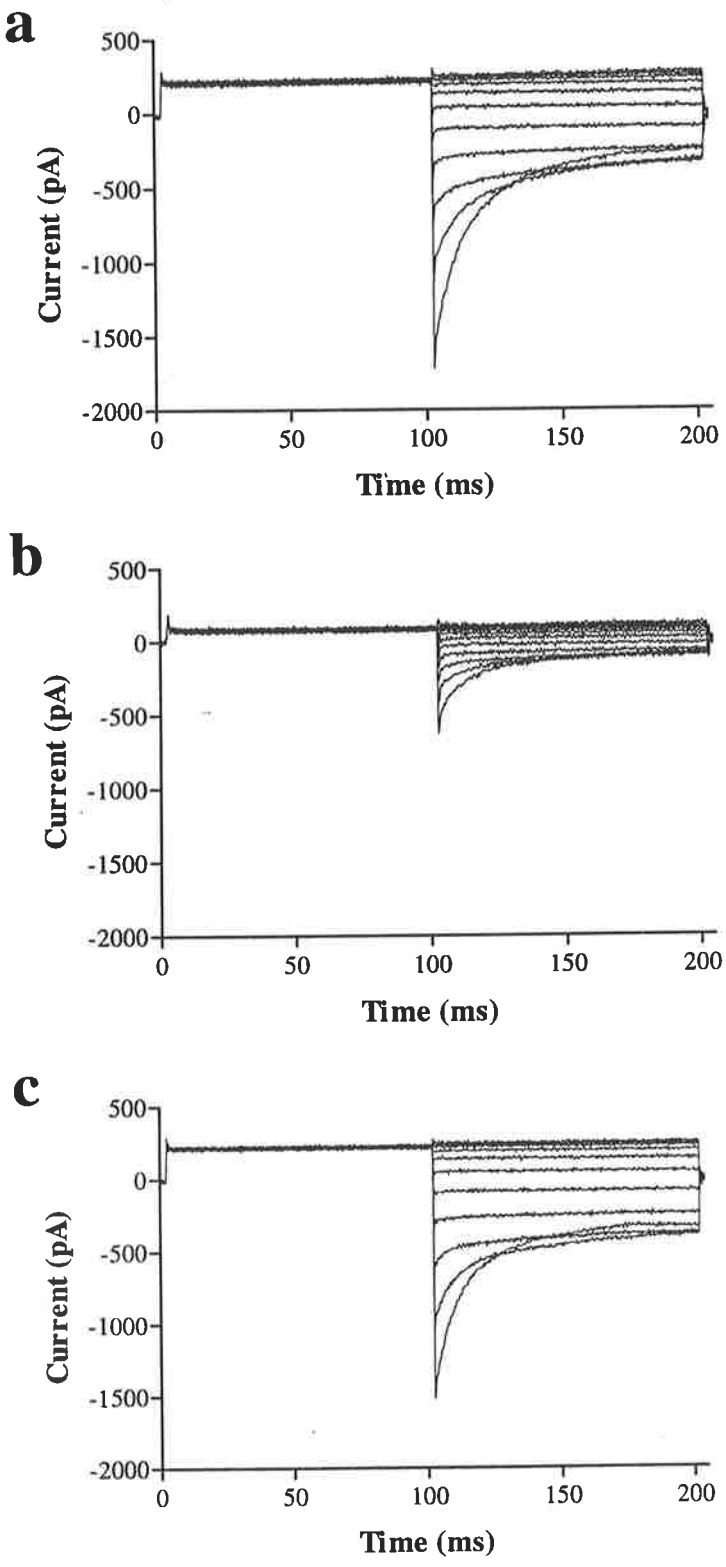

Figure 5.3: Whole cell currents measured in the same cell (**a**) before and (**b**) after addition of 100μM A9C. **c:** The same cell after rinsing with 10ml of normal bath solution.

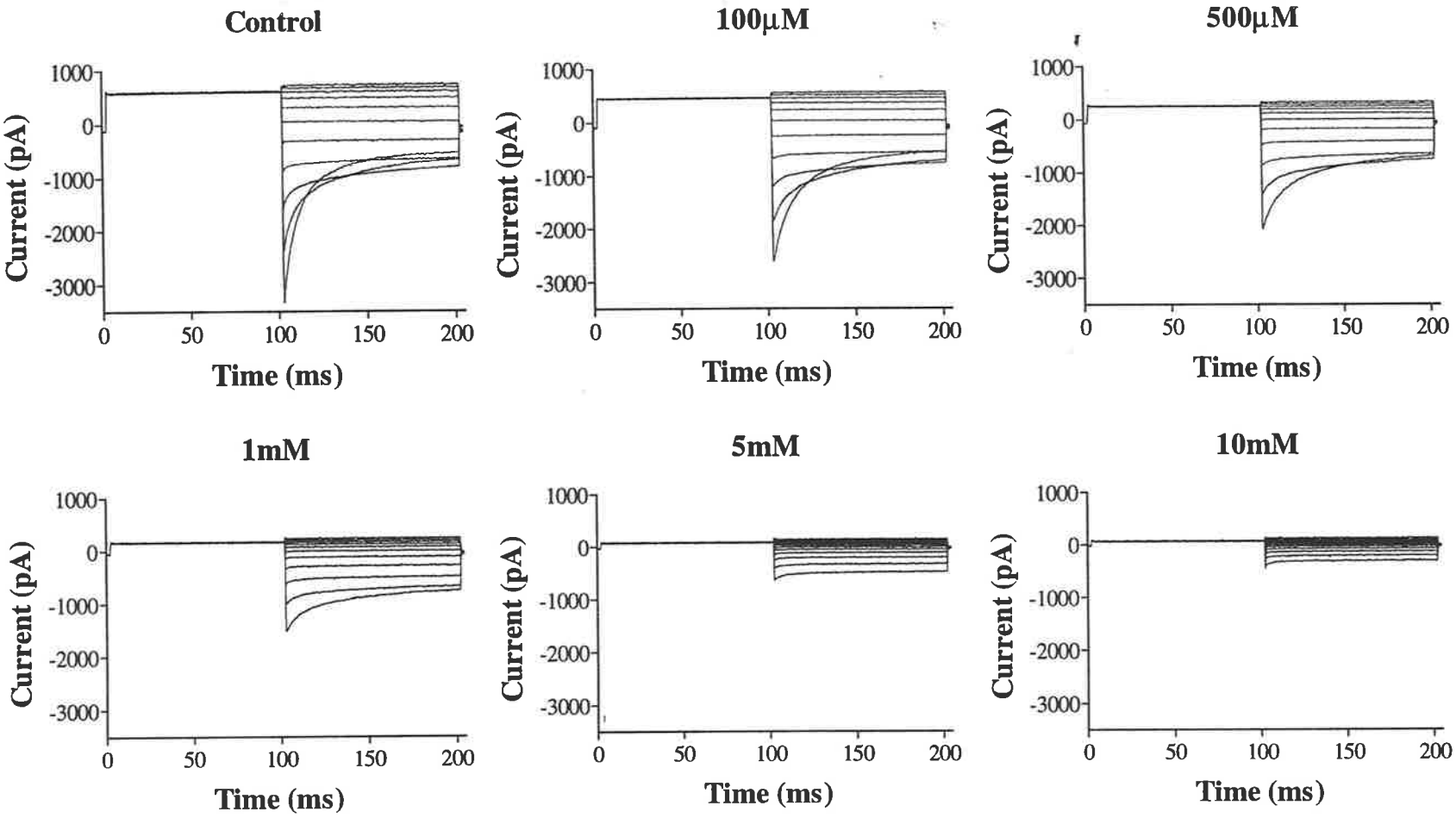

Figure 5.4: Typical families of current traces elicited using the activation voltage protocol in the presence of the concentration of perrhenate indicated above each graph. All sets of traces were recorded from the same cell.

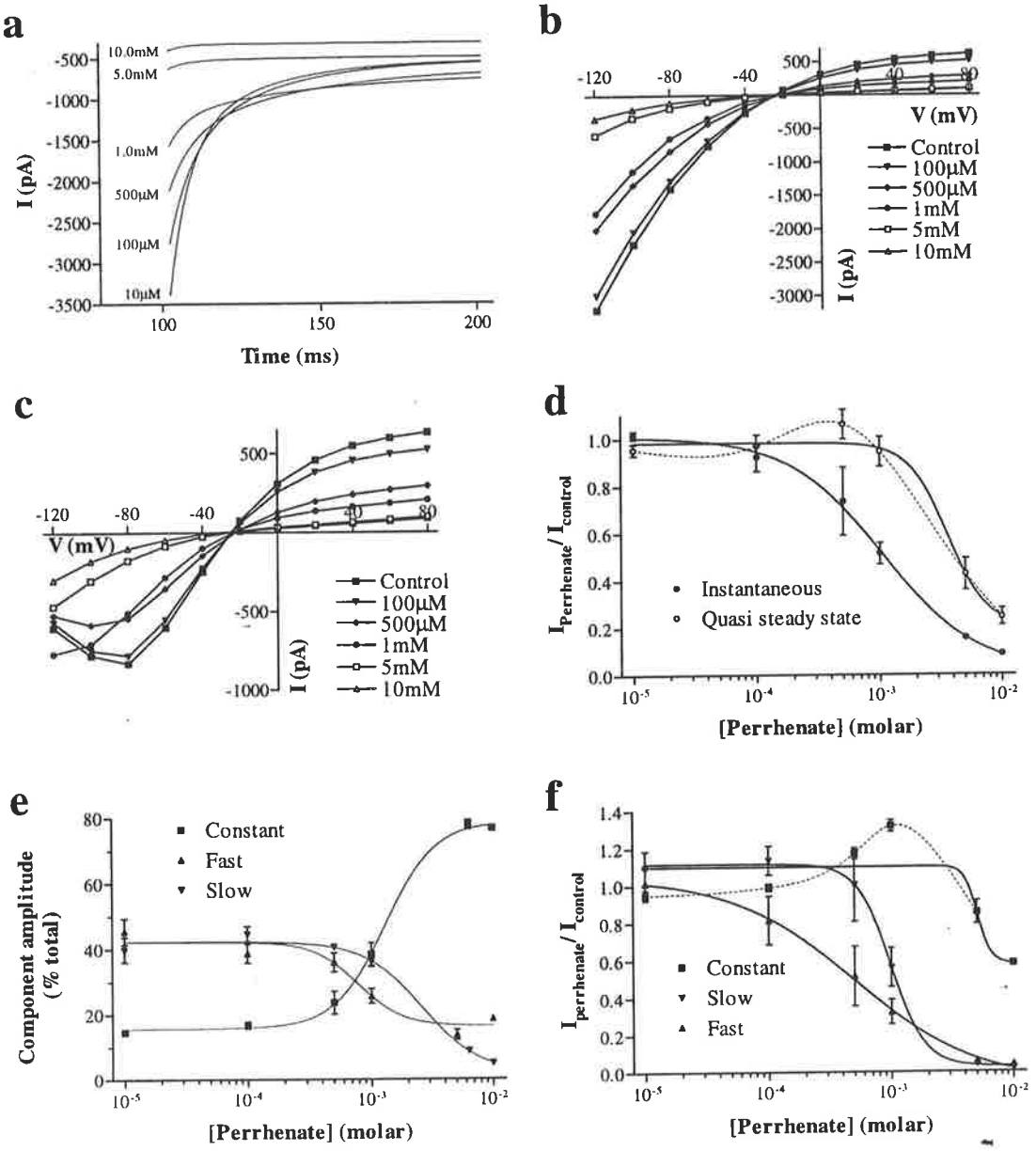

Figure 5.5: **a:** Currents elicited by -120mV test pulses each preceded by a 100ms prepulse to +40mV measured in a single cell in the presence of the indicated concentrations of perrhenate. Currents shown are averaged data from 3 separate cells and are fitted with curves as described in Section IV. **b and c:** Current/voltage relationships for instantaneous (b) and quasi-steady state (c) currents measured from the same cell in the presence of the concentrations of perrhenate indicated on the graphs. **d:** Cumulative dose response data (n=3) **e:** Relative component amplitudes in the presence of the indicated concentrations of perrhenate. **f:** Cumulative dose response data for each current component. Data in **d**, **e** and **f** are fitted with sigmoidal functions (solid line) as described in materials and methods or cubic splines (broken line).

At concentrations above 500μM the relative amplitudes of all three components were markedly altered. The contribution of both exponentially decaying components to the total current is reduced with a concomitant increase in the relative amplitude of the constant component (Figure 5.5e). Calculation of IC_{50} values for each component, using currents measured in response to a -120mV voltage pulse, indicated a differing sensitivity to perrhenate for each. The fast decaying component showed an apparent IC_{50} of 490μM whilst the slow component returned a value of 1mM. Data for the constant component was not well fitted by a sigmoidal dose response function, thus the calculated IC_{50} of 11.5mM is unlikely to reflect the true value (Figure 5.5f).

As with A9C, block was easily reversible (Figure 5.6) regardless of the concentration applied. In contrast to A9C, however, duration of exposure had no effect on the ease with which control currents could be restored.

V.3.3 2-(4-chlorophenoxy)-propionate

V.3.3.1 Racemate

As its racemic mixture this compound began to alter current amplitudes at concentrations as low as 100nM (Figure 5.7). Instantaneous inward currents initially showed an increase in amplitude and were not noticeably reduced below 10mM. Blockade was easily reversible with minimal rinsing regardless of concentration used (Figure 5.8a-c). Current/voltage curves demonstrated that quasi-steady state currents were more markedly reduced and at lower concentrations than instantaneous currents (Figure 5.8d, e). In the case of quasi-steady state currents, inward currents were reduced in a concentration dependent manner at concentrations of 100μM and higher whilst outward currents were not noticeably reduced until 10mM. In contrast, instantaneous inward and outward currents were relatively equally affected but only at very high (10mM) concentrations.

Concentrations above 100μM led to a distinct change in the kinetics of both inward and outward currents. Steps to positive potentials evoked an activating outward current which, like the deactivating current seen at hyperpolarising potentials, could be fitted with the sum of 2 exponential and one constant component. This is most clearly seen in the currents elicited by the prepulses used in the -80mV deactivation protocol (Figure 5.9). At very high concentrations (10mM) saturation of outward currents was also noticeably reduced.

The changes in inward current kinetics were seen as faster deactivation predominantly due to a change in the relative amplitudes of the three current components (Figure 5.10a, b). At CPP concentrations above 100μM there was a marked increase in the contribution of the fast exponential component at the expense of the other two (Figure 5.10b). The change in relative component amplitudes was found to be significant by analysis of variance ($P<0.0001$). Using the -80mV deactivation protocol, the apparent open probability was calculated and the curve found to shift to more positive potentials in the presence of CPP concentrations of ≥100μM (Figure 5.10c). A large and significant shift in $V_{1/2}$ was observed between the controls and cells measured in the presence of 10mM CPP, the values being -86.7 ± 2.9 and -5.4 ± 2.8mV for control and 10mM measurements respectively. The calculated gating charge remained at around -1 at all concentrations tested.

Calculation of IC_{50}s (currents at -100mV) returned values of 6.3mM and 730μM for the instantaneous and quasi-steady state currents respectively (Figure 5.10d). Given that the maximal current reduction achieved with the instantaneous current was less than 30%, the accuracy of the calculated IC_{50} for this parameter is questionable. IC_{50} values calculated for the separate components, at the same voltage, gave similar

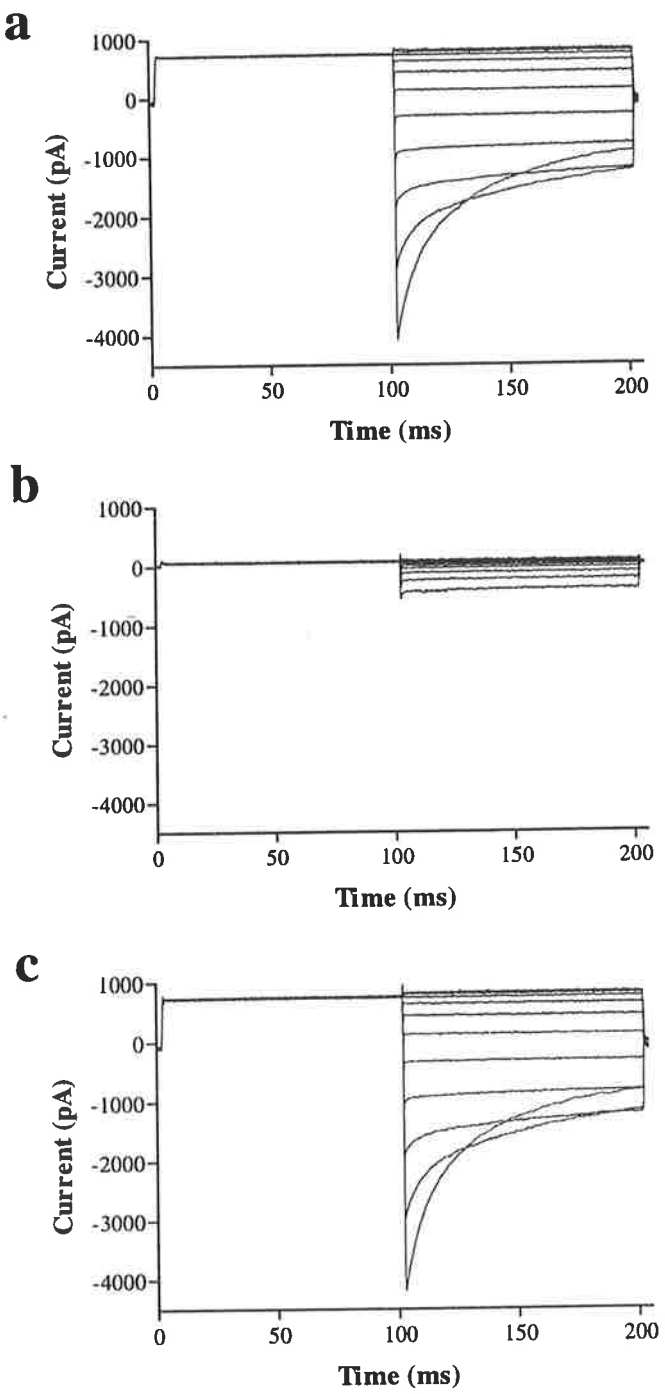

Figure 5.6: Current traces measured from the same cell elicited using the activation voltage protocol before (**a**) and after (**b**) addition of 10mM perrhenate. **c:** Currents measured from the same cell after rinsing with 10ml of normal bath solution.

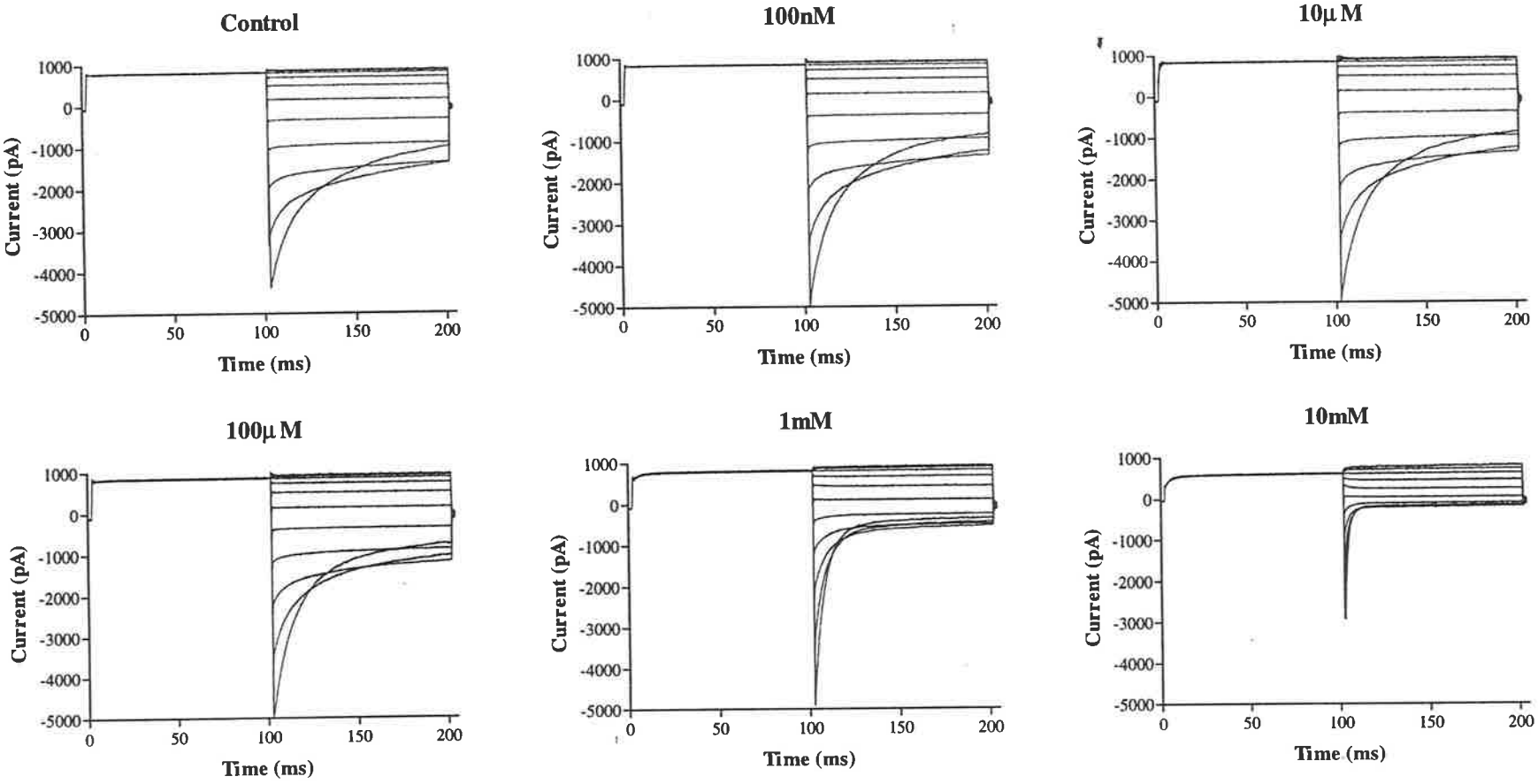

Figure 5.7: Typical families of current traces, all recorded from the same cell, elicited using the activation voltage protocol in the presence of the concentration of CPP racemate indicated above each graph.

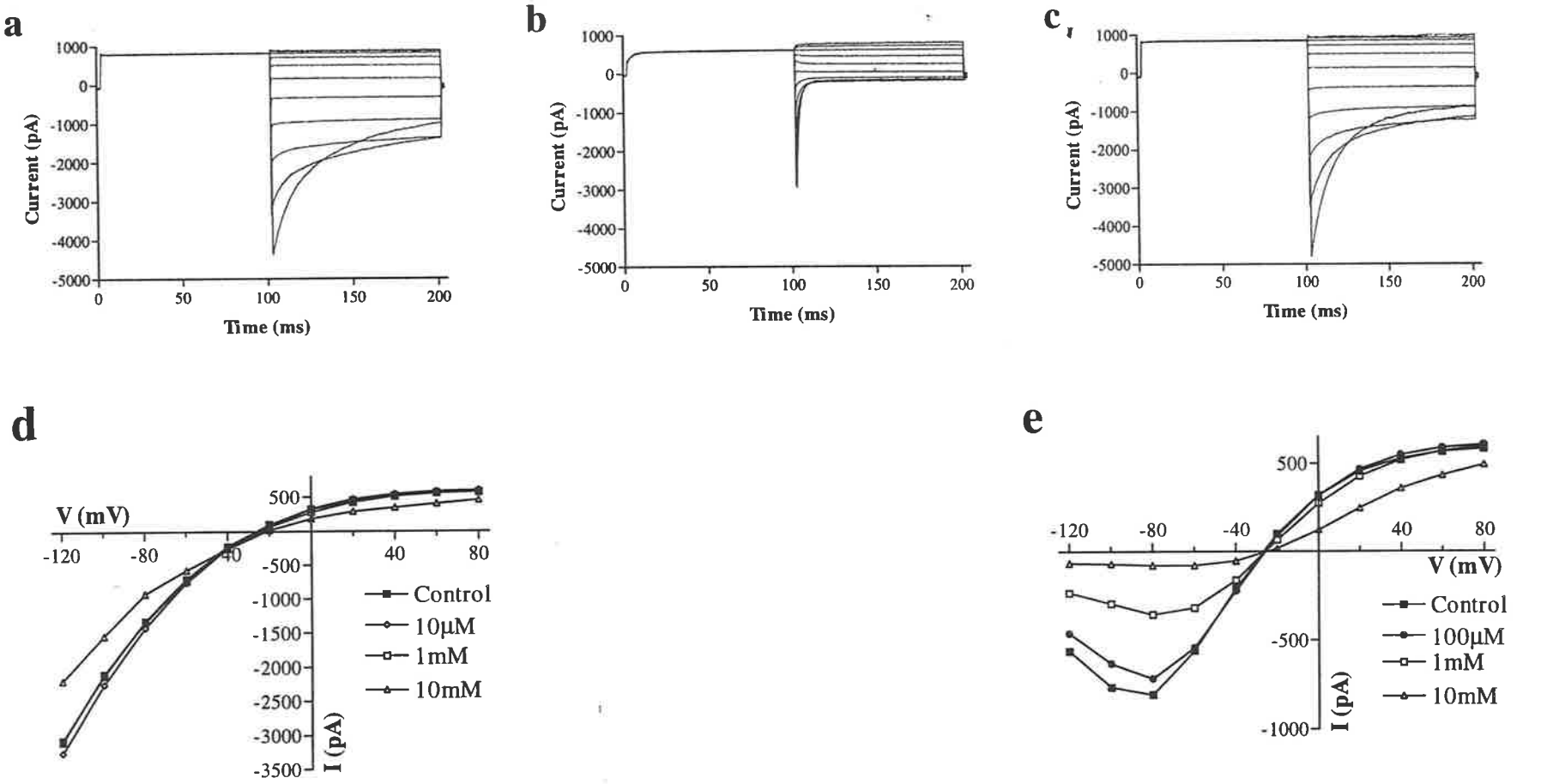

Figure 5.8: a, b: Current traces, elicited using the activation voltage protocol, recorded in the same cell before (**a**) and after (**b**) addition of 10mM CPP racemate. **c:** The same cell after rinsing with 10ml of normal bath solution. **d, e:** Instantaneous (**d**) and quasi-steady state (**e**) current/voltage relationships at the concentrations of CPP racemate indicated on the graphs.

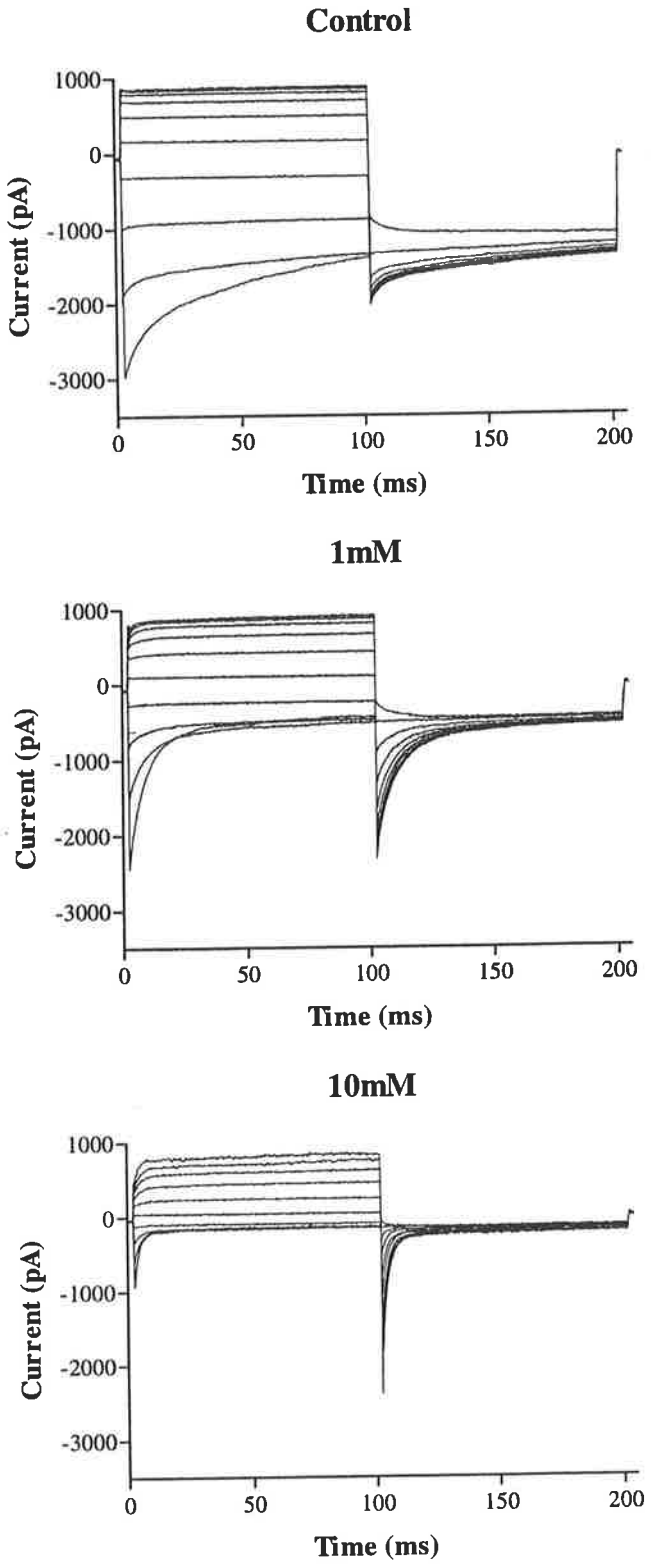

Figure 5.9: Current traces elicited using the -80mV deactivation voltage protocol in a single cell at the concentrations of CPP racemate indicated above each graph.

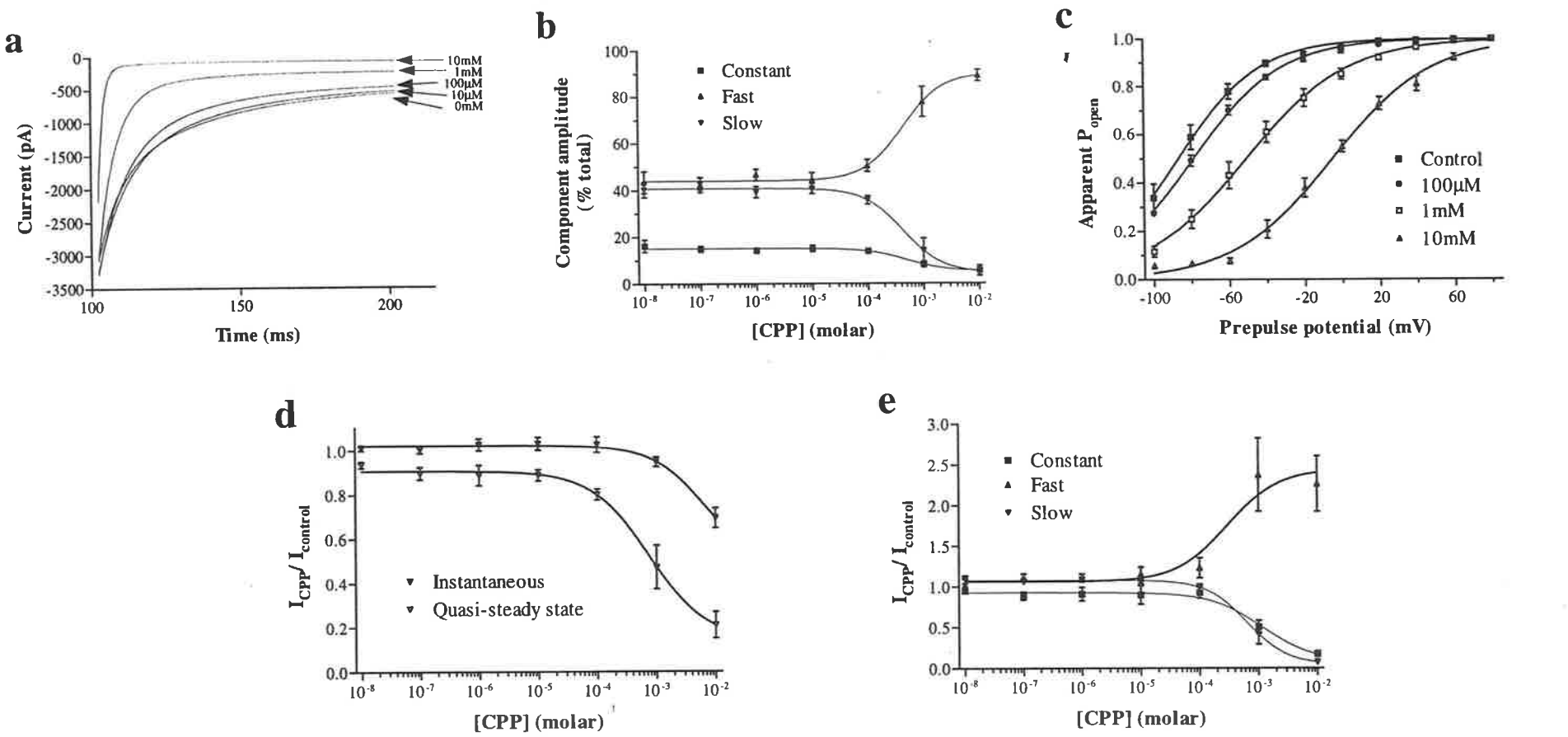

Figure 5.10: **a:** Currents elicited by -120mV test pulses, each preceded by a 100ms prepulse to +40mV, measured in a single cell in the presence of the indicated concentrations of CPP racemate. **b:** Relative component amplitudes measured at different concentrations of CPP. **c:** Apparent open probabilities vs prepulse potential at various CPP concentrations. Curves represent fitting of Boltzmann functions as described in Section IV. **d:** Dose response data for instantaneous and quasi-steady state currents. **e:** Dose response data for separate components. Data in **b**, **d** and **e** are fitted with sigmoidal dose response functions as described in materials and methods.

results for all three ie. 620μM, 1.1mM and 300μM for the slow and constant component decreases and the half maximal effect for the increase in the amplitude of the fast component respectively (Figure 5.10e).

V.3.3.2 Enantiomers

V.3.3.2.1 S(-)

The S(-) enantiomer of CPP produced similar effects to the racemic mixture but exhibited a higher potency (Figure 5.11). Slight but consistent reductions in inward quasi-steady state currents were detectable with concentrations as low as 10nM although outward quasi-steady state currents were not noticeably reduced below 1mM (Figure 5.12a, b). As was the case with the racemate, instantaneous currents, either inward or outward, were not significantly reduced at sub-mM concentrations.

Similar changes in current kinetics were also observed. In response to steps to positive potentials, in the presence of mM concentrations, outward current activation was seen (Figure 5.12c-e) from which the usual three components could be extracted. With increasing concentrations, more rapid deactivation was observed in response to hyperpolarising potentials (Figure 5.13a). As was the case with the racemate, the kinetic changes were due to significant ($P<0.0001$) changes in the relative amplitudes of the three current components. At concentrations above 100μM a marked increase was seen in the contribution to the total current from the fast exponentially decaying component at the expense of the other two (Figure 5.13b).

Calculated IC_{50} values at -120mV were 940μM for instantaneous and 190μM for quasi-steady state currents (Figure 5.13c). As with the racemate, block of the instantaneous current appears not to have reached anything like its possible maximum. The IC_{50} value for this parameter is therefore at best a rough approximation. As with the racemate, IC_{50} calculations, at the same potential, for the separate components

returned similar values for each. The values for the slow exponential and constant components were 240μM and 440μM respectively (Figure 5.13d) whilst the fast component increase showed a half maximal effect at 430μM. Also similar to the racemic mixture was the effect on relative open probability. A significant shift of $V_{1/2}$ of approximately 72mV (-99.8 ± 6.3 vs -27.9 ± 3.1mV) was noted between control and 1mM measurements (Figure 5.13e). The gating charge remained unchanged at around -1 at all concentrations tested.

V.3.3.2.2 R(+)

This enantiomer when applied at mM concentrations produced effects similar to both the racemate and S(-) isomer (Figure 5.14, 5.15, 5.16a). Whilst some cells showed a slight decrease in instantaneous inward current amplitudes at high concentrations (10mM) (Figure 5.16e), averaged data shows instantaneous currents were not measurably different from control values at this concentration. A more noticeable and consistent reduction in quasi-steady state currents was observed. Calculated IC_{50} values of 1.8 and 5.2mM were obtained for instantaneous and quasi-steady state currents respectively (Figure 5.16b). Again, given the small effect on instantaneous currents and poor fit of the sigmoidal function, the IC_{50} for this parameter is not likely to represent the true value. As was the case with the other enantiomer and racemate, concentrations above 100μM alter the relative component amplitudes (Figure 5.16c) there being an increase in the fast component with concomitant decrease in the other two. Again the change in relative component amplitudes was found to be significant ($P<0.0001$). The effect with R(+) is, however, not as marked. Data for the changes in component amplitudes were not well fitted by sigmoidal dose response functions.

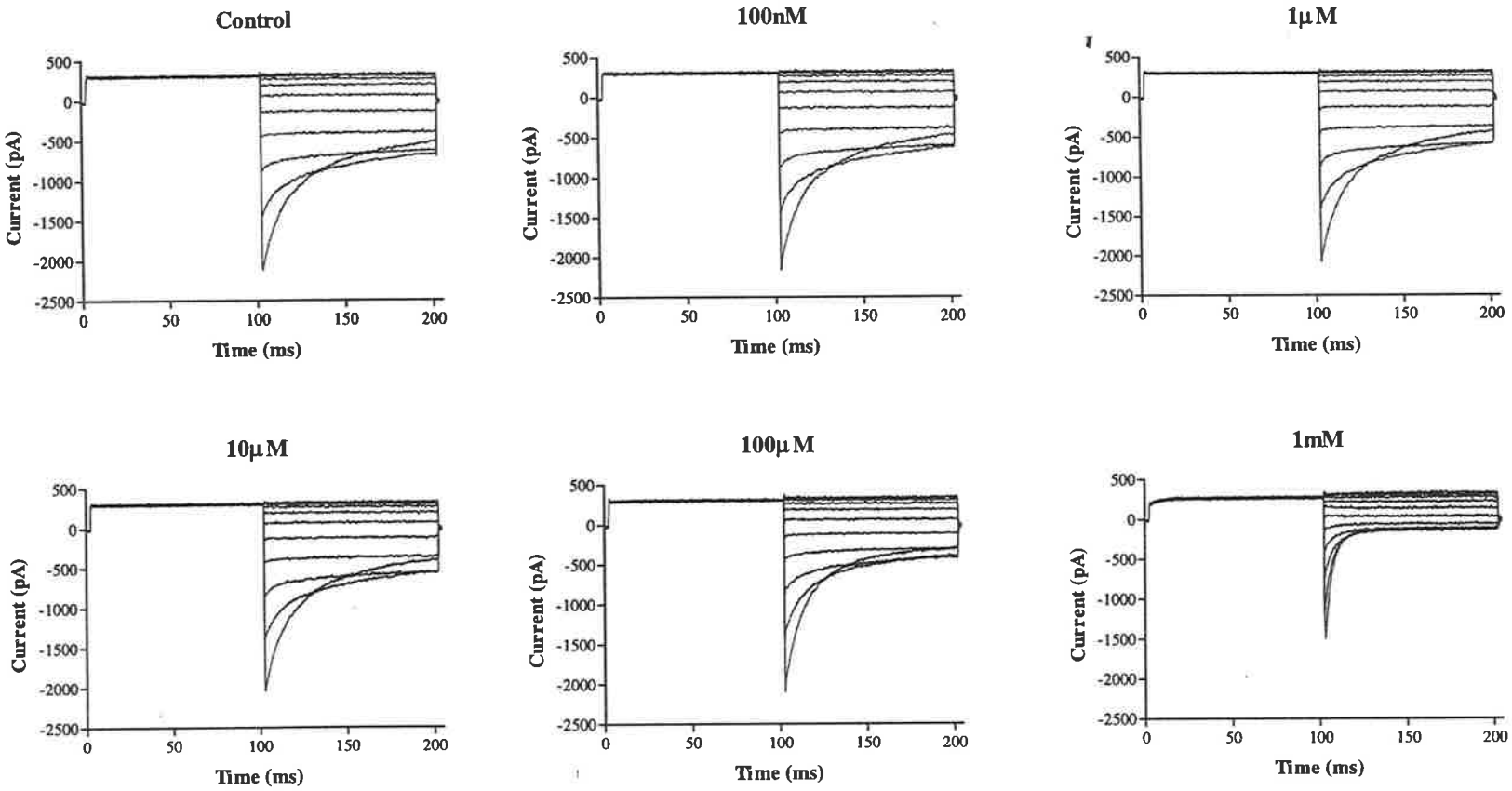

Figure 5.11: Typical families of current traces, all recorded from the same cell, elicited using the activation voltage protocol in the presence of the concentration of CPP S(-) enantiomer indicated above each graph.

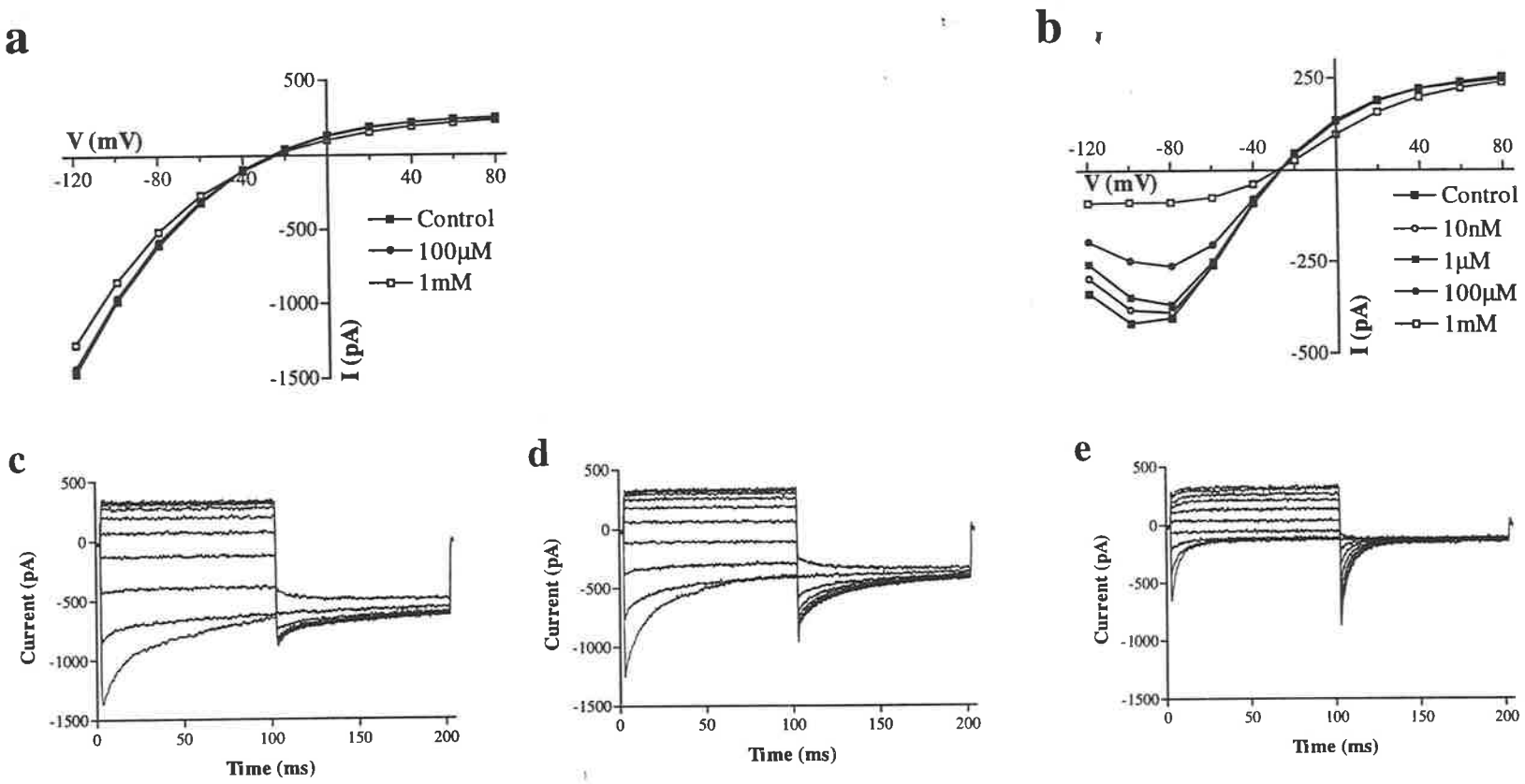

Figure 5.12: a, b: Instantaneous (**a**) and quasi-steady state (**b**) current/voltage relationships at the concentrations of CPP S(-) enantiomer indicated on the graphs. **c - e:** Current traces elicited by the -80mV deactivation voltage protocol and recorded in the same cell before (**c**) and after application of 100µM (**d**) or 1mM (**e**) CPP S(-).

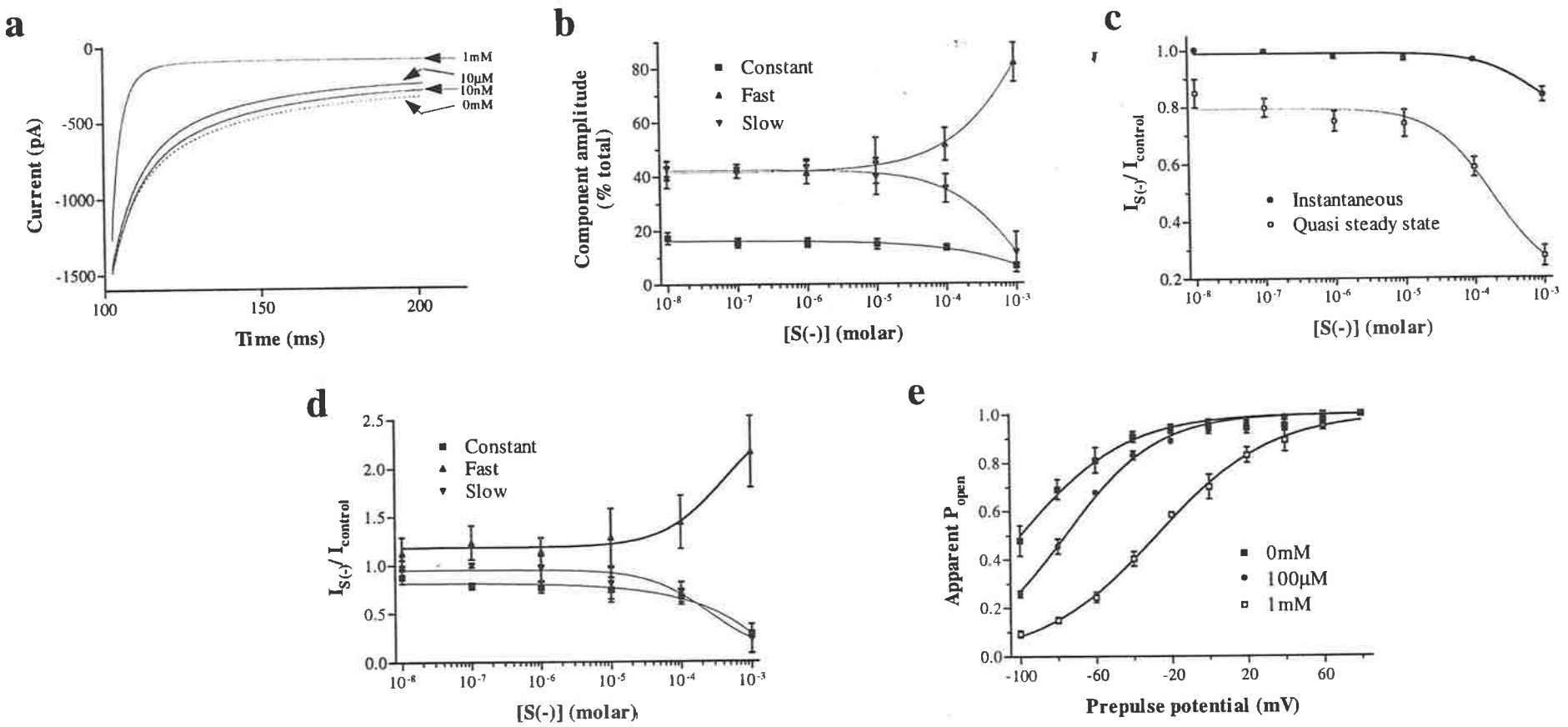

Figure 5.13: **a:** Currents elicited by -120mV test pulses, each preceded by a 100ms prepulse to +40mV, measured in a single cell in the presence of the indicated concentrations of CPP S(-). **b:** Relative component amplitudes measured at different concentrations of CPP S(-). **c:** Dose response data for instantaneous and quasi-steady state currents. **d:** Dose response data for separate components. Data in **b**, **c** and **d** are fitted with sigmoidal dose response functions as described in materials and methods. **e:** Apparent open probabilities vs prepulse potential at various CPP S(-) concentrations. Curves represent fitting of Boltzmann functions as described in Section IV.

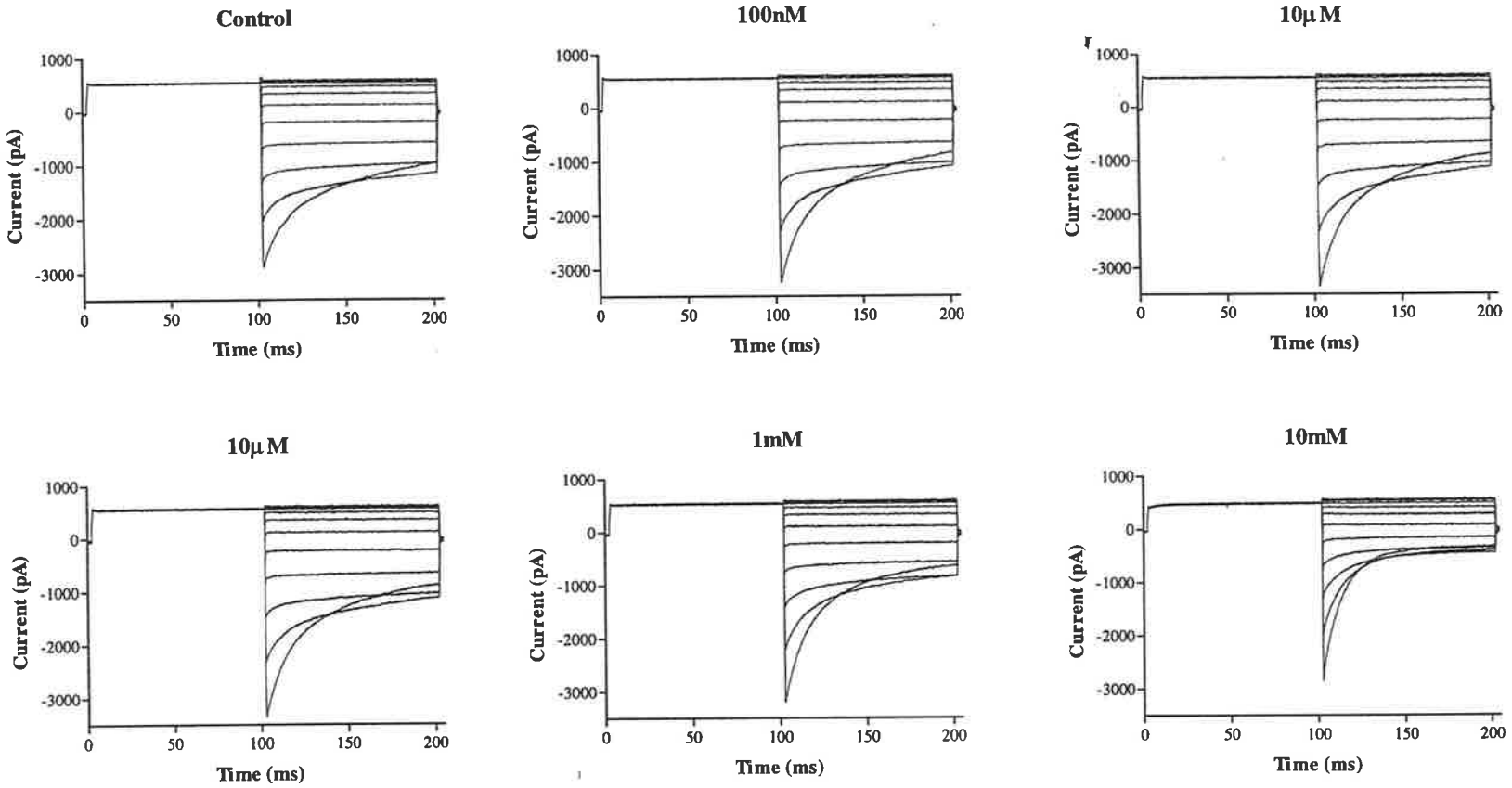

Figure 5.14: Typical families of current traces, all recorded from the same cell, elicited using the activation voltage protocol in the presence of the concentration of CPP R(+) enantiomer indicated above each graph.

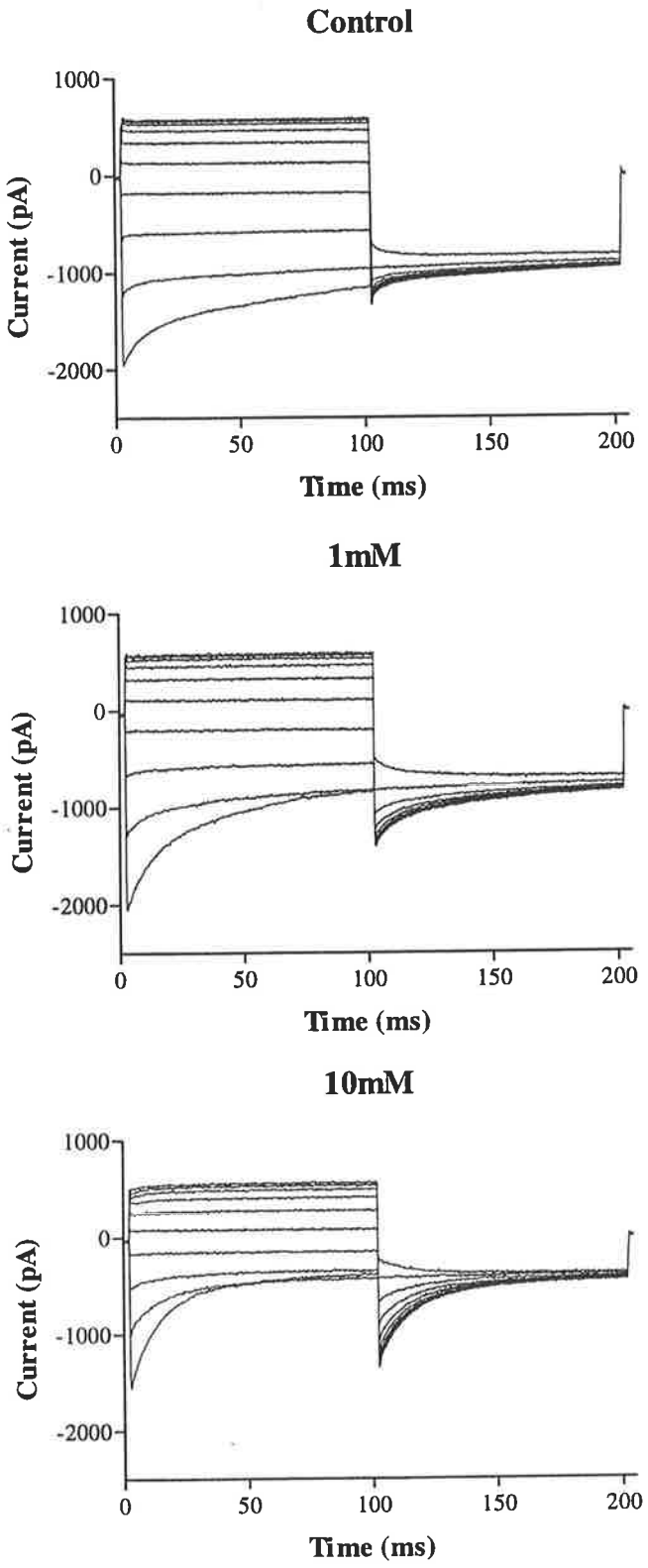

Figure 5.15: Current traces elicited using the -80mV deactivation voltage protocol in a single cell at the concentrations of CPP R(+) enantiomer indicated above each graph.

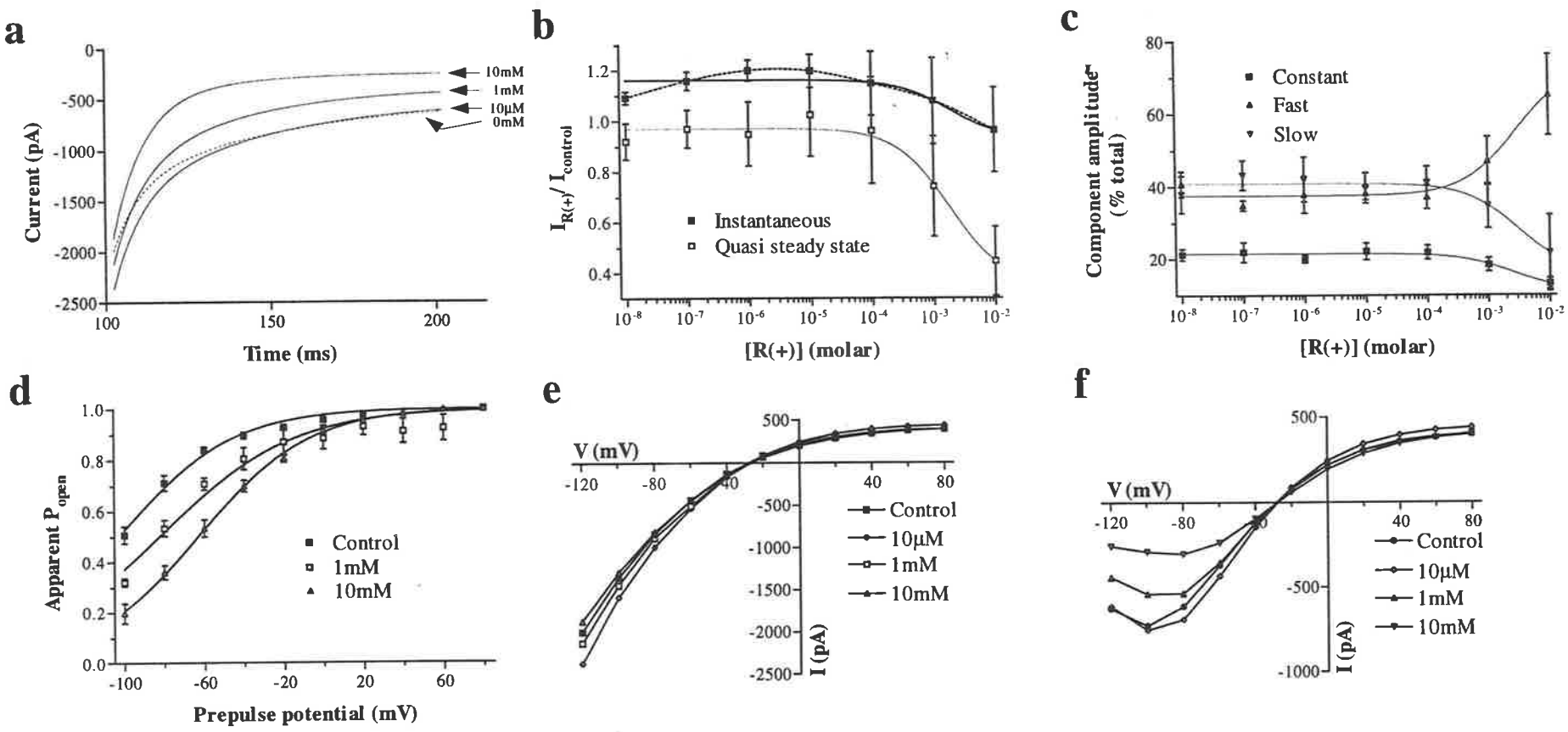

Figure 5.16: **a:** Currents elicited by -120mV test pulses, each preceded by a 100ms prepulse to +40mV, measured in a single cell in the presence of the indicated concentrations of CPP R(+). **b:** Dose response data for instantaneous and quasi-steady state currents. **c:** Relative component amplitudes measured at different concentrations of CPP R(+). Data in **b** and **c** are fitted with sigmoidal dose response functions (solid line) as described in materials and methods. Data for instantaneous currents in **b** are also fitted with a cubic spline (broken line) **d:** Apparent open probabilities vs prepulse potential at various CPP R(+) concentrations. Curves represent fitting of Boltzmann functions as described in Section IV. **e, f:** Instantaneous (**e**) and quasi-steady state (**f**) current/voltage relationships in the presence of CPP R(+) indicated on each graph.

Activation of current in response to positive voltages was beginning to become apparent at 10mM (Figure 5.15) and a significant shift of the open probability curve was also observed (Figure 5.16d). This shift was, as with other aspects of the R(+) effect, less marked than for the S(-) isomer or racemate being only 37mV (-102.8 ± 3.6 vs -63.1 ± 2.4mV) between the control and 10mM measurements. Again the apparent gating charge remained at approximately -1.

Where this enantiomer does differ from the racemate and S(-) is its effect at low concentrations. Both instantaneous and quasi-steady state currents were increased in the presence of sub-mM concentrations. Whilst an increase in instantaneous current was also seen with the racemate, the effect is more marked with R(+). Instantaneous inward current increased after exposure to doses above 10nM to a peak at 1 - 10μM before decreasing in a dose dependent manner, only returning to control values after addition of 10mM R(+) (Figure 5.16a, b, e). The difference between values measured in the presence of 1μM and controls was statistically significant (paired t-test, P = 0.021). Outward instantaneous current was not measurably different from control values except in the presence of doses between 1 and 100μM where a slight, but not statistically significant (paired t-test), increase was noted. In the case of the quasi-steady state current, a slight increase in both inward and outward current was noted at 10μM whilst a dose dependent decrease in inward current was found with mM concentrations (Figure 5.16f). At all other concentrations tested, currents across the entire tested voltage range did not detectably differ from controls.

V.3.4 Indanyloxyacetate 94/95

Only small reductions in instantaneous and quasi-steady state currents were detected with this compound when applied at sub-millimolar concentrations (Figure 5.17).

Addition of 1mM led to a distinct reduction in both inward and outward instantaneous and quasi-steady state currents without changing the overall shape of current/voltage curves (Figure 5.18a, b). No appreciable change in deactivation kinetics or relative component amplitudes was noted at any of the tested concentrations (Figure 5.18c) although a slightly greater reduction in instantaneous current relative to quasi-steady state was noted.

Calculation of IC_{50} values, for currents at -100mV, returned figures of 650μM and 1.4mM for instantaneous and quasi-steady state currents respectively (Figure 5.18d). In contrast to most other blockers used here, IAA was slow to act requiring at least 10 minutes to produce an effect. Although flushing with normal bath solution resulted in reduced block, complete restoration of pretreatment currents was never achieved even after rinsing with large volumes (>50ml).

V.3.5 Zinc

Application of zinc evoked a concentration dependent block of inward and outward currents (Figure 5.19) which was irreversible even after extensive washing (>50ml) with normal bath solution. No qualitative change in the general shape of current/voltage curves or current kinetics was noted until 5mM at which point both instantaneous and quasi-steady state I/V curves become linear with current amplitudes similar to those found in negative control cells (Figure 5.20a, b). Cumulative dose response data returned similar IC_{50} values of 1.8 and 2.1mM for instantaneous and quasi-steady state currents respectively (Figure 5.20c).

V.3.6 Preliminary results with other compounds

V.3.6.1 2-(3-trifluoromethylanilino)-nicotinic acid

Niflumate reduced instantaneous and quasi-steady state inward and outward currents when applied at concentrations above 10μM (Figure 5.21) with marked block being

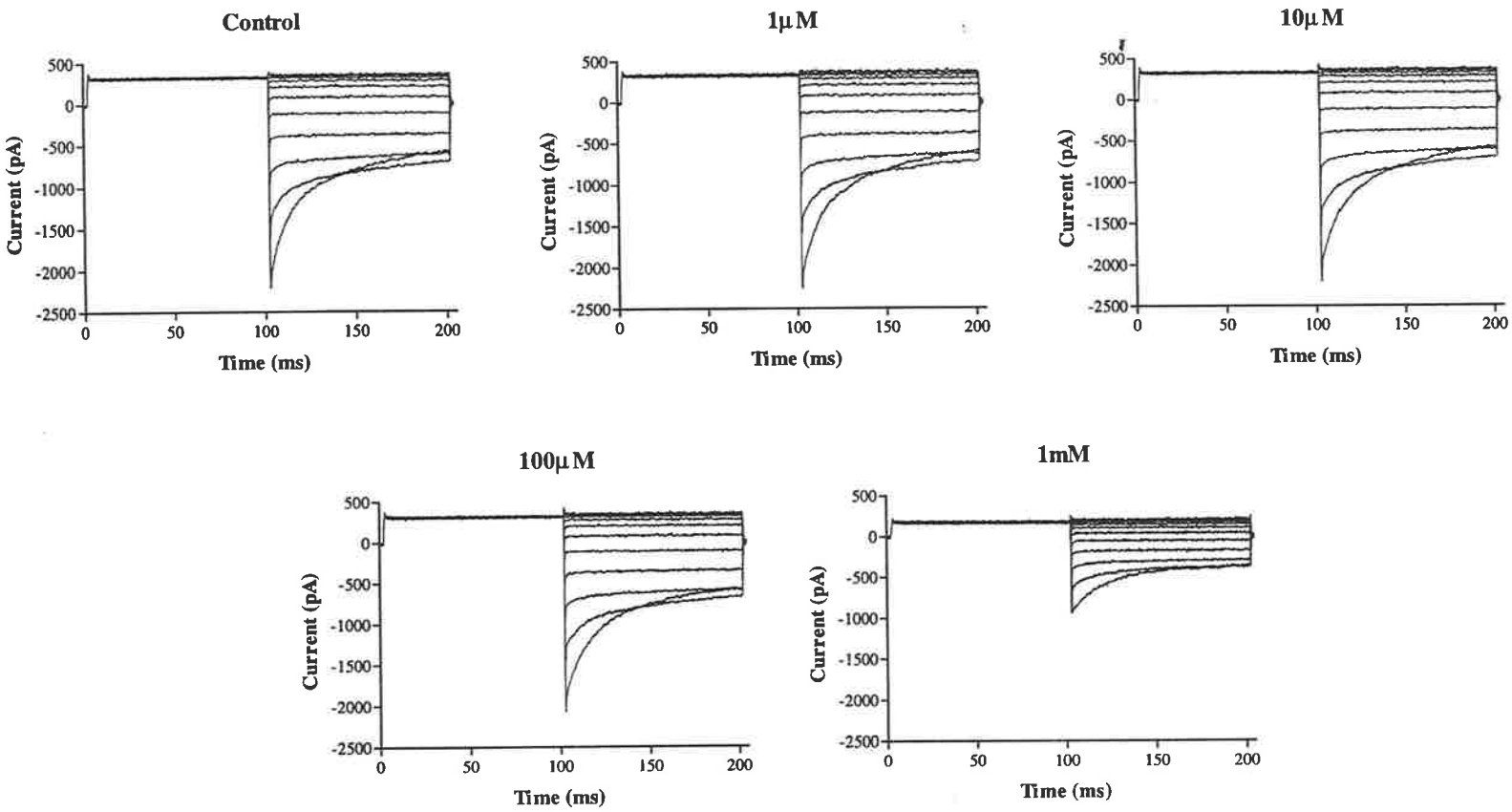

Figure 5.17: Typical families of current traces, all recorded from the same cell, elicited using the activation voltage protocol in the presence of the concentration of IAA indicated above each graph.

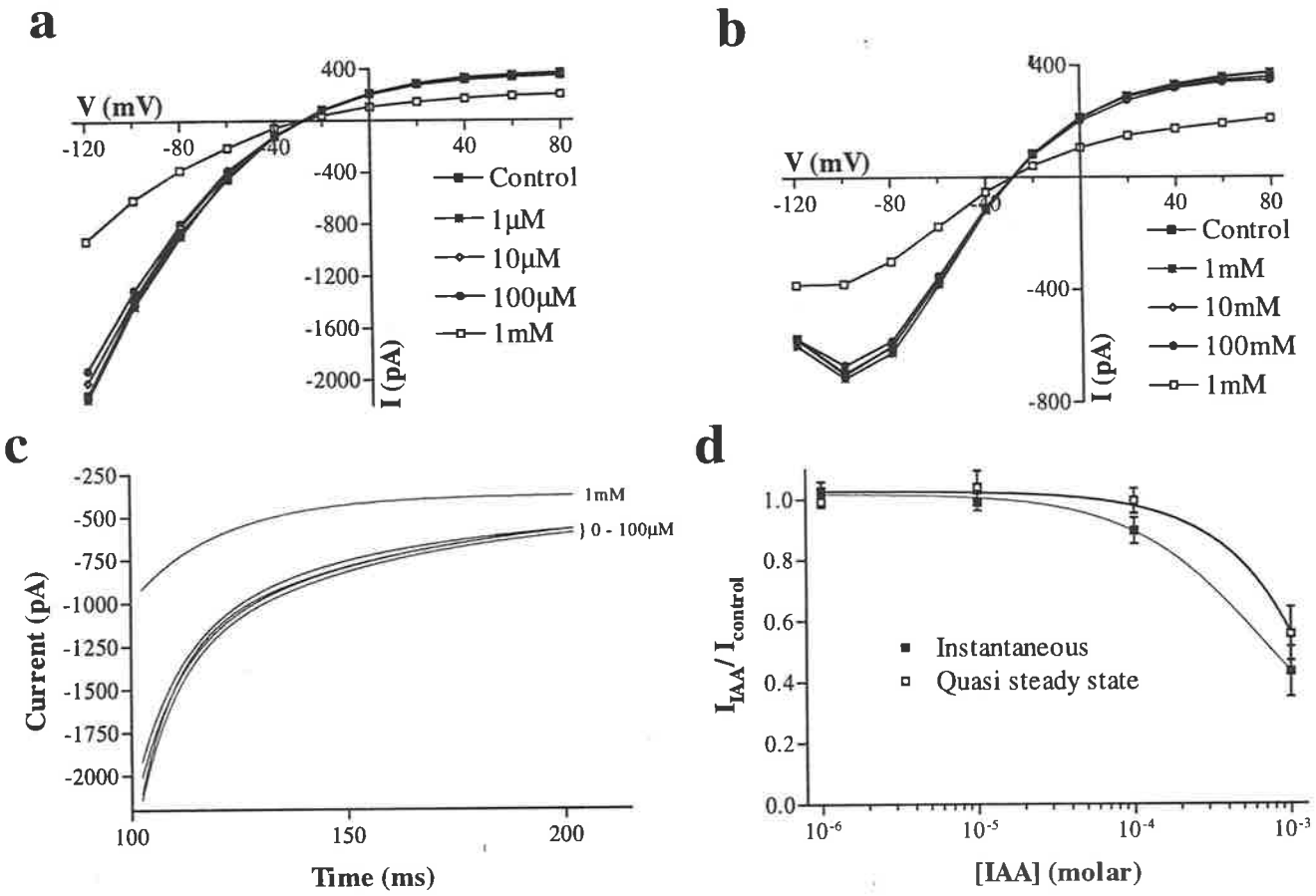

Figure 5.18: a,b: Instantaneous (**a**) and quasi-steady state (**b**) current/voltage relationships measured in the same cell in the presence of the concentrations of IAA indicated on each graph. **c:** Current traces elicited by a -120mV test pulse following a 100ms prepulse to +40mV in the presence of the indicated concentrations of IAA. **d:** Cumulative dose response data for instantaneous and quasi-steady state currents. Curves represent sigmoidal functions as described in materials and methods.

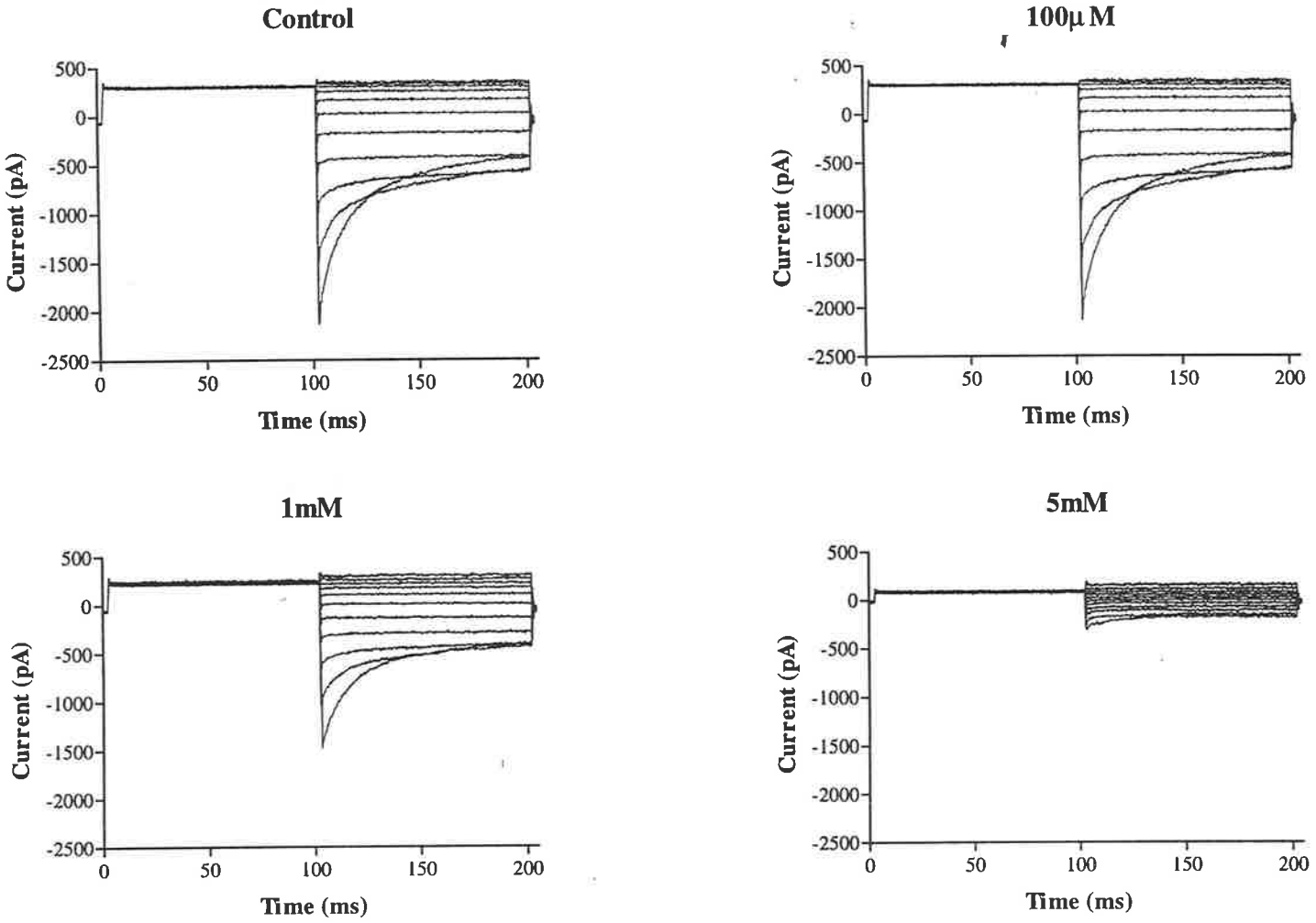

Figure 5.19: Typical families of current traces, all recorded from the same cell, elicited using the activation voltage protocol in the presence of the concentration of Zn^{++} indicated above each graph.

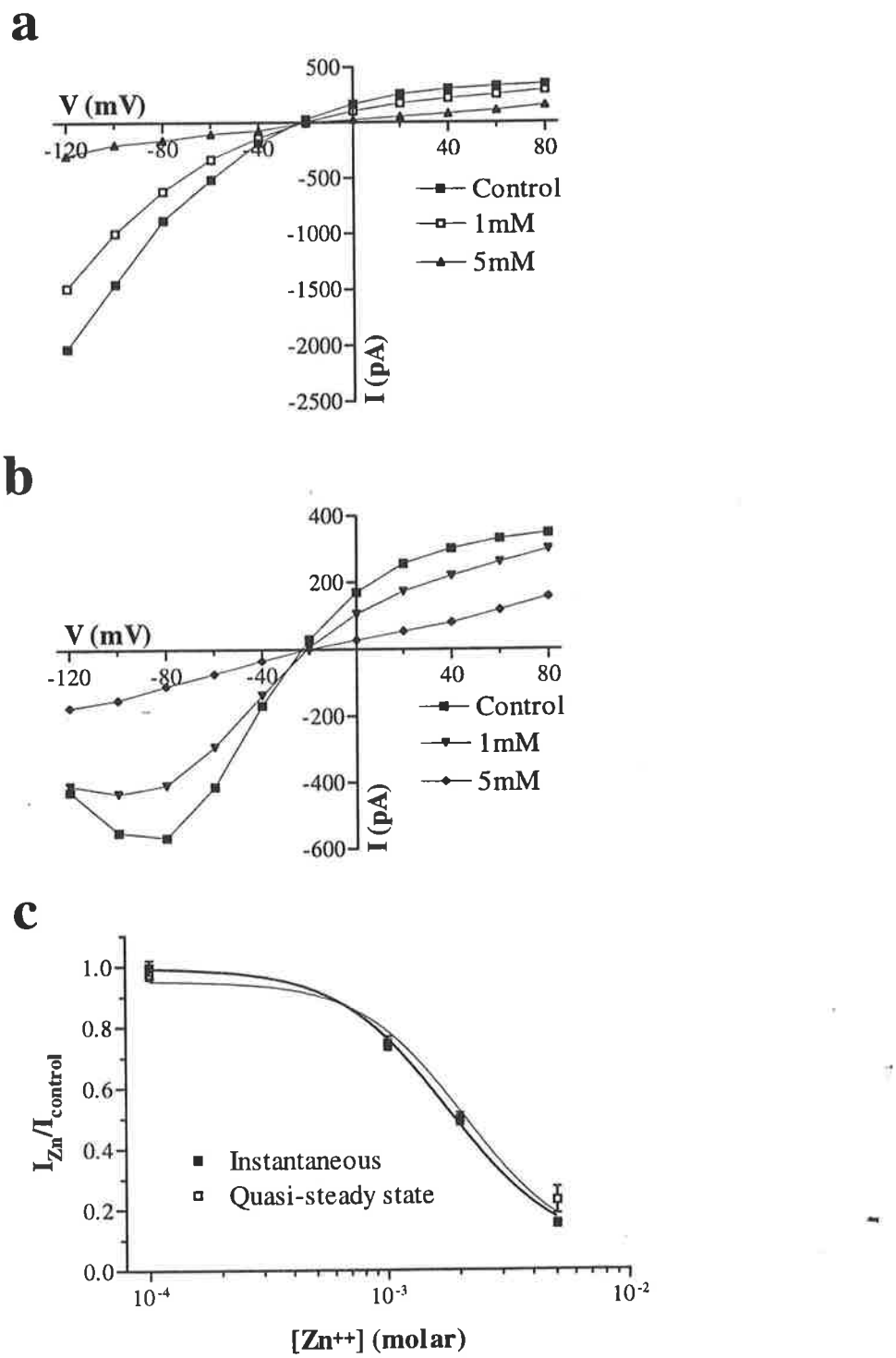

Figure 5.20: a, b: Current/voltage relationships for instantaneous (**a**) and quasi-steady state (**b**) currents measured in the presence of the indicated concentrations of Zn^{++}. **c:** Cumulative dose response data for instantaneous and quasi-steady state currents. Curves represent fit of sigmoidal dose response functions as described in materials and methods.

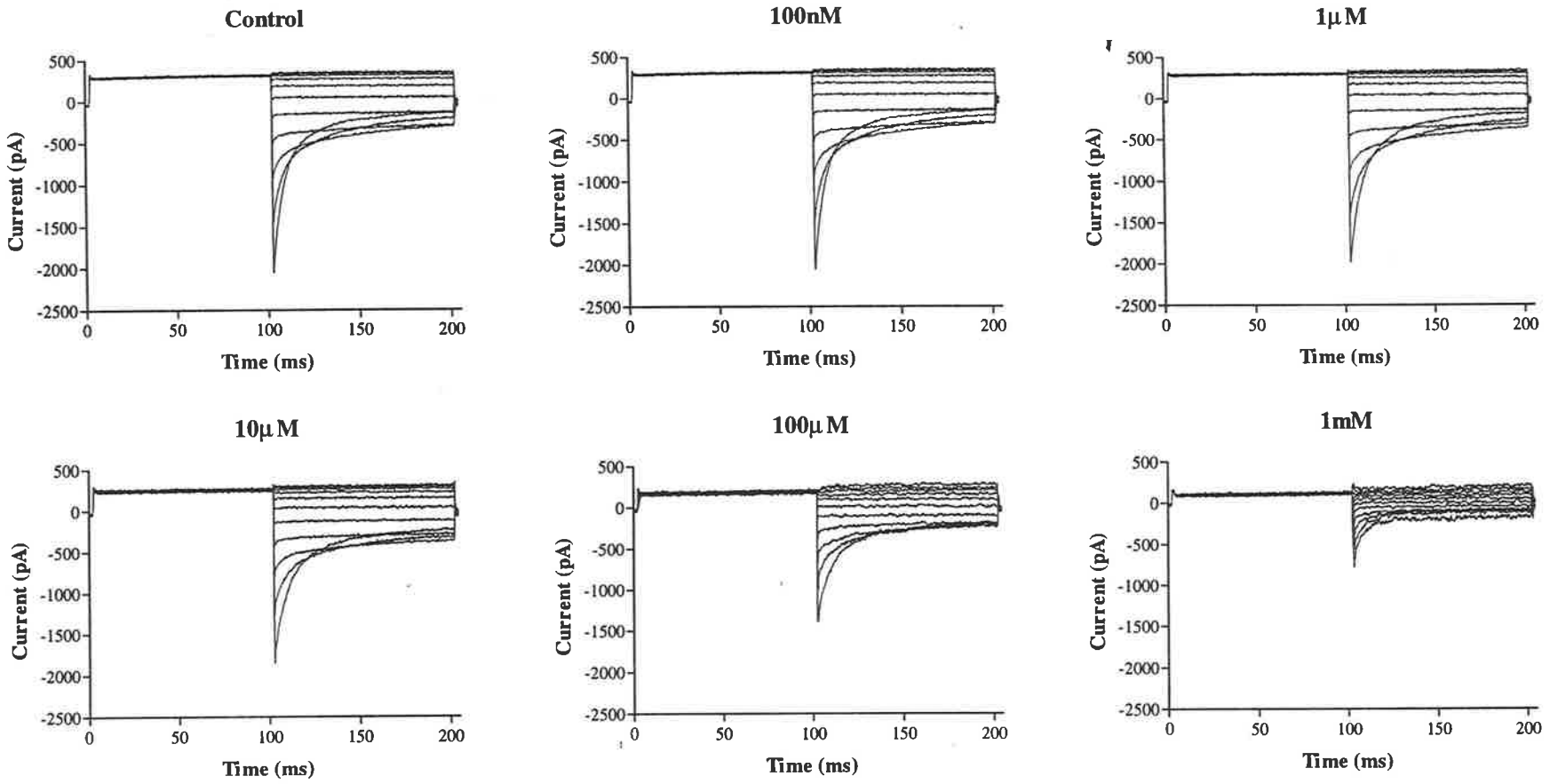

Figure 5.21: Typical families of current traces, all recorded from the same cell, elicited using the activation voltage protocol in the presence of the concentration of niflumate indicated above each graph.

observed at a concentration of 1mM. The general shape of current/voltage curves did not alter appreciably (Figure 5.22a, b).

Calculation of IC_{50} values for instantaneous currents returned a value of 53μM (Figure 5.22c) at a test potential of -100mV (n=1). Dose response data for quasi-steady state currents at test potentials negative to -60mV were generally not well fitted by a sigmoidal function. At more positive potentials however values in the μM range were calculated eg. 100μM at -60mV (Figure 5.22c).

The only change seen in current kinetics was a slow activation of outward current following application of mM concentrations, the effect being easily reversed with minimal washing (Figure 5.23).

V.3.6.2 2,4-dichlorophenoxyacetate

Application of 2,4-D at 2.5mM induced, within seconds, a marked reduction in both instantaneous and quasi-steady state currents (Figure 5.24). As with most blockers used in this study, block was easily reversed with minimal washing (Figure 5.24).

A change in current kinetics similar to that seen with CPP was also noted. Steps to positive potentials evoked activating currents, from which 3 components could be extracted, and inward rectification was reduced. These phenomena were best illustrated when using the deactivation voltage protocols (Figure 5.24d-e).

Calculation of apparent open probabilities at the various test potentials revealed a shift in $V_{1/2}$ of approximately 61mV toward more positive potentials (-88.5 vs –27.1mV) in the presence of 2.5mM 2,4-D (Figure 5.25).

V.3.6.3 diphenylamine-2-carboxylate

Application of 1mM DPC produced very similar effects to 2,4-D (Figure 5.26). Currents decreased within seconds of application and block was relatively easily

reversed, although in the particular case illustrated, control currents were not fully restored before loss of the seal (Figure 5.26).

As with 2,4-D, current kinetics were altered with activation being seen when stepping to positive potentials along with a reduction in the degree of outward current saturation (Figure 5.26d-f). Relative open probability curves were prepared from measurements taken in the presence and absence of DPC. In contrast to other blockers, the control measurements were taken immediately following establishment of whole-cell configuration resulting in a less negative control $V_{1/2}$ value. Despite the fact that $V_{1/2}$ normally drifts toward more negative potentials during the first 20 or so minutes of whole-cell recording (vide Section IV), the $V_{1/2}$ value calculated from data collected 5 minutes after patch perforation of -67.5mV was still markedly different from the +1.5mV measured in the presence of 1mM DPC (Figure 5.27).

V.3.6.4 5-nitro-2-(3-phenylpropylamino) benzoate

Application of NPPB at 1mM markedly reduced inward and outward instantaneous and quasi-steady state currents (Figure 5.28). As with most other blockers restoration of control currents was achieved with minimal washing. Instantaneous inward currents, in the one cell tested thus far, appeared to be reduced more markedly than quasi-steady state (Figure 5.28).

V.4 Discussion

V.4.1 Potency

As can be seen from the summarised IC_{50} data, presented in Table Vb, the efficacy of different compounds varies widely. A9C is the most potent compound tested here with half maximal block occurring at ca. 20μM. This value is within the range of that reported by Palade and Barchi (1977b) in rat skeletal muscle. Most other blockers for which IC_{50}s were calculated appear to be effective in the mM concentration range. A

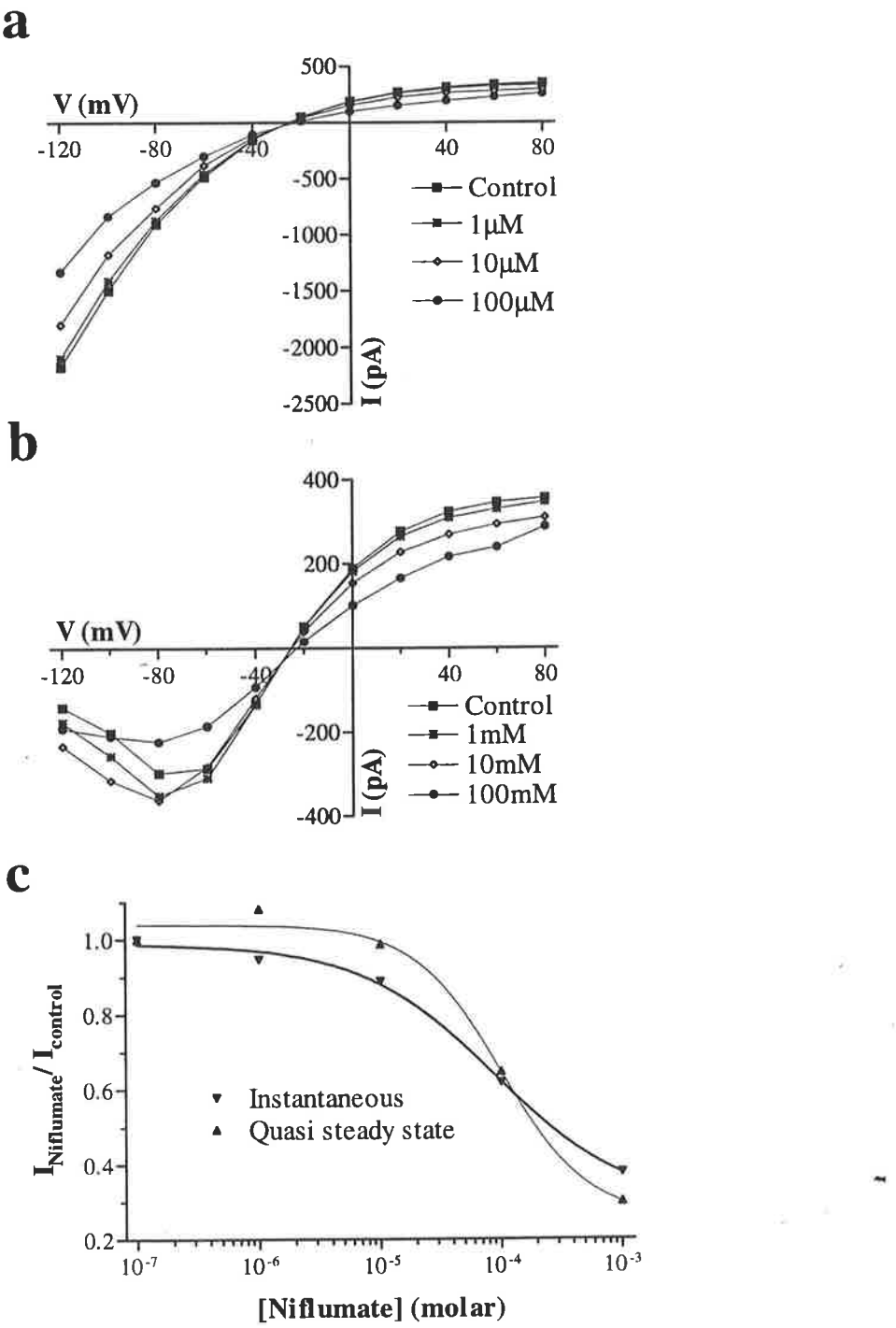

Figure 5.22: a, b: Instantaneous (**a**) and quasi-steady state (**b**) current/voltage relationships at the indicated concentrations of niflumate. **c:** Dose response data for instantaneous and quasi-steady state currents (n=1) measured at -60mV (quasi-steady state) or -100mV (instantaneous) Data are fitted with sigmoidal dose response functions as described in materials and methods.

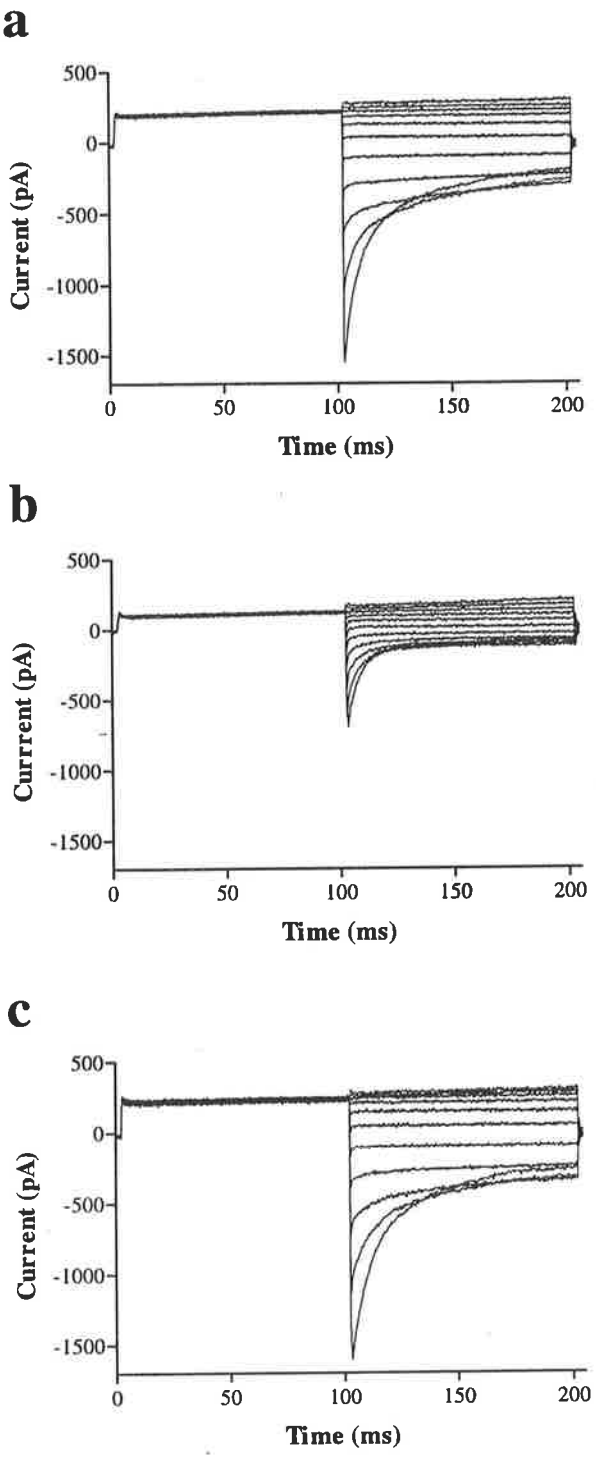

Figure 5.23: **a**, **b**: Current traces recorded in the same cell before (**a**) and after (**b**) addition of 1mM niflumate. **c**: the same cell after rinsing with 10ml of normal bath solution.

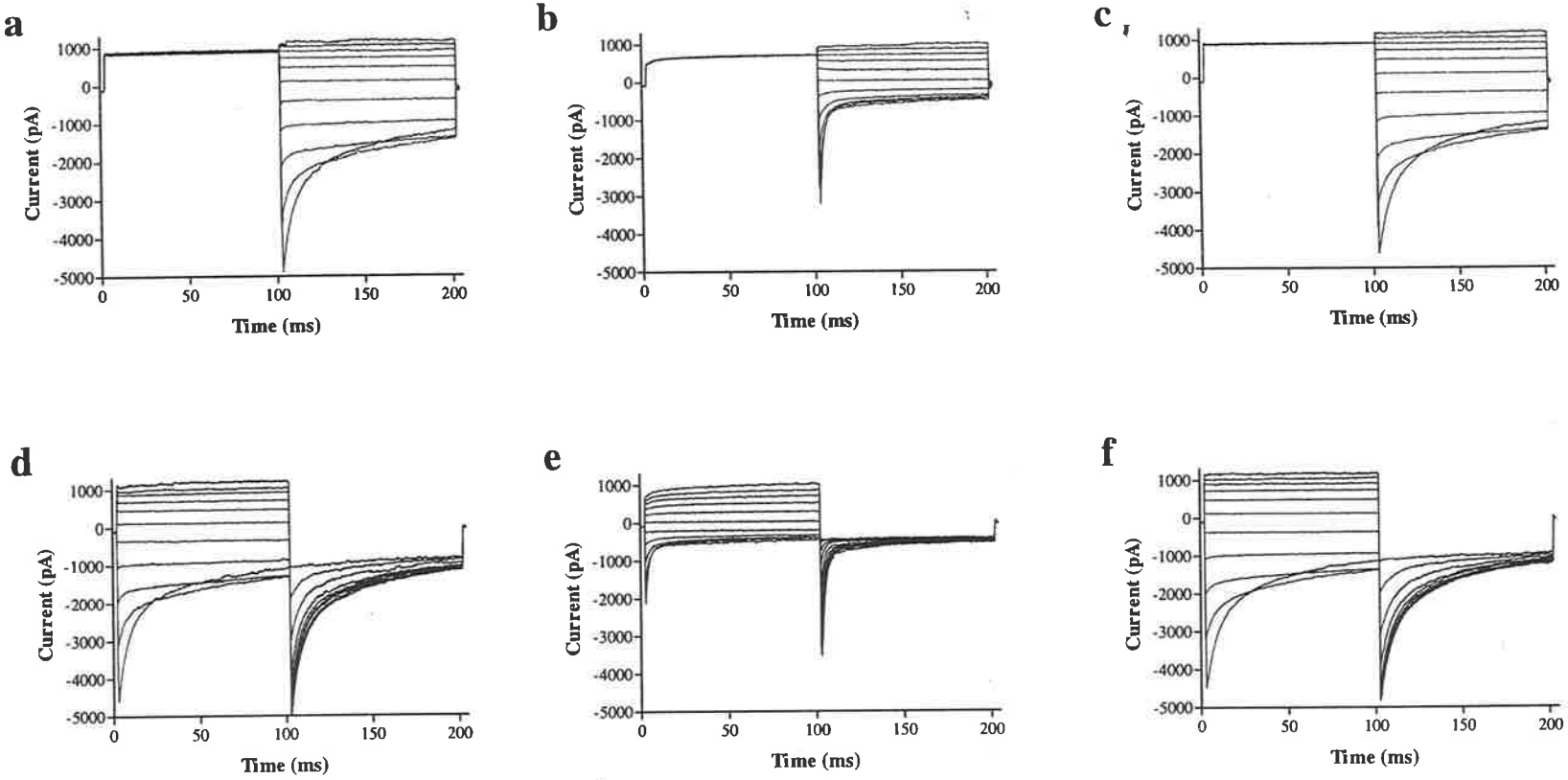

Figure 5.24: a - c: Currents elicited using the activation voltage protocol before (**a**) and after (**b**) addition of 2.5mM 2,4-D. **c:** Currents recorded from the same cell after rinsing with 10ml of normal bath solution. **d - e:** Currents recorded from the same cell as in **a - c** elicited using the -120mV deactivation voltage protocol before (**d**) and after addition of 2.5mM 2,4-D and following rinsing with 10ml of normal bath solution (**f**).

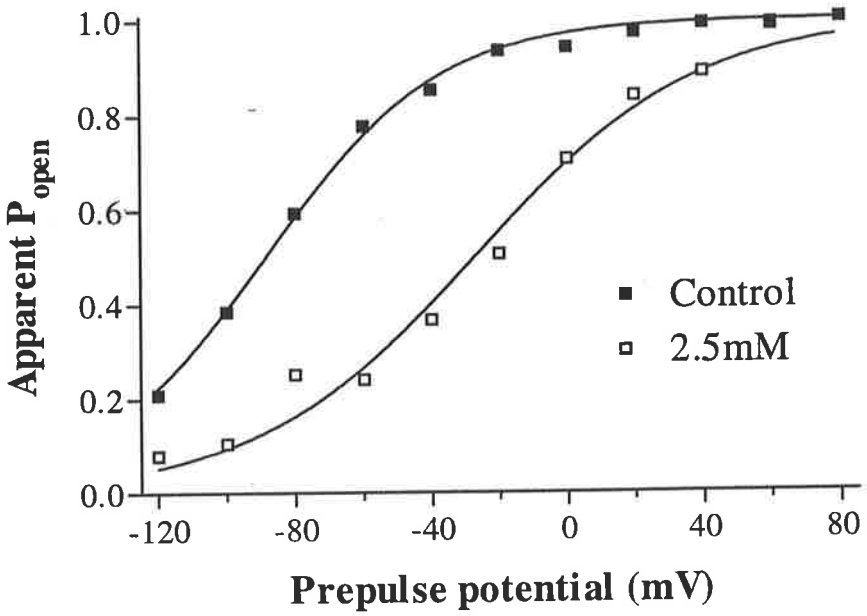

Figure 5.25: Apparent open probabilities in the presence and absence of 2.5mM 2,4-D (n=1). Curves represent fitting of Boltzmann functions as described in Section IV.

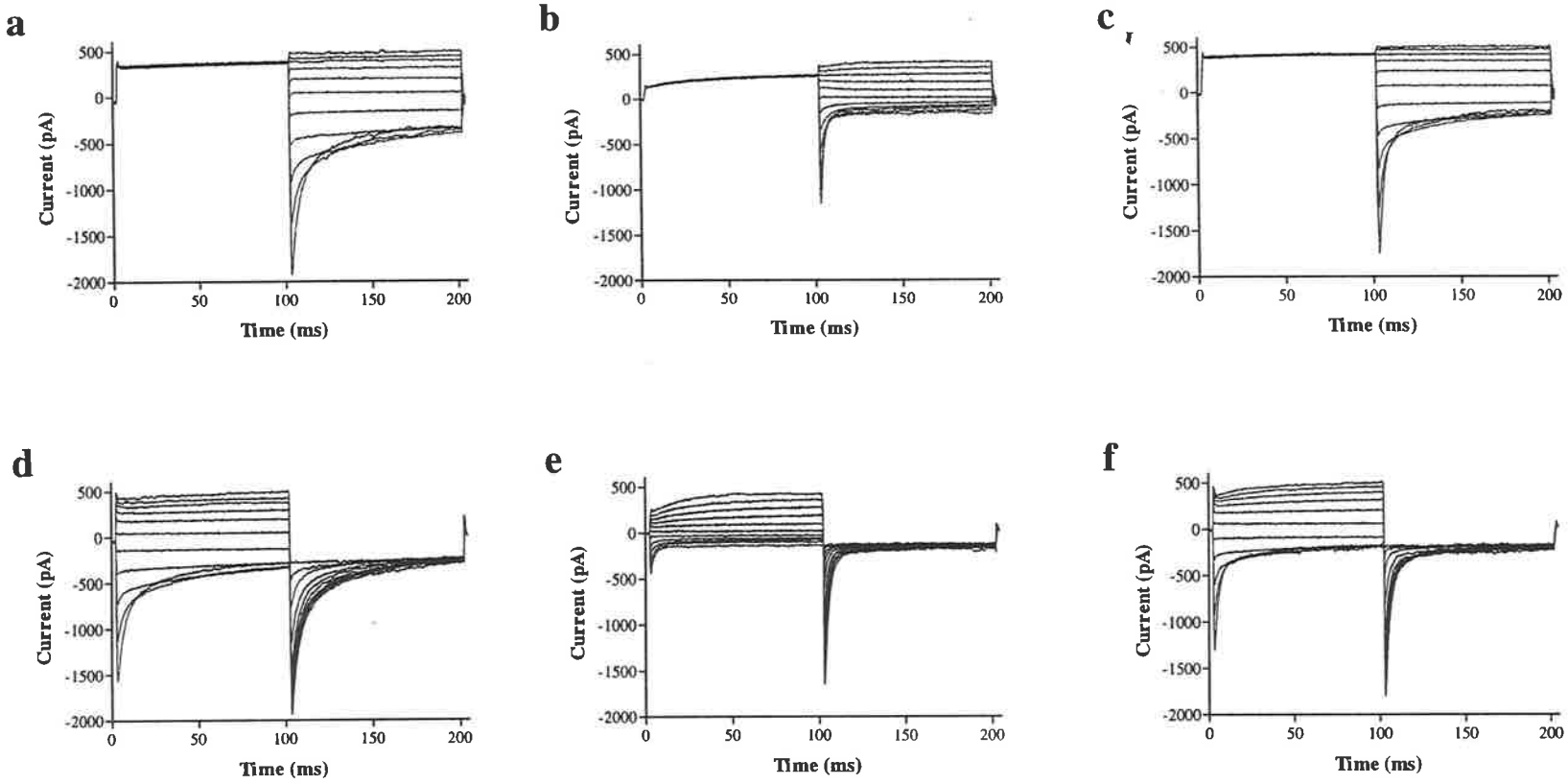

Figure 5.26: a - c: Currents elicited using the activation voltage protocol before (**a**) and after (**b**) addition of 1mM DPC. **c:** Currents recorded from the same cell after rinsing with 10ml of normal bath solution. **d - e:** Currents recorded from the same cell as in **a - c** elicited using the -120mV deactivation voltage protocol before (**d**) and after (**e**) addition of 1mM DPC and following rinsing (**f**) with 10ml of normal bath solution.

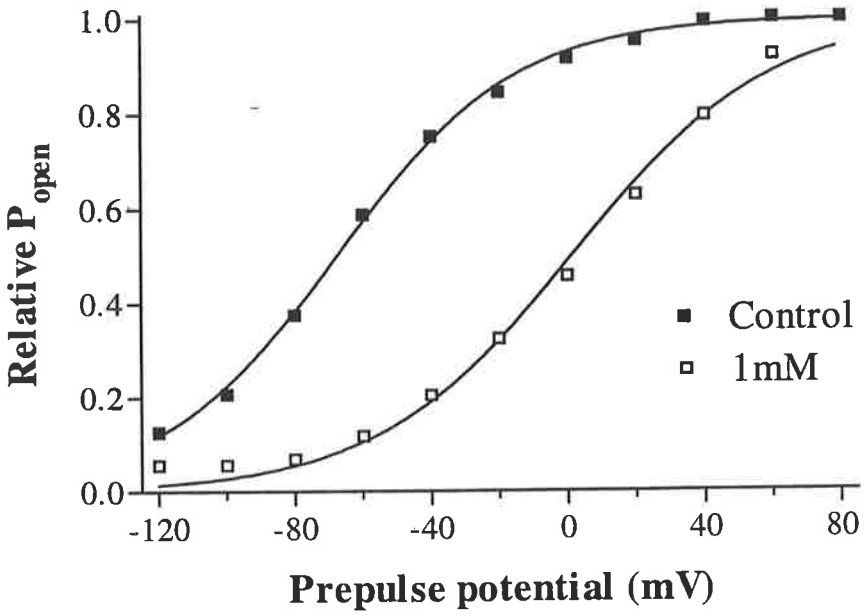

Figure 5.27: Apparent open probabilities in the presence and absence of 1mM DPC (n=1). Curves represent fitting of Boltzmann functions as described in Section IV.

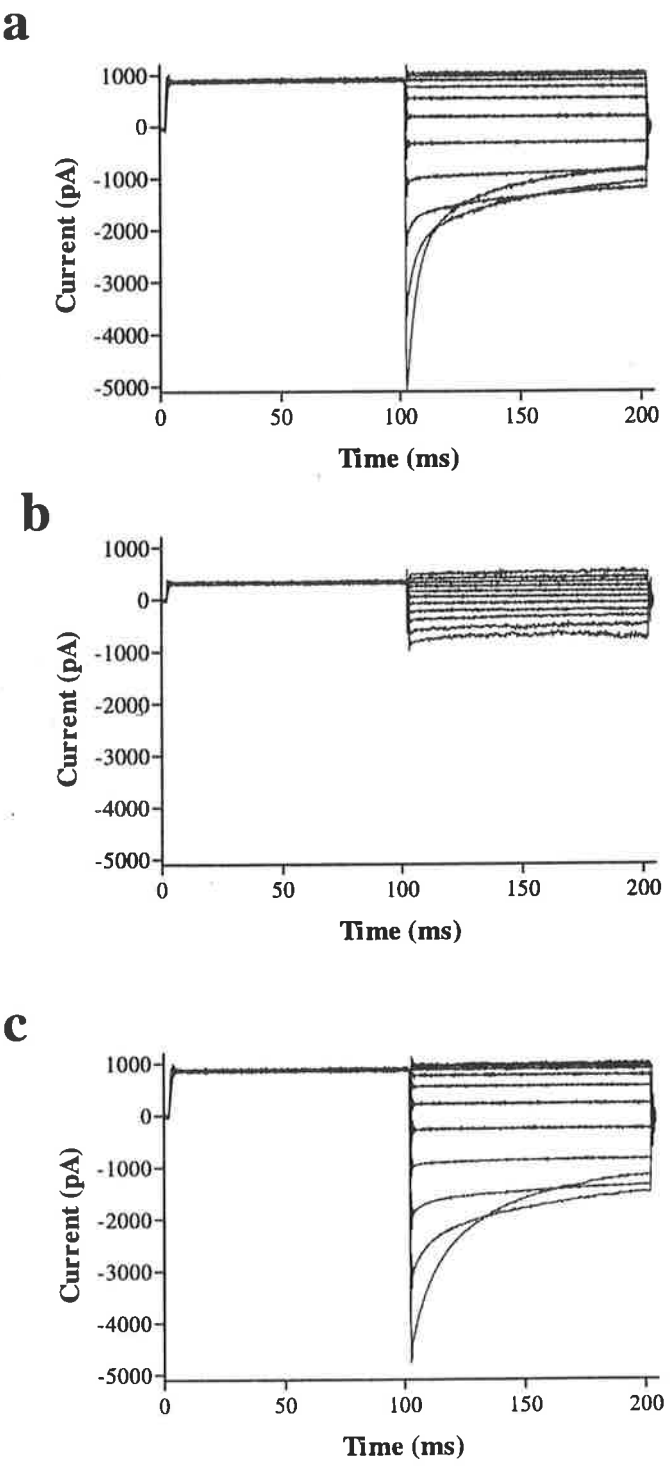

Figure 5.28: **a,b:** Currents elicited using the activation voltage protocol in the absence (**a**) and presence (**b**) of 1mM NPPB. **c:** Currents recorded from the same cell following rinsing with 10ml of normal bath solution.

Compound	Total Current	
	Instantaneous	Quasi-steady state
Antrhacene-9-carboxylate	21μM	29μM
2-(4-chlorophenoxy) propionate		
Racemate	6.3mM	730μM
R(+) enantiomer	1.8mM*	5.2mM*
S(-) enantiomer	940μM*	190μM
Indanyloxyacetate	650μM	1.4mM
2-(3-trifluoromethylanilino)-nicotinic acid	53μM	100μM
Perrhenate	1.1mM	3.5mM
Zinc	1.8mM	2.1mM

Table Vb.1: Summary of blocker potencies on total instantaneous and quasi-steady state currents. * = $R^2 < 0.8$

Compound	Current Component		
	Fast	Slow	Constant
2-(4-chlorophenoxy) propionate			
Racemate	300μM♦	620μM	1.1mM
R(+) enantiomer	8mM*♦	8mM*	5.3mM*
S(-) enantiomer	430μM♦	240μM	440μM
Perrhenate	490μM	1mM	11.5mM*

Table Vb.2: Summary of blocker potencies on individual current components.
* = $R^2 < 0.8$ ♦ = increasing amplitude

possible exception is niflumate for which preliminary results suggest an IC_{50} in the sub-millimolar range.

The calculated potencies of CPP and its enantiomers were found to be much lower than reported in studies on whole muscle preparations (Bettoni et al., 1987; Conte-Camerino et al., 1988b; De Luca et al., 1992). Conte-Camarino et al., De Luca et al. and Bettoni et al. report IC_{50} values for the racemic mixture and S(-) enantiomer 10 to 100 times lower than calculated here. With regard to the R(+) enantiomer, an exact potency was not presented by any of the previous investigators, the IC_{50} being reported as >230μM. A direct comparison of the effect on total currents cannot therefore be made. However, the concentration range at which current increases are seen in this work is almost identical to that reported for the studies in whole muscle. Compared to the previously published work, there is a difference in the behaviour of the R(+) form at higher concentrations. Whole muscle studies indicated a maximal inhibition of 25% of control conductance at concentrations above 100μM. No such plateau in current reduction was seen here, the degree of block in the mM range being relatively proportional to concentration.

There is a difference in the methods used to separate the enantiomers in this work compared to previous studies. Previous investigators used brucine/ ethanol crystallisation as a separation tool whilst enantiomers used in this study were separated by application of chromatography employing a chiral column. This, however, is unlikely to account for the discrepancies. In fact the compounds used in this work, prepared by Prof. SH Bryant, a co-author in the previously mentioned reports, were found to be of higher purity, as judged by chromatographic analysis, than those prepared using brucine salts (SH Bryant, personal communication). The

only other major difference between the two studies is the environment in which the chloride channel has been investigated. In the whole muscle studies there are numerous other contaminating conductances which need to be accounted for. In the muscle fibre studies, chloride conductance was assessed by measuring the cable parameters of test fibres in chloride-containing and chloride-free solutions before and after the addition of the test compound. Membrane conductance attributable to chloride was calculated by subtraction of the conductance in chloride free solution, presumed to be largely potassium conductance, from that in chloride-containing bathing solution. Using this indirect method it is possible that if CPP and its enantiomers also induce a relative increase in membrane conductance in chloride free solutions then this could lead to a calculated IC_{50} lower than is actually the case. However, the increase in membrane conductance required to account for a discrepancy of the size found is unlikely to have gone unnoticed. At this stage, therefore, this author has no reasonable explanation for the discrepancy between the two sets of data. IAA 94/95 has been found to be a potent blocker of chloride conductance in epithelial tissues (Landry et al., 1987; Tilmann et al., 1991) with IC_{50}s reported in the μM range. No IC_{50} value has previously been reported for its effect on skeletal muscle although the 94 enantiomer has been reported to be highly effective when injected into single muscle fibres (Weber-Schürholz et al., 1993). The slow onset of block and poor reversibility reported here are consistent with an intracellular site of action as has previously been proposed (Weber-Schürholz et al., 1993). The relatively high IC_{50} may therefore simply be a reflection of application at an inappropriate site and the dependence on diffusion across the membrane before the compound can take effect. Preliminary experiments in our laboratory applying IAA intracellularly via the pipette have, however, failed to elicit any detectable reduction in whole-cell currents

(Rychkov and Astill, unpublished observations). Even allowing for the differences in concentration of the 94 form between purified enantiomer and racemic preparations, this result is at odds with reports of intracellular block in whole muscle (Weber-Schürholz et al., 1993). It is clear that further work, in particular using the 94 form of IAA, needs to be done if this issue is to be resolved.

V.4.2 Possible modi operandi

The blockers used in this study can be broadly divided into three groups on the basis of their effect on whole-cell current kinetics. Group 1 encompasses substances which do not detectably alter kinetics eg. A9C, IAA and zinc. Group 2 includes compounds which produce alterations, in some cases quite subtle, in one or more aspect(s) of current kinetics eg. perrhenate, niflumate and NPPB. Finally, group 3 contains blockers which perturb almost every kinetic parameter to some degree eg. CPP, 2,4-D and DPC. Whilst this is a convenient basis on which to classify compounds for the purposes of this discussion, it should be kept in mind that this form of classification does not reflect any structural similarities between different molecules and that compounds which induce similar responses need not necessarily act at the same site nor via exactly the same mechanism.

V.4.2.1 Group 1

Upon application of these substances, instantaneous and quasi-steady state currents are relatively equally affected and no significant change in deactivation, inward rectification or relative component amplitudes is seen at any concentration. This finding alone would seem to suggest that the compounds in this group do not act via interference with the gating mechanism.

Of these compounds, zinc appears to interact with the channel in the simplest manner. Given its charged nature, hydrophilicity, small size and rapid effect, it seems likely

that this divalent cation interacts with the channel at residues exposed to the aqueous environment. The characteristics of the block induced are consistent with occlusion of the pore. However, given that cation channel pores are found to have an overall negative charge, which acts to attract cations into the permeation pathway, and that these channels can be blocked by foreign cations (cf. for example Stanfield et al., 1994; Ikeda and Korn, 1995; Kirsch et al., 1995; Pascual et al., 1995) we would logically expect the pore of an anion-selective channel such as ClC-1 to exhibit an overall positive charge. This being the case, direct interaction between the pore of ClC-1 and Zn^{++} would appear unlikely. It is possible that Zn^{++} binds to a site remote from the actual pore but that in doing so it causes some residue(s) to interfere sterically with the passage of chloride into the pore proper, producing blocking characteristics indistinguishable from simple occlusion. Given the small size of this divalent cation and that most channels investigated to date appear to have rather wide external mouths, which only narrow closer to the selectivity filter (cf. for example Lü and Miller, 1995; Pascual et al., 1995), it is suggested that zinc induces some sort of conformational change leading to either channel closure or inaccessibility of the chloride binding site(s). The lack of reversibility even with extensive rinsing implies that zinc binds tightly to the protein and considering the pH at which this binding occurs, single or multiple histidine residues would be likely candidates for Zn^{++} binding by coordination bonding via their imidazole moiety (*vide* Section VI).

A9C shows slightly different behaviour in that although it takes effect rapidly and does not alter kinetics, its effect is initially fully reversible but it becomes increasingly difficult to remove with increasing duration of exposure. There are a number of possible explanations for this sort of behaviour. Given the rapid onset and constant degree of block at a given concentration, it would seem likely that A9C binds with a

fast on, and off, rate to a specific site. The slowed apparent off rate with longer exposure may be indicative of a second binding site, interaction with which also induces blockade, to which A9C binds more strongly with slower on and off rates. Thus with prolonged exposure more blocker molecules become bound to the slow on/ off site with the result that block is more difficult to reverse.

Previous investigators working with this compound have suggested that A9C interacts with the channel via both a hydrophobic and hydrophilic site (Bryant and Morales-Aguilera, 1971; Palade and Barchi, 1977b). Bryant and Morales-Aguilera (1971) suggested that the molecule anchors itself to the "lipid rim" of the channel via its flat multiple ring structure and the carboxyl interacts within the pore to sterically inhibit conduction. Palade and Barchi (1977b) suggested, on the basis of A9C-induced changes in the conductivity sequence of halide anions, that a change in protein conformation seemed more likely. These investigators also suggested an intramembrane site of action. The data presented here can be used to support this hypothesis. A9C may induce a conformational change as a result of interaction with an intramembrane site and the reduced reversibility with increased time of exposure may simply reflect accumulation of A9C in the membrane. Any molecules removed from their binding site(s) during rinsing may be so rapidly replaced by others in close proximity to the channel that no obvious reduction in block is detected. Prolonged exposure has been reported to be cytotoxic to muscle fibres (Palade and Barchi, 1977b) and this also appears to be the case with Sf9 cells. This could be due to some change/ damage to the Sf cell plasmalemma induced by an intramembrane accumulation of A9C as proposed above. Thus, at this stage it is not possible to rule out the hypotheses of either Palade and Barchi (1977b) or Bryant and Morales-Aguilera (1971).

Recent experiments performed in our laboratory by Dr. G Rychkov indicate that the potency of A9C increases with reduced chloride concentration (Astill et al., 1995a). Whilst this might imply that A9C and chloride compete for a common site, presumably within the channel pore, it does not exclude the possibility that A9C binds at a site remote from that which interacts with chloride. It could be envisaged that binding of A9C to a site remote from the pore may induce a reversible change in protein conformation which either destroys one or more chloride binding sites or renders them inaccessible. Conversely, when chloride is bound to its site(s) the channel may be unable to undergo this A9C-induced conformational change and/or bound blocker may be displaced. According to this scenario an equilibrium between chloride and A9C binding would exist which would clearly be shifted in favour of the blocker with reduced chloride concentration. Given the evidence to date that both ClC-0 (Pusch et al., 1995a) and ClC-1 (Rychkov et al., 1995) are gated by the permeating anion, the characteristics of A9C-induced block are not unexpected since it appears to prevent interaction of chloride with the channel protein. Once closed, this leads to the inability of the channel to gate to the open conformation.

Experiments, again performed by Dr. G. Rychkov, in our laboratory (Astill et al., 1995b) have revealed another interesting aspect of A9C-induced block, this being a change in the calculated IC_{50} under conditions of reduced pH. Changing the extracellular pH from 7.4 to 5.5 results in a more than 20 fold increase in potency. Titration experiments using 1μM A9C give a pKa for this shift of 6.4 with a Hill coefficient of 1. The pKa is in the range expected for the involvement of histidine residues. Thus it would appear that altering the protonation state of probably a single histidine residue increases the affinity of the protein for A9C. This effect does not necessarily indicate the involvement of a histidyl residue in the binding site and may

simply reflect a charge effect where the increase in positive charge brought about by protonation increases the attraction between ClC-1 and negatively charged A9C molecules making them more likely to interact.

IAA 94/95 also appears to reduce inward and outward instantaneous and quasi-steady state currents relatively proportionally which is suggestive of a single site of action. As mentioned above, the results obtained with this compound suggest an intracellular site of action however no supporting evidence has been obtained in preliminary experiments where application was made via the pipette. It is possible that this compound interacts with the same site as A9C accounting for its similar effects on current without appreciably altering kinetics. If there are two sites of interaction with A9C, one fast and one slow, then IAA interaction with the slow, more strongly interacting site would be consistent with the slow onset of block and poor reversibility observed with this compound. Further experiments with this compound and its enantiomers are required before any firm conclusions can be drawn.

V.4.2.2 Group 2

Given its structure one would predict that perrhenate could only interact with parts of ClC-1 exposed to the aqueous environment, for example the ion conduction pathway. An expected modus operandi for this compound would be simple occlusion of the pore. Its behaviour, however, suggests that a more complex interaction occurs between the channel protein and this anion. Whilst movement of chloride into the cell is perturbed in a simply concentration dependent manner, consistent with possible occlusion, the increase in chloride movement out of the cell, represented by inward current, at concentrations close to the IC_{50} cannot be explained by such a simple model. This compound appears to interfere with gating, in particular, impeding the activation of the molecular process responsible for the fast deactivating exponential

component. It is the effect on this component, beginning at μM concentrations, which results in the marked reduction in instantaneous inward currents.

As to a mechanistic explanation for the kinetic changes, it is tempting to suggest the involvement of two, or more, separate binding sites. Binding at one site could conceivably interfere with a fast gate responsible for the fast current component. This interaction may also exhibit fast on and off rates resulting in a flicker type block, for example similar to that induced by stilbene-sulphonate derivatives, IAA and NPPB with the ICOR chloride channel (Tilmann et al., 1991). Binding at a second site may interfere with a second slow gate tending to hold it in an open conformation. To fit this proposal with the data presented here, access to the second binding site must only occur when the channel is open and when mM concentrations are applied. At sub mM concentrations, the channel could be rapidly gating between closed and open states as a result of the binding to the site on the fast gate. During times that the channel is open, binding to the second site, which impedes closing and consequently increases quasi-steady state current amplitudes, could occur. As the perrhenate concentration is increased beyond 1mM, the probability of binding to the fast gate approaches 1. This results in the channel open probability approaching 0 a possible consequence of which could be the second site becoming inaccessible in turn resulting in the only detectable effects being due to interaction with the fast on/ off (blocking) site. This would be seen as a relatively proportional and marked reduction in both the instantaneous and quasi-steady state inward and outward current. The results also raise the possibility that the molecular basis for at least the two exponentially decaying components involve structurally distinct moieties.

The slowly activating outward current seen in the presence of mM concentrations of niflumate and in response to strongly depolarising potentials was a consistent

phenomenon (n = 4). Since there was no measurable shift in either the cell membrane potential or the reversal potential under these conditions, the possibility that this current is due to increasing leakage was ruled out. The implication from these results is that niflumate interferes with the gating process slowing the transition from closed to open state in response to stepping to a positive membrane potential. At this stage there is too little information to draw any firm conclusions about this behaviour.

As yet, no detailed information has been obtained with NPPB. There is a hint that this compound may interfere with the gating process as evidenced by its more marked effect on instantaneous than quasi-steady state currents. Further work will reveal what effects this blocker induces when applied at lower concentrations. Until these experiments are completed no meaningful comments can be made regarding its possible mode of action.

V.4.2.3 Group 3

All blockers in this group appear to alter both the sensitivity of the gating process to voltage and the kinetics of deactivation.

The shift of the open probability curve to more positive potentials is difficult to explain in terms of direct interaction with a voltage sensor of the type seen in cation channels (for review see Franciolini, 1994) simply on the basis of bound blocker altering the charge of a gating "particle". For example, direct interaction could add a negative charge to the sensor reducing the positivity of a positively charged particle and vice versa for a negative particle. A reduction in net positive charge would make the sensor less sensitive to both intracellular positivity and negativity making the channel less likely to gate regardless of the membrane potential. Increasing the negativity of a negative particle would make it more sensitive to voltage, the result being opening at less positive and closing at less negative potentials. Since neither

situation appears to fit the experimental results, an indirect effect induced when blocker binds at a site, or sites, remote from the voltage sensor appears more likely. The inability to explain the experimental data on the basis of interaction with a charged gating particle is perhaps not unexpected given the finding that in ClC-0 (Pusch et al., 1995a) and possibly ClC-1 (Rychkov et al., 1995) the permeating anion acts as the gating charge.

The finding that the permeating anion needs to be bound to a site within the pore of ClC-0 for it to open (Pusch et al., 1995a) may provide some clue as to the shift in voltage sensitivity seen with ClC-1 in the presence to these compounds. Given the similar behaviour seen with ClC-1 (Rychkov et al., 1995), the shift in the voltage dependence of gating induced by this group of blockers could be explained on the basis of the introduction of a negative charge adjacent to a chloride binding site to which chloride must bind to open the channel. Under normal circumstances, at depolarising potentials chloride is drawn toward this binding site and repelled under conditions of hyperpolarisation. If a negative charge were introduced near this site, a stronger driving force would be required to attract the permeating anion toward the site ie. a more positive intracellular potential. Similarly, the anion would be more strongly repelled at less negative intracellular potentials. Thus the result would be a shift of the open probability curve to the right.

Recently a series of ClC-1 point mutations found in autosomal dominant human myotonia congenita have been investigated *in vitro* (Pusch et al., 1995b). The changes in biophysical behaviour found with these mutants are very similar to those induced by this group of blockers ie. the most marked change is a shift of the open probability curve to more positive potentials without any appreciable change in the apparent gating charge. No comments were made by Pusch et al. regarding deactivation

kinetics or relative component amplitudes although the current traces presented in their report do appear to show slightly faster deactivation and possibly a reduced amplitude of the slow exponential component in the mutant channels, particularly R317Q and Q552R. The cause of the shift in voltage sensitivity seen in these mutants was proposed to be an alteration in the thermodynamic stabilities of the open and closed states. It is possible that the interaction of this group of blockers with ClC-1 produces a similar effect. Interestingly, the residues involved, I290, R317, P480 and Q552, are fully conserved in both the rat and human sequences. It would be an interesting exercise to examine the response of these mutants to this group of compounds.

The apparent correlation between the potency of block and the degree of shift in the open probability curves seen with CPP and its enantiomers suggests that conductance and voltage sensitivity are perturbed by binding of blocker at the same site(s). Furthermore, the minimal effect on instantaneous inward and outward currents suggests that these blockers interfere with the gating process without markedly perturbing ion permeation ie. whilst the voltage sensitivity of the channel has been shifted to more positive potentials, once gated to the open conformation, the channel is still able to conduct anions freely even in the presence of relatively high concentrations of these blockers.

The differential action of the R and S enantiomers are in keeping with the two binding site model proposed by De Luca et al (1992 and *vide* V.1.2.2), discrepancies in the degree of block by R(+) at mM concentrations notwithstanding. Interaction with the blocking site appears primarily to perturb the molecular process involved in the slow deactivating current component. Binding of R(+) to the second site, proposed to be involved in channel opening (De Luca et al., 1992), appears predominantly to alter the

ability of the channel to conduct chloride out of the cell, albeit a small effect, without any appreciable change in deactivation kinetics.

A modified version of the model proposed by De Luca et al. could also be used to explain the data. R(+) could interact with the blocking site exclusively, with a sensitivity in the mM range. Both enantiomers may also bind at a second site with a relatively equal K_d. Due to their structures, the orientation of the carboxyl and methyl groups of enantiomers bound at this site would differ with respect to the protein. It is possible that the positioning of the charged carboxyl and/ or methyl on the S(-) isomer allows it to interact with the protein in a manner which causes stabilisation of the closed state. This interaction may, for example, hold in the closed position a residue, which normally moves during the gating process. With the R(+) isomer, the altered orientation of the charged carboxyl and methyl groups allows it to act in a manner which tends to stabilise the open conformation. This could be visualised as the interacting group on the enantiomer being positioned in such a way as to hold the residue involved in gating toward the opposite end of its plane of movement ie. the open position. Thus whilst it could be successfully argued that both isomers interact at the same site, one as a blocker and the other as an opener, the involvement of a second inhibitory site has to be evoked to explain the blocking behaviour of R(+).

The non-chiral compounds 2,4-D and DPC appear only to act as blockers. The changes in current kinetics induced by these two compounds are suggestive of interaction with the same site as that involved in CPP-induced blockade. The apparent reduction in saturation of outward current seen with all these compounds probably reflects the shift in voltage dependence. It seems likely that if it were possible to measure currents at more positive potentials, eg between +140 and +180mV, that saturation may be detected.

Clearly there are numerous possible explanations which can account for the action of this group of compounds. The most fruitful approach for further investigation of these findings is likely to be site-directed mutagenesis.

V.4.3 Blocker structure vs effect

The use of such a varied group of blocking agents has clearly revealed different effects and possibly sites of interaction with ClC-1. The results obtained with these compounds also demonstrate that molecules of differing structure are capable of producing remarkably similar changes in the behaviour of the channel. Given the diversity of the compounds used it is not surprising that no obvious correlation between structure and effect has emerged.

CPP and 2,4-D both incorporate chloride groups on their rings and have carboxyl groups which are separated from the ring by an oxygen and carbon. These characteristics are not however shared by DPC which induces very similar changes in current kinetics. Double ring structures like niflumate, NPPB and DPC all differ in their effect as do more complex structures like IAA and A9C. Given the complexity of the various structures and the different effects they induce, it is obvious that the most appropriate approach to investigate blocker structure vs effect is to use series of related compounds with slight structural variations as have been reported elsewhere (Palade and Barchi, 1977b; Wangemann et al., 1986; Landry et al., 1987).

V.4.4 Concluding remarks/ future directions

The variability of effect of the blockers tested here implies interaction by different compounds via a number of separate sites on the ClC-1 molecule. This may make them useful as molecular probes in localising particular molecular structures involved in various aspects of channel behaviour. For example, the "group three" compounds appear to interact primarily with the portion of the channel involved in the slow

deactivating current component and although interaction at a site remote from the actual molecular structure involved in this aspect of channel behaviour cannot at this stage be ruled out, these compounds may be useful in mapping this particular structure. Much information is likely to be gained by combining analysis of the effect of blockers with site-directed mutagenesis techniques looking for mutants which respond differently to particular compounds and/ or which exhibit different current kinetics. This approach is already being pursued in our laboratories and is beginning to produce some interesting results (*vide* Section VI).

VI
Mutagenesis

VI.1 Introduction

VI.1.1 ClC-1 Mutations

Since the identification and sequencing of the gene encoding the major chloride permeation pathway through mammalian skeletal muscle (Steinmeyer et al., 1991a, b; George et al., 1993), numerous reports have appeared in the literature describing mutations associated with myotonia. Nonsense and missense mutations of ClC-1 in mice have been reviewed by Gronmeier et al. (1994). In humans, mutations in this gene (ClCN1) have been demonstrated in patients suffering from autosomal dominant myotonia congenita (MC) (George et al., 1993, 1994; Steinmeyer et al., 1994; Pusch et al., 1995b), autosomal recessive generalised myotonia (RGM) (Koch et al., 1992; Heine et al., 1994; Lorenz et al., 1994; Meyer-Kleine et al., 1994) and myotonia levior (Lehmann-Horn et al., 1995).

Mutations reported to date in RGM pedigrees include 2 different frame shift deletions (Heine et al., 1994; Meyer-Kleine et al., 1994), 2 nucleotide substitutions affecting mRNA splice sites (Lorenz et al., 1994; Meyer-Kleine et al., 1995) and 16 point mutations (12 missense, 4 nonsense) (Koch et al., 1992; George et al., 1994; Meyer-Kleine et al., 1995). In MC pedigrees, 5 missense (George et al., 1993; Steinmeyer et al., 1994; Meyer-Kleine et al., 1995) and 1 nonsense mutation (George et al., 1994; Meyer-Kleine et al., 1995), which is also found in RGM, have been reported thus far (for recent reviews see Jentsch et al., 1995b; Meyer-Kleine et al., 1995). Additionally, two benign polymorphisms have been detected in the ClCN1 gene (Steinmeyer et al.,

1994; Meyer-Kleine et al., 1995) as well as numerous examples of compound heterozygosity (reviewed in Meyer-Kleine et al., 1995).

At the time of writing, 11 of these mutations, 5 from RGM, 5 from MC and 1 found in both pedigrees, had been reproduced, expressed and investigated *in vitro*. Two of these mutants, R300Q, detected in a MC pedigree, (Steinmeyer et al., 1994) and V327I, identified in a RGM patient, (Lorenz et al., 1994) were reported not be detectably different from wild type channels with regard to their biophysical behaviour. These results confirmed the R300Q mutation as being a likely benign polymorphism whilst V327I was speculated to exert its *in vivo* effect via interference with mRNA splicing. Two other RGM mutations, R496S (Lorenz et al., 1994) and D136G (Heine et al., 1994; Fahlke et al., 1995b), were found to differ profoundly from wild type channels. R496S failed to form functional chloride channels when expressed in *Xenopus* oocytes and was also shown in co-expression studies not to interfere with the function of normal channel proteins, this latter finding being totally consistent with its recessive inheritance pattern. In contrast, D136G when expressed in oocytes and HEK293 cells was found to produce chloride-selective channels (Fahlke et al., 1995b) but with biophysical properties dramatically different from wild type ClC-1. The predominant alteration appears to affect the voltage sensitivity of the channel with hyperpolarisation inducing a slowly activating rather than deactivating current.

Mutations G230E, P480L and Q552R, detected in MC pedigrees, when expressed in oocytes in isolation failed to produce chloride-selective currents (Steinmeyer et al., 1994; Pusch et al., 1995b). Co-expression studies have demonstrated that subunits carrying these dominant mutations suppress the activity of wild type subunits in a dose dependent manner with the effect being more pronounced with some mutations, eg.

P480L, than others eg. G230E. This finding has been interpreted as strong evidence that ClC-1 exists in the membrane as a homooligomer, calculations of the dose dependent effect suggesting the multimer consists of between 2 and 4 subunits (Steinmeyer et al., 1994).

Biophysical investigation of the MC mutations I290M, R317Q, P480L and Q552R by expression *in vitro*, as homo and/ or heteromultimers, has shown that their voltage sensitivity is shifted toward more positive potentials (Pusch et al., 1995b). The result is channels which are only open in a voltage range where they cannot contribute to recovery from an action potential. Clinically this manifests itself as myotonia.

Recent expression studies of the R894X mutation which has been found in both RGM and MC pedigrees indicated that currents though mutant homomultimers, whilst showing the same general biophysical characteristics as wild type channels, were smaller (Meyer-Kleine et al., 1995). In interpreting these data the authors suggest that this mutation is likely to cause effects intermediate between typical recessive and dominant mutations and is therefore likely to exhibit either a recessive or dominant inheritance pattern depending on the genetic background.

VI.1.2 Mutagenesis of ClC-0 and ClC-2

ClC-0 has been subjected to site-directed mutagenesis in an attempt to identify residues involved in its fast gating behaviour (Pusch et al., 1995a). Channels incorporating single point mutations which neutralised each of the charged residues in transmembrane domains, with the exception of K519, when expressed in oocytes were either non functional or indistinguishable from wild type. Gating and permeation were, however, found to be distinctly different in mutants K519Q, K519E and K519H, whereas K519R was described as intermediate to wild type. Currents measured in channels with alterations in lysine 520 and residues 515 to 518 did not differ

significantly from wild type. The K519E mutant was studied in detail and found to be altered in its speed of gating, single channel conductance and mole fraction behaviour indicating an important role for this positively charge residue in anion permeation.

ClC-2 mutants have also been investigated. Extensive mutagenesis of the ClC-2 N-terminus has revealed an inactivation ball and chain like structure (Gründer et al., 1992), akin to that found in cation channels (Armstrong and Bezanilla, 1977; Hoshi et al., 1990; Zagotta and Aldrich, 1990), contained in the first 100 amino acids of the protein. Chimeras of ClC-2, ClC-1 and ClC-0 were also produced in this study, the results revealing that the inactivating properties of the ClC-2 N-terminus are specific to that channel. Transplanting the inactivating sequence to the C-terminus of ClC-2 produced a channel with normal gating behaviour providing good evidence that both termini are located on the same side of the membrane.

VI.2 Aim/ Approach

At the time of writing, no reports had appeared in the literature describing *in vitro* expressed ClC-1 mutants which had not previously been identified in human pedigrees. The aim of this work was to extend these studies by specifically mutating other residues in the ClC-1 protein that might be expected to be involved in ion permeation and/ or channel gating. The approach taken was to mutate highly conserved, positively charged residues on the basis that highly conserved residues are likely to be important in channel function and that positive charges could possibly play a role in the interaction of anions with the protein. It was decided to reverse the charge of positive residues rather than simply neutralise them based on the logic that this would be more likely to produce an obvious effect. On this basis, fully conserved arginine residues at positions 304 and 370 were replaced by glutamic acid residues.

The effects of one of these mutations, R304E, on the biophysical and pharmacological characteristics of ClC-1 are reported here.

VI.3 Materials and methods

VI.3.1 Chemicals and solutions

All chemicals were of either Analar or molecular biology grade. All solutions were prepared using MQ quality water (resistance >18MΩ).

VI.3.2 Molecular biology

All standard molecular methods were as described in Section II.

Site-directed mutagenesis work was performed by Honours student J.D. Clarke under the supervision of the author and Dr. B.P. Hughes (School of Pharmacy and Medical Sciences, Uni. of Sth. Australia).

Production of baculovirus expression vector BVDA6-R304E and all patch-clamping experiments were performed by the author.

VI.3.2.1 Site-directed mutagenesis

The entire ClC-1 insert from plasmid pDA6bvr was excised and subcloned into vector pALTER-1 (*Promega*) via the *Bam*H1 and *Kpn*I sites. Mutagenesis of the arginine codon (TCG) at position 304 to a glutamic acid codon (TTC) was achieved using the Altered Sites System (*Promega*) following the manufacturers protocols utilising the mutagenic oligonucleotide designated JC304. In the process of altering the arginine codon JC304 also eliminates an *Mnl*I restriction site.

Following mutagenesis, DNA was extracted from ampicillin resistant clones using the mini-prep method (*vide* appendix b). The sequence spanning the mutation site (codons 272 to 393) was then amplified by PCR using primers JCSEQ1 and JCSEQ2. PCR products were then screened for the loss of the *Mnl*I restriction site using standard techniques. PCR products from two *Mnl*I negative clones were then

sequenced using the dye-labelled terminator method (*Applied Biosystems*) using the amplification primers.

Mutated cDNA was excised from pALTER-1 using *Xba*I and *Kpn*I and subcloned into pBacPAK8 (*Clonetech*). Resultant ampicillin resistant clones were screened for the presence and orientation of insert DNA using *Eco*RV, *Kpn*I and *Xba*I singly and in various combinations. One clone was selected at random and designated pDA6-R304E.

Oligonucleotides were purchased from the Department of Haematology, Institute of Medical and Veterinary Science, Frome Rd. Adelaide, 5000 and were produced as described in Section II. Sequences were as follows:

JCR304 5'-GGAAT TACTG GGAGG GATTC TTTGC-3'
JCSEQ1 5'-GCCGT GGGGG GTCGG TTGCT GT-3'
JCSEQ2 5'-ATAGA GCAGG CGGTG CTTAG C-3'

VI.3.3 Virus Production

Plasmid pDA6-R304E was used to produce baculovirus expression vectors following the methods described in Section II.

Four plaques produced by co-transformation of Sf21 cells with pDA6-R304E and linearised Bac6 virus were selected at random and screened for protein expression as described in Section II. One clone was selected for use in electrophysiological analyses and was designated BVDA6-R304E.

VI.3.4 Electrophysiology

All electrophysiological, data analysis and statistical methods were as described in Section IV. Since current kinetics were found to change over the first 10 to 20 minutes of whole-cell recording (vide Section IV) and in an effort to minimise inconsistency, all kinetic parameters were measured in R304E-expressing cells immediately following perforation of the cell-attached patch. These data were then

directly compared with those recorded in cells expressing wild type ClC-1 at the same time point (t = 0). Graphically presented data are displayed as mean ± SEM. IC_{50} and pKa values for zinc are stated as mean ± 95% confidence interval as are $V_{1/2}$ values taken from the fitted Boltzmann functions. When comparing two IC_{50}, pKa or $V_{1/2}$ values, differences were considered significant if the mean of each of the two values being compared lay outside the 95% C.I. of the other

VI.3.5 Pharmacology

VI.3.5.1 Blockers

All pharmacological methods using channel blockers were as described in Section V. Except where stated otherwise, cells were held in whole-cell configuration until current parameters had stabilised (typically 10 - 20 minutes post cell-attached patch perforation) prior to the addition of solutions containing blocking agents.

VI.3.5.2 pKa of Zn^{++} block

For solutions with a pH above 6, normal bath solution was prepared using HEPES buffer and the pH adjusted to the required value using 1M NaOH. Where a pH less than 6 was required, MES replaced HEPES at an equimolar concentration and the pH was adjusted as above. Zinc was prepared as a 1M stock solution of $ZnSO_4$ in MQ water and added to bath solution to the required final concentration just prior to use. Control readings were taken at the pH to be tested with the highest pH being applied first. This solution was then replaced with the next pH in the series and so on until the lowest test pH was reached. Bath solutions containing zinc were then added beginning with the lowest pH, a reading then being taken, and the next solution in the series used to replace the last until reaching the highest test pH. The degree of block at a given pH was calculated by division of the instantaneous current in the presence of Zn^{++} at that pH by the current measured using the corresponding control solution.

Data were fitted with sigmoidal dose response curves as described in Section V and pKa values calculated therefrom.

VI.4 Results

VI.4.1 Mutagenesis

Sequencing of both clones revealed successful alteration of the sequence from TCG to TTC. All other nucleotides were identical to the wild type sequence.

Mutated DNA was successfully excised from pALTER-1 and subcloned into pBacPAK8 as indicated by restriction analysis of resulting clones.

VI.4.2 Virus production

Standard plaque assay of the pDA6-R304E/ linearised Bac6 co-transformation supernatant exhibited a titre of 5×10^3 pfu/ml. Titres of primary virus stocks produced by amplification of the four isolated plaques were between 1 and 3×10^8 pfu/ml.

VI.4.3 Protein expression

PAGE analysis of cells infected with primary virus stocks revealed the presence of protein products with apparent molecular masses of 116 and 200kDa (not shown) as in cells infected with BVDA6 but not detected in uninfected cells or those infected with negative control virus BVDA2. As occurred with other expression vectors, there was some variation in the level of protein expression between different clones (not shown). One clone showing a high level of expression was selected for use in further experiments.

VI.4.4 Electrophysiology

VI.4.4.1 Kinetics

Currents recorded from BVDA6-R304E infected cells using whole-cell configuration were very similar to those of BVDA6 infected cells (Figure 6.1a). As with wild type

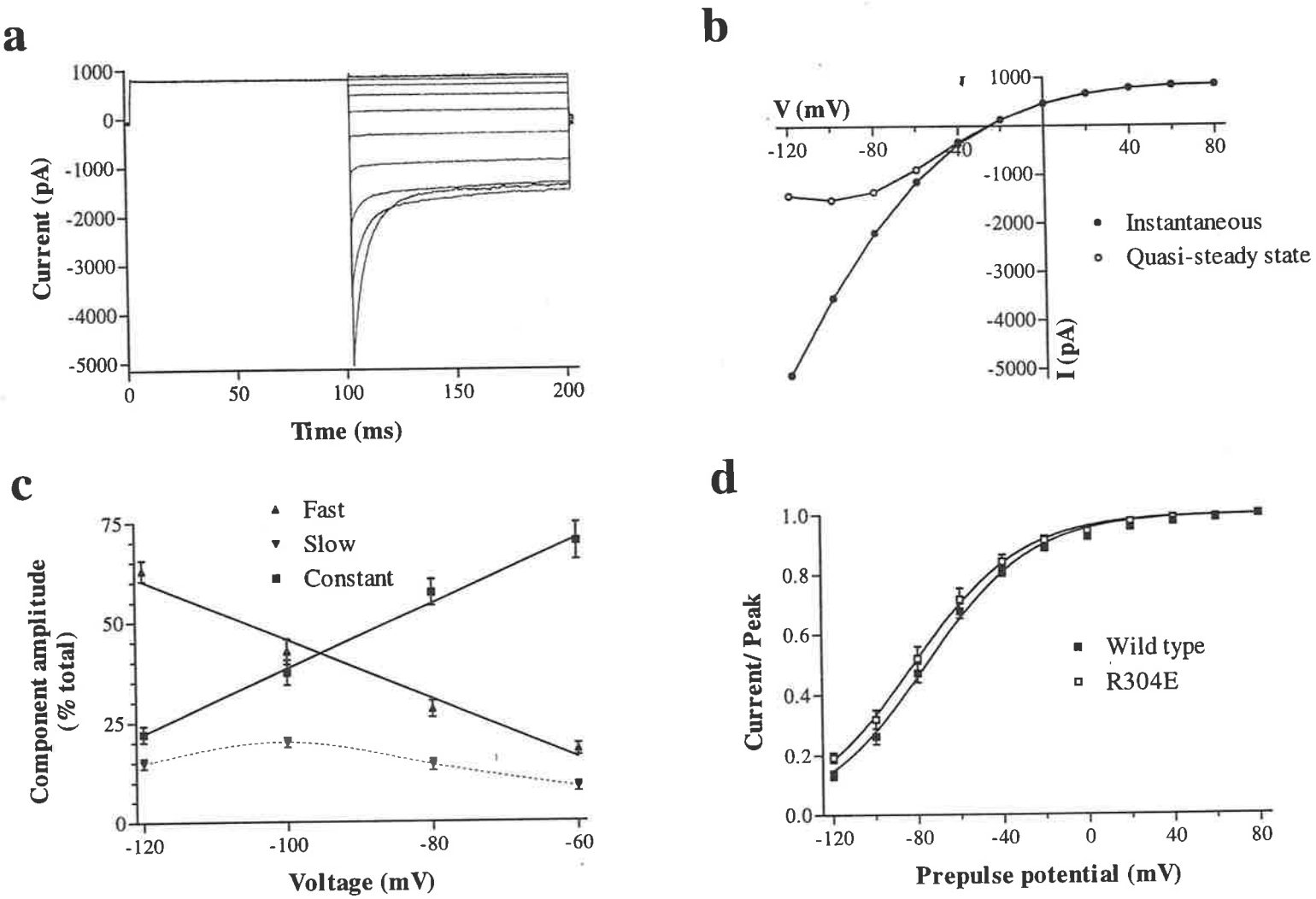

Figure 6.1: **a:** Currents elicited by the activation voltage protocol measured in a typical R304E expressing Sf9 cell. **b:** Instantaneous and quasi-steady state current/voltage relationships derived from currents in **a**. **c:** Relative component amplitudes of R304E inward currents. Data are fitted with regression lines (solid line) or cubic spline (broken line). **d:** Apparent open probabilities of ClC-1, wild type (n = 8) and R304E mutant (n = 4). Data are fitted with Boltzmann functions as described in Section IV.

ClC-1, deactivating current was elicited by voltages negative to -40mV whilst steps to positive potentials induced rectification with saturation evident at potentials positive to +40mV. The general shape of current/voltage curves was not different from those seen with the wild type channel (Figure 6.1b).

Three components could be extracted from the deactivating current, these being two exponentially decaying components, one fast and one slow, and a constant component. Time constants for the exponential components measured immediately following establishment of whole-cell configuration (see Table VI) were similar to those for wild type ClC-1, analysis of variance finding them not to be significantly different from the wild type channel measured at the same time point. The time constants of both components showed the same trend with respect to voltage as is seen with the wild type channel ie. the fast exponent became faster as the voltage became less negative whilst the slow component became slower.

The contribution of each component to the total instantaneous current showed the same trend with respect to voltage as occurred with the wild type ie. the fast component amplitude decreased as the voltage became less negative whilst the slow component amplitude first increased, reaching a peak at around -100mV, then decreased. The contribution from the constant component steadily increased as the membrane potential became less negative (Figure 6.1c). The relative component amplitudes measured immediately following perforation of the cell-attached patch were, however, significantly different from those measured in the wild type channel at the same time point. The contribution from the constant component was significantly larger ($P<0.0001$) at all voltages whilst the relative amplitudes of both exponential components were smaller ($P<0.0001$).

Apparent open probabilities at the various test voltages were calculated using the deactivation protocol immediately following perforation of the cell-attached patch due to the high level of stability and consistency of results when measured at this time point. P_{open} values measured in R304E were found to differ significantly from wild type ClC-1. The open probability curve was shifted to more hyperpolarising potentials with $V_{1/2}$ changing from -76.1 ± 2.3 mV (n = 8) for the wild type to -82.2 ± 1.3 mV (n = 4) for R304E (Figure 6.1d).

VI.4.5 Selectivity

Testing of foreign anions, Br^-, NO_3^- and I^-, demonstrated the same conductivity series as seen with the wild type channel (Figure 6.2).

VI.5 Pharmacology

VI.5.1 Anthracene-9-carboxylate

The response of currents measured in BVDA6-R304E infected cells to the presence of A9C was not noticeably different from that in BVDA6 infected cells. There was a concentration dependent decrease in current with instantaneous and quasi-steady state currents being relatively equally effected (Figure 6.3a, b, c). The calculated IC_{50}, for currents recorded at -120mV, was 15.6μM (n=1, Figure 6.3d) which is comparable to that measured with wild type ClC-1.

VI.5.2 2-(4-chlorophenoxy)propionate

As was the case with A9C, the response to this blocker was not detectably different from that seen with wild type protein (Figure 6.4a, b). Faster deactivation of inward current was still a feature as was the appearance of an activating current at positive potentials in the presence of mM concentrations (Figure 6.4c, d, e). The calculated IC_{50} for the racemate was found to be 3.9mM (n = 1, Figure 6.4f) for instantaneous

Wild Type		**Membrane potential** (mV)			
Component	**Parameter**	-120	-100	-80	-60
Fast	Amplitude	47.2 ± 1.7	33.1 ± 1.7	21.4 ± 1.0	12.6 ± 0.8
	τ_1	5.9 ± 0.2	5.1 ± 0.1	4.0 ± 0.1	3.0 ± 0.2
Slow	Amplitude	43.6 ± 1.9	49.6 ± 1.7	42.4 ± 2.4	25.4 ± 2.6
	τ_2	26.1 ± 1.4	39.9 ± 2.0	59.2 ± 2.2	80.4 ± 4.2
Constant	Amplitude	9.1 ± 0.6	17.7 ± 1.7	36.1 ± 2.7	62.1 ± 2.8
R304E					
Fast	Amplitude	63.0 ± 2.6	42.6 ± 3.1	28.2 ± 2.0	19.0 ± 1.5
	τ_1	6.4 ± 0.7	5.2 ± 0.3	4.7 ± 0.4	2.7 ± 0.2
Slow	Amplitude	14.9 ± 1.3	20.0 ± 1.2	14.5 ± 14.5	9.7 ± 1.2
	τ_2	36.2 ± 36.2	40.0 ± 2.3	60.2 ± 4.6	74.7 ± 5.4
Constant	Amplitude	22.1 ± 2.1	37.4 ± 3.2	57.3 ± 3.2	71.3 ± 4.7

Table VI:
Relative component amplitudes, expressed as percentage of total current, and time constants, in milliseconds, (mean ± SEM) measured in Sf9 cells expressing R304E mutant ClC-1 (n = 12 throughout). Wild type measurements collected over the same voltage range are also presented for comparison (n values are as presented in Table IVa).

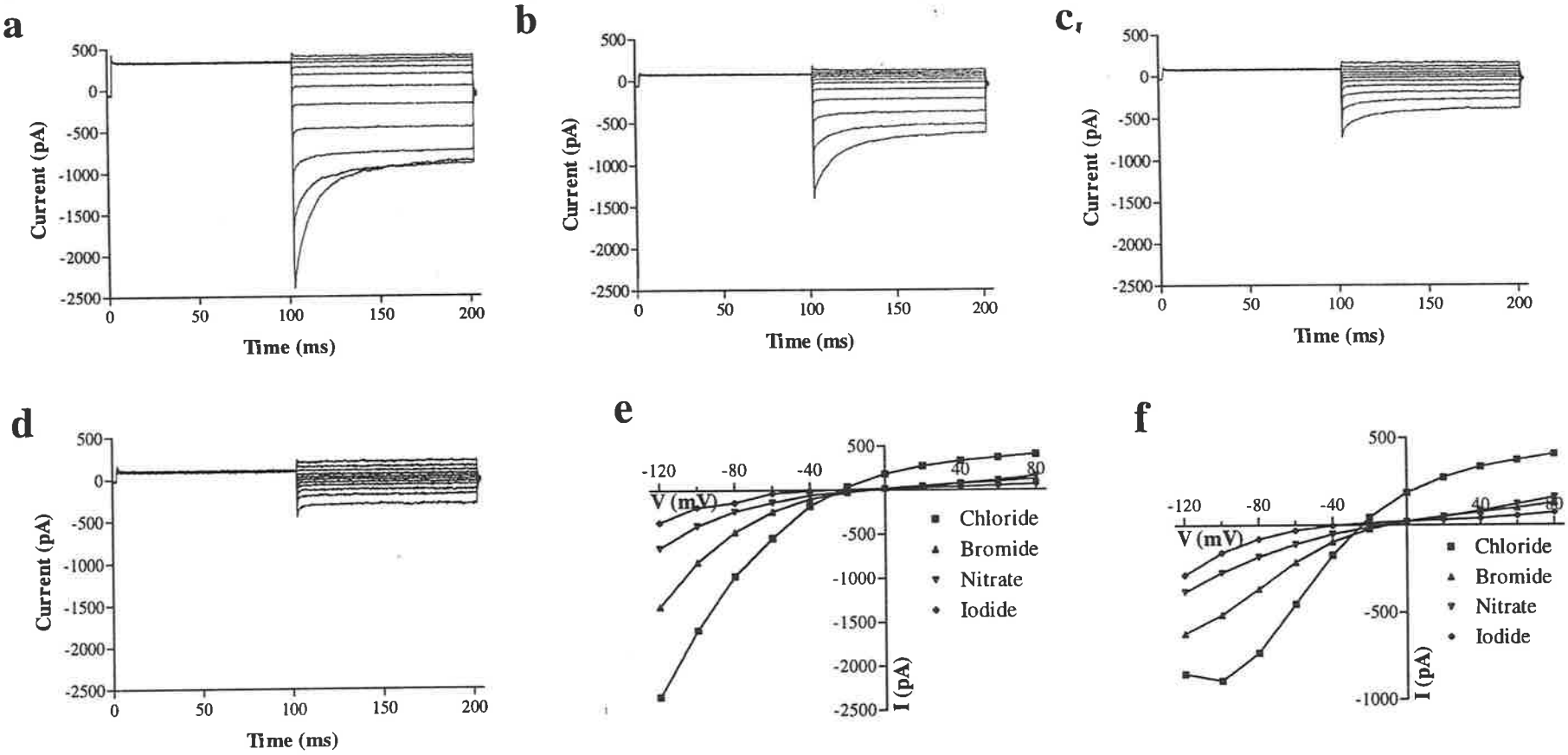

Figure 6.2: Currents measured in the same cell in the presence of various anions. Methods as described in section IV. **a:** Chloride **b:** Bromide. **c:** Nitrate. **d:** Iodide. **e, f:** Instantaneous (**e**) and quasi-steady state (**f**) current/voltage relationships measured in the presence of different anions.

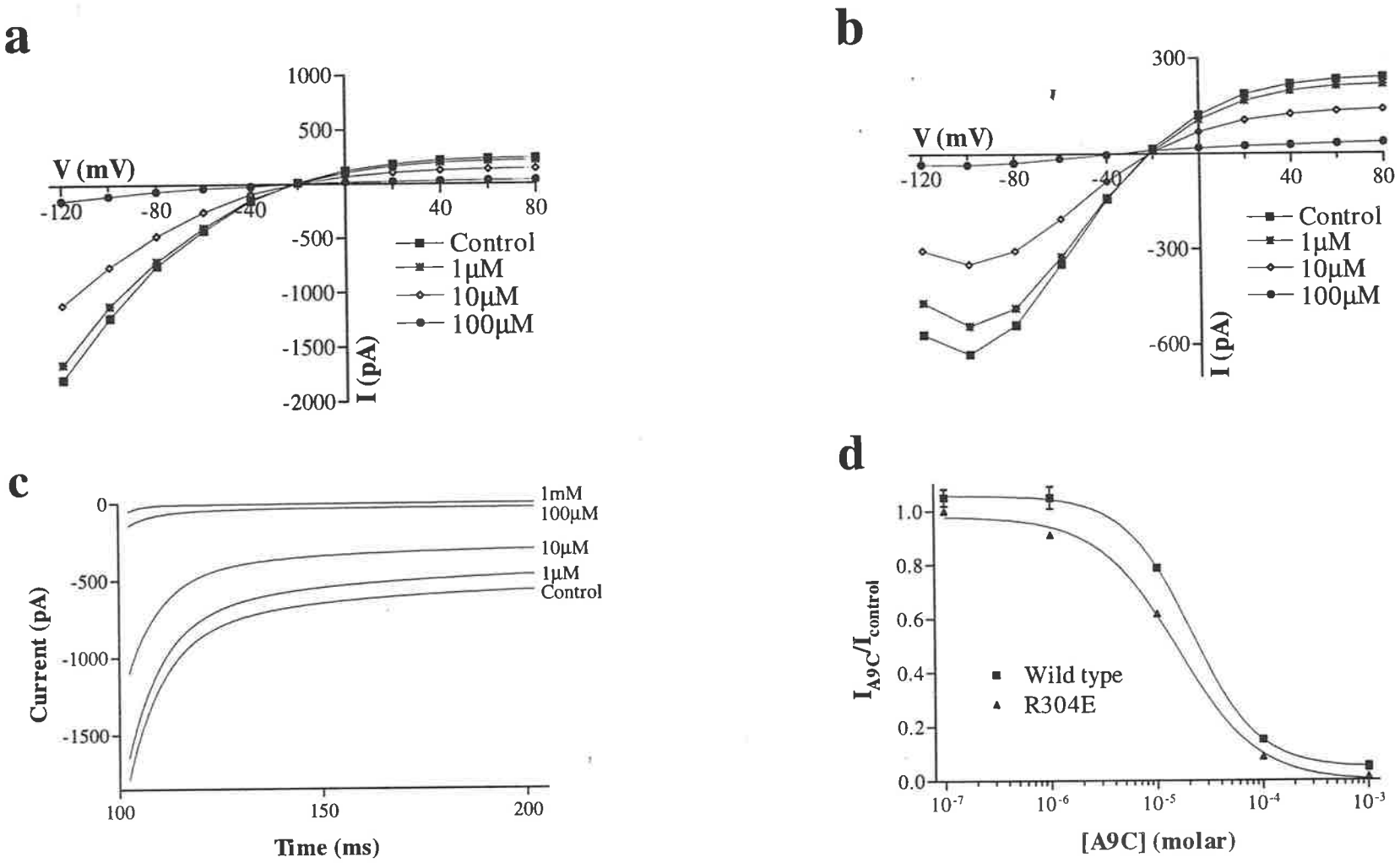

Figure 6.3: Effect of A9C on ClC-1 mutant R304E. **a, b:** Instantaneous (**a**) and quasi-steady state (**b**) current/voltage relationships measured in the same cell at the indicated concentrations of A9C. **c:** Currents elicited by a -120mV voltage pulse at the concentrations of A9C indicated on the graph. **d:** Degree of current reduction by A9C, wild type vs R304E. Data are fitted with sigmoidal functions as described in Section V.

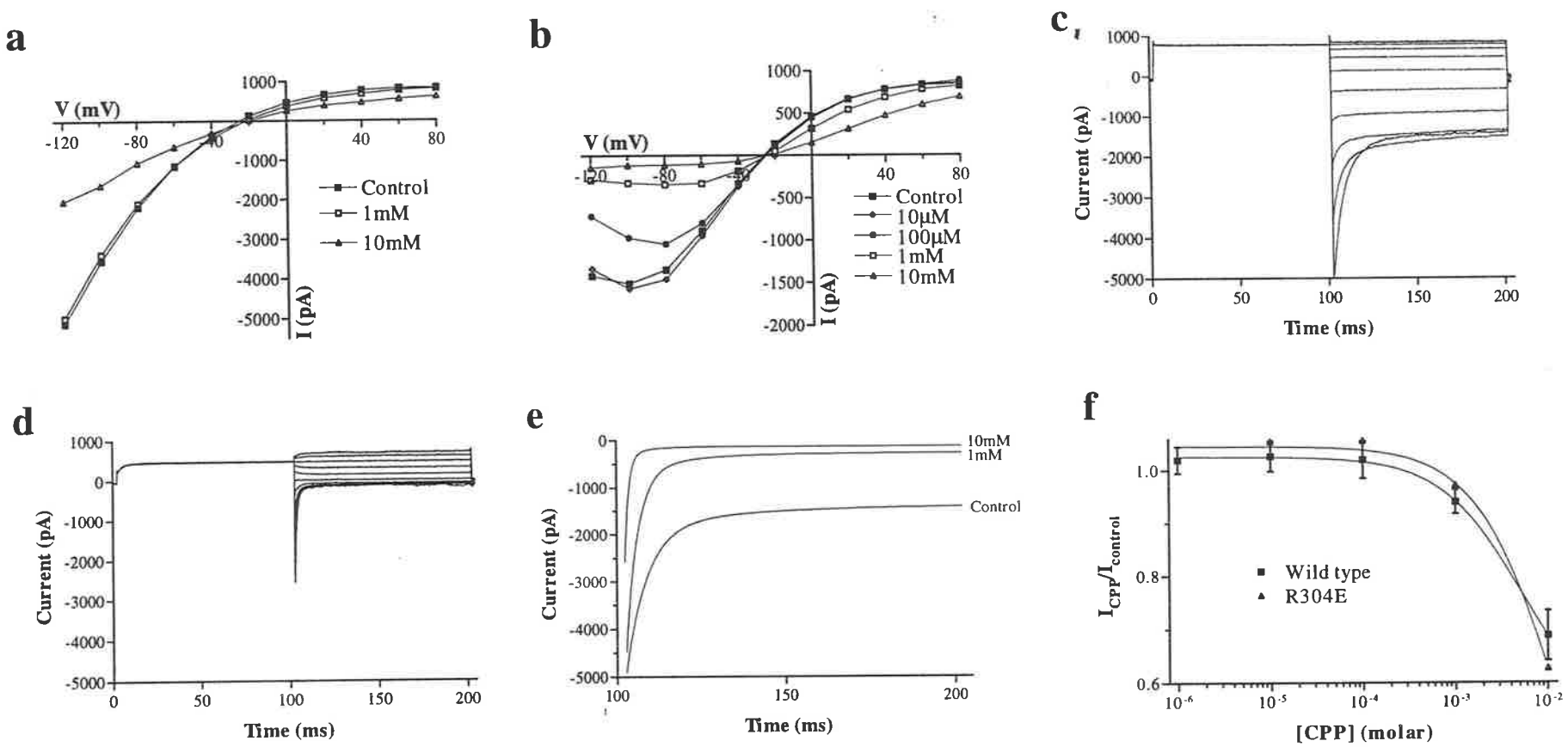

Figure 6.4: Effect of CPP racemate on ClC-1 mutant R304E. **a, b:** Instantaneous (**a**) and quasi-steady state (**b**) current/voltage relationships measured in the same cell at the indicated concentrations of CPP. **c, d:** Currents elicited using the activation voltage protocol measured in the same cell before (**c**) and after (**d**) addition of 10mM CPP. **e:** Currents measured during a -120mV voltage pulse at the concentrations of CPP indicated on the graph. **f:** Degree of current reduction by CPP, wild type vs R304E. Data are fitted with sigmoidal functions as described in Section IV.

current measured at -100mV. Again, this result is similar to the value measured with the wild type protein.

VI.5.3 Perrhenate

As with CPP and A9C, the response to this blocker was not noticeably altered with the R304E mutant (Figure 6.5a, b). A concentration dependent decrease in instantaneous current was seen as occurs with wild type ClC-1. The increase in quasi-steady state current seen for -120mV steps with the wild type channel at a concentration of 1mM is also seen with the mutant (Figure 6.5c). The calculated IC_{50} for instantaneous current measured at -120mV was 840μM (n = 1, Figure 6.5d). As with the other two blockers, this result was not qualitatively different from that obtained with the wild type protein.

VI.5.4 Zinc

In the case of zinc, there was a noticeable difference in the sensitivity of the currents to block. Whilst this cation was still able to induce a concentration dependent decrease in both instantaneous and quasi-steady state current amplitudes (Figure 6.6a, b, c), the concentrations required to obtain block equivalent to that seen with the wild type channel were significantly higher, as judged by comparison of confidence intervals. The calculated IC_{50} was found to be 4.2 ± 1.5mM (n = 4, Figure 6.6d), compared to 1.8mM for the wild type channel (*vide* V.3.5).

VI.5.5 pKa of Zn^{++} interaction

Testing of the level of block induced by 5mM Zn^{++} at pHs ranging from 5.5 to 7.5 clearly indicated a strong pH dependence for the interaction of this cation with ClC-1 (Figure 6.7). More detailed investigation of this pH dependence in the range pH 6.5 - 7.5 yielded data which were well fitted by a sigmoidal dose response function. From

the curves fitted to data obtained with both wild type and mutant proteins pKa values of 6.70 ± 0.07 (n = 4) and 6.89 ± 0.06 (n = 4) respectively (Figure 6.7) were obtained. Comparison of 95% confidence intervals finds this difference to be significant..

VI.6 Discussion

There are distinct differences between the biophysical characteristics of R304E and the wild type channel. Whilst the possibility cannot be ruled out that the change in charge at position 304, induced directly by the amino acid substitution, may alter the protein's tertiary structure, the changes found could be explained by an increased level of protonation of one or more histidine residues.

The open probability and relative component amplitudes measured with wild type ClC-1 are altered at reduced extracellular pH (Rychkov et al., 1995). At pH 7.4, the R304E mutant shows characteristics similar to those of the wild type channel at reduced extracellular pH ie. an increase in the contribution from the constant component at the expense of the exponential components and a shift of the open probability curve to more negative potentials. The pKa of this pH-induced change in kinetics observed with the wild type protein is found to be in the range expected for protonation of histidine residues in proteins (Kilmartin and Rossi-Bernardi, 1973; Stoesz et al., 1979). Further, the interaction of transition metals with proteins, in this pH range, has previously been shown to be most effectively facilitated via coordination bonding between the cation and imidazole moieties in His residues (Sundberg and Martin, 1974; Sigel and Martin, 1982; Sulkowski, 1987). The pKa of interaction of His residues with transition metal ions is in the range of that measured for the interaction of Zn^{++} with ClC-1. The change in pKa measured in the R304E mutant can be accounted for on the basis of a change in the micro-environment of one,

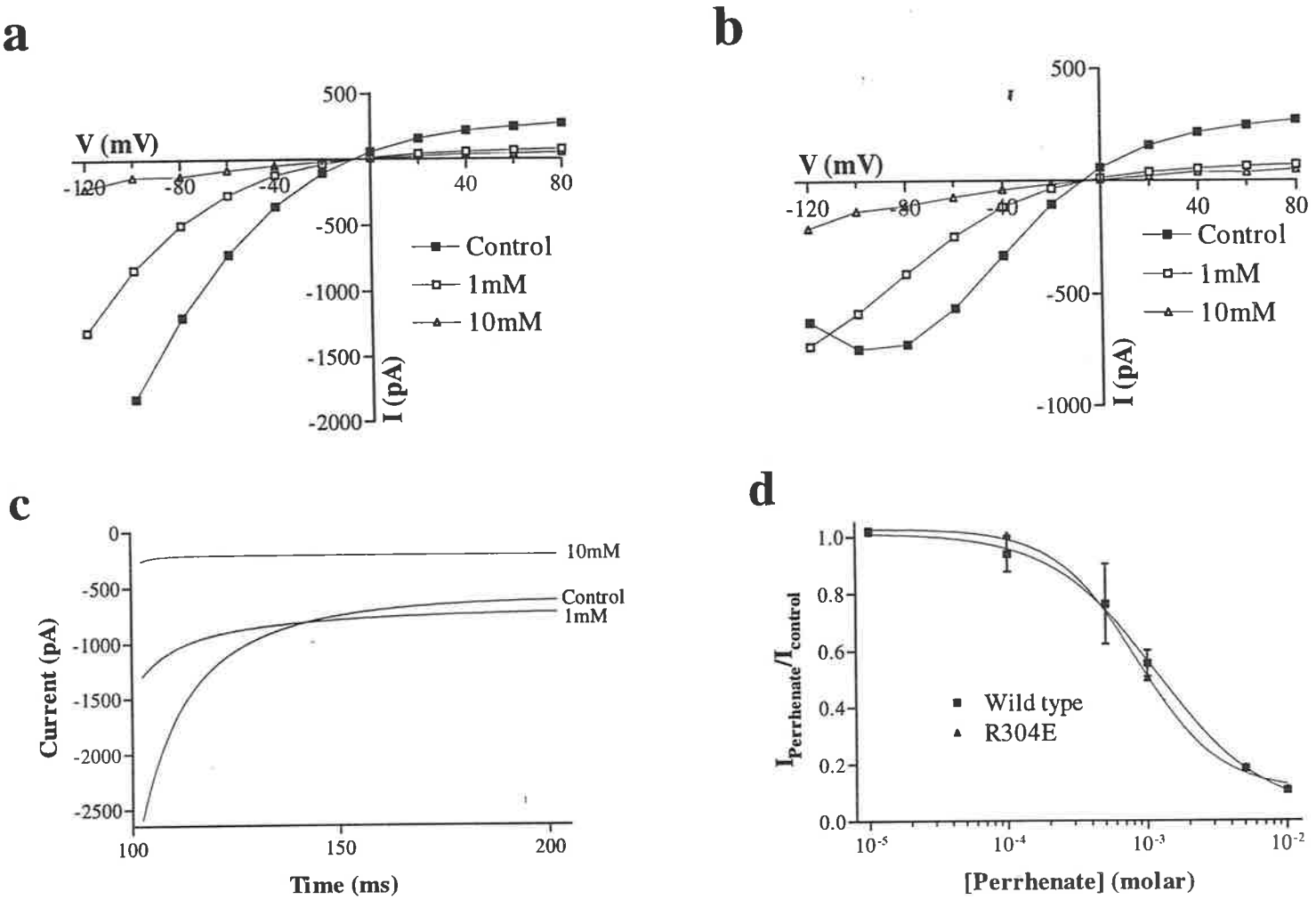

Figure 6.5: Effect of perrhenate on ClC-1 mutant R304E. **a, b:** Instantaneous (**a**) and quasi-steady state (**b**) current/voltage relationships measured in the same cell at the indicated concentrations of perrhenate. **c:** Currents elicited by a -120mV voltage pulse at the concentrations of perrhenate indicated on the graph. **d:** Degree of current reduction by perrhenate, wild type vs R304E. Data are fitted with sigmoidal functions as described in Section V.

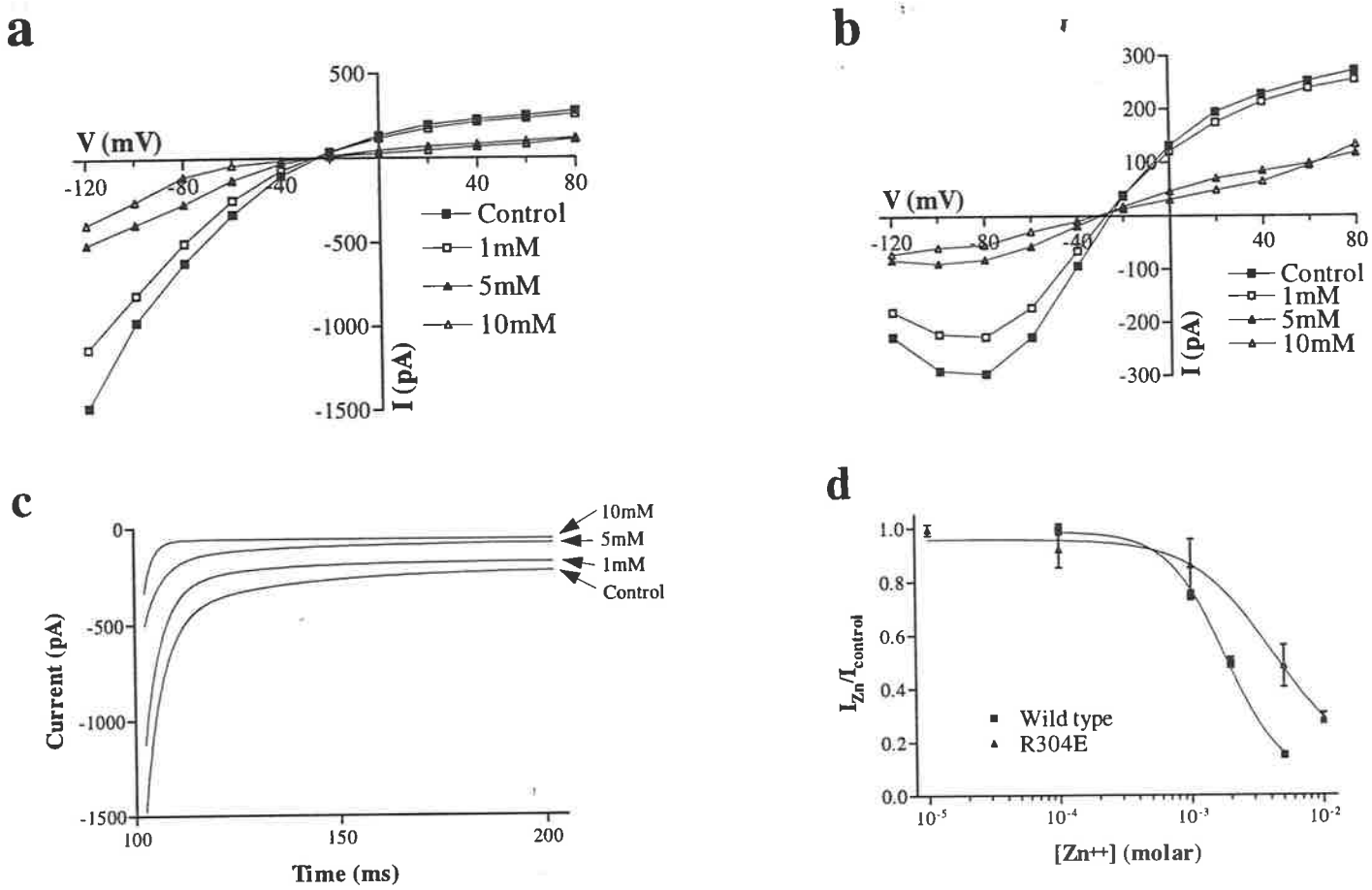

Figure 6.6: Effect of Zn^{++} on ClC-1 mutant R304E. **a, b:** Instantaneous (**a**) and quasi-steady state (**b**) current/voltage relationships measured in a typical cell at the indicated concentrations of Zn^{++}. **c:** Currents elicited by a -120mV voltage pulse, recorded from the same cell as in **a** and **b**, at the concentrations of Zn^{++} indicated on the graph. **d:** Degree of reduction of instantaneous current by Zn^{++}, wild type vs R304E. Data are fitted with sigmoidal functions as described in Section V.

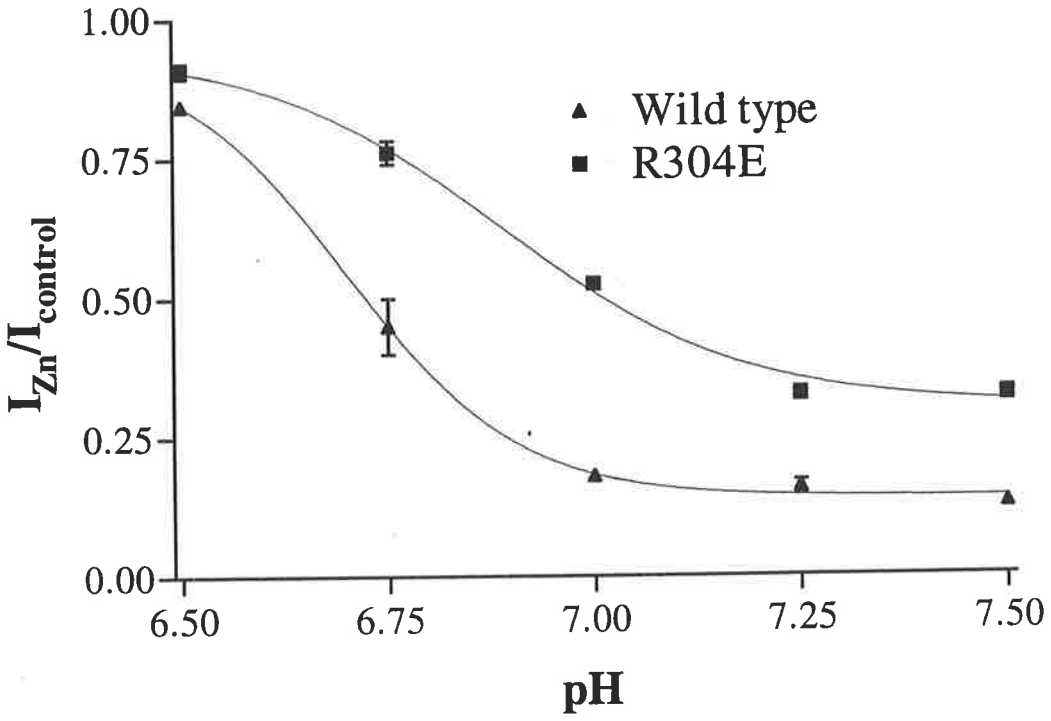

Figure 6.7: Effect of pH on zinc induced block of wild type and R304E mutant ClC-1. Data are fitted with sigmoidal functions as described in Section V.

or more, of the imidazole side chains involved in the coordinate bonding process. Such a change has previously been reported where a glutamic acid residue adjacent to a histidine tends to stabilise the protonation of the imidazole ring by virtue of its negative charge (Sulkowski, 1987). It has also been found that the potency of A9C increases with reduced pH (Astill et al., 1995b), a change of 2 pH units resulting in a 25 fold decrease in IC_{50}. There is a slight reduction in IC_{50} for A9C with R304E compared to wild type (15 vs 20μM) and whilst this change cannot at this stage be tested for statistical significance (n=1) it is in keeping with the subtle changes in pKa induced in this mutant.

Under the current proposed topological model for ClC-1 (Jentsch et al., 1995a) arginine 304 is placed at the internal face of the membrane at the beginning of the domain designated D6 (Figure 6.8a). Preliminary experiments performed in our laboratory indicate that ClC-1 is not blocked by addition of transition metal ions intracellularly (G. Rychkov, unpublished observations). Thus, if channel block is induced by an interaction between transition metal ions and histidine residues, the histidine(s) involved would be expected to be located in a position accessible from the extracellular milieu, perhaps closer to the extracellular than intracellular face of the plasmalemma. This being the case, for a glutamate residue at position 304 to exert its effect it too would need to be located extracellularly so as to bring it into close juxtaposition with an externally located imidazole moiety. This can be accomplished by modification of the current topological model. In an effort to keep the apparently utilised glycosylation site between domains D8 and D9 external (Kieferle et al., 1994) and minimise the changes required, it is suggested that D4 be reinstated as a membrane spanning region and D8 be changed from a membrane spanning domain to a loop which enters and exits the membrane from the extracellular side (Figure 6.8b).

In this configuration three histidine residues, which are interestingly also evenly spaced in the linear sequence (positions 369, 379, 389), are now brought into a position where they may potentially be in close proximity to residue 304 in the tertiary/ quaternary protein structure.

VI.7 Future directions

Clearly the method of choice to resolve the issue of which residues are involved in zinc and pH-induced effects is site-directed mutagenesis coupled to patch-clamping. At the time of writing, this approach was being vigorously pursued in our laboratories with particular attention being focused on the histidine residues mentioned above.

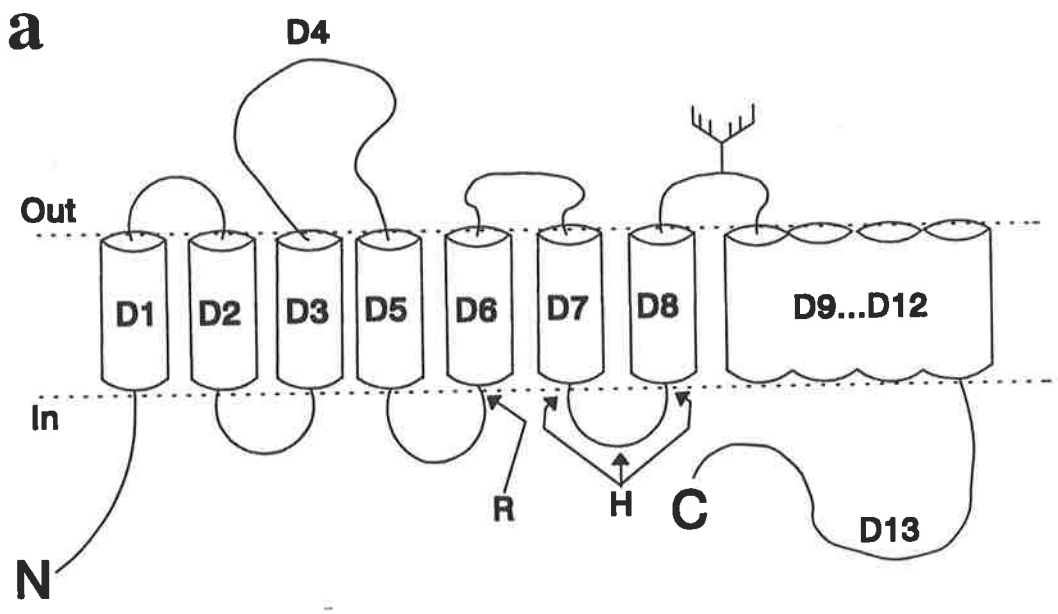

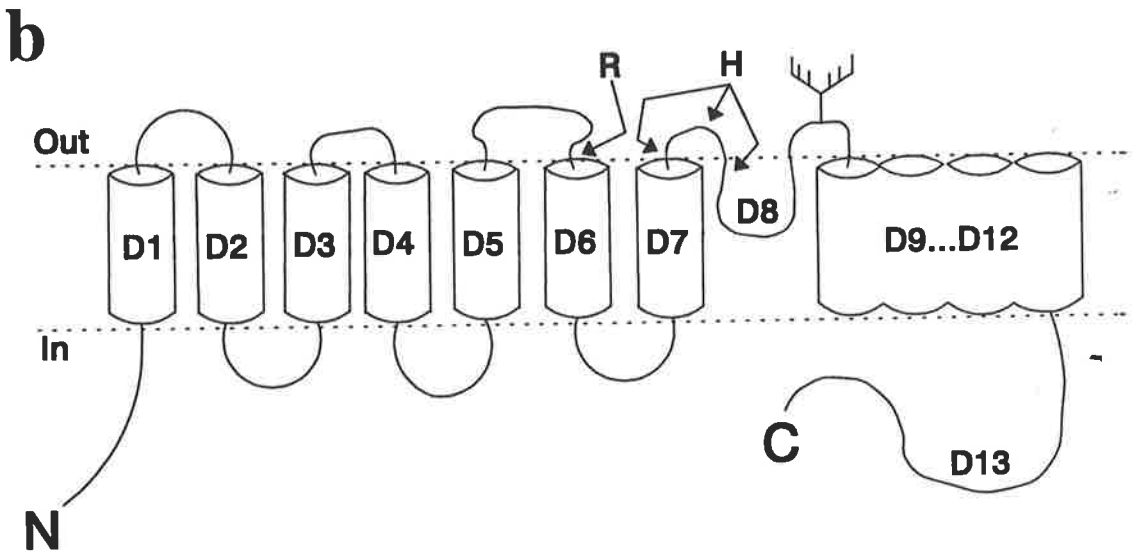

Figure 6.8: **a:** Current proposed topological model for ClC-1. **b:** Revised structure proposed by the author on the basis of data obtained with point mutant R304E.
R = arginine 304. **H** = histidine residues at positions 369, 379 and 389.

VII
General Discussion

VII.1 Baculovirus Sf cell system

It is clear from the results presented here that the expression system employed is well suited to the production and investigation of ClC-1 *in vitro*. The high yield of protein and ease with which cultures can be "scaled up" make it an appropriate system for protein purification/ reconstitution experiments. Additionally, the amenability of Sf9 cells to patch-clamping and their low background conductance makes them ideal for the investigation of heterologously expressed ion channels. The stability/ longevity of patches also allows for numerous manipulations to be carried out on a single cell over relatively long (60+ minutes) periods.

VII.2 ClC-1 characteristics

Comparison of the biophysical characteristics of ClC-1 expressed in Sf and other cell types shows that the channel behaves very similarly in all systems (*Xenopus* oocytes (Steinmeyer et al., 1991b, 1994) HEK293 (Pusch et al., 1994; Fahlke et al., 1995b), muscle fibres (Fahlke and Rüdel, 1995)) thus far investigated, slight differences in kinetics notwithstanding. Furthermore, the behaviour of currents through ClC-1 measured *in vitro*, in various preparations, is in keeping with the general characteristics of G_{Cl} measured in whole muscle fibres and thus data gained from the heterologously expressed channel would appear to be generally applicable to the situation in intact myocytes.

With regard to the deactivation seen at negative potentials, it is tempting to suggest a two step change in protein conformation accounting for the two exponential components extractable from these currents. However, the possibility of a third

exponentially decaying component, with a time constant in the hundreds of milliseconds range, requires further investigation. The slowing of the deactivation kinetics, along with an increase in current amplitude, seen over the first 10 to 20 minutes post perforation of the cell-attached patch also suggests modulation of the deactivation process by some soluble cytoplasmic factor. Additionally, the possibility that the deactivation behaviour of ClC-1 might be due to voltage dependent block should not be neglected.

As yet there is no mechanistic explanation of the rectification process seen at positive membrane potentials. The reduction in inward rectification seen with high concentrations of some blockers (CPP, DPC, 2,4-D) may make these compounds useful in the investigation of this particular biophysical characteristic.

VII.3 Pharmacology

The results gained with the various compounds used in this work are indicative of the existence of numerous different sites of interaction with the channel. This should make these substances useful probes in future structure/ function investigations. There is evidence that whilst most of the tested compounds act to reduce the flow of chloride through ClC-1, some are able to induce the opposite effect eg. CPP R(+) and perrhenate. The shift in the apparent open probability curve induced by the "group 3" compounds is remarkably similar to that seen with the majority of ClC-1 mutations causing dominant myotonia congenita (Pusch et al., 1995b). This leads to the possibility that, after further investigation, a compound may be found, or even designed, which could act *in vivo* to shift the open probability back toward the normal range, in the process alleviating myotonic symptoms.

VII.4 Future directions

Future experiments need to be designed to address a number of unresolved questions as well as expand our understanding of the general biophysical and pharmacological properties of ClC-1.

The differences in the time constants of the exponential components extracted from the deactivating currents induced by hyperpolarisation reported by different laboratories is a question worthy of further investigation. Recordings need to be made using longer time scales to investigate the possibility of the existence of a third exponentially decaying component and to test the hypothesis that the discrepancies reported by different laboratories are due to examination of different pairs of components.

The proposal that deactivation of ClC-1 may be due to voltage dependent block is another area which requires examination. Investigations along these lines have already begun in our laboratory. Results thus far suggest that deactivation may be the result of voltage dependent block by cytoplasmic hydroxyl ions (Rychkov and Bretag, unpublished results). Replacement of all extracellular cations (except H^+) with Tris does not alter the deactivation kinetics (Astill et al., 1995a). Further, reducing the extracellular pH causes a reduction, rather than increase, in the level of deactivation (Rychkov et al., 1995). Replacement of intracellular anions with glutamate does not lead to any alteration of deactivation kinetics but changing internal pH leads to obvious kinetic changes, increasing pH inducing more rapid inactivation whilst reducing pH has the opposite effect (Rychkov et al., 1995). Whilst these results could be explained on the basis of changes in the internal OH^- concentration, the possibility that they reflect alterations in the protonation state of a negatively charge region of the protein, which acts as an inactivating particle, cannot be excluded.

Production of specific anti-ClC-1 antibodies is another area worth pursuing. Particularly with reference to the application of such antibodies to the identification of the larger protein band seen in extracts prepared from ClC-1-expressing Sf9 cells, the tracking of protein through solubilisation and purification techniques and the problem of membrane topology.

The changes in current amplitudes and kinetics which occur following perforation of the cell-attached patch also suggest possible metabolic control of ClC-1 as another area requiring investigation. The effects of protein kinase-induced phosphorylation is an obvious starting point given the finding that muscle chloride conductance is influenced by the activity of protein kinase C (Brinkmeier and Jockusch, 1987; Bryant and Conte-Camerino, 1991; Tricarico et al., 1991; Rosenbohm et al., 1995).

The results obtained with the various blockers suggest interaction with the channel at discrete sites by different compounds. Application of these blockers to site-directed mutants of ClC-1 should therefore be useful in the investigation of channel structure. For example, mutants which respond differently to perrhenate may suggest residues which are exposed to the aqueous environment and/ or form part of the channel pore whereas mutations which affect A9C binding are more likely to be in hydrophobic regions. The apparent lack of activity of blockers when applied internally should give clues as to which residues are exposed on the external side of the membrane. Identification of residues involved in the interaction with transition metal ions should provide useful information regarding which residues form the channel pore or are at least adjacent thereto. The apparent ability of some blockers to alter gating, eg. CPP and perrhenate, may also be useful in defining regions of ClC-1 involved in this process.

Isolation of ClC-1 homologues from other species is an additionally possibly fruitful area for investigation. The protein sequence, biophysical and pharmacological behaviour of these channels should provide clues about areas involved in particular properties of mammalian ClC-1. For example, the exquisite sensitivity of the avian channel to iodide (Morgan et al., 1975) and the reduced sensitivity of the frog channel to A9C (Bretag et al., 1980) should provide useful hints as to which regions of the mammalian protein are involved in interaction with these substances.

In the relatively short term, it is envisaged that the major thrust of future work will focus on two areas. Firstly, much information is to be gained by production and investigation ClC-1 mutants. On the basis of the result gained in this work, and in other experiments (Rychkov et al., 1995), the most obvious residues to pursue at this stage are histidines. In particular those at positions 369, 379 and 389 in the linear sequence, since these appear likely to participate in the interaction with Zn^{++} and possibly the channel's sensitivity to extracellular pH. Other highly conserved residues are also worth investigation eg. arginine 370. Production of expression vectors carrying these mutations is currently under way in our laboratories as well as a random mutagenesis approach using high error rate PCR.

The second area is that of protein purification. The histidine tagged construct is well expressed in the baculovirus Sf cell system and should prove useful, via the application of immobilised metal affinity chromatography, for this purpose. It is envisaged that purified protein would be reconstituted into lipid bilayers for biophysical investigation. Despite the reported low unitary conductance of ClC-1 (Pusch et al., 1994), it is possible that single channel recordings may still be obtained using ultra low noise recording techniques, particularly if, in the absence of cellular components, the single channel conductance of ClC-1 increases. Ultimately, it is

hoped that purified protein may be crystallised and the structure examined by X-ray diffraction techniques.

In summary, the work presented in this thesis has added to the basic knowledge of the biophysical and pharmacological characteristics of ClC-1 and has, perhaps more importantly, provided a basis for decisions about the direction of future research.

VIII Appendices

Appendix a

Baculoviruses

General biology and life cycle

The family Bacuoliviridae includes over 600 members all of which have been isolated from invertebrates. Most members of the family have been isolated from insects, predominantly lepidoptera. All exhibit enveloped, rod shaped nucleocapsids 36nm wide and ranging in length from 200 - 400nm depending on the size of the isolate's genome (Harrap, 1972b; Fraser, 1986). The genome consists of covalently closed, circular, double stranded DNA ranging in size from 80 to 200 kilobase pairs (Burgess, 1977). Many species produce virus-containing occlusions within host cell nuclei during the final stages of infection (for review see Kozlov et al., 1986; and see Vlak et al., 1988). The family can be broadly subdivided into three subgroups according to the type of nuclear occlusions (if any) produced. Subgroup A, the nuclear polyhedrosis viruses (NPVs), produce occlusions known as polyhedra made up of a polyhedrin protein matrix surrounded by a surface coat (calyx) (Harrap, 1972a; O'Reilly et al., 1994). There are several enveloped viral particles within each polyhedron and each envelope may contain single or multiple nucleocapsids. On this criterion subgroup A isolates are described as either singly (SNPVs) or multiply (MNPVs) embedded or enveloped. Subgroup B, the granulosis viruses (GVs), produce occlusions made up of granulin protein containing a single nucleocapsid per "granule". The Subgroup C viruses, the non occluded baculoviruses (NOBs), as the name suggests, do not produce occlusions. Each virus is also generally named after the species from which it was isolated. As an example, the virus most commonly used in heterologous expression systems is a subgroup A virus which produces polyhedra

containing multiply embedded nucleocapsids and was isolated from larvae of the "alfalfa looper" (*Autographa californica*). It is therefore named *Autographa californica* Multiply embedded Nuclear Polyhedrosis Virus (*Ac*MNPV).

The life cycle of the NPVs has been studied in some detail (reviewed in Blissard and Rohrmann, 1990 and O'Reilly et al., 1994) and proceeds as follows. In the environment, these viruses are found, within their protective polyhedra, on vegetation and in soil. Once ingested by a permissive host, viruses are released from the polyhedron as it dissolves in the alkaline environment of the insect's midgut. The virions then penetrate the peritropic membrane lining the gut and fuse with the plasma membrane of gut cells, a process facilitated by the virions lipoprotein envelope. The now intracellular nucleocapsids move to the host cell nucleus and, by a process which is yet to be elucidated, release their DNA therein. During the course of infection, the virus produces two distinct forms of progeny in a bi-phasic replication cycle. In infected gut cells, progeny nucleocapsids form in the nucleus by ca. 8 hours post infection (hpi). At around twelve hpi they begin to bud through the nuclear membrane. As they move though the cytoplasm they lose their nuclear membrane derived envelope and finally are released from the cell by budding through the plasmalemma. In the process they acquire a plasma membrane derived, lipid envelope studded with a 67kDa, virally encoded glycoprotein (gp67) (Volkman, 1986; Whitford et al., 1989). This form of virion, variously known as budded or extracellular virus (ECV), has been shown to be 1000 times more infectious than those released from polyhedra. The ECV is released into the host haemolymph via which the infection is disseminated. The ECV of *Ac*MNPV exhibits a broad tissue tropism infecting tissues including fat bodies, nerve cells, hypodermis and haemocytes. Cells infected by ECV produce more ECV but also produce occluded virus within their nuclei. Occluded

viruses are genetically identical to ECV but gain their lipid envelope *de novo* within the nucleus. This envelope does not contain gp67. By the late stages of infection virtually the entire host is infected and finally liquefies to release polyhedra thus completing the cycle.

Molecular biology

*Ac*MNPV is relatively easy to propagate *in vitro*. The cell lines most commonly used for this purpose are derived from pupal ovarian tissue of the "fall army worm" (*Spodoptera frugiperda*). The two most frequently used Sf cell lines, derived from the original cell line IPLB-Sf-21 (Vaughn et al., 1977), are Sf-21AE and a clonal derivative thereof known as Sf9. Both cell lines exhibit very similar characteristics (see Section I). Using ECV to infect these cultured cells the molecular events occurring during viral replication have and are being investigated.

In vitro, *Ac*MNPV enters cells via adsorptive endocytosis (reviewed in Volkman, 1986). The nucleocapsid migrates through the cytoplasm and gains access to the nucleoplasm wherein viral replication is initiated. Groups of viral genes are expressed in a regulated cascade comprising four consecutive, overlapping phases, these being immediate early (*IE* or α), delayed early (β), late (χ) and very late (δ) (for reviews see Friesen and Miller, 1986; Blissard and Rohrmann, 1990 and O'Reilly et al., 1994). Over 100 distinct viral RNA transcripts have been described, a number of which have had polypeptides assigned (Friesen and Miller, 1986 and see O'Reilly et al., 1994 for recent review).

Immediate early genes are defined as those which can be transcribed in the presence of protein synthesis inhibitors ie. they can be transcribed immediately by the host cell machinery. *IE* gene products transactivate the β genes. As an example, the *IE*-1 (Guarino and Summers, 1986) and *IE*-N (Carson et al., 1988) gene products

transactivate the transcription of a delayed early gene encoding a 39kDa protein. IE-1 alone is able to transactivate production of this protein but the effect is augmented by IE-N (Carson et al., 1988). The *IE*-N gene product does not appear effective in the absence of IE-1. All delayed early genes begin to be transcribed after the *IE* genes at ca. 3 - 6 hpi.

Late and very late gene expression, which is dependent on the expression of earlier genes, begins at around the same time as viral DNA replication, which may occur at multiple origins throughout the genome (Pearson,M et al., 1992). Inhibition of viral DNA synthesis also inhibits the transcription of χ and δ genes. Products of χ genes include a viral DNA polymerase (Wang,X and Kelly, 1983; Tomalski et al., 1988) and various structural proteins including basic protein (Tweeten et al., 1980; Kelly et al., 1983), capsid protein (Thiem and Miller, 1989) and gp67 (Whitford et al., 1989). The late and very late genes are transcribed by an α-amanitine resistant RNA polymerase (Grula et al., 1981; Fuchs et al., 1983). This unusual polymerase is thought to be either virally encoded or a modified host enzyme. The delayed early gene encoding a 39kDa product mentioned above is also transcribed during this phase but using a different initiation site situated 25 nucleotides upstream of the early mRNA start site (Chisholm and Henner, 1988). Using this later initiation site the gene is expressed until 18 or more hpi.

Very late genes are expressed from around 15 hpi during the so called occlusion phase. These genes are transcribed from highly efficient promoters (*vide infra*) resulting in their hyperexpression. By the end of the infective process the proteins encoded by these genes can account for up to 50% (w/w) of the total cell protein. In NPVs, two δ genes have been investigated in some detail, these being *polh*

(polyhedrin) and *p10*. The *p10* product forms a matrix in the host nucleus and cytoplasm, the role of which is unclear. P10 protein may play a role in control of host cell lysis and is not required for production of polyhedra nor is it a component thereof (Vlak et al., 1988; Williams et al., 1989; O'Reilly et al., 1994). Polyhedrin forms the nuclear occlusions in which viral particles are embedded (reviewed in Rohrmann, 1986, *vide supra*).

Baculovirus promoters

The promoter elements of baculoviral genes have attracted a great deal of interest (for reviews see Blissard and Rohrmann, 1990; O'Reilly et al., 1994) particularly those of the δ genes. Initiation of transcription begins at a TAAG motif in all χ and δ genes. This sequence is to be found 50 base pairs (bp) and 70 bp upstream of the start codon of the *polh* (Possee and Howard, 1987) and *p10* genes (Kuzio et al., 1984) respectively. Investigation of the importance of the sequences from the TAAG motif to the polyhedrin start codon have shown that the entire sequence is required for optimal gene expression (Matsuura et al., 1987; Possee and Howard, 1987). Deletion analysis of this region indicated a direct correlation between its length and the efficiency of transcription. In other studies, (Rankin et al., 1988; Ooi et al., 1989) point mutations introduced into the TAAG motif lead to virtually complete loss of promoter activity. Mutations introduced into the nucleotides (nts) immediately adjacent to this motif (4 bp either side) result in only a minor reduction in promoter efficiency. Further work has shown that the 20 bp 5' of the transcription initiation site are required for maximum expression but that their influence is minimal compared with those between TAAG and the start codon. Interestingly, in the work done by Ooi et al (1989) point mutations introduced between 12 and 20 nts 5' of the initiation signal led to a 50% increase in promoter activity. Very similar results have also been

obtained with the *p10* promoter (Kuzio et al., 1984; Vlak et al., 1988; Weyer and Possee, 1989).

Promoter elements of other genes have also been investigated. *IE*-1 is transcribed from 2 separate initiation sites and is therefore thought to have 2 promoters. The first is active from around 0 - 2 hpi and produces a 2.1kb, spliced transcript whose start site is ca. 4kbp 5' of the second initiation site. This second site leads to the production of a 1.9kb transcript. Studies of both RNA species have shown that the larger transcript encodes a product identical to the smaller variant but for an additional 54 amino acids at the N-terminus (Chisholm and Henner, 1988). Steady state mRNA levels for the latter transcript are achieved by around 30' after the adsorption period and continue throughout the course of the infection. Dual initiation sites are also used for the genes encoding the 39kDa delayed early protein (Nissen and Friesen, 1989), the viral DNA polymerase (Tomalski et al., 1988) and possibly a 25kDa structural protein (Goh, 1993) expressed from around 6 hpi. In the case of the former two genes, both sites are utilised during the early stages of infection.

IE-1 transactivated expression of β genes is also influenced by enhancer elements. In *Ac*MNPV, they are found to consist of 5 regions of homologously repeated sequences containing multiple *Eco*R1 restriction sites (Guarino et al., 1986). When linked in *cis* with α or β genes they induce an increase in transcription of up to 1000 fold.

The demonstration of the non-essential nature of the δ gene products for *in vitro* viral replication led to the investigation of the use of their promoters for expression of foreign proteins (see Section I).

Appendix b

Solutions and buffers

Blunt end Ligation buffer
Tris-Cl (pH 7.6) 50mM, $MgCl_2$ 10mM, dithiothreitol 10mM, Acetylated BSA 50µg/ml, ATP 0.5mM

Insect cell lysis solution
50mM Tris-Cl (pH 8), 5% β-mercaptoethanol, 0.4% SDS, 10mM EDTA.

Klenow (End fill) buffer
50mM Tris-Cl (pH 7.2), 10mM $MgSO_4$, 0.1mM dithiothreitol, 5µg/ml acetylated BSA, dNTPs 10mM each

Phosphate-citrate buffer
40mM citric acid, 170mM Na_2HPO_4. Adjust pH to 5.0.

PAG Electrophoresis
Sample buffer
100mM Tris-Cl (pH 6.8), 4% w/v SDS, 20% glycerol, 0.2% bromophenol blue, 200mM dithiothreitol (add just prior to use).
Running buffer
25mM Tris, 0.1% w/v SDS, 250mM glycine.
Resolving gel (9%)
Mix 3ml acrylamide (30% (w/v)), 0.930ml bis-acrylamide (2.5% (w/v)) and 2.5ml 1.5M Tris-Cl (pH 8.8). Add water to a final volume of 10ml to give final concentrations of 9.23% total monomer and 2.5% cross linker. Degas and polymerise by addition of 50µl of freshly prepared 10% (w/v) ammonium persulfate and 5µl of TEMED.
Stacking gel (4%)
Mix 1.3ml acrylamide (30% (w/v)), 0.426ml bis-acrylamide (2.5% (w/v)) and 1.25ml 1M Tris-Cl (pH 6.8). Add water to a final volume of 10ml to give final concentrations of 4% and 2.66% total monomer and cross-linker respectively. Degas and polymerise by addition of 50µl of freshly prepared 10% (w/v) ammonium persulfate and 10µl of TEMED.
Fix/ Stain
Coomassie Brilliant blue R250 (*Sigma*) 0.25% (w/v) in destian.
Destain
25% (v/v) ethanol, 10% (v/v) glacial acetic acid in H_2O.

TAE (1X)
40mM acetate, 40mM Tris-Cl, 2mM EDTA.

Taq reaction buffers
Bresatec
15mM $(NH_4)_2SO_4$, 50mM Tris-Cl (pH 8.8), 0.15% Triton X-100, 200µg/ml BSA.
Boerhinger Mannheim
50mM KCl, 1.5mM $MgCl_2$ 10mM Tris-Cl (pH 8.3)

TE
10mM Tris-Cl (pH 8), 1mM EDTA (pH 8)

Plasmid mini-prep method
(Sambrook et al., 1989)

Solutions
I: 50mM glucose, 25mM Tris-Cl (pH 8), 10mM EDTA (pH 8)
II: 0.2N NaOH, 1% SDS (make on day of use).
III: 3M K^+/ 5M acetate

Method
Spin 1.5ml of overnight culture in a microcentrifuge (15000X g/ 30s) and remove all supernatant. Resuspend pellet in 100µl of solution I using a vortex mixer. Add 200µl of solution II and mix by inversion (DO NOT VORTEX). Add 150µl of solution III and vortex briefly (10s) in an inverted position. Incubate on ice for 3-5 minutes. Spin (15000X g/ 5 min/ 4°C), transfer supernatant to a fresh tube and extract with an equal volume of TE equilibrated phenol/ $CHCl_3$ (1:1 (v/v)) and recentrifuge (15000X g/ 2 min/ 4°C). Transfer aqueous phase to a fresh tube and precipitate plasmid DNA by addition of 2X volume of 100% ethanol. Mix by vortex and stand at room temperature for 2 minutes. Pellet DNA by centrifugation (15000X g/ 5 min/ 4°C) and remove all supernatant by aspiration. Wash DNA by addition of 500µl 70% ethanol and recentrifugation. Again remove all supernatant, air dry (room temperature/ 10 min) and resuspend pellet in 50µl of TE (pH 8) containing 20µg/ ml RNAase A. Store at -20°C.

Sf cell DNA extraction for PCR
(King and Possee, 1992)

Resuspend PBS washed cells (see II 2.12.7) in 250µl TE (pH 8), add 250µl of insect cell lysis solution, 12.5µl Proteinase K (10mg/ ml) and 2.5µl RNAase A (10mg/ ml), mix gently and incubate at 37°C for 30 minutes. Add 500µl of TE equilibrated phenol/ $CHCl_3$ (1:1 (v/v)) and mix by inversion for 5 minutes. Spin (15000X g/ 2 min) and transfer aqueous phase to a fresh tube. Repeat phenol/ $CHCl_3$ extraction, recentrifuge and transfer

aqueous phase to a fresh tube. Precipitate DNA by addition of 50µl sodium acetate (3M, pH 5.2) and 1000µl 100% ethanol. Pellet by centrifugation (15000X g/ 5 min). Wash pellet twice by addition of 500µl of 70% ethanol and repelleting. Air dry DNA at room temperature for 10 minutes, add 100µl of TE (pH 8) and soak overnight at 4°C. Warm DNA/ TE at 37°C for 10 minutes and gently resuspend. Use 10µl in PCR reaction.

Appendix c: Entire clc-1 cDNA

Sequence composed of 83 bp 5' untranslated sequence, 2985 bp open reading frame (underlined) and 458 bp 3' untranslated region.

CAAAAGCAGA GGCTTAAGGA GGTACTAGGG GGAGACTAGG AGCAAGCAGG CCAAGGCCTG
GCTGGGGCTT GGGGGGAGGA CACATGGAGC GGTCCCAGTC CCAGCAACAT GGAGGTGAAC
AAAGCTGGTG GGGCACTGCC CCCCAGTACC AGTACATGCC CTTCGAACAT TGTACCAGCT
ATGGACTGCC CTCAGAGAAT GGGGGCCTTC AGCACCGGCC CCGAAAGGAC CTGGGTCCCA
GGCACAATGC CCACCCAACA CAGATATATG GCCATCACAA AGAACAATAT TCATATCAGG
CACAGGACAG GGGAATACCC AAGAAGACGG ACTCCAGTTC TACTGTGGAC AGCTTGGATG
AGGACCACTA TTCTAAATGT CAAGACTGTG TCCATCGCCT GGGACGTGTG CTGAGAAGGA
AGCTGGGGGA AGACTGGATC TTTCTTGTGC TCCTGGGCCT ACTGATGGCT CTTGTCAGCT
GGTGCATGGA CTATGTTAGC GCCAAGAGCC TTCAGGCCTA CAAGTGGACC TATGCCCAGA
TGCAGCCCAG CCTTCCTCTA CAGTACTTGG CCTGGGTCAC CTTCCCACTT ATCCTCATCC
TCTTCAGTGC CCTCTTTTGC CAACTCATCT CTCCCCAGGC TGTGGGCTCT GGAATCCCTG
AGATGAAGAC AATTCTTCGT GGTGTTGTCT TGAAGGAATA CCTCACACTC AAGGCCTTTG
TAGCCAAGGT GGTGGCCTTG ACAGCCGGTC TGGGCAGTGG TATCCCTGTG GGGAAAGAGG
GTCCCTTTGT TCACATTGCC AGCATCTGTG CTGCTGTCCT CAGCAAATTC ATGTCCATGT
TCTCTGGTGT CTATGAGCAG CCATACTATT ACACTGACAT CCTGACAGTG GGCTGTGCCG
TGGGGGTCGG TTGCTGTTTT GGAACACCAC TTGGAGGAGT GCTGTTCAGC ATCGAGGTCA
CCTCTACCTA CTTTGCCGTT CGGAATTACT GGCGAGGATT CTTTGCAGCC ACCTTCAGTG
CCTTTGTGTT CCGCGTCCTG GCAGTGTGGA ACAAGGATGC TGTCACTATT ACTGCTCTGT
TCAGAACTAA TTTCCGGATG GATTTCCCCT TTGACCTGAA GGAACTCCCA GCTTTTGCTG
TCATTGGGAT TTGCTGCGGG TTCTTGGGAG CTGTTTTTGT TTATCTGCAT CGCCAAGTCA
TGCTCGGTGT CCGAAAGCAC AAGGCTCTCA GCCAGTTTCT TGCTAAGCAC CGCCTGCTCT
ATCCTGGAAT CGTTACTTTT GTCATCGCCT CACTCACCTT TCCACCAGGA ATGGGTCAAT
TCATGGCTGG AGAGCTGATG CCCCGTGAAG CTATCAGCAC CCTCTTTGAC AACAACACAT
GGGTAAAGCA CATAGGTGAT CCCAAAAGCT TGGGCCAGTC AGCTGTGTGG ATTCACCCCC
AGGTCAACGT GGTCATCATC ATCCTTCTCT TCTTCGTCAT GAAGTTTTGG ATGTCCATTG
TGGCCACGAC TATGCCCATA CCCTGTGGAG GCTTCATGCC TGTTTTTGTG CTAGGAGCTG
CCTTTGGAAG GCTGGTAGGA GAGATCATGG CCATGCTGTT CCCTGAGGGT ATCTTATTTG
ATGATATCAT CTATAAGATC TTACCAGGGG GCTATGCAGT GATTGGAGCA GCAGCTTTGA
CAGGGGCTGT CTCTCACACA GTCTCCACAG CTGTGATTTG CTTCGAATTA ACTGGTCAGA
TTGCTCACAT CCTGCCCATG ATGGTGGCTG TTATCTTGGC CAACATGGTG GCCCAAAGTC
TGCAGCCCTC CCTCTATGAC AGCATCATCC AGGTCAAGAA GCTTCCCTAT TTGCCAGACC
TTGGTTGGAA CCAGCTCAGC AAATTTACAA TTTTTGTTGA GGACATCATG GTACGTGACG
TGAAGTTTGT TTCAGCTTCT TGTACATACG GGGAACTAAG AAACCTACTC CAGACCACCA
CAGTCAAGAC TTTACCATTG GTTGACTCCA AAGATTCAAT GATCCTGCTA GGCTCTGTGG
AACGCTCAGA ACTGCAGTCC CTCCTGCAGC GCCACCTGTG TGCAGAGCGA AGGTTGAAGG
CTGCCCAGGA CATGGCTCGA AAGTTATCAG AGCTGCCCTA TAATGGCCAG GCTCAGCTGG
CTGGGGAGTG GCATCCTGGT GGTCGACCTG AGTCCTTTGC CTTCGTAGAT GAAGATGAAG
ATGAGGACGT CTCCCGGAAG ACAGAGCTTC CACAGACTCC AACTCCTCCT CCTCCTCCCC
CTCCTCCTCT GCCTCCCCAG TTTCCTATTG CTCCATCATA CCCTGAAGAG CCTAACGGGC
CACTGCCCAG CCACAAACAG CCCCCTGAAG CTTCAGACTC TGCAGATCAA AGGTCCTCCA
TCTTCCAGCG CCTGCTGCAC TGCTTACTGG GCAAAGCTCA CTCCACAAAG AAGAAAATAA
CCCAGGATTC AACAGATTTA GTGGATAACA TGTCACCTGA AGAGATTGAG GCCTGGGAGC
GGGAGCAGCT GAGCCAGCCT GTGTGTTTTG ATTTCTGCTG CATTGACCAG TCTCCCTTCC
AGCTGGTGGA GCAGACAACT CTGCACAAGA CTCATACACT CTTCTCACTT CTTGGCCTCC
ATCTTGCCTA TGTGACCAGC ATGGGGAAGC TCAGAGGTGT CTTGGCACTA GAAGAGCTAC
AGAAAGCTAT CAAGGGCCAC ACCAAATCTG GAGTGCAGCT TCGCCCTCCA CTTGCCAGCT
TCCGGAATAC AACTTCAATT CGGAAGACCC CTGGGGGGCC ACCCCCTCCT GCAGAGAGCT
GGAATGTGCC TGAGGGTGAA GATGGAGCTC CTGAAAGAGA AGTCATGGTT CCTACCATGC
CAGAGACTCC TGTCCCACCA CCATCTCCAG AGGTCCCTTC CTGCCTGGCC CCAGCCAGAG
TGGAGGGTGA GCTGGAGGAA CTGGAGATGG TGGGGAACCT AGGGCCTGAG GAGGACCTGG
CTGACATCTT GCATGGCCCC AGTCTGCGGT CCACTGATGA GGAAGATGAG GACGAGCTGA
TCCTGTGAAC AACACCCTCC AAGCTTTCTT CATAAAAACC ACAGGGCCCA TGTCAGAGAG
TGGGCTTGTA TATGAAATGG GTGCCCTGAA GTTGGGGAGA CCTCCATTTC ATCGTTGTTC
CTACCCCACT ATGAAAGGTG ATGGTTGATG GATCTTAAGG AGAACTTGAT CTTGGGCAGG
GAAGAATTTG GGTCCATCAA GACCCCCCTC CCCATTTCCA GGGAGGGTTC AAGCCCCCAT
GCTCAAAGGA CTTCTGTGTT CCTGCTGTGC AGGTTCAGTC CCTGTCACTC TAATGCCCCA
CAGTTCCCAG TGTCATTCTG TCACCATCCT GGCCCGGCAT GCCTGTCTAT ATTTCAGTTT
CCATATGGAG TAGGTGAGTG GAGGCCCAGA TTGAAAGAAT CCGCAAGTGT CACATTGGAA
GGGCATGTGG GACCACAATA TTGCCATGTG GATTGACTAC CCTAAA

Appendix d

CLC-1 Protein sequence.

994 amino acids, predicted molecular mass 110068Da. Hydrophobic domains underlined, proposed transmembrane domains double underlined, sequence which may or may not be within membrane indicated by broken underline (Pusch et al., 1994). Domains numbered according to Steinmeyer et al. (1991b). Arginine residue 304 boxed, histidine residues at positions 369, 379 and 389 circled.

```
MERSQSQQHG GEQSWWGTAP QYQYMPFEHC TSYGLPSENG GLQHRPRKDL  50
GPRHNAHPTQ IYGHHKEQYS YQAQDRGIPK KTDSSSTVDS LDEDHYSKCQ 100
DCVHRLGRVL RRKLGEDWIF LVLLGLLMAL VSWCMDYVSA KSLQAYKWTY 150
AQMQPSLPLQ YLAWVTFPLI LILFSALFCQ LISPQAVGSG IPEMKTILRG 200
VVLKEYLTLK AFVAKVVALT AGLGSGIPVG KEGPFVHIAS ICAAVLSKFM 250
SMFSGVYEQP YYYTDITLTV GCAVGVGCCF GTPLGGVLFS IEVTSTYFAV R 300
NYWRGFFAAT FSAFVFRVLA VWNKDAVTIT ALFRTNFRMD FPFDLKELPA 350
FAVIGICCGF LGAVFVYLHR QVMLGVRKHK ALSQFLAKHR LLYPGIVTFV 400
IASLTFPPGM GQFMAGELMP REAISTLFDN NTWVKHIGDP KSLGQSAVWI 450
HPQVNVVIII LLFFVMKFWM SIVATTMPIP CGGFMPVFVL GAAFGRLVGE 500
IMAMLFPEGI LFDDIIYKIL PGGYAVIGAA ALTGAVSHTV STAVICFELT 550
GQIAHILPMM VAVILANMVA QSLQPSLYDS IIQVKKLPYL PDLGWNQLSK 600
FTIFVEDIMV RDVKFVSASC TYGELRNLLQ TTTVKTLPLV DSKDSMILLG 650
SVERSELQSL LQRHLCAERR LKAAQDMARK LSELPYNGQA QLAGEWHPGG 700
RPESFAFVDE DEDEDVSRKT ELPQTPTPPP PPPPPLPPQF PIAPSYPEEP 750
NGPLPSHKQP PEASDSADQR SSIFQRLLHC LLGKAHSTKK KITQDSTDLV 800
DNMSPEEIEA WEREQLSQPV CFDFCCIDQS PFQLVEQTTL HKTHTLFSLL 850
GLHLAYVTSM GKLRGVLALE ELQKAIKGHT KSGVQLRPPL ASFRNTTSIR 900
KTPGGPPPPA ESWNVPEGED GAPEREVMVP TMPETPVPPP SPEVPSCLAP 950
ARVEGELEEL EMVGNLGPEE DLADILHGPS LRSTDEEDED ELIL        994
```

Bibliography

Adamo HP, Caride AJ, Penniston JT. Use of expression mutants and monoclonal antibodies to map the erythrocyte Ca^{2+} pump. J. Biol. Chem. **267**:14244-14249 (1992)

Armstrong RW, Bezanilla F. Inactivation of the sodium channel. II. Gating current experiments. J. Gen. Physiol. **70**:567-590 (1977)

Astill DStJ, Rychkov GY, Clarke JD, Hughes BP, Roberts ML, Bretag AH. Characteristics of skeletal muscle chloride channel ClC-1 and point mutant R304E expressed in Sf-9 insect cells. Biochim. Biophys. Acta **in press** (1995a)

Astill DStJ, Rychkov GY, Hughes BP, Bretag AH, Roberts ML. The involvement of histidine in the function of ClC-1, the skeletal muscle chloride channel. Proc. Aust. Physiol. Pharmacol. Soc. **26**:268P (1995b) (*abstract*)

Barry PH, Lynch JW. Liquid junction potentials and small cell effects in patch-clamp analysis. J. Membr. Biol. **121**:101-117 (1991)

Bauer CK, Steinmeyer K, Schwarz JR, Jentsch TJ. Completely functional double-barreled chloride channel expressed from a single *Torpedo* cDNA. Proc. Natl. Acad. Sci. USA **88**:11052-11056 (1991)

Belyaev AS, Roy P. Development of baculovirus triple and quadruple expression vectors: co-expression of three or four bluetongue virus proteins and the synthesis of bluetongue virus-like particles in insect cells. Nucleic Acids Res. **21**:1219-1223 (1993)

Bennett MVL. Modes of operation of electric organs. Ann. N.Y. Acad. Sci. **94**:458-509 (1961)

Bettoni G, Loiodice F, Tortorella V, Conte-Camerino D, Mambrini M, Ferrannini E, Bryant SH. Stereospecificity of the chloride ion channel: The action of chiral clofibric acid analogues. J. Med. Chem. **30**:1267-1270 (1987)

Birnboim HC, Doly J. A rapid alkaline extraction procedure for screening recombinant plasmid DNA. Nucleic Acids Res. **7**:1513-1523 (1979)

Birnir B, Tierney ML, Howitt SM, Cox GB, Gage PW. A combination of human α_1 and β_1 subunits is required for formation of detectable GABA-activated chloride channels in Sf9 cells. Proc. R. Soc. Lond. B **250**:307-312 (1992)

Blatz AL, Magleby KL. Single voltage-dependent chloride-selective channels of large conductance in cultured rat muscle. Biophys. J. **43**:237-241 (1983)

Blatz AL, Magleby KL. Single chloride-selective channels active at resting membrane potentials in cultured rat skeletal muscle. Biophys. J. **47**:119-123 (1985)

Blatz AL, Magleby KL. Quantitative description of three modes of activity of fast chloride channels from rat skeletal muscle. J. Physiol. **378**:141-174 (1986)

Blissard GW, Rohrmann GF. Baculovirus diversity and molecular biology. Annu. Rev. Entemol. **35**:127-155 (1990)

Bretag AH. Muscle chloride channels. Physiol. Rev. **67**:618-724 (1987)

Bretag AH, Dawe SR, Moskwa AG. Chemically induced myotonia in amphibia. Nature **286**:625-626 (1980)

Brewster BS, Jeal S, Strong PN. Identification of a protein product of the myotonic dystrophy gene using peptide specific antibodies. Biochem. Biophys. Res. Commun. **194**:1256-1260 (1993)

Brinkmeier H, Jockusch H. Activators of protein kinase C induce myotonia by lowering chloride conductance in muscle. Biochem. Biophys. Res. Commun. **148**:1383-1389 (1987)

Brown MGM, Weston A, Saunders JR, Humphreys GO. Transformation of *Eschericia coli* C600 by plasmid DNA at different phases of growth. FEMS Micro. Lett. **5**:219-222 (1979)

Brown TA (ed) (1991) Molecular Biology Labfax. Bios Scientific, Oxford

Bryant SH, Conte-Camerino D. Chloride channel regulation in skeletal muscle of normal and myotonic goats. Pflugers Arch. **417**:605-610 (1991)

Bryant SH, Morales-Aguilera A. Chloride conductance in normal and myotonic muscle fibres and the action of monocarboxylic aromatic acids. J. Physiol. **219**:367-383 (1971)

Burgess S. Molecular weights of Lepidopteran baculovirus DNAs: derivation by electron microscopy. J. Gen. Virol. **37**:501-510 (1977)

Burton F, Dörstelmann U, Hutter OF. Single-channel activity in sarcolemmal vesicles from human and other mammalian muscles. Muscle and Nerve **11**:1029-1038 (1988)

Butler VP, Beiser SM. Antibodies to small molecules: Biological and clinical applications. Adv. Immunol. **17**:255-310 (1973)

Cameron IR, Possee RD, Bishop DHL. Insect cell culture technology in baculovirus expression systems. Trends Biotech. **7**:66-70 (1989)

Carson DD, Guarino LA, Summers MD. Functional mapping of an AcNPV immediately early gene which augments expression of the IE-1 *trans*-activated 39K gene. Virology **162**:444-451 (1988)

Casadei JM, Gordon RD, Lampson LA, Schotland DL, Barchi RL. Monoclonal antibodies against the voltage-sensitive Na^+ channel from mammalian skeletal muscle. Proc. Natl. Acad. Sci. USA **81**:6227-6231 (1984)

Chisholm GE, Henner DJ. Multiple early transcripts and splicing of the *Autographa californica* nuclear polyhedrosis virus IE-1 gene. J. Virol. **62**:3193-3200 (1988)

Chua M, Betz WJ. Characterization of ion channels on the surface membrane of adult rat skeletal muscle. Biophys. J. **59**:1251-1260 (1991)

Conte-Camerino D, Mambrini M, DeLuca A, Tricarico D, Bryant SH, Tortorella V, Bettoni G. Enantiomers of clofibric acid analogs have opposite actions on rat skeletal muscle chloride channels. Pflugers Arch. **413**:105-107 (1988a)

Conte-Camerino D, Tortorella V, Bettoni G, Bryant SH, De Luca A, Mambrini M, Tricarico D, Grasso G. A stereospecific binding site regulates the Cl^- ion channel in rat skeletal muscle. Pharm. Res. Comm. **20**:1077-1080 (1988b)

Conte Camerino D, De Luca A, Mambrini M, Vrbovà G. Membrane ionic conductances in normal and denervated skeletal muscle of the rat during development. Pflugers Arch. **413**:568-570 (1989)

Cutting GR. Spectrum of mutations in cystic fibrosis. J. Bioen. Biomemb. **25**:7-10 (1993)

De Greef C, Sehrer J, Viana F, Van Acker K, Eggermont J, Mertens L, Raeymaekers L, Droogmans G, Nilius B. Volume-activated chloride currents are not correlated with P-glycoprotein expression. Biochem. J. **307**:713-718 (1995)

De Luca A, Tricarico D, Wagner R, Bryant SH, Tortorella V, Conte-Camerino D. Opposite effects of enantiomers of clofibric acid derivative on rat skeletal muscle chloride conductance: Antagonism studies and theoretical modelling of two different receptor site interactions. J. Pharmacol. Exp. Therap. **260**:364-368 (1992)

DeTomaso AW, Xie ZJ, Liu G, Mercer RW. Expression, targeting, and assembly of functional Na, K-ATPase polypeptides in baculovirus-infected insect cells. J. Biol. Chem. **268**:1470-1478 (1993)

Dulhunty AF. Distribution of potassium and chloride permeability over the surface and T-tubule membranes of mammalian skeletal muscle. J. Membr. Biol. **45**:293-310 (1979)

Dulhunty A. Effect of chloride withdrawal on the geometry of the T-tubules in amphibian and mammalian muscle. J. Membr. Biol. **67**:81-90 (1982)

Dulhunty A, Carter G, Hinrichsen C. The membrane capacity of mammalian skeletal muscle fibres. J. Muscle Res. Cell Mot. **5**:315-332 (1984)

Eldefrawi AT, Eldefrawi ME. Receptors for γ-aminobutyric acid and voltage-dependent chloride channels as targets for drugs and toxicants. FASEB J. **1**:262-271 (1987)

Ey PL. Use of stable 6-amionhexyl derivatives for labelling polysaccharides with haptens and for preparing polysaccharide immunosorbents. J. Immunol. Methods **160**:135-137 (1993)

Fahlke C, Rüdel R. Chloride currents across the membrane of mammalian skeletal muscle fibres. J. Physiol. **484**:355-368 (1995)

Fahlke C, Zachar E, Rüdel R. Single-channel recordings of chloride currents in cultured human skeletal muscle. Pflugers Arch. **421**:108-116 (1992)

Fahlke C, Zachar E, Rüdel R. Chloride channels with reduced single-channel conductance in recessive myotonia congenita. Neuron **10**:225-232 (1993)

Fahlke C, George AL, Rosenbohm A, Rüdel R. Effect of pH on the gating properties of a recombinant human muscle chloride channel, hClC-1. Pflugers Arch. **429** (supplement):R15 (1995a) (*abstract*)

Fahlke C, Rüdel R, Mitrovic N, Zhou M, George AL. An aspartic acid residue important for voltage-dependent gating of human muscle chloride channels. Neuron **15**:463-472 (1995b)

Fisher SE, Black GCM, Lloyd SE, Hatchwell E, Wrong O, Thakker RV, Craig IW. Isolation and partial characterization of a chloride channel gene which is expressed in kidney and is a candidate for Dent's disease (an X-linked hereditary nephrolithiasis). Hum. Molec. Genet. **3**:2053-2059 (1994)

Franciolini F. The S4 segment and gating of voltage-dependent cationic channels. Biochim. Biophys. Acta **1197**:227-236 (1994)

Franciolini F, Petris A. Chloride channels of biological membranes. Biochim. Biophys. Acta **1031**:247-259 (1990)

Fraser MJ. Ultrastructural observations of virion maturation in *Autographa californica* nuclear polyhedrosis virus infected *Spodoptera frugiperda* cell cultures. J. Ultrastruct. Molec. Struct. Res. **95**:189-195 (1986)

Friesen PD, Miller LK. The regulation of baculovirus gene expression. Curr. Top. Microbiol. Immunol. **131**:31-49 (1986)

Fuchs LY, Woods MS, Weaver RF. Viral transcription during *Autographa californica* nuclear polyhedrosis virus infection: a novel RNA polymerase induced in infected *Spodoptera frugiperda* cells. J. Virol. **48**:641-646 (1983)

Fuller CM, Howard MB, Bedwell DM, Frizzell RA, Benos DJ. Antibodies against the cystic fibrosis transmembrane regulator. Am. J. Physiol. **262**:C396-C404 (1992)

Gearing KL, Possee RD. Functional analysis of a 603 nucleotide open reading frame upstream of the polyhedrin gene of *Autographa californica* nuclear polyhedrosis virus. J. Gen. Virol. **71**:251-262 (1990)

George AL, Crackower MA, Abdalla JA, Hudson AJ, Ebers GC. Molecular basis of Thomsen's disease (autosomal dominant myotonia congenita). Nature Genet. **3**:305-310 (1993)

George AL, Sloan-Brown K, Fenichel GM, Mitchell GA, Spiegel R, Pascuzzi RM. Nonsense and missense mutations of the muscle chloride channel gene in patients with myotonia congenita. Hum. Molec. Genet. **3**:2071-2072 (1994)

Germann UA, Willingham MC, Pastan I, Gottesman MM. Expression of the human multidrug transporter in insect cells by a recombinant baculovirus. Biochemistry **29**:2295-2303 (1990)

Gill DR, Hyde SC, Higgins CF, Valverde MA, Mintenig GM, Sepúlveda FV. Separation of drug transport and chloride channel functions of the human multidrug resistance P-glycoprotein. Cell **71**:23-32 (1992)

Goh DKS. Identification and immunocharacterization of a 25K structural protein in *Autographa californica* nuclear polyhedrosis virus (AcMNPV). Virus Res. **28**:141-152 (1993)

Goldberg AFX, Miller C. Solubilization and functional reconstitution of a chloride channel from *Torpedo californica* electroplax. J. Membr. Biol. **124**:199-206 (1991)

Grabenhorst E, Hofer B, Nimitz M, Jäger V, Conradt HS. Biosynthesis and secretion of human interleukin 2 glycoprotein variants from baculovirus-infected Sf21 cells: Characterization of polypeptides and posttranslational modifications. Euro. J. Biochem. **215**:189-197 (1993)

Greger R. Chloride channel blockers. Methods Enzymol. **191**:793-809 (1990)

Greger R (1992) Cl^- -channels. In: DePont, JJHHM (ed) New Comprehensive Biochemistry: Molecular Aspects of Transport Proteins, vol 21. Elsevier, Amsterdam

Grisshammer R, Tate CG. Overexpression of integral membrane proteins for structural studies. Quart. Rev. Biophys. **28**:315-422 (1995)

Gronemeier M, Condie A, Prosser J, Steinmeyer K, Jentsch TJ, Jockusch H. Nonsense and missense mutations in the muscular chloride channel gene *Clc-1* of myotonic mice. J. Biol. Chem. **269**:5963-5967 (1994)

Gründer S, Thiemann A, Pusch M, Jentsch TJ. Regions involved in the opening of ClC-2 chloride channel by voltage and cell volume. Nature **360**:759-762 (1992)

Grula MA, Buller PL, Weaver RF. α-Amanitin-resistant viral RNA synthesis in nuclei isolated from nuclear polyhedrosis virus-infected *Heliothis zea* larvae and *Spodoptera frugiperda* cells. J. Virol. **38**:916-921 (1981)

Guarino LA, Summers MD. Functional mapping of a *trans*-activating gene required for expression of a baculovirus delayed-early gene. J. Virol. **57**:563-571 (1986)

Guarino LA, Gonzalez MA, Summers MD. Complete sequence and enhancer function of the homologous DNA regions of *Autographa californica* nuclear polyhedrosis virus. J. Virol. **60**:224-229 (1986)

Gurnett CA, Kahl SD, Anderson RD, Campbell KP. Absence of skeletal muscle sarcolemma chloride channel ClC-1 in myotonic mice. J. Biol. Chem. **270**:9035-9038 (1995)

Hanke W, Miller C. Single chloride channels from *Torpedo* electroplax: Activation by protons. J. Gen. Physiol. **82**:25-45 (1983)

Hara T, Nonaka K, Kawaguchi H, Ogata S, Etou N. Effects of temperature on *Escherichia coli* β-galactosidase expression in baculovirus-insect cell system. Biosci. Biotech. Biochem **57**:996-997 (1993)

Harlow E, Lane D (1988) ANTIBODIES: A Laboratory Manual. Cold Spring Harbour Laborotory, Cold Spring Harbour, New York

Harrap KA. The structure of the nuclear polyhedrosis viruses I: The inclusion body. Virology **50**:114-123 (1972a)

Harrap KA. The structure of the nuclear polyhedrosis viruses II: The virus particle. Virology **50**:124-132 (1972b)

Heine R, George AL, Pika U, Deymeer F, Rüdel R, Lehmann-Horn F. Proof of a non-functional muscle chloride channel in recessive myotonia congenita (Becker) by detection of a 4 base pair deletion. Hum. Molec. Genet. **3**:1123-1128 (1994)

Heiny JA, Jong D, Bryant SH, Conte-Camerino D, Tortorella V. Enantiomeric effects on excitation-contraction coupling in frog skeletal muscle by a chiral phenoxy carboxylic acid. Biophys. J. **57**:147-152 (1990a)

Heiny JA, Valle JR, Bryant SH. Optical evidence for a chloride conductance in the T-system of frog skeletal muscle. Pflugers Arch. **416**:288-295 (1990b)

Hopp TP, Woods KR. Prediction of protein antigenic determinants from amino acid sequences. Proc. Natl. Acad. Sci. USA **78**:3824-3828 (1981)

Hoshi T, Zagotta WN, Aldrich RW. Biophysical and molecular mechanisms of *shaker* potassium channel inactivation. Science **250**:533-538 (1990)

Huang M-E, Chuat J-C, Galibert F. A voltage-gated chloride channel in the yeast *Saccharomyces cerevisiae*. J. Molec. Biol. **242**:595-598 (1994)

Hutter OF, De Mello WC, Warner AE (1969) An application of the field strength theory. In: Tosteson, DC (ed) Molecular basis of membrane function. Prentice-Hall, Englewood Cliffs, NJ

Ikeda SR, Korn SJ. Influence of permeating ions on potassium channel block by external tetraethylammonium. J. Physiol. **486**:267-272 (1995)

Jarvis DL. Baculovirus expression vectors: A review and update. Ann. N.Y. Acad. Sci. **646**:240-247 (1991)

Jentsch TJ. Chloride channels. Curr. Opin. Neurobiol. **3**:316-321 (1993)

Jentsch TJ, Steinmeyer K, Schwarz G. Primary structure of *Torpedo marmorata* chloride channel isolated by expression cloning in *Xenopus* oocytes. Nature **348**:510-514 (1990)

Jentsch TJ, Günther W, Pusch M, Schwappach B. Properties of voltage-gated chloride channels of the ClC gene family. J. Physiol. **482.P**:19S-25S (1995a)

Jentsch TJ, Lorenz C, Pusch M, Steinmeyer K. Myotonias due to CLC-1 chloride channel mutations. Soc. Gen. Physiol. Ser. **50**:149-159 (1995b)

Joyce KA, Atkinson AE, Bermudez I, Beadle DJ, King LA. Synthesis of functional $GABA_A$ receptors in stable insect cell lines. FEBS Lett. **335**:61-64 (1993)

Kamb A, Korenbrot JI, Kitajewski J. Expression of ion channels in cultured cells using baculovirus. Methods Enzymol. **207**:423-431 (1992)

Kartner N, Hanrahan JW, Jensen TJ, Naismith AL, Sun S, Ackerley CA, Reyes EF, Tsui Lap-C, Rommens JM, Bear CE, Riordan JR. Expression of the cystic fibrosis gene in non-epithelial invertebrate cells produces a regulated anion conductance. Cell **64**:681-691 (1991)

Kawasaki M, Uchida S, Monkawa T, Miyawaki A, Mikoshiba K, Marumo F, Sasaki S. Cloning and expression of a protein kinase C-regulated chloride channel abundantly expressed in rat brain neuronal cells. Neuron **12**:597-604 (1994)

Kawasaki M, Suzuki M, Uchida S, Sasaki S, Marumo F. Stable and functional expression of the ClC-3 chloride channel in somatic cell lines. Neuron **14**:1285-1291 (1995)

Kelly DC, Brown DA, Ayres MD, Allan CJ, Walker IO. Properties of the major nucleocapsid protein of *Heliothis zea* singly enveloped nuclear polyhedrosis virus. J. Gen. Virol. **64**:399-408 (1983)

Kieferle S, Fong P, Bens M, Vandewalle A, Jentsch TJ. Two highly homologous members of the ClC chloride channel family in both rat and human kidney. Proc. Natl. Acad. Sci. USA **91**:6943-6947 (1994)

Kilmartin JV, Rossi-Bernardi L. Interaction of hemoglobin with hydrogen ions, carbon dioxide, and organic phosphates. Physiol. Rev. **53**:836-890 (1973)

King LA, Possee RD (1992) The baculovirus expression system: A laboratory guide. Chapman and Hall, London

Kirsch GE, Pascual JM, Shieh C-C. Functional role of a conserved aspartate in the external mouth of voltage-gated potassium channels. Biophys. J. **68**:1804-1813 (1995)

Kitts PA, Possee RD. A method for producing recombinant baculovirus expression vectors at high frequency. Biotechniques **14**:810-817 (1993)

Kitts PA, Ayres MD, Possee RD. Linearization of baculovirus DNA enhances the recovery of recombinant virus expression vectors. Nucleic Acids Res. **18**:5667-5672 (1990)

Klaiber K, Williams N, Roberts TM, Papazian DM, Jan LY, Miller C. Functional expression of *shaker* K^+ channels in a baculovirus-infected insect cell line. Neuron **5**:221-226 (1990)

Koch MC, Steinmeyer K, Lorenz C, Ricker K, Wolf F, Otto M, Zoll B, Lehmann-Horn F, Grzeschik K-H, Jentsch TJ. The skeletal muscle chloride channel in dominant and recessive human myotonia. Science **257**:797-800 (1992)

Kozlov EA, Levitina TL, Gusak NM. The primary structure of baculovirus inclusion body proteins. Evolution and structure-function aspects. Curr. Top. Microbiol. Immunol. **131**:135-164 (1986)

Krapivinsky G, Gordon EA, Wickman K, Velimirovic B, Krapivinsky L, Clapham DE. The G-protein-gated atrial K^+ channel I_{KACh} is a heteromulimer of two inwardly rectifying K^+-channel proteins. Nature **374**:135-141 (1995)

Kuzio J, Rohel DZ, Curry CJ, Krebs A, Carstens EB, Faulkner P. Nucleotide sequence of the p10 gene of *Autographa californica* nuclear polyhedrosis virus. Virology **139**:414-418 (1984)

Laemmli UK. Cleavage of structural proteins during the assembly of the head of bacteriophage T4. Nature **227**:680-685 (1970)

Landry DW, Reitman M, Cragoe EJ, Al-Awqati Q. Epithelial chloride channels: Development of inhibitory ligands. J. Gen. Physiol. **90**:779-798 (1987)

Lehmann-Horn F, Mailänder V, Heine R, George AL. Myotonia levior is a chloride channel disorder. Hum. Molec. Genet. **4**:1397-1402 (1995)

Li Z, Smith CD, Smolley JR, Bridge JHB, Frank JS, Philipson KD. Expression of the cardiac Na^+-Ca^{2+} exchanger in insect cells using a baculovirus vector. J. Biol. Chem. **267**:7828-7833 (1992)

Licari P, Bailey JE. Factors influencing recombinant protein yields in an insect cell-baculovirus expression system: Multiplicity of infection and intracellular protein degradation. Biotech. Bioeng. **37**:238-246 (1991)

Livingstone C, Jones I. Baculovirus expression vectors with single strand capability. Nucleic Acids Res. **17**:2366 (1989)

Lorenz C, Meyer-Kleine C, Steinmeyer K, Koch MC, Jentsch TJ. Genomic organization of the human muscle chloride channel ClC-1 and analysis of novel mutations leading to Becker-type myotonia. Hum. Molec. Genet. **3**:941-946 (1994)

Luckow VA (1991) Cloning and expression of heterologous genes in insect cells with baculovirus vectors. In: Prokop, A, Bajpai, RK, Ho, CS (eds) Recombinant DNA technology and applications. McGraw-Hill, Inc., New York

Luckow VA, Summers MD. Trends in the development of baculovirus expression vectors. Bio/Technology (N.Y.) **6**:47-55 (1988)

Luckow VA, Lee SC, Barry GF, Olins PO. Efficient generation of infectious recombinant baculoviruses by site-specific transposon-mediated insertion of foreign genes into a baculovirus genome propagated in *Eschericia coli*. J. Virol. **67**:4566-4579 (1993)

Lü Q, Miller C. Silver as a probe of pore-forming residues in a potassium channel. Science **268**:304-307 (1995)

Malinowska DH, Kupert EY, Bahinski A, Sherry AM, Cuppoletti J. Cloning, functional expression, and characterization of a PKA-activated gastric Cl^- channel. Am. J. Physiol. **268**:C191-C200 (1995)

Matsuura Y, Possee RD, Overton HA, Bishop DHL. Baculovirus expression vectors: the requirements for high level expression of proteins, including glycoproteins. J. Gen. Virol. **68**:1233-1250 (1987)

Mehrke G, Brinkmeier H, Jockusch H. The myotonic mouse mutant ADR: Electrophysiology of the muscle fiber. Muscle and Nerve **11**:440-446 (1988)

Meyer-Kleine C, Ricker K, Otto M, Koch MC. A recurrent 14 bp deletion in the CLCN1 gene associated with generalized myotonia (Becker). Hum. Molec. Genet. **3**:1015-1016 (1994)

Meyer-Kleine C, Steinmeyer K, Ricker K, Jentsch TJ, Koch MC. Spectrum of mutations in the major human skeletal muscle chloride channel gene (CLCN1) leading to myotonia. Am. J. Hum. Genet. **57**:1325-1334 (1995)

Middleton RE, Pheasant DJ, Miller C. Reconstitution of detergent-solubilized Cl^- channels and analysis by concentrative uptake of $^{36}Cl^-$ and planar lipid bilayers. Methods **6**:28-36 (1994)

Miller C. Open-state substructure of single chloride channels from *Torpedo* electroplax. Phil. Trans. R. Soc. Lond. B **299**:401-411 (1982)

Miller C, White MM. A voltage-dependent chloride conductance channel from *Torpedo* electroplax membrane. Ann. N.Y. Acad. Sci. **341**:534-551 (1980)

Miller C, White MM. Dimeric structure of single chloride channels from *Torpedo* electroplax. Proc. Natl. Acad. Sci. USA **81**:2772-2775 (1984)

Miller LK. Baculoviruses as gene expression vectors. Annu. Rev. Microbiol. **42**:177-199 (1988)

Morgan KG, Entrikin RK, Bryant SH. Myotonia and block of chloride conductance by iodide in avian muscle. Am. J. Physiol. **229**:1155-1158 (1975)

Mroczkowski BS, Huvar A, Lernhardt W, Misono K, Nielson K, Scott B. Secretion of thermostable DNA polymerase using a novel baculovirus vector. J. Biol. Chem. **269**:13522-13528 (1994)

Nissen MS, Friesen PD. Molecular analysis of the transcriptional regulatory region of an early baculovirus gene. J. Virol. **63**:493-503 (1989)

Ooi BG, Rankin C, Miller LK. Downstream sequences augment transcription from the essential initiation site of a baculovirus polyhedrin gene. J. Molec. Biol. **210**:721-736 (1989)

O'Reilly DR, Miller LK, Luckow VA (1994) Baculovirus expression vectors: A laboratory manual. Oxford University Press, New York

Palade PT, Barchi RL. Characteristics of the chloride conductance in muscle fibers of the rat diaphragm. J. Gen. Physiol. **69**:325-342 (1977a)

Palade PT, Barchi RL. On the inhibition of muscle membrane chloride conductance by aromatic carboxylic acids. J. Gen. Physiol. **69**:879-896 (1977b)

Pascual JM, Shieh C-C, Kirsch GE, Brown AM. Multiple residues specify external tetraethylammonium blockade in voltage-gated potassium channels. Biophys. J. **69**:428-434 (1995)

Patel G, Nasmyth K, Jones N. A new method for the isolation of recombinant baculovirus. Nucleic Acids Res. **20**:97-104 (1992)

Pearson M, Bjornson R, Pearson G, Rohrmann G. The *Autographa californica* baculovirus genome: Evidence for multiple replication origins. Science **257**:1382-1384 (1992)

Pearson WR, Lipman DJ. Improved tools for biological sequence comparison. Proc. Natl. Acad. Sci. USA **85**:2444-2448 (1988)

Pennock GD, Shoemaker C, Miller LK. Strong and regulated expression of *Escherichia coli* ß-galactosidase in insect cells with a baculovirus vector. Molec. Cell. Biol. **4**:399-406 (1984)

Possee RD, Howard SC. Analysis of the polyhedrin gene promoter of the *Autographa californica* nuclear polyhedrosis virus. Nucleic Acids Res. **15**:10233-10248 (1987)

Power JF, Reid S, Radford KM, Greenfield PF, Nielsen LK. Modeling and optimization of the baculovirus expression vector system in batch suspension culture. Biotech. Bioeng. **44**:710-719 (1994)

Pusch M, Jentsch TJ. Molecular physiology of voltage-gated chloride channels. Physiol. Rev. **74**:813-827 (1994)

Pusch M, Steinmeyer K, Jentsch TJ. Low single channel conductance of the major skeletal muscle chloride channel, ClC-1. Biophys. J. **66**:149-152 (1994)

Pusch M, Ludewig U, Rehfeldt A, Jentsch TJ. Gating of the voltage-dependent chloride channel ClC-0 by the permeant anion. Nature **373**:527-531 (1995a)

Pusch M, Steinmeyer K, Koch MC, Jentsch TJ. Mutations in dominant human myotonia congenita drastically alter the voltage-dependence of the CLC-1 chloride channel. Neuron **in press** (1995b)

Rankin C, Ooi BG, Miller LK. Eight base pairs encompassing the transcriptional start point are the major determinant for baculovirus polyhedrin gene expression. Gene **70**:39-49 (1988)

Ratcliff SW, Luh J, Ganesan AT, Behrens B, Thompson R, Montenegro MA, Morelli G, Trautner TA. The genome of *Bacillus subtilis* phage SPP1: The arrangement of restriction endonuclease generated fragments. Molec. Gen. Genet. **168**:165-172 (1979)

Reuveny S, Kim YJ, Kemp CW, Shiloach J. Production of recombinant proteins in high-density insect cell cultures. Biotechnol. Bioeng. **42**:235-239 (1993)

Rivet-Bastide M, Fahlke C, Seewald MJ, Rüdel R. Rat skeletal muscle chloride channels reconstituted on patch pipettes. Pflugers Arch. **422**(Suppl. 1):R28 (1993) (*abstract*)

Rohrmann GF. Polyhedrin structure. J. Gen. Virol. **67**:1499-1513 (1986)

Rosenbohm A, George AL, Rüdel R, Fahlke C. Effect of activators of protein kinase C (PKC) on the muscle chloride channel, ClC-1, studied in native and heterologous expression systems. Pflugers Arch. **429**(supplement):R25 (1995) (*abstract*)

Rüdel R, Lehmann-Horn F. Membrane changes in cells from myotonia patients. Physiol. Rev. **65**:310-356 (1985)

Rüdel R, Ricker K, Lehmann-Horn F. Transient weakness and altered membrane characteristic in recessive generalised myotonia (Becker). Muscle and Nerve **11**:202-211 (1988)

Rychkov GY, Pusch M, Astill DStJ, Roberts ML, Jentsch TJ, Bretag AH. Concentration and pH dependence of skeletal muscle chloride channel ClC-1. J. Physiol. **submitted** (1995)

Sambrook J, Fritsch EF, Maniatis T (1989) Molecular cloning: A laboratory manual, 2nd edn. Cold Spring Harbour Laboratory Press, New York

Sawadogo M, Van Dyke MW. A rapid method for the purification of deprotected oligonucleotides. Nucleic Acids Res. **19**:674 (1991)

Schorderet DF, Pescia G, Bernasconi A, Regli F. An additional family with Startle disease and a G1192A mutation at the Â1 subunit of the inhibitory glycine receptor gene. Hum. Molec. Genet. **3**:1201 (1994)

Shiang R, Ryan SG, Zhu Y-Z, Hahn AF, O'Connell P, Wasmuth JJ. Mutations in the α_1 subunit of the inhibitory glycine receptor cause the dominant neurologic disorder, hyperekplexia. Nature Genet. **5**:351-357 (1993)

Sigel H, Martin RB. Coordinating properties of the amide bond. Stability and structure of metal ion complexes of peptides and related ligands. Chem. Rev. **82**:385-426 (1982)

Smith CD, Hirayama BA, Wright EM. Baculovirus-mediated expression of the Na^+/glucose cotransporter in Sf9 cells. Biochim. Biophys. Acta **1104**:151-159 (1992)

Smith GE, Fraser MJ, Summers MD. Molecular engineering of the *Autographa californica* nuclear polyhedrosis virus genome: deletion mutations within the polyhedrin gene. J. Virol. **46**:584-593 (1983)

Stanfield PR, Davies NW, Shelton PA, Sutcliffe MJ, Khan IA, Brammer WJ, Conley EC. A single aspartate residue is involved in both intrinsic gating and blockage by Mg^{2+} of the inward rectifier, IRK1. J. Physiol. **478**:1-6 (1994)

Steinmeyer K, Klocke R, Ortland C, Gronemeier M, Jockusch H, Gründer S, Jentsch TJ. Inactivation of muscle chloride channel by transposon insertion in myotonic mice. Nature **354**:304-308 (1991a)

Steinmeyer K, Ortland C, Jentsch TJ. Primary structure and functional expression of a developmentally regulated skeletal muscle chloride channel. Nature **354**:301-304 (1991b)

Steinmeyer K, Lorenz C, Pusch M, Koch MC, Jentsch TJ. Multimeric structure of ClC-1 chloride channel revealed by mutations in dominant myotonia congenita (Thomsen). EMBO J. **13**:737-743 (1994)

Stephenson FA. The $GABA_A$ receptors. Biochem. J. **310**:1-9 (1995)

Stoesz JD, Malinowski DP, Redfield AG. Nuclear magnetic resonance study of solvent exchange and nuclear overhauser effect of the histidine protons of bovine superoxide dismutase. Biochemistry **18**:4669-4675 (1979)

Sulkowski E (1987) Immobilized metal affinity chromatography of proteins. In: Burgess, R (ed) Protein purification: Micro to Macro. Alan R Liss Inc., New York

Summers MD, Smith GE (1987) A manual of methods for baculovirus vectors and insect cell culture procedures. Texas Agricultural Experiment Station, College Station, Texas, Bulletin No. 1555

Sundberg RJ, Martin RB. Interactions of histidine and other imidazole derivatives with transition metal ions in chemical and biological systems. Chem. Rev. **74**:471-517 (1974)

Thiem SM, Miller LK. Identification, sequence, and transcriptional mapping of the major capsid protein gene of the baculovirus *Autographa californica* nuclear polyhedrosis virus. J. Virol. **63**:2008-2018 (1989)

Thiemann A, Gründer S, Pusch M, Jentsch TJ. A chloride channel widely expressed in epithelial and non-epithelial cells. Nature **356**:57-60 (1992)

Tilmann M, Kunzelmann K, Fröbe U, Cabantchik I, Lang HJ, Englert HC, Greger R. Different types of blockers of the intermediate-conductance outwardly rectifying chloride channel in epithelia. Pflugers Arch. **418**:556-563 (1991)

Tomalski MD, Wu J, Miller LK. The location, sequence, transcription, and regulation of a baculovirus dna polymerase gene. Virology **167**:591-600 (1988)

Tricarico D, Conte Camerino D, Govoni S, Bryant SH. Modulation of rat skeletal muscle chloride channels by activators and inhibitors of protein kinase C. Pflugers Arch. **418**:500-503 (1991)

Tweeten KA, Bulla LA, Consigli RA. Characterization of an extremely basic protein derived from granulosis virus nucleocapsids. J. Virol. **33**:866-876 (1980)

Uchida S, Sasaki S, Furukawa T, Hiraoka M, Imai T, Hirata Y, Marumo F. Molecular cloning of a chloride channel that is regulated by dehydration and expressed in kidney medulla. J. Biol. Chem. **268**:3821-3824 (1993)

Vaitukaitis JL. Production of antisera with small doses of immunogen: Multiple intradermal injections. Methods Enzymol. **73**:46-52 (1981)

Valverde MA, Diaz M, Sepúlveda FV, Gill DR, Hyde SC, Higgins CF. Volume-regulated chloride channels associated with the human multidrug-resistance P-glycoprotein. Nature **355**:830-833 (1992)

Van Bueren AM, Moholt-Seibert M, Begley DE, McCall AL. An immunization method for generation of high affinity antisera against glucose transporters useful in immunohistochemistry. Biochem. Biophys. Res. Commun. **197**:1492-1498 (1993)

Van Regenmortal MVH, Briand JP, Muller S, Plau S (1988) Synthetic polypeptides as antigens: Laboratory techniques in biochemistry and molecular biology. Elsevier Science Publishers, Amsterdam, The Netherlands

van Slegtenhorst MA, Bassi MT, Borsani G, Wapenaar MC, Ferrero GB, de Conciliis L, Rugarli EI, Grillo A, Franco B, Zoghbi HY, Ballabio A. A gene from the Xp22.3 region shares homology with voltage-gated chloride channels. Hum. Molec. Genet. **3**:547-552 (1994)

Vaughn JL, Goodwin RH, Tompkins GJ, McCawley P. The establishment of two cell lines from the insect *Spodoptera frugiperda* (Lepidoptera: Noctuidae). In Vitro **13**:213-217 (1977)

Vlak JM, Klinkenberg FA, Zaal KJM, Usmany M, Klinge-Roode EC, Geervliet JBF, Roosien J, Van Lent JWM. Functional studies on the p10 gene of *Autographa californica* nuclear polyhedrosis virus using a recombinant expressing a p10-β-galatctosidase fusion gene. J. Gen. Virol. **69**:765-776 (1988)

Volkman LE. The 64K envelope protein of budded *Autographa californica* nuclear polyhedrosis virus. Curr. Top. Microbiol. Immunol. **131**:103-118 (1986)

Voss T, Ergülen E, Ahorn H, Kubelka V, Sugiyama K, Maurer-Fogy I, Glössl J. Expression of human interferon ω1 in Sf9 cells. No evidence of complex-type N-linked glycosylation or sialylation. Euro. J. Biochem. **217**:913-919 (1993)

Walter G. Production and use of antibodies against synthetic peptides. J. Immunol. Methods **88**:149-161 (1986)

Wang M-Y, Vakharia V, Bentley WE. Expression of epoxide hydrolase in insect cells: A focus on the infected cell. Biotech. Bioeng. **42**:240-246 (1993)

Wang X, Kelly DC. Baculovirus replication: Purification and identification of the *Trichoplusia ni* nuclear polyhedrosis virus-induced DNA polymerase. J. Gen. Virol. **64**:2229-2236 (1983)

Wangemann P, Wittner M, Di Stefano A, Englert HC, Lang HJ, Schlatter E, Greger R. Cl^--channel blockers in the thick ascending limb of the loop of Henle. Structure activity relationship. Pflugers Arch. **407**(Suppl. 2):S128-S141 (1986)

Weber-Schürholz S, Wischmeyer E, Laurien M, Jockusch H, Schürholz T, Landry DW, Al-Awqati Q. Indanyloxyacetic acid-sensitive chloride channels from outer membranes of skeletal muscle. J. Biol. Chem. **268**:547-551 (1993)

Weyer U, Possee RD. Analysis of the promoter of the *Autographa californica* nuclear polyhedrosis virus p10 gene. J. Gen. Virol. **70**:203-208 (1989)

White MM, Miller C. A voltage-gated anion channel from the electric organ of *Torpedo californica*. J. Biol. Chem. **254**:10161-10166 (1979)

Whitford M, Stewart S, Kuzio J, Faulkner P. Identification and sequence analysis of a gene encoding gp67, an abundant envelope glycoprotein of the baculovirus *Autographa californica* nuclear polyhedrosis virus. J. Virol. **63**:1393-1399 (1989)

Williams GV, Rohel DZ, Kuzio J, Faulkner P. A cytopathological investigation of *Autographa californica* nuclear polyhedrosis virus p10 gene function using insertion/deletion mutants. J. Gen. Virol. **70**:187-202 (1989)

Zagotta WN, Aldrich RW. Voltage-dependent gating of *shaker* A-type potassium channels in *Drosophila* muscle. J. Gen. Physiol. **95**:29-60 (1990)